THE UNIVERSITY
of EDINBURGH

The role of novel pro-viral cellular proteins in the replication of *Vaccinia virus*

Kate Harrison

Doctor of Philosophy

University of Edinburgh

2017

Table of Contents

Declaration 1

Acknowledgements 2

List of Publications 3

Abstract 4

Lay Abstract 6

List of Abbreviations 8

1 Introduction 13

1.1. Vaccinia virus 13

1.1.1. History of VACV and first generation vaccines 13

1.1.2. Post-eradication Vaccinia vaccines 15

1.1.3. Vaccini*a* post-eradication 16

1.1.4. Life cycle and morphogenesis 17

1.1.4.1 Entry 17

1.1.4.2 Genome replication and the transcription cascade 19

1.1.4.3 The formation of immature virion crescents and intracellular mature virions 22

1.1.4.4 Intracellular and extracellular enveloped virions 23

1.1.4.5 Release 32

1.2. MKK3 34

1.2.1. Mitogen activated protein kinases 34

1.2.1.1 ERK1/ERK2 34

1.2.1.2 JNK 36

1.2.1.3 ERK5/BMK1 36

1.2.2. MKK3 and the p38 pathway 37

1.2.3. p38 in infection and inflammation 38

1.3. Vps52 41

1.3.1. Retrograde Transport 41

1.3.1.1 Vesicle transport 41

1.3.1.2 The retrograde transport pathway 43

1.3.2. The GARP complex 44

1.3.3. Retrograde transport and infection 48

1.4. Aims and Objectives 50

2 Materials and Methods 51

2.1. Cell lines and viruses 51

2.1.1. Cell lines 51

2.1.2. Viruses 51

2.1.3. Preparation of viral stocks 51

2.2. siRNA transfection 52

2.3. Western blotting 54

2.3.1. Protein collection and protein concentration calculation 54

2.3.2. Sodium dodecyl sulphate – polyacrylamide gel electrophoresis (SDS-PAGE) and western blotting 54

2.4. Growth curves 56

2.4.1. Fluorescent growth curves 56

2.4.2. Plaque assay growth curve 56

2.4.3. Staining and counting cells 57

2.5. MKK3 *In vivo* experiments 57

2.5.1. In vivo VACV infection time course in MKK3 knockout and wild type mice 57

2.5.2. Viral titration from mouse tissues 58

2.5.3. Histopathology of mouse tissues 58

2.5.4. Cytokine array of mouse tissues 58

2.6. Immunofluorescence 59

2.6.1. Immunofluorescence 59

2.6.2. IMARIS image analysis 60

2.7. Retro-2-based assays 60

2.7.1. Shiga toxin survival assay 60

2.7.2. Retro-2 growth curve assays 61

2.7.3. *In vivo* VACV infection time course in Retro-2 treated mice 61

3 The cellular MAPK Kinase protein MKK3 is not required for VACV growth *in vitro* or *in vivo* 62

3.1. Introduction 62

3.2. Aims 66

3.3. Results 67

3.3.1. Transfection of HeLa cells with MKK3-targeting siRNA inhibits protein expression 67

3.3.2. MKK3 knockdown reduces VACV growth as measured by fluorescence 68

3.3.3. MKK3 knockdown does not influence production of infectious virions 70

3.3.4. MKK3 loss does not affect VACV infection *in vivo* 72

3.3.5. MKK3-dependent cytokine expression is not essential for VACV clearance *in vivo* 75

3.3.6. MKK3 knockdown does not reduce total or phosphorylated p38 levels 79

3.3.7. MKK3 loss affects production of VACV proteins 81

3.4. Discussion 84

4 Blocking cellular retrograde transport by destabilising the GARP complex inhibits VACV morphogenesis 90

4.1. Introduction 90

4.2. Aims 93

4.3. Results....94

4.3.1. siRNA targeting Vps52 reduces the levels of Vps52 in HeLa cells 94

4.3.2. Vps52 knockdown affects retrograde transport, but not Golgi morphology 96

4.3.3. Knockdown of Vps52 inhibits VACV infection....99

4.3.4. Knockdown of any GARP component inhibits replication of VACV....101

4.3.5. Vps52 loss affects extracellular enveloped virion production....104

4.3.6. Expression of GARP complex is reduced in *Wobbler* MEFs....105

4.3.7. The *Wob* MEF mutation reduces VACV replication through inhibition of EEV production....107

4.3.8. Loss of GARP Affects IEV production and produces aberrant B5-containing vesicles 109

4.4. Discussion....113

5 VACV uses retromer-independent, Retro-2 susceptible retrograde transport to facilitate IEV wrapping....116

5.1. Introduction....116

5.2. Aims....121

5.3. Results....122

5.3.1. B5 and F13 colocalise independently of VACV capsids in GARP deficient cells 122

5.3.2. Retromer knockdown does not affect VACV growth....124

5.3.3. Retro-2 inhibits VACV growth....128

5.3.3.1 Retro-2 treatment protects against shiga toxin-2 by blocking retrograde transport.128

5.3.3.2 Retro-2 treatment inhibits VACV growth....130

5.3.3.3 Retro-2 related compounds also inhibit VACV growth 131

....133

5.3.3.4 Retro-2 and related compounds inhibit EEV production....134

5.3.3.5 Retro-2 treatment displays additional effects on VACV to the *Wob* mutation....135

5.3.3.6 Retro-2 treatment affects IEV production and causes formation of aberrant B5 vesicles 136

5.3.4. Retro-2 treatment prior to infection inhibits VACV growth, and alleviates systemic disease symptoms *in vivo* 138

5.4. Discussion 142

5.4.1. F13 and B5 142

5.4.2. Retromer 144

5.4.3. Retro-2 145

6. General Discussion 148

6.1. Thesis aims and overview. 148

6.2. Conclusions and implications 148

6.2.1. MKK3 148

6.2.2. Vps52 150

6.3. Overall Discussion 154

Bibliography 158

Declaration

I declare that this thesis is my own composition and that the work and results contained in it are entirely my own, unless the specific contribution of other are acknowledged. This work has not been submitted for any other degree or professional qualification.

Kate Harrison

June 2017

Acknowledgements

I would like to thank my supervisors Dr Pip Beard and Professor Paul Digard for their support and advice. I would also like to thank Dr Colin McInnes for proof-reading my thesis, and wish to acknowledge the Roslin Institute and the University of Edinburgh for my Principal's Career Development Scholarship. Many of the results contained here would not have been possible without the reagents kindly donated by Dr Thomas Schmitt-John (Aarhus University, Denmark), Daniel Gillet (CEA Saclay) and Dr Kenny Baillie (The Roslin Institute). I would like to thank Dr Ismar Haga and Dr Tali Pechenick-Jowers for their support and teaching in the lab, and for looking after my cells while I was on holiday. The public engagement aspect of my scholarship would not have been possible without the help and advice of Dr Nicola Stock. On a personal level, there are so many friends, family and colleagues who have supported me during the last few turbulent years, that it's almost impossible to list them all. First and foremost, I am forever indebted to my wonderful parents, for their advice and love, as well as putting up with endless sobbing phone calls, and ensuring I haven't had to buy my own loo roll in 8 years. Thank you to my sister Beth and my best friend Maria for listening to my venting and providing unfailing entertainment and distraction, and just generally being top buds. I would like to thank Fiona, Andrew, Graham, Brendan, John, Laura, Dave, Carys, Enrique and Seema for making lunchtime the highlight of everyday at the Roslin, and particularly Andrew, Graham and Beans for being ace writing-up pals. A huge thank you goes to Gwen, Sandi, Casper, Laura, Sarah and everyone at the Watermelon Studio for the classes, the laughs, the video-bombing and the late night gossip/stretch sessions. Mostly though, thank you for being my escape. Thank you to the wonderful friends I made at The Chocolate Tree: Shaz, Maggie, Euan, Sara, Cat, Michael for being the perfect distraction from writing and particularly Adelina for helping me get the job in the first place, pure nepotism. I would also like to acknowledge my fantastic friends Fiona (for the day trips and rat cuddles), Tali (for the cocktails), Pippa (for the Yeni's), Amy (generally just a top bud), and Jamie (for all the emotional support and helping me deal with all these lemons).

I would also like to thank my new colleagues in Oxford who have been so welcoming and supporting and finally, thank you to my housemates past and present, particularly Emily and Isabel who have dealt admirably with the Thesis Gremlin, and made me feel instantly at home in a new city.

List of Publications

Harrison, K., Haga, I.R., Jowers, T.P., Jasim, S., Cintrat, J.C., Gillet, D., Schmitt-John, T., Digard, P. and Beard, P.M., 2016. Vaccinia Virus Uses Retromer-Independent Cellular Retrograde Transport Pathways To Facilitate the Wrapping of Intracellular Mature Virions during Virus Morphogenesis. *Journal of Virology*, *90*(22), pp.10120-10132.

Abstract

Vaccinia virus (VACV), the prototypic poxvirus, undergoes a complex life cycle, with multiple stages that are not yet fully understood. This work studied two cellular proteins which had previously been identified by siRNA screens as playing proviral roles in the replication cycle of VACV: the dual specificity mitogen-activated protein kinase kinase 3 (MKK3) and vacuolar protein sorting 52 (Vps52).

MKK3 is an upstream regulator in the p38 pathway which, along with MKK6, phosphorylates and therefore activates p38. In HeLa cell cultures, siRNA depletion experiments confirmed that MKK3 supported VACV replication. MKK3 knockdown reduced production of both early and late-class VACV proteins, suggesting that it facilitates viral gene expression. However, this difference did not translate to an *in vivo* model, as comparison between wild type and MKK3 knockout mice infected with VACV revealed no significant differences in virus replication or overall disease.

The Golgi-associated retrograde protein complex (GARP) is composed of four large heteromeric proteins: Vps51, Vps52, Vps53 and Vps54, and plays a key role in retrograde transport from endosomes to the TGN. The effects of loss of GARP function were investigated using three techniques: mouse embryonic fibroblasts (MEFs) containing the hypomorphic Vps54 "wobbler" mutation, Vps52-targetting siRNA in HeLa cells and pharmacological inhibition of retrograde transport using the drug Retro-2. GARP loss resulted in a marked reduction in VACV spread due to a reduction specifically in "double wrapped" extracellular enveloped virion (EEV) production. Investigation of the mechanism by which GARP facilitates EEV production revealed a disruption of the VACV morphogenesis pathway prior to the double wrapping event, resulting in mislocalisation and aggregation of the viral membrane protein B5 within the cytoplasm. The effects of GARP loss translated to an in vivo model, as mice infected with VACV and treated with Retro-2 exhibited reduced viral replication and overall disease. These results identify GARP as a pro-viral host complex required for EEV production, and suggest that cellular retrograde transport pathways are required for double-wrapping of VACV virions.

Overall, the study illustrates both the potential pitfalls of carrying out genetic screens in a transformed cell line and the power of such studies to nevertheless identify novel features of virus biology as well as druggable targets for antiviral intervention.

Lay Abstract

Vaccinia virus (VACV) is a complex poxvirus with multiple life cycle stages which are not yet fully understood. VACV is most well-known as the vaccine for Smallpox, but also has applications in biotechnology and vaccine development for other diseases. This work investigated how specific host proteins are used in the VACV replication cycle. Two proteins that had previously been identified in large genetic screens as aiding VACV growth were focussed on: the dual specificity mitogen-activated protein kinase kinase 3 (MKK3) and vaculolar protein sorting 52 (Vps52).

MKK3 is an enzyme which, when activated by environmental stress, triggers subsequent enzymes which are involved in controlling the cellular growth cycle. This chain of events is known as the p38 pathway. When MKK3 production in cells was inhibited, VACV replication was reduced. MKK3 inhibition also reduced the production of viral proteins from early and late stages in the VACV life cycle, suggesting that it plays role in viral protein synthesis. However, this difference was not seen in a whole animal model, infecting genetically normal mice and mice lacking the MKK3 protein with VACV showed no significant differences in virus growth or disease symptoms.

In cells, proteins are packaged for transport at the Golgi apparatus near the centre of the cell, before being trafficked to their destination. The retrograde transport pathway transports proteins from the periphery of the cell back in to the trans-Golgi network (TGN), for reuse or recycling. The Golgi-associated retrograde protein complex (GARP) is a key part of retrograde transport and is made up of four large proteins: Vps51, Vps52, Vps53 and Vps54. The effects of GARP loss were investigated using three techniques: inhibition of Vps52 protein production, cells containing the wobbler mutation which increases the rate at which GARP is degraded, and pharmacological inhibition of retrograde transport using the drug Retro-2. GARP loss resulted in a marked reduction in VACV replication and spread, due to a reduction specifically in extracellular enveloped virion (EEV) production. EEVs are a stage in the VACV life cycle in which a small fraction of intracellular virions are wrapped in an extra double-layer membrane, and released before the cell dies for long-range spread of the virus. Investigation of how GARP is involved in EEV production revealed a disruption in VACV formation before the double-wrapping event, resulting in proteins usually found in the EEV membrane forming large, wrongly-trafficked aggregates. The effects of GARP loss translated to an animal-model, as

when mice with the wobbler mutation, and therefore reduced levels of GARP, were infected with VACV, a reduction was seen in both viral replication and overall disease symptoms. These results identify host complex GARP as having a key role in EEV production, and suggests that cellular retrograde transport pathways are required for double-wrapping of VACV.

Overall, the study illustrates both the potential pitfalls of carrying out large genetic screens, and the power of such studies to nevertheless identify new features of virus biology as well as potential future targets for antiviral treatment.

List of Abbreviations

4E-BP	Eukaryotic translation initiation factor 4F binding protein
AAV	Adeno-associated virus
ANOVA	Analysis of variance
ALS	Amyotrophic lateral sclerosis
Ang	Another new gene
ATF	Activating transcription factor
BMK	Big mitogen activated protein kinase
CatD	Cathepsin-D
CATCHR	Complex associated with tethering containing helical rods
CAV	Cell-associated virion
CCL	(C-C) motif ligand
CEV	Cell-associated enveloped virion
CI-MPR	Cation independent mannose-6-phosphate receptor
CMC	Carboxymethylcellulose
COP	Coat protein complex
CORVET	Class C core vacuole/endosome tethering
CPXV	Cowpox virus
CPY	Carboxy peptidase Y
CTx	Cholera toxin
CXCL	(C-X-C) motif ligand
DMEM	Dulbecco's modified Eagle's medium
DMSO	Dimethyl sulphoxide
dpi	Days post infection
dVV-L	Defective vaccinia Lister
EEV	Extracellular enveloped virion
EFC	Entry/fusion complex
EGFP	Enhanced green fluorescent protein
EGRT	Endosome to Golgi retrograde transport

EGRTP	Endosome to Golgi retrograde transport pathway
EHEC	Enterohaemorrhagic *Escherichia coli*
eIF4F	Eukaryotic translation initiation factor 4
Env	Human immunodeficiency virus envelope glycoprotein
ER	Endoplasmic reticulum
ERK	Extracellular signal regulated protein kinase
FBS	Foetal bovine serum
GAG	Glycosaminoglycan
GARP	Golgi associated retrograde pathway
GM-CSF	Granulocyte/macrophage colony stimulating factor
HBV	Hepatitis B virus
HIV	Human immunodeficiency virus
HOPS	Homotypic fusion and vacuole protein sorting/class C Vps
hpi	Hours post infection
HPV	Human papilloma virus
HRP	Horseradish peroxidase
HSV	Herpes simplex virus
IEV	Intracellular enveloped virion
IFN	Interferon
IL	Interleukin
IMCBH	N1-isonicotinoyl-N2-3-methyl-4-chlorobenzoylhydrazine
IMV	Intracellular mature virion
IP	Interferon gamma-induced protein
IRAK	Interleukin receptor associated kinase
ISG	Interferon stimulated genes
IV	Immature virion
JNK	c-Jun NH2 terminal kinase
kd	Knock down
KLC	Kinesin light chain

LC3	Microtubule-associated protein 1A/1B-light chain 3
LC16m8	Lister clone 16 medium pock size clone 8
LPS	Lipopolysaccharide
MAPK	Mitogen activated protein kinase
MAPKAPK	Mitogen activated protein kinase activated protein kinase
MPKK/MAP2K/MEK	Mitogen activated protein kinase kinase
MPKKK/MAP3K/MEKK	Mitogen activated protein kinase kinase kinase
MPKKKK/MAP4K	Mitogen activated protein kinase kinase kinase kinase
MCP	Monocyte chemoattractant protein
MIG	Monokine induced by gamma interferon
MEF	Mouse embryonic fibroblasts
MIP	Macrophage inflammatory protein
MLK	Mixed-lineage protein kinase
Mnk	Mitogen activated protein kinase-interacting kinase
MOI	Multiplicity of infection
MPR	Mannose-6-phosphate receptor
MTC	Multi-subunit tethering complex
MV	Mature virion
MVA	Modified vaccine Ankara vaccinia virus
MU	*Wobbler* MEF cells
NF-κB	Nuclear factor kappa-light-chain-enhancer of activated B cells
NT	Non-targeting
NYVAC	New York vaccinia
ORF	Open reading frame
PBS	Phosphate buffered saline
pfu	Plaque forming units
PEx	*Pseudomonas* toxin
PKR	Protein kinase R
PLD	Phospholipase D

PLK	Polo-like kinase
PRK-AB1	5'-AMP-activated protein kinase subunit beta-1
Rab	Small GTPase of the Ras superfamily
RAF	Rapidly accelerated fibrosarcoma
RANTES	Regulated on activation, normal T cell expressed and secreted
RAP	RNA polymerase-associated protein
Rho	Ras homolog gene family, member
RIG	Retinoic acid-inducible gene I
ROS	Reactive oxygen species
RPO	Viral RNA polymerase
RT	Room temperature
SCR	Short consensus repeat
siRNA	Small interfering RNA
SEM	Standard error of the mean
SNAP	Soluble N-ethylamide factor attachment protein
SNARE	Soluble N-ethylamide factor attachment protein receptor
SNX	Sorting nexin
ST-246	4-trifluoromethyl-N-(3,3a,4,4a,5,5a,6,6a-octahydro-1,3-di oxo-4,6-ethenocycloprop [f]isoindol-2(1 H)-yl)-benzamide
STx	Shiga toxin
STxB	Shiga toxin subunit B
TAB	Transforming growth factor β-activated protein kinase binding protein 1
TAK	Transforming growth factor- β-activated kinase
TGF	Transforming growth factor
TGN	Trans-Golgi network
TIMP	Tissue inhibitor of metalloproteinase
TK	Thymidine kinase
TNF	Tumour necrosis factor
TR-tfn	Texas-red conjugated transferrin

TRAF	TNF-receptor associated factor
TREM	Triggering receptor expressed on myeloid cells
VACV	*Vaccinia* virus
VACV-A5-EGFP	*Vaccinia* virus A5 enhanced fluorescent green protein
VACV-IHD-J	*Vaccinia* virus International Health Department-J
VACV-WR	*Vaccinia* virus Western Reserve strain
VAMP	Vesicle associated membrane protein
VARV	*Variola* virus
VCP	Viral complement control factor
VETF	Vaccinia early transcription factor
VITF	Vaccinia intermediate transcription factor
VLTF	Vaccinia late transcription factor
VGF	Vaccinia growth factor
VIG	Vaccinia immunoglobulin
VPEF	Vaccinia penetration factor
Vps	Vacuolar protein sorting
VTF	Vaccinia early transcription termination factor
Vti	Vesicle transport through interaction with t-SNAREs homolog
WHO	World Health Organisation
WT	Wild type

1 Introduction

1.1. Vaccinia virus

In the last two centuries, the impact that infectious diseases have on humanity has lessened significantly. For the most part, this is thanks to the advent of vaccines, and the ability to comprehensively prevent disease. Therefore, it can be argued that the prototypic orthopoxvirus, *Vaccinia* virus (VACV), as the very first widely used vaccine, is the most important virus in human history. While genetically distinct from other orthopoxviruses such as *Variola* virus (VARV) and *Cowpox virus* (CPXV), VACV carries enough antigenic similarities to provide cross-protection to all viruses in this genus (Roberts & Smith, 2008). VACV's large genome allows it to encode many of its own replication and transcription factors, which enables it, unlike most DNA viruses, to replicate in viral factories in the cytoplasm of the cell, rather than being dependent on the nucleus (Broyles, 2003). VACV has a highly complex life cycle, several parts of which are still heavily debated and not fully understood, such as the site of extra-membrane wrapping. VACV is considered the prototypic poxvirus, and has many applications as a vaccine vector and as a tool to study cellular biology. Therefore, further investigation and characterisation of these poorly understood areas may reveal novel applications for VACV.

1.1.1. History of VACV and first generation vaccines

Though it was use of VACV that resulted in the final eradication of smallpox, it was CPXV with which Edward Jenner began his famous vaccination experiments in the late 19th century. Although CPXV and VACV are closely related, they remain genetically distinct (Baxby, 1977). At some point during the last century, VACV replaced CPXV as the prevalent source of vaccination for VARV, though the time and method of this transition is unknown, as is the original host of VACV (Roberts & Smith, 2008). Theories for the origins of VACV include the now extinct horsepox, or an attenuating hybridisation of VARV and CPXV, as these viruses do show the possibility of hybridisation under experimental conditions (Alcami & Smith, 1996; Bedson & Dumbell, 1964). However, no theory has been conclusively confirmed as yet.

Smallpox is unique among infectious human diseases in that it is the only pathogen that has been successfully removed from nature by man. The widespread use of VACV to induce VARV immunity resulted in the last naturally occurring smallpox case being recorded in 1977, the World Health Organisation (WHO) declaring official eradication in 1980 (Meyer, 2013). As a vaccine, VACV is extremely effective, but not without risk. Vaccines developed and used during the smallpox eradication are known as first generation vaccines. First generation vaccines used during the eradication, such as the Lister strain, Dryvax and Tian Tan (Midgley *et al.,* 2008) replicate in the dermis after subcutaneous injection, resulting in mild fever, local lymphadenopathy and a pustule at the site of infection. This pustule begins as a papule, before becoming vesicular at 5-8 days post infection. In a normal infection, the pustule reaches its maximum size at day 10 before scabbing over by day 14 post inoculation, and shedding the scab by day 21 (Cono, *et al.,* 2003; Bray, 2003). However, as all the first generation vaccines were replication competent viruses, there was a relatively high risk of complications, including eczema vaccinatum, post vaccinal encephalitis, generalised vaccinia, and progressive vaccinia, all of which had the potential to be fatal (Cono *et al.*, 2003; Meyer, 2013). Generalised vaccinia can occur at random, regardless of immune status of the vaccinee and results in extensive maculopapular lesions, both around the site of inoculation and all over the body, due to dissemination of the virus in the blood (Goldstein *et al.*, 1975; Gibson & Langsten, 2004) In comparison, progressive vaccinia is associated with immunodeficiency and the significant expansion of the pustule, both across the dermis and into deeper tissues, is often compounded by bacterial superinfection, resulting in osteomyelitis and necrosis (Goldstein *et al.,* 1975; Bray & Wright, 2003). Eczema vaccinatum occurs in cases of atopic dermatitis, in both primary vaccines and through secondary contact, with over half of cases seen in children under 5 (Vora *et al.,* 2008). Post vaccinal encephalitis and encephalomyelitis are the rarest, but most severe of the potential VACV complications, and have no link with immunodeficiency. Symptoms, including convulsions, paralysis and coma manifest within two weeks post inoculation, and have a 30% mortality rate (Goldstein *et al.*, 1975). For progressive and generalised vaccinia, and eczema vaccinatum, treatment can be administered using Vaccinia immunoglobulin (VIG) from recently, successfully vaccinated individuals, or oral or topical application of the anti-poxvirus drug ST-146 (Bray, 2003; Lederman *et al.,* 2012). Despite a relatively high rate of complications, the overall rate of fatal complications from

VACV inoculation was thought to be less than one per million vaccinations during the eradication (Bray, 2003).

In addition to these complications, first generation vaccines were often passaged in ovine or bovine skin, or in chicken eggs, resulting in contaminations and wide variations in virulence, immune protection and genetic sequences (Medaglia *et al.,* 2015) Genetic examination of first generation vaccine strains has shown that not only were these vaccines not clonal, there was more genetic diversity within the vaccine strain Dryvax, than between the major and minor strains of VARV (Qin *et al.,* 2011). Therefore, improved and genetically homogenous VACV strains were developed for use in vaccination.

1.1.2. Post-eradication Vaccinia vaccines

In the years since the eradication of smallpox, several attenuated 2nd and 3rd generation vaccines have been developed in order to reduce side effects and bacterial contamination, such as Modified Vaccine Ankara (MVA), New York Vaccinia (NYVAC) and Lister clone 16 medium pock size clone 8 (LC16m8). While these vaccines have been used in clinical settings, their efficacy has never been tested in an endemic situation (Meyer, 2013). These attenuated vaccines are produced by extensive passaging of fully pathogenic VACV strains, such as MVA, a non-replicating, avirulent VACV strain developed in Germany in 1975. The original VACV Ankara strain was passaged 575 times in primary chick embryo fibroblasts until it became highly attenuated in mammalian cells (Mayr, 2003). Six major deletions, totalling 24kb have been identified, in the MVA genome compared to the fully virulent Western Reserve strain (WR). However, these major deletions are not sufficient to cause the level of attenuation seen in MVA, suggesting the avirulence stems from additional or co-operative mutations. (Altenburger *et al.*, 1989; Meisinger-Henschel *et al.,* 2010). Several of the major deletions affect genes involved in host range, the late stages of morphogenesis, and several immunomodulatory proteins usually found in orthopoxvirues such as receptors for interferon-γ (IFN-γ), IFN-α/β, and certain chemokines (Blanchard, *et al.,*1998; Altenburger, *et al.*, 1989; Moss, 1996). Consequently, MVA has been used without complications in over 150,000 vaccinations, even in cases of immunodeficiency (Mayr, 2003), and has been shown to induce humoral and cellular immunity comparable to fully-virulent strains in mice, as well as protecting against monkeypox in non-human

primates (Earl *et al.,* 2004; McCurdy *et al.,* 2004). Another highly attenuated strain, LC16m8 was developed at the same time in Japan, this time from the Lister strain through several intermediates (Hasizume, 1975). A frame-shift from a single deletion mutation results in no B5R gene, and therefore a decreased ability for the virus to attain long-range spread. However, since the B5 protein is the major target for immune responses against extracellular enveloped virions (EEVs), it is possible that an immune response generated against LC16m8 is not as potent as those from wild type strains, and therefore may not be the ideal vaccine candidate (Johnson *et al.,* 2011). Though it is possible for LC16m8 to revert back to more virulent forms, it has been used in over 100,000 successful, complication-free vaccinations and has been shown to be 100 fold more effective than MVA (Kidokoro, *et al.,* 2005). A more recent 3rd generation vaccine, defective vaccinia Lister (dVV-L) has been derived from Lister and Elstree strains, as a vector rather than a vaccine. dVV-L is infectious, but contains a replication block at late gene expression due to the deletion of the gene for uracil DNA glycoslylase, D4R, which is essential for vaccinia replication (Holzer & Falkner, 1997). Unlike LC16m8, dVV-L cannot regain its full pathogenic status, and is shown to induce similar levels of humoral and cellular immune responses to MVA (Ober *et al.,* 2002).

1.1.3. Vaccini*a* post-eradication

Despite the eradication of VARV in the 1970s, VACV still remains important in biological research, not only as an insight into other poxviruses such as VARV, but also as a tool to investigate cellular mechanisms, such as actin polymerisation (Frischknecht *et al.,* 1999), and immune evasion (Smith, 1999). Due to its large, easy to manipulate genome, VACV can be used as a vector for the delivery of other vaccine epitopes, such as MVA expressing influenza proteins haemagluttinin, neuraminidase and Matrix-protein 1 in order to stimulate humoral and cellular immunity (Breathnach *et al.,* 2004; Mullin *et al.,* 2016). Several other infectious diseases such as *Mycobacterium tuberculosis* and West Nile fever have also been successfully protected against under experimental conditions using a VACV vector (Zhu *et al.,* 1997; Volz *et al.,* 2016). As well as protection against microbial disease, VACV is currently under investigation as a potential oncolytic virotheraputic, as it has the potential to infect a broad range of cancerous cell types. An early paper on the topic showed that deletion of the Vaccinia growth factor (VGF) gene and thymidine kinase (TK) gene produces an attenuated virus that replicates specifically in tumour cells *in vivo,* and highlighted VACV as a key potential oncolytic

(McCart *et al.,* 2001). Since then, several strains of VACV have shown anti-tumour activity, including the WR strain which, when containing targeted gene deletions is able to inhibit the growth of certain tumours, in human patients (Zeh *et al.,* 2015).

1.1.4. Life cycle and morphogenesis

The life cycle of VACV is complex and progresses through several different stages and morphologies, with the virion consisting of a conserved DNA protein core surrounded by varying numbers of lipid membranes. The number and structure of the membranes present is dependent on the life cycle stage. Replication begins with the entry of an uncoated viral core into the cytoplasm of a host cell, where it is transported on microtubules further into the cytoplasm (Carter *et al*., 2003). Unlike the majority of DNA viruses, VACV replicates exclusively in the cytoplasm, and never enters the nucleus. Instead, VACV creates viral factories in peri-nuclear areas of the cytoplasm (Minnigan & Moyer, 1985). These factories begin to appear approximately two hours post infection, as dense accumulations of filaments and granules, and are the site of the viral DNA replication, transcription, and the initial stages of morphogenesis. Between 10 and 24 hours post infection the number and size of these factories rapidly increases, until the cell is filled by virion replication (Dales & Siminovitch 1961). Vaccinia virus virions are formed from initial membrane crescents which associate with viroplasm to form immature virions (IVs) which then develop further to intracellular mature virions (IMVs), intracellular enveloped virions (IEVs), cell-associated enveloped virions (CEVs) and extracellular enveloped virions (EEVs). The existence of different virion forms results in different methods of cells entry and cell exit.

1.1.4.1 Entry

Vaccinia exhibits more than one method of entry, due to the structural and antigenic differences in mature virions (MVs) and EEVs. For both MVs and EEVs, initial adsorption is required to begin the entry process and although both forms of virion adsorb at the same rate, IMVs are internalised at a faster rate than EEVs (Payne & Norrby, 1978; Vanderplasschen & Smith, 1997).

Two methods of MV entry have been observed: macropinocytosis, and entry via the fluid phase endocytic pathway. Direct fusion is initiated by the binding of MV proteins such as D8 and A27 to

glycosaminoglycans (GAGs) on the cellular surface, including chondroitin sulphate and heparin sulphate respectively (Chung *et al.,*1997; Hsaio *et al.,* 1999). Once adsorbed, a large, multi-protein complex known as the entry fusion complex (EFC) is required for fusion with the plasma membrane and entry into the cytoplasm. The complex consists of several MV proteins including A16, A21, A28, G2, G9, H2 J5, L1 and L5, and although its exact role is as yet unknown, loss of any of the proteins results in the same phenotype and an inability to enter cells (Senkevich *et al.,* 2005). On the cellular side, vaccinia virus penetration factor (VPEF) is required for entry, along with actin signalling cascade signalling cascade which includes Ras homolog gene family, member A (RhoA), Cell division control protein 42 (Cdc42) and small GTPase Ras-related C3 botulinum toxin substrate 1 (Rac1). This cascade results in the formation of filopodia to ensure the largest possible surface area of the plasma membrane is in contact with the virion (Vanderplasschen *et al.,* 1998; Locker *et al.,* 2000; Huang *et al.,* 2008). Fusion then occurs consisting of direct continuity of the viral and plasma membranes, and the ejection of the naked viral core and the lateral bodies into the cell cytoplasm, ready for early transcription and DNA replication to begin (Armstrong *et al.,* 1973; Carter *et al.,* 2005). This model of entry is consistent with the hypothesis that the IMV/MV has only one membrane, and indeed the Carter *et al.* study in 2005 proved this conclusively using tilt series analysis.

Direct fusion of the virus with the membrane appears to be the preferred entry mechanism for IMVs early on in infection, while entry via macropinocytosis predominates at later stages (Armstrong *et al,* 1973). This fluid-phase endocytic entry involves virally induced, rapid blebbing on the cell surface, followed by the low pH- and dynamin-dependent engulfment of the MV into an endosome. Once internalised, the MV then fuses with the endosomal membrane for release into the cytoplasm (Mercer & Helenius, 2008; Huang *et al.,* 2008).

EEV entry is more complex than MV, as it has an extra membrane which must be removed before entry can occur. GAGs on the cell surface interact with EEV proteins B5 and A34 to induce membrane rupture, in a process called ligand-dependent non-fusogenic dissolution. The EEV membrane does not fuse with the plasma membrane, but instead drapes over the virion core while it fuses, most likely to protect it from immune system attack. (Law *et al.,* 2006; Roberts *et al.,* 2009). It

is also thought that EEVs can enter via endocytosis. Ichihashi, *et al.,* (1996) put forward the hypothesis that low-pH dependent endocytosis encloses EEVs in endosomes where the outer membrane is disrupted to allow the MV core to fuse with the endosomal membrane for release into the cytoplasm.

1.1.4.2 Genome replication and the transcription cascade

The VACV genome encodes over 200 open reading frames (ORFs), which must be selectively expressed at the correct point in replication. To achieve this regulation, VACV exerts control at a transcriptional level, expressing its genome in a cascade mechanism, in which genes are classified as early, intermediate and late, and transcription of each class is initiated by the gene products of the previous class (Broyles, 2003; Keck *et al.,* 1990).

Once the virions are uncoated, early transcription begins with early mRNA being seen within 12 minutes of cell infection, before DNA replication. This is possible as VACV contains all the components required for early transcription, already-synthesised in the viral core (Kates & McAuslan, 1967; Munyon et al., 1967). Further research showed that this early transcription machinery consisted primarily of Vaccinia early transcription factor (VETF), RNA polymerase associated protein (RAP94) and the viral RNA polymerase (RPO), as well as capping and methylating enzymes, poly(A) polymerase, and ATPases; all of which are transcribed from late genes and packaged into virion cores before dissemination (Broyles, 2003; Gershon & Moss, 1990; Ahn & Moss, 1992; Munyon *et al.*1967). The presence of a virally encoded, DNA dependent RNA polymerase is unusual, as usually invading viruses seek to hijack the cellular RNA polymerase for their own use. During early transcription, the VACV RPO is recruited to the site of early promoters by VETF, in order to initiate transcription. (Broyles, *et al.,* 1988). VETF is composed of two independently produced subunits transcribed by late genes: an 82kDa polypeptide encoded by the A8L gene (Hu *et al.,* 1997), and the slightly smaller 70kDa gene product of D6R (Broyles and Fesler, 1990; Gershon and Moss, 1990). The 70kDa subunit contains an ATP binding site, which has been shown to be the main source of the ATPase activity that drives early transcription, thus showing that VETF is required for the continued progress of RPO, as well as transcription initiation (Broyles and Fesler, 1990). The remaining component of early transcription machinery, RAP94, is a transcription specificity factor and ensures

that only early genes are transcribed during early transcription, by controlling the association of RPO and VETF by the formation of a link between the two (Yang and Moss, 2009). RAP94 is also essential for early transcription termination, through its interaction with the Vaccinia early transcription termination factor (VTF) and the ATPase nucleoside triphosphate phosphohydrolase-1 (NPH1) at the UUUUUNU termination motif (Piacente *et al.,* 2008)

The VACV genome begins to replicate after early transcription, at around 2h post infection, as the DNA replication machinery is translated from early viral mRNAs. DNA replication, RNA transcription and translation all occur inside viral factories located close to the cell nucleus, which are also later the site of IMV morphogenesis (Kastafanas & Moss, 2007). The VACV genome consists of one continuous polynucleotide chain with incompletely paired, AT-rich hairpins at each end. DNA replication is initiated near these terminal hairpins, and initially forms concatermeric intermediates before the new genome is completed (Pogo *et al.,* 1984; Moss, 2013). As with transcription, VACV encodes much of its own DNA replication machinery, minimising its dependence on cellular factors. This includes the VACV polymerase Pol, encoded by the E9L gene, which previous evidence has shown to be homologous to several eukaryotic DNA polymerases (Wang *et al.,*1989). Multiple other viral proteins are required for successful DNA replication in addition to Pol, including nucleotide hydrolysis catalyst D5 which forms a complex with processivity factors A20 and D4, all of which are essential for genome replication (Ishii & Moss,2001). Once genome replication is complete and the intermediate concatemers are resolved, the resulting DNA nucleoids are packaged into viral membrane crescents before the membranes close off to become spherical intermediate virions (IVs) (Moss, 2013), a process discussed in more detail later on in this section.

Of the VACV genome, 115 genes are considered early genes, comprising approximately half of the entire genome (Yang *et al.,* 2010). Several of these genes code for the necessary machinery for intermediate transcription and the continuation of the cascade. Vaccinia intermediate transcription factors (VITF) are synthesised *de novo,* but as they are products of early genes they do not require DNA replication for their formation. Where early transcription requires only one specific transcription factor, the transcription of intermediate genes requires several: VITF-1, VITF-2, VITF-3, as well as capping enzyme VITF-A and the RPO. However, while VITF-1 is the 30kDa gene product

of viral gene E4L (Rosales *et al.,* 1994a), the 68kDa VITF-2 is a cellular factor, as it can be isolated from the nuclei of uninfected cells (Rosales, *et al.*, 1994b). Further investigation revealed VITF-2 to be a heterodimer of cellular factors cytoplasmic activation/proliferation-associated protein p137, and Ras-GTPase-activating protein SH3 domain-binding protein G3BP (Katsafanas & Moss, 2004) A third transcription factor of 100kDa, originally designated as VITF-3, is composed of 35kDa and 45kDa subunits encoded by viral genes A8R and A23R respectively (Sanz & Moss, 1999). All three factors are required to form a complex with RPO for the transcription of intermediate genes. However, as RPO is required for all stages of transcription, VITF-3 also provides stage specificity, so that only intermediate genes are transcribed at this time (Sanz & Moss, 1999).

The final stage of the transcription cascade consists of the synthesis of late genes, a process initiated by products of intermediate transcription. DNA replication is also required, as late genes can only be transcribed from progeny, not parental DNA (Keck & Moss, 1990). Again, RPO is required, along with several newly synthesised trans-activating transcription factors: Vaccinia late transcription factor-1 (VLTF-1), VLTF-2, VLTF-3 and VLTF-X. VLTF-1, VLTF-2 and VLTF-3 are all viral genes, encoded by G8R, A1L and A2L respectively (Wright *et al.,* 1991; Wright & Coroneos, 1993; Hubbs & Wright, 1996). In comparison, the transcription factor originally designated as VLTF-X has now been shown to be a cellular heterodimer. Wright *et al.,* 2001 showed that VLTF-X activity co-purified with cellular single stranded nucleic acid binding proteins: Putative RNA-binding protein 3 (RBM3) and Heterogeneous ribonucleoprotein particle (hnRNP) A2/B1. These factors are initially expressed at approximately 4.5 hours post infection, then accumulate to a peak between 12 and 24 hours post infection (Wright *et al.,* 1991), forming a complex for late transcription with extensive protein-protein interactions (Dellis *et al.,* 2004). Once late transcription is initiated, the viral gene product G2R aids elongation, before interacting with the DNA dependent ATPase and DNA helicase A18 for transcription termination and mRNA release (Black and Condit, 1995; Condit *et al*., 1996). Many of the products of late genes are involved in early transcription and DNA replication, and are packaged into progeny virions for the immediate initiation of viral replication in new cells.

1.1.4.3 The formation of immature virion crescents and intracellular mature virions

The formation of the initial precursors through to mature virions occurs in viral factories very early on in infection, with the first membranes recorded at 3-3.5 hours post infection. This occurs almost immediately after DNA replication, as the majority of progeny DNA is produced between 2.5-3 hours post infection (Dales & Mosbach, 1968). The first stage of virion morphogenesis is the formation of membrane crescents which, despite displaying similarities to cellular membranes in terms of their structural and chemical make-up, are unique from any host membranes (Dales & Mosbach, 1968). The single lipid bilayer crescents surround electron-dense viroplasm filaments, in order to become spherical IVs containing a nucleoid (Morgan, 1976; Heuser, 2005). The successful association of viroplasm and membranes to become IVs is regulated by a highly conserved, seven-protein complex, consisting of core components A30 and G7, and F10, as well as A15, D2, D3 and J1. All seven proteins are required for the correct functioning of the complex, as the same phenotype is seen if any one of the proteins is repressed: no association between membranes and viroplasm (Szajner *et al.,* 2004). The curvature and rigidity of the membrane crescents, and subsequently the IV membrane, is regulated by the association of 65kDa structural protein trimer D13. D13 forms a honeycomb-like lattice of hexagons and pentagons on the convex surface of the membrane crescents, and the outside of IVs in order to maintain their shape (Heuser, 2005; Szajner *et al.,* 2005). As D13 itself doesn't display a transmembrane domain, it is able to stabilise the membrane via binding to the N-terminal of IV membrane protein A17 (Bisht, *et al.,* 2009).

Proteolytic cleavage of core proteins such as the processing of P4a and P4b to major IMV proteins 4a and 4b; and intramolecular disulphide bond formation occurs in the IV core in order to convert the IV through a series of brief transitional intermediate forms into the brick-shaped IMV (Szajner et al., 2004; Senkevich et al., 2002; Cepeda & Esteban, 2014). A range of virion core proteins are essential for this process, including A19 and A6, as loss of either factor arrests VACV morphogenesis at the IV stage, and prevents IMV formation (Meng *et al.,* 2007; Satheshkumar *et al.,* 2013). Other proteins, such as the scaffold protein D13 are no longer required once transition from IV to IMV begins. Proteolysis of A17 by viral protease I7 results in the disassembly of the D13 lattice, so that by the time IMV formation is completed, no D13 is detected on the IMV surface (Bisht, *et al.,* 2009). The

source of the IMV membrane is complex and highly debated. Analysis of purified IMVs has not shown any cellular membrane proteins, or evidence of signal peptides that would indicate trafficking through cellular secretory pathways. However, several IMV membrane proteins have been seen to localise by the rough endoplasmic reticulum (ER) and the ER-Golgi intermediate compartment, suggesting a role for these organelles in membrane formation (reviewed in depth in Moss, 2015). The number and exact structure of membranes enclosing IMVs was also controversial, and debated for decades, but it has now been conclusively shown that IMVs have only a single, 5nm thick lipid bilayer, covered by an 8nm thick protein coat, and have no continuity with cellular membranes (Hollinshead *et al.,* 1999; Heuser, 2005).

1.1.4.4 Intracellular and extracellular enveloped virions

IMVs are by far the most abundant form of VACV, and the vast majority remain as such in the cell until lysis occurs, when they are released for short-range dissemination. However, a small percentage

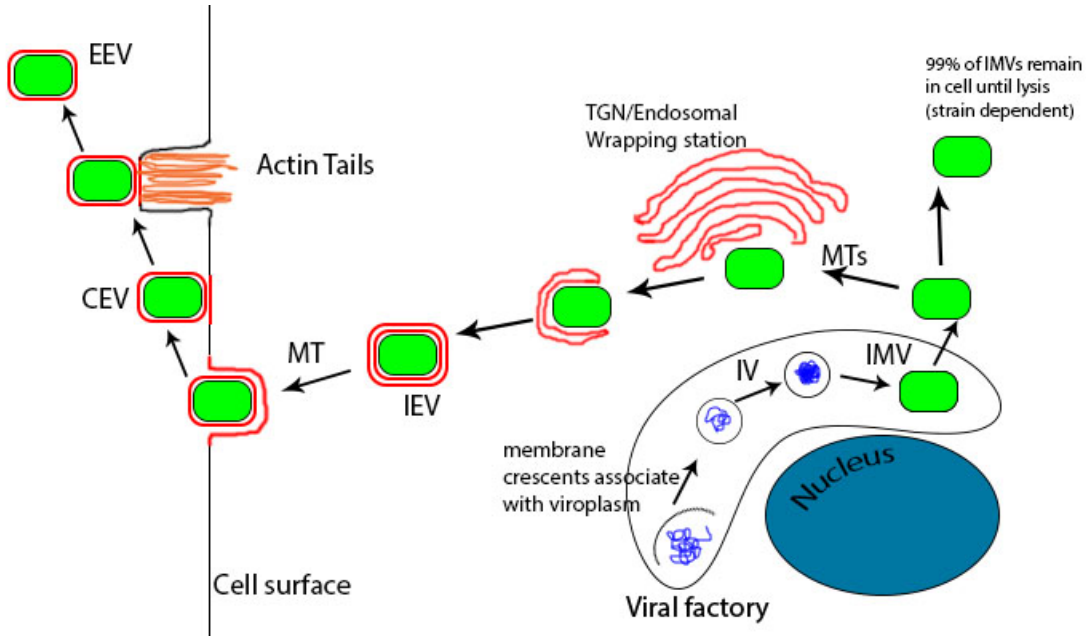

Figure 1.1 VACV replication and morphogenesis. Adapted from Smith *et al.*, 2002. Initial stages of replication occur in juxta-nuclear viral factories. Viral membranes initially form crescents, which surround electron-dense viroplasm to form immature virions (IVs). IVs are then formed into brick shaped intracellular mature virions (IMVs). IMVs leave the viral factory, and the majority of remain in the cell until lysis. A small percentage of IMVs are transported on microtubules (MTs) to a wrapping station thought to be located near the *trans*-Golgi network (TGN). Here they are wrapped in a double layer membrane to become intracellular enveloped virions (IEVs), then are transported on MTs to the cell surface. At the cell surface, the outer IEV membrane fuses with the plasma membrane to form cell-associated enveloped virions (CEVs) which are pushed away from the cell on actin tails. CEVs can also be released as extracellular enveloped virions (EEVs). Virions are coloured green here to represent an enhanced green fluorescent protein (EGFP)-tagged VACV strain, which allows fluorescence to be measured as a representative of viral growth.

of IMVs are wrapped in an extra double layer membrane to become IEVs, before being transported to the cell surface where they are released as CEVs and EEVs for long range dissemination (Appleyard *et al*, 1971; Payne, 1980). Microtubules are used to transport IMVs to the wrapping station, regulated by the viral A27 protein (Sanderson *et al.,* 2000), and once IEV formation is complete, microtubules are used again to transport the wrapped virions to the cell surface for release, this time mediated by the A36 and F12 IEV proteins (Herrero-Martinez *et al.,* 2005; Johnston *et al.,* 2009). The proportion of IMVs that become IEVs varies according to the strain of VACV in question. VACV-Western Reserve (WR) wraps only 1% of it progeny to become IEVs, while infection with the International Health Department-J (IHD-J) strain results in 25-30% IEVs, and elongated plaques known as 'comets', due to the high levels of EEV release (Payne, 1980).

Much like the IMV membrane, the source of the IEV membrane has been a topic of much debate. Cases have been made for both the intermediate compartment, between the endoplasmic reticulum (ER) and the Golgi network (Sodeik *et al.,* 1993; Van Eijl *et al.,* 2002) and the Golgi and *trans*-Golgi network (TGN) (Ichihashi *et al.,* 1971; Hiller & Weber, 1985; Schmelz *et al.,* 1994) as the origin of the extra IEV double membrane. However, it has more recently been shown that IEV membranes can be labelled with fluid phase marker horseradish peroxidase (HRP), indicating an endosomal origin (Van Eijl *et al.,* 2002). None of these hypotheses have yet been conclusively proved, and the wide range in opinions most likely stems from highly increased traffic through the ER, Golgi and TGN during VACV infection, making pinpointing a specific origin extremely difficult (Van Eijl *et al.,* 2002). As EEVs are responsible for long distance dissemination, and are essential for a fully infectious virus, the production of IEVs and EEVs is an attractive target for pharmaceutical intervention. One of the earliest anti-VACV drugs to target this stage of the infection cycle was N1-isonicotinoyl-N2-3-methyl-4-chlorobenzoylhydrazine (IMCBH). Treatment of cells with this compound inhibits EEV double membrane formation, without affecting the IMV stage, and helped to prove the existence of the IEV double membrane (Payne & Kristenson, 1979). Although IMCBH is a useful method of inhibiting IEV production *in vitro*, further research has shown that it is ineffective both *in vivo* and against other poxviruses, ruling it out as a viable anti-poxvirus drug for anything but laboratory use (Payne & Kristenson, 1979; Schmutz *et al.,* 1991). A more recently characterised anti-poxvirus drug, 4-trifluoromethyl-N-(3,3a,4,4a,5,5a,6,6a-octahydro-1,3-di oxo-4,6-ethenocycloprop

[f]isoindol-2(1 H)-yl)-benzamide (ST-246), was first discovered during a high-throughput screening for small molecule compounds with anti-VACV activity (Yang *et al.,* 2005). Again, this drug does not affect IMV production but is able to significantly inhibit viral spread and multi-cycle growth by targeting the IEV/EEV membrane protein F13 in order to prevent wrapping. However, as it targets a key viral protein, ST-246 is susceptible to survival mutations and resistance to the drug can occur (Yang *et al.,* 2005; Duraffour *et al.,* 2015)

The presence of an additional stage in the poxvirus life cycle was initially observed as an antigenic difference between intracellular and extracellular virus from lysed cells infected with rabbitpox, and

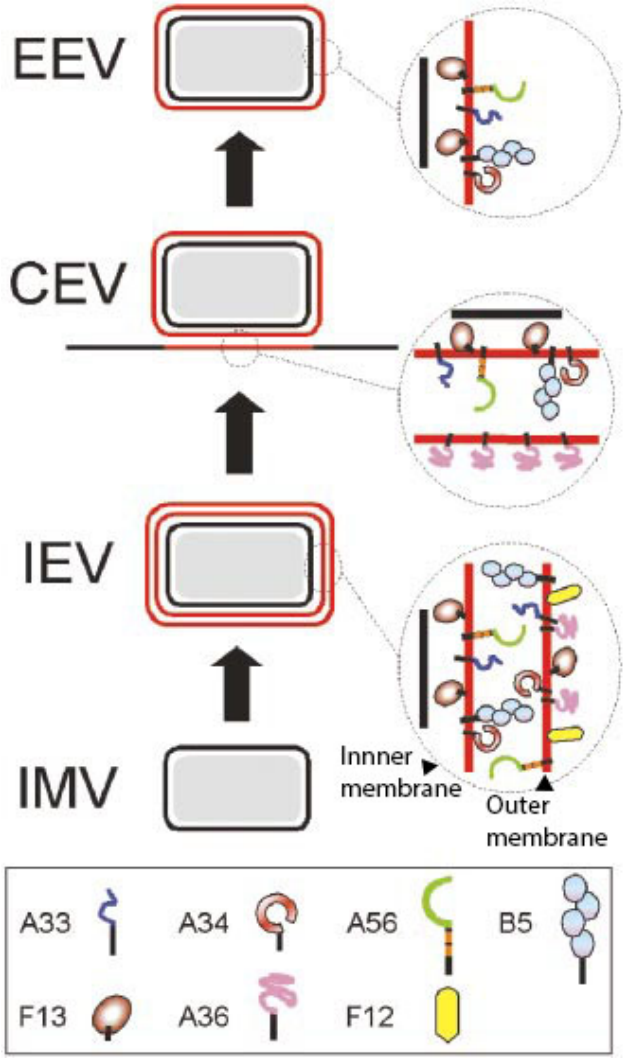

Figure 1.2 Location of VACV IEV/EEV membrane proteins. Taken from Smith *et al.,*2002.IEV and EEV membrane proteins are shown, along with their orientation. Of the seven proteins associated with the IEV membrane, not all are localised to both layers of the double membrane. A36 and F12 are present on the outer membrane of the IEV, and are not seen on EEVs or CEVs. B5, A56, A34 and A33 face outwards on the EEV/CEV membrane, while F13 faces inwards between the membrane and capsid.

further investigation using electron microscopy also showed a morphological difference with the presence of an extra membrane wrapping the extracellular virions (Appleyard *et al.,* 1971). Further investigation by Payne, (1980) demonstrated that immunisation with whole IMV or whole EEV conferred protection against both intra- and extracellular virus, while immunisation with purified EEV envelopes alone only protected against EEV, not IMV. This confirmed not only that an antigenic difference in IMV and EEV membranes is conserved in VACV, but also that the EEV membrane contains of a number of proteins that are not seen in the IMV. To date, a total of seven proteins have been identified as being specific components of the IEV and/or EEV: A33 (Roper *et al.,* 1996), A34 (Duncan & Smith, 1992), A36 (Parkinson & Smith, 1994), A56 (Payne & Norrby, 1976), B5 (Engelstad *et al.,* 1992), F12 (Zhang *et al.,* 2000), and F13 (Hirt *et al.,* 1986). The functions and structures of these proteins will be discussed in the following sections

B5

One of the most studied IEV/EEV proteins, B5 is a 45kDa, glycosylated protein transcribed from a late promoter, that also has some early activity, as production reaches a peak at 6-7 hours post infection (hpi), but is also seen in low level amounts early on in infection (Engelstad *et al.,* 1992). B5 deletion mutants exhibit a very strong EEV inhibition phenotype of tiny plaques and loss of comet formation, due to a 90% reduction in EEV levels, almost completely inhibited IMV wrapping, and lack of IEV migration within the cell. IMV production is unaffected. (Engelstad & Smtih, 1993; Wolffe *et al.,* 1993).

B5 has a complex structure, including four short consensus repeats (SCRs) in its extracellular domain, which play key parts in its EEV release activity. All four SCRs are required to ensure that B5 is correctly formed, and the deletion of any one SCR results in a loss of intracellular actin tail formation which ultimately leads to a small plaque phenotype (Mathew *et al.,* 1998). Wrapping of IMVs to form EEVs, and IEV transport within the cell were not affected by SCR loss, which indicated that that other areas of the B5 protein were required for overall IEV/EEV production, and the 90% reduction in EEV levels seen in the B5 negative mutants described above (Herrera *et al.,* 1998; Engelstad & Smith, 1993). The transmembrane domain has been implicated in the signalling required for ER to Golgi transport, while the cytoplasmic tail has been suggested to control the speed and timing of this

movement, as well as the accumulation of the protein in the Golgi before wrapping occurs (Ward & Moss, 2000; Mathew *et al.,* 2001). The cytoplasmic tail is also required for the transport of B5 (and therefore the IEV) from the Golgi to the plasma membrane after wrapping has occurred, as deletion of the cytoplasmic tail reduces B5 expression on the cell surface (Mathew *et al.,* 2001). B5 is one of the few VACV IEV proteins that is able to maintain its standard distribution pattern in the cell even when expressed alone, in the absence of virions and other IEV proteins (Lorenzo *et al.,* 2000). Intense juxtanulcear staining, around the Golgi region is seen in both full infections and when B5 is expressed alone. Only the punctate peripheral staining indicating the presence of IEVs are not seen. This indicates that the targeting of the B5 to the Golgi is down to its own cytoplasmic and transmembrane domains and is not dependent on any other IEV protein, despite associations with A33 and A34 described below (Katz *et al.,* 1997; Lorenzo *et al.,* 2000).

A33

The 25kDa A33R gene product is classed as a type II membrane protein, and is localised in the outer envelope of the IEV, as well as the Golgi complex and its surrounding area, and the plasma membrane (Roper *et al.,* 1996; Lorenzo *et al.,* 2000). Loss of A33 results in a small plaque phenotype usually characteristic of inefficient or reduced EEV production. However, these plaques exhibit a comet-like shape, usually seen in the replication of IHD-J. Comets are seen in IHD-J plaques due to the high EEV levels seen in this strain, suggesting an increase in EEV in A33 null mutants (Roper *et al.,* 1998). Despite this increase, fully wrapped IEVs are almost completely absent inside the cells, and the only evidence of IEV production is in partially wrapped IEVs, suggesting that the EEVs released by A33 mutant virus are not fully formed (Roper *et al.,* 1998). Indeed, only 1 in 12.9 EEV genomes created by A33 mutant viruses are able to form a plaque, compared to 1 in 1.6 genomes in a GFP-labelled wild type (WT) virus, confirming a severe loss of infectivity caused by A33 deletion (Chan & Ward, 2010). In addition, actin tails that would usually push CEVs away from the host cell, for cell-to-cell spread, are not seen in A33 mutant viruses, indicating that A33 is required for actin microvilli production, though this lack of actin tail formation may be linked to the loss of fully wrapped IEVs (Roper *et al.,* 1998).

A33 also directly interacts with several other envelope proteins: A34, A36 and B5. A33 and A36 interact via their cytoplasmic domains, and the deletion of either interaction site results in both less A36 localising to IEVs, suggesting that A33 plays a role in A36 recruitment (Ward *et al.,* 2003). A33 may play a large role as a recruiter of other IEV proteins, as neither B5 nor A34 are correctly glycosylated or targeted into IEVs in the absence of A33, though B5 is still targeted to the general Golgi area (Lorenzo *et al.,* 2000; Perdiguero & Blasco, 2006; Breiman *et al.,* 2013).

A34

Like A33, A34 is another type II integral membrane protein, and is encoded by the 23kDa A34R gene at late stages of infection (Duncan & Smtih 1992). Infection with A34 deletion viruses show a similar phenotype to A33 mutants in that they can only form small plaques, despite an increase in EEV presence. This combination of seemingly contrasting phenotypes shows that A34 is involved not in IEV production, but in EEV infectivity (McIntosh & Smith, 1996). Membrane disruption of the EEVs formed during an A34 mutant infection results in normal, fully infectious IMVs, and confirms that the EEVs do not express a fully competent outer membrane. This is most likely due to the role that A34 plays in regulating the direct recruitment of A36, B5 and the indirect recruitment of A33, into the enveloped virions (McIntosh & Smith, 1996; Perdiguero *et al.,* 2008). A34 is also involved in the production of actin-containing microvilli required for cell-to-cell spread of CEVs, as infection with A34 mutant virus results in a loss of actin tail formation and thickened, inefficient microvilli (Wolffe *et al.,* 1997). A34 is particularly key in VACV infection, as a single point mutation changing its Lysine to Glutamine at position 151 has been linked to the difference in EEV release seen in VACV-WR and VACV-IHD-J strains. This is most likely due to the role of A34 in actin tail formation, as VACV-WR exhibits more EVs retained at the cell surface than IHD-J (Blasco *et al.,* 1993).

A34 typically exhibits a similar distribution pattern to A33, in that it can be visualised in a juxtanuclear, larger-than-Golgi area, and small membrane structures in the cell periphery, potentially due to the strong associations between the two proteins. However, when expressed alone, without the intact virion or other IEV proteins, A33 exhibits similar staining to a full infection just with less intense labelling, while A34 is retained close to the nucleus in an area that does not correspond with

Golgi staining (Lorenzo *et al.,* 2000), confirming that A34 is more reliant on other EV proteins for correct targeting than A33 (Perdiguero & Blasco, 2006;)

A36

The third protein required for IEV production is the 45kDa A36R gene product, which exhibits type 1b topology, and is integral to the IEV membrane via attachment at the N-terminal (Parkinson & Smith, 1994; Van Eijl *et al.,* 2000). Like the previously described proteins, loss of A36 results in the classic small plaque phenotype with an absence of actin tails. However, unlike the majority of the EV proteins, A36 is found only on the outer of the IEV double membranes and is not seen on EEVs. (Parkinson & Smith, 1994; Van Eijl *et al.,* 2000). The presence of A36 is only required on IEV outer membranes as it is responsible for interacting with the actin cytoskeleton. Specifically, A36 phosphorylates tyrosine residues at positions 112 and 132, and inducing actin nucleation for the formation of actin tails and EEV release. Therefore, A36 remains at the cell surface during IEV egress, present only directly underneath tethered CEVs, in order to create actin tails. If A36 undergoes a mutation at the specific tyrosine 112 and 132 residues, EEV production is reduced as virions remain attached to the plasma membrane due to tight, viral protein-protein interactions (Van Eijl *et al.,* 2000; Horsington *et al.,* 2013). A36 is also involved in the transport of IEVs to the cell surface, although it does not directly interact with kinesin as IEVs with an A36 deletion mutation are still able to move on microtubules. However, movement of these mutated virions is slower, with shorter periods of uninterrupted movement, and they are far more dispersed within the cell than the wild type IEVs (Herrero Martinez *et al.,* 2005; Johnston *et al.,* 2009).

F12

The most recently characterised EV protein is the 65kDa, late gene product F12 which, like A36, is only found on the outer IEV membrane and is not seen to be associated with EEVs (Van Eijl et al., 2002). As with A36 protein, F12 is required for the production of normal-sized plaques. (Zhang et al., 2000), indicating that like A36, F12 is key for the production of actin tails. However, while A36 is an integral membrane protein, F12 is only membrane associated and has no transmembrane domain, and so is easily left behind when the IEV is released from the cell (Van Eijl et al., 2002; Johnston et al.,

2009). F12 interacts with the IEV membrane via binding with A36 using motifs at amino acid residues 351-458 and 91-111. As this interaction with A36 is the only way that F12 associates with the IEV, it is essential for the prevention of the small plaque phenotype and actin tail production (Zhang et al., 2000; Johnston et al., 2009). Actin tail formation is highly dependent on F12 as this protein is responsible for the movement of IEVs on microtubules (MT). F12 shares a structural similarity to kinesin light chains (KLCs), a key part of the microtubule transport machinery which form a bridge between kinesin heavy chains and cargo, in this case IEVs, to allow movement along MTs (Morgan et al., 2010). The F12 motifs required for interaction with A36 overlap the tetracopeptide-like repeats that confer the KLC similarity, and both A36 and F12 are essential for MT movement (Johnston et al., 2009; Morgan et al., 2010).

F12 also shares similarities in action with B5, both are transported to the cell periphery even after IEV formation is arrested and IMVs are retained in the viral factories. Once at the periphery, they are seen to colocalise in endosomes labelled with fluid phase marker horseradish peroxidase (HRP) (Van Eijl *et al.,* 2002).

F13

The unglycosylated, palmitoylated F13, which was previously known as p37 due to its molecular weight is the most abundant protein in the EEV membrane, composing 5-7% of the total EEV protein levels (Hirt *et al.,* 1986; Hiller *et al.,* 1981). Once again, F13 loss results in a small plaque phenotype (Vliegen *et al.,* 2012). F13 is a late protein, and is not produced until 6 hpi. Soon after synthesis, it associates with the cytosolic face of the TGN in transitional vesicles before becoming incorporated into the IEV membranes (Hiller & Weber, 1985; Schmutz *et al.,* 1995; Baek *et al.,* 1997). Once integrated into virion, F13 is located on the inner side of the IEV membrane, as well as between the membrane and the IMV. Consequently, F13 is found on the cytosolic rather than the extracellular side of the plasma membrane after EEV exit (Schmutz *et al.,* 1995).

While the other five IEV proteins are glycosylated, F13 is palmitoylated to allow association with the IEV membrane (Husain & Moss, 2003). Although unique in this manner, F13 also shares several similarities with B5, with which it has been seen to associate (Payne, 1992; Husain & Moss, 2002).

For example, like B5, F13 is still correctly targeted to the Golgi area when expressed in the absence of virions and other IEV proteins (Lorenzo *et al.,* 2000). Another unique feature of F13 is its phospholipase activity. F13 contains a partially conserved sequence between amino acid residues 313 and 329 known as the (H)KD domain, which is essential for phospholipase action and is shared with lipases such as phospholipase D (PLD) (Sung *et al.,* 1997*;* Baek *et al.,* 1997). Though F13 doesn't express the conserved histidine in this motif, it is still able to exert PLD-like enzymatic activity and produce lipids such as diaglycerol, choline phosphate and lysophosphatidylcholine (Baek *et al.,* 1997; Husain & Moss, 2002). Both A36 and B5 are able to interact with PLD, and inhibition of phospholipase activity with butanol-1, or mutation of the (H)KD domain results in accumulation of F13 in the Golgi, and prevention of normal plaque and comet formation, indicating that the HKD-like domain is essential for F13 function (Sung *et al.,* 1997; Husain & Moss, 2002). Vesicle budding from the Golgi membrane requires the presence of human PLD, so it may be that it is the presence of F13 in IEVs at the TGN that triggers the trafficking of IEVs to the surface (Sung *et al.,* 1997).

A56

Originally identified as the VACV haemaglutinin due to its irreversible interactions with red blood cells, A56 was the first protein to be classified as an IEV protein (Payne & Norrby, 1976). Unlike the other 5 IEV proteins however, A56 is the only one that plays no direct role in EEV and CEV release and dissemination. Instead, it complexes with another viral protein, K2 and is expressed on the cell surface in order to prevent superinfection (Wagenaar & Moss, 2009). The A56/K2 complex binds to the entry/fusion complex (EFC), on the approaching virion, thereby preventing it from interacting with the cellular glycosaminoglyans that would otherwise allow entry. The repellent action of the A56/K2 complex is such that if transfected and expressed on the surface of an uninfected cell, it can prevent initial infection with VACV (Wagenaar & Moss, 2009).

In another EEV independent role, A56 is also thought to exhibit complement regulation activity, through interaction with the viral complement control protein (VCP). VCP is essential for an *in vivo* infection, and requires interaction with A56 via disulphide bond formation at the A56 N-terminal for its expression at the cell surface, where it is able to interfere with the complement immune cascade at several different stages (DeHaven *et al.,* 2010).

1.1.4.5 Release

As VACV exhibits two different infectious forms, IMV and IEV, with different structures and membrane antigens, it follows that there is more than one method of cell egress seen in VACV infection. Although they are the most abundant form of viral progeny, IMV release is a poorly researched area of VACV exit. The vast majority of IMVs accumulate in the cell and are not released until lysis occurs, for short range dissemination. However, while EEVs and CEVs are predominantly released during earlier stages of infection (Tsutsui, 1983), several studies have suggested that IMV release, via budding, is the most common form of viral release in the later stages of infection (Tsutsui, 1983; Ulaeto *et al.,* 1996; Meiser *et al.,* 2003). These studies suggested that IEV production plateaus relatively early in infection, and the majority of IMVs are formed after this point (Ulaeto *et al.,* 1996). As IMV synthesis increases, the unwrapped virions accumulate in the cell periphery, and cytoplasmic packets are formed on the plasma membrane. Filaments extend from these packets, and release IMVs from their ends (Tsutsui, 1983). However, IMVs never directly fuse with the plasma membrane on exit as EEVs do. Instead, it is suggested that the unwrapped mature virions make use of B5 remaining on the cell surface from EEV release for their own egress (Tsutsui, 1983; Meiser *et al.,* 2003). However, since these studies were performed, there has no further evidence to support this theory.

Little is known about IMV budding in comparison to the most well-characterised form of virion exit – the actin-based motility and fusion of EEVs and CEVs. CEVs are involved in direct, cell-cell transmission, while EEVs are required to spread through the extracellular matrix, and the bloodstream *in vivo,* for more long-range spread. The proportions of EV released as CEV compared to EEV differs according to the infecting viral strain. VACV-WR for example, retains a higher percentage of virions attached to the plasma membrane as CEVs compared to VACV IHD-J which exhibits less actin tails and more EEVs, creating the characteristic "comet" shaped plaque formation (Blasco & Moss, 1992). This is most likely due to the IHD-J single point mutation in the actin-tail forming A34 protein, as mentioned previously (Blasco *et al.,* 1993).

The first step in the formation of the actin tails that push CEVs towards adjacent cells is the disruption of actin stress fibres by VACV infection. Cortical actin is instead formed into intracellular microvilli, each of which measure between 6.4 -9.6μm long and exhibits an IEV associating with the

tip (Cudmore *et al.,* 1995). Formation of the actin tails requires a complex signalling pathway which includes not only IEV proteins such as A34 and A36, but also the involvement of cellular factors. Phosphorylation of A36 recruits actin nucleation factors such as Nck, WASP, Grb2 and the Arp2/3 complex to the virion in order to begin actin tail formation from G-actin (Cudmore *et al.,* 1996; Scaplehorn *et al.,* 2002). The microfilament extends in a tapering shape by addition of actin monomers to free ends in the vicinity of the virion, as nucleation is stimulated only by the association with the CEV (Cudmore *et al.,* 1996). Eventually, the CEV inside the filament fuses with the plasma membrane at the tip of the tail, and emerges for insertion into another cell (Payne & Kristensson, 1979). EEV release also occurs through fusion of its outer membrane with the plasma membrane, although this is rarely seen in progress and so is thought to occur rapidly (Payne & Kristenson, 1979).

The rate at which a virus spreads can be predicted by its replication kinetics. However, even taking into account the ability of EEVs to promote long range spread, it has been shown that VACV is able to infect new, distant cells at a rate four-fold higher than expected. (Doceul *et al.* 2010). This is due to a phenomenon known as 'trampolining'. Should a virion come into contact with a cell that is already infected, it would be pointless for the virus to attempt to enter. Invading virions are alerted to an already-established VACV infection in a cell by the presence of the A56/K2 complex on the cell surface, which, as discussed earlier prevents further entry (Wagenaar & Moss, 2009). However, this complex binds the EFC, which is found on the IMV surface and is therefore not exposed on EEVs/CEVs, indicating that another method for the prevention of super-infection must exist. While the IEV/EEV proteins A33 and A36 are responsible for the production of actin tails to expel progeny enveloped virions from the cell before lysis (Roper *et al.,* 1998; Horsington *et al.,* 2013), Doceul *et al.,* showed in their 2010 study that these proteins can also induce the formation of actin tails under superinfecting virions, in order to push them away to uninfected cells, therefore accelerating viral spread.

1.2. MKK3

A 2014 high throughput screen (Beard *et al.)* identified a component of the p38 mitogen activated protein (MAP) kinase pathway as a pro-viral factor in a successful VACV infection. This cellular protein, MAP kinase kinase 3 (MKK3) is involved in activation of the p38 pathway, in order to subsequently activate various cellular processes. This activation, along with the other MAP kinase pathways, will be discussed in the following sections.

1.2.1. Mitogen activated protein kinases

All cells must be able to adapt to changes in their environment. Extracellular stimuli, such as UV radiation, osmotic stress, and toxins all demand a response from the cell, ranging from apoptosis to conformational changes that allow survival. These responses are mediated by a number of complex, overlapping kinase pathways which culminate in the activation of transcription factors by MAPKs, and the subsequent expression of stimuli-appropriate genes. MAPKs are the terminal components of what is usually a 3-kinase cascade, and are activated by dual phosphorylation of a Thr-Xaa-Tyr motif, by upstream MAPK kinases. (Jonak & Hirt, 1994). These MAPK Kinases (MAPKK/MAP2Ks) are in turn activated by dual phosphorylation of Ser and Thr residues in a similar activation loop by MAPK kinase kinases (MAPKKK/MAP3Ks). There are four known MAPK cascade families: the extracellular signal regulated protein kinases (ERK1), the c-Jun NH2 terminal kinases (JNK) family, the p38 isoforms, and the ERK5/Big MAPK 1 (BMK1) cascade (Raman & Cobb, 2003; Wang & Tournier, 2006). Although each family contains at least two very specific MAP2Ks, and three more promiscuous, often inter-family MAP3Ks, certain stimuli result in the activation of extremely specific regulatory responses and genes, due to the presence of several controlling mechanisms, such as scaffold proteins, crosstalk with other signalling pathways and differential use of MAP2K and MAP3Ks (Raman & Cobb, 2003; Shaul & Seger, 2006).

1.2.1.1 ERK1/ERK2

The first MAPK cascade to be characterised was the ERK pathway. Initially thought to be triggered by growth factor signalling, further investigation showed it to be involved in a wide range of cellular processes, including cell proliferation, differentiation, survival and apoptosis (Seger & Krebs, 1995;

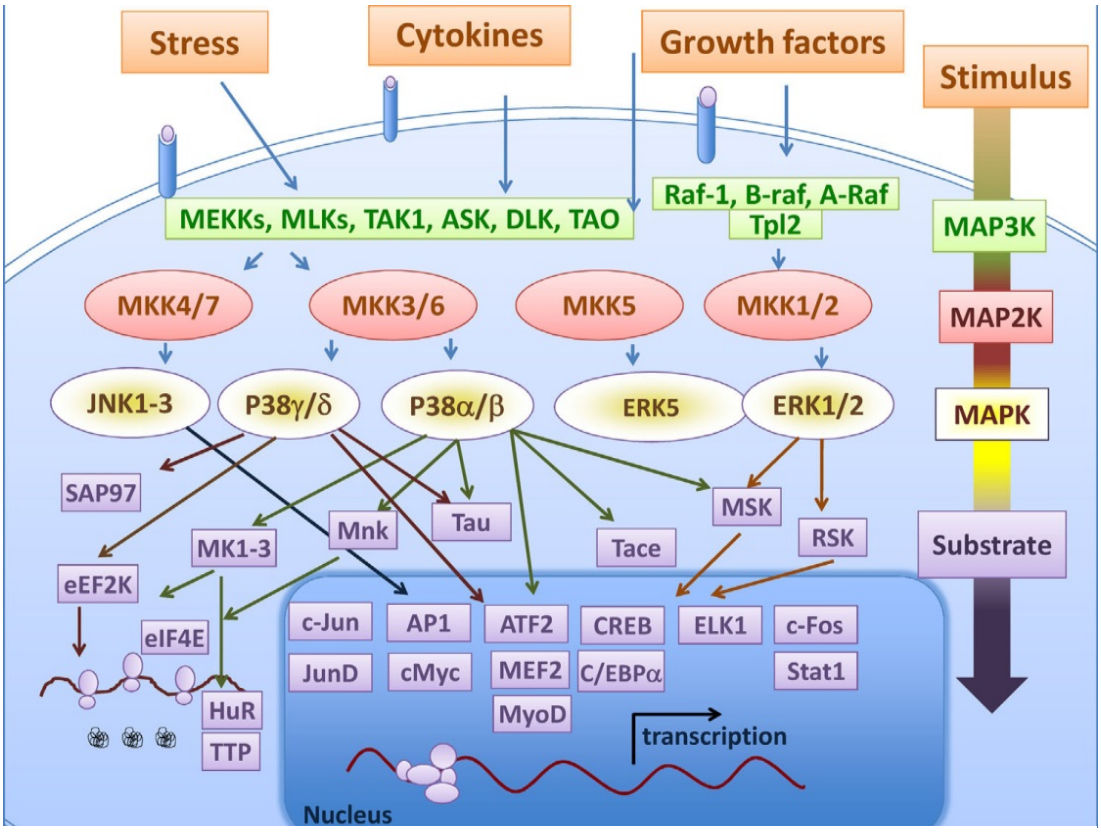

Figure 1.3 MAPK signalling cascades. Taken from Sabio & Davis, 2014**.** MAP kinase pathways consist of three core components, initiated by a signal from an external stimulus. A MAP3K activates a MAP2K by dual phosphorylation which then activates a MAPK by the same method. There are four classical families of mammalian MAP kinases. The core ERK pathway is initiated by MAP3Ks, RAFs, and Tpl2.. These kinases activate MKK1 and MKK2, which in turn phosphorylate ERK1 and ERK2 for the activations of multiple subtrates The p38 and JNK pathways share several promiscuous MAP3Ks, including MEKKs, MLKs and TAK1. In the p38 pathway, these MAP3Ks activate MKK3 and MKK6, which in turn activate the 4 isoforms of p38. In the JNK pathway, these MAP3Ks activate the MAP2Ks MKK4 and MKK7, followed by activation of JNK1-3.. Finally, the core ERK5 pathway is initiated by the MAP3Ks MEKK2 and MEKK3, which phosphorylate MKK5, which in turn activates ERK5. All the pathways then go on to activate multiple transcription and translation factors.

Shaul & Seger, 2006). The ERK cascade consists of 3 core levels – MAPK, MAP2K and MAP3K - but can extend to further tiers, including MAP4Ks and MAPK-activated protein kinase (MAPKAPK) (Shaul & Seger, 2006). In the ERK cascade, growth factors activate GTP- binding protein Ras, which in turn activates MAP3Ks, including the protein kinase rapidly accelerated fibrosarcoma (RAF). RAF then activates mitogen-activated protein/ERK kinase kinase 1 (MEK1) by dual phosphorylation of Ser217 and Ser221, which is then ready to phosphorylate the next tier of the cascade (Alessi *et al*, 1994). The MEKs, the MAP2Ks of the ERK cascade, are extremely specific to ERK1 and 2, and activate their substrates by dual phosphorylation at Thr188 and Tyr190 (Seger *et al.,* 1992). At the final stage in the cascade, ERK1 and 2 phosphorylate their substrates at a Pro-Xaa-Ser/Thr-Pro motif, where Xaa is any neutral or basic amino acid (Gonzalez *et al.,* 1991).

1.2.1.2 JNK

The MAPK JNK is present in three isoforms in mammals; JNK1 and JNK2 are ubiquitous throughout the body, while JNK3 is found only in the brain, heart and testes. The most well studied substrates of JNK are the transcription factor component and proto-oncogene c-Jun, and activating transcription factor 2(ATF2) (Davies, 2000; Vlahopoulos & Zoumpourlis, 2004). Although JNK is not essential for cell growth and proliferation, one of its key roles is the mediation of stress-induced apoptosis, most notably due to cytokine induced reactive oxygen species (ROS). Cytokines such as interleukin (IL)-1 and tumour necrosis factor (TNF)-α induce ROS, which activate the JNK cascade, resulting in the expression of c-Jun. TNF-family proteins can also differentially activate the JNK pathway in order to induce further cytokine response, via TNF-receptor associated factor (TRAF) signalling. (Lo *et al.,* 1994; Davies, 2000; Vlahopolous & Zoumpourlis, 2004). The JNK pathway contains a number of MAP3Ks, including MEKK 1-4, and mixed lineage protein (MLK)1-3, though it is not yet fully understood which are relevant to which stimuli. At the second tier of the cascade, there are only two MAP2Ks that can activate JNK: MKK4 and MKK7, though several isoforms of these kinases exist for specific stimulation. Both kinases activate JNK by dual phosphorylation on Thr180 and Tyr182 and are required for full and optimal JNK activation, though MKK4 preferentially activates Tyr, and MKK7 is preferential to the Thr residue (Davies, 2000; Tournier *et al.,* 2001). This preference of the MAP2Ks for different activating residues shows another mechanism of maintaining specificity in the signalling cascade, particularly since MKK4 and MKK7 are non-redundant, and are activated by different external stimuli (Tournier *et al.,* 1999). For example, MKK4 activation by MEKK1 is essential for JNK response to heatshock and treatment with protein synthesis inhibitor anisomycin. Both MKK4 and MKK7 are required for optimal activation during UV radiation-induced stress; and only MKK7 is required for the cascade to respond to TNF-α and IL-1 stimulus (Yang *et al.,* 1997; Tournier *et al.,* 2001).

1.2.1.3 ERK5/BMK1

Of the MAPK cascades, the ERK5/BMK1 pathway is the least well characterised. ERK5 was originally identified along with its specific MAP2K, MEK5, and is found in a wide range of mammalian tissues, particularly the heart and skeletal muscle (Zhou *et al.,* 1995). ERK5 is heavily

involved in cardiovascular development, as well as cell proliferation, neuronal cell survival and tumour malignancy (Wang & Tournier, 2006). MEK5 is currently the only known activator of ERK5, phosphorylating the MAPK at Tyr221 and Thr219. However, several MAP3Ks are known to activate MEK5, including MEKK1, MEKK2 and MEKK3 (Mody *et al.,* 2003; Wang & Tournier, 2006). In addition to its role in the ERK5 cascade, MEKK1 is also a key activator in the JNK1 cascade, while JNK MAP3K MLK-3 is also involved in the p38 pathway, demonstrating the promiscuity of MAP3Ks. (Enslen *et al.,* 1998; Davies, 2000).

1.2.2. MKK3 and the p38 pathway

p38, the fourth MAPK pathway was first identified through the activation and phosphorylation of a 38kDa MAPK in response to lipopolysaccharide (LPS) stimulation, and was determined to be unique to other MAPK families by specific amino acid sequences surrounding the phosphorylation sites (Han *et al.,* 1993; Han *et al.,* 1994). The p38 cascade can be activated by a range of stimuli, including UV radiation, heat shock, osmotic shock, growth factors, and certain families of cytokines. These stimuli activate small Rho GTPases, which in turn phosphorylate the non-specific MAP3Ks of the cascade, including MLK1 and MEKK1(Raingeaud *et al.,*1996; Zarubin & Han, 2005). In comparison, the second tier of the cascade is far more specific, and the two major MAP2Ks, MKK3 and MKK6 activate only p38. However, a third p38 activating MAP2K, MKK4 is also involved in activating the JNK pathway (Derijard *et al.,* 1995; Han *et al.,* 1996; Moriguchi *et al.,* 1996; Raingeaud *et al.,*1996). Once phosphorylated and activated by MAP2Ks, p38 activates its own substrates, including heat shock protein 27, transcription factor ATF1, and the first discovered MAPK substrate, MAPK-activated protein kinase (MAPKAPK). Activation of p38 has been linked to a wide range of biological processes, such as inflammation, particularly in autoimmune diseases, apoptosis, cell cycle progression, tumour suppression and cell differentiation (Rouse *et al.,* 1994; Zarubin & Han, 2005). The activators and roles of p38 are extremely diverse, and dependent on a variety of conditions, such as the nature of the stimuli and cell type. For example, in foetal neurons, p38 activity is inhibited by up to 90% by insulin treatment, whereas insulin significantly stimulates p38-dependent glucose transport in adipocytes (Heidenreich & Kummer, 1996; Sweeney *et al.,* 1999).

There are four p38 isoforms: p38α, p38β, p38γ and p38δ. All isoforms are activated in the same manner, instigated by a similar range of stimuli, but their localisation and response to activation varies (Raingeaud *et al.,*1996; Jiang *et al.,* 1997). For example, although p38α, p38β and p38δ are all able to successfully activate ATF2, the β isoform shows most activity towards the transcription factor, and p38δ the least. In comparison p38γ doesn't activate ATF2 at all, but is able to activate a unique 7kDa skeletal muscle protein that the other isoforms cannot (Jiang *et al.,*1996; Li *et al.,* 1996; Jiang *et al.,* 1997). The isoforms are also differently regulated by MAP2Ks. MKK6 is able to interact with, and activate all isoforms; MKK3 phosphorylates p38α, p38γ and p38δ, and MKK4, which is not a strong p38 activator, interacts with p38α, and weakly with p38δ and p38γ (Enslen *et al.,*1998; Enslen *et al.,* 2000). Despite this differential regulation, MKK3 and MKK6 exhibit extremely similar *in vivo* knockout phenotypes, and loss of one of the two MAP2Ks does not entirely inhibit p38 phosphorylation. This, along with their ability to selectively activate p38 indicates a level of redundancy between the two proteins, and suggests that they are able to compensate for each other to a certain extent (Raingeaud *et al.,* 1996; Brancho *at al.,* 2003; Ma *et al.,*2007).

All p38 isoforms are activated in the same manner by MAP2Ks, through dual phosphorylation of Thr180 and Tyr182 in the p38 activation loop (Raingeaud *et al.,* 1994; Enslen *et al.,* 2000). Before this can occur however, the MAP2K must bind to the MAPK at a docking site, which contains hydrophobic residues in an ØA-Xaa-ØB motif, where ØA and ØB represent any combination of Leu, Ile or Val, and Xaa is any amino acid (Chang *et al.,* 2002; Weston *et al.,* 2003). This docking site is also the same domain to which MAPK substrates bind. The MAPK docking domain interacts with a docking groove in the C-terminal of the MAP2K or MAPK substrate, causing a conformational change in the proteins, which allows phosphorylation and therefore activation to occur. It is thought that different MAP2Ks cause differing conformational changes in p38, thereby inserting another level of specificity (Chang *et al.,* 2002; Weston *et al.,* 2003).

1.2.3. p38 in infection and inflammation

One of the key roles of the p38 pathway is its involvement in inflammation during infection. Differential activation of p38 by MKK3 or MKK6 gives rise to the production of different cytokines and other inflammatory effects. Both TNF-α and transforming growth factor (TGF)-β, two essential

inflammatory mediators, activate varying p38 isoforms via MKK3, giving MKK3 a critical role in downstream cytokine production. (Wysk *et al.,*1999; Wang *et al.* 2002). Loss of MKK3 expression results in a significant reduction in not only TNF-α induced cytokines such as IL-1 and IL-6, but also a wide range of other cytokines, including IL-5, IL-12(p70), IL-17, eotaxin and granulocyte/macrophage colony stimulating factor (GM-CSF), a reduction that is seen both intra- and extracellularly (Wysk *et al.,* 1999; Srivastava *et al.,* 2015). Type 1 interferons, such as IFN-α are able to activate downstream p38 by rapidly engaging both MKK3 and MKK6 after IFN receptor binding. The expression of interferon stimulated genes (ISGs) are then directly influenced by p38, as the MAPK phosphorylates the ISG mediator, signal transducer and activator of transcription (STAT1). Consequently, MKK3, MKK6 and p38 are required for inducing innate inflammation, and cytokine storms (Li *et al.,* 2005; Börgeling *et al.,* 2014). Conversely, p38 can also be involved in the anti-inflammatory response, as it is required for the expression of the anti-inflammatory cytokine IL-10, which inhibits IL-6 and TNF-α, thereby causing p38 to regulate its own activity (Hammaker *et al.,* 2014).

The pathogenesis of several diseases has been linked to the p38 pathway, including influenza A. During influenza A infection, p38 is thought to be responsible, either partially or fully, for the expression of 94% of virus-induced genes, and demonstrates a role the adaptive immune response in addition to the innate immune response. Activation of p38 in T-cells not only increases IFN-γ expression in $CD4^+$ and $CD8^+$ T-cells, but also selectively targets $CD8^+$ cells for apoptosis during influenza infection (Conze *et al.,* 2000; Börgeling *et al.,* 2014). As this is a counterintuitive measure during infection, a protective environment is produced in the lungs in which IL-6 regulates T-cell death, and inhibits p38 activity. Since p38 is responsible for initial TNF-α stimulated production of IL-6, this demonstrates another way in which p38 is able to regulate its own activity (Wysk *et al.,* 1999; Conze *et al.,* 2000).

p38 has been implicated in the pathology of the number of diseases in addition to influenza, by increasing inflammation-associated damage and inducing apoptosis. For example, p38 is thought to be responsible for injury and apoptosis on neurons during HIV infection, leading to HIV-associated neurocognitive disorders, by activating monocytes that release neurotoxins (Medders & Kaul, 2011).

In dengue virus infection, p38, ERK and JNK are all activated in endothelial cells, but p38 specifically leads to increased expression of TNF-α, IL-8 and RANTES, as well as contributing to vascular leakage (Fu *et al.,* 2014).

The key roles of MKK3, MKK6 and p38 in inflammation and disease make this cascade an attractive target for therapeutic mediation, and indeed, several p38 inhibitors already exist, including p38 MAPK specific pyridinyl imidazoles SB202190 and SB203580, and berberine, a plant-derived isoquinoline alkaloid (Engelman *et al.,* 1998; Shin *et al.,* 2015). However, clinical trials so far have been unsuccessful due to low levels of efficiency *in vivo* and adverse side effects (Choi *et al.,* 2016).

1.3. Vps52

The 2014 high throughput screen for cellular factors involved in VACV infection (Beard *et al.)* also identified a tethering factor complex, the Golgi associated retrograde pathway (GARP) complex. GARP is involved in retrograde transport of cargo from the cell periphery back to the Golgi body. This complex, along with general vesicle transport , will be discussed in the following sections.

1.3.1. Retrograde Transport

1.3.1.1 Vesicle transport

A eukaryotic cell requires the constant movement of cargo throughout the cell for continued existence. Anterograde transport describes the transfer of molecules through the ER and Golgi to the cell surface. However, in order for balance and transport homeostasis to be maintained within the cell, retrograde, or recycling transport of cargo back to, for example, the Golgi area is also required. It is this form of retrograde transport which will be focused on here. Both anterograde and retrograde transport utilise the same general mechanism, as outlined in the vesicular transport hypothesis. Specific proteins in a donor compartment are sorted and selected before budding from said compartment in a vesicle. Vesicles are then targeted to a specific acceptor compartment, where the vesicular and acceptor membranes fuse and the cargo is delivered (Bonifacino & Glick, 2004). Each stage of these pathways involves multiple and specific regulators and facilitators (reviewed in Faini *et al.,* 2013).

Transport is initiated by recruitment of vesicle coat proteins to the donor compartment. These coat proteins are responsible for selecting and sorting the cargo to be transported, as well as initiating the budding formation of the endosome. There are three main types of vesicles: Coat protein complex (COP)I-coated, COPII-coated and clathrin-coated. The coat proteins form a scaffold on the outside of the donor membrane surface and induce membrane curvature, which subsequently become budding vesicles (McMahon & Mills, 2004). COPI-coated vesicles are found predominantly in Golgi to ER transport, as well as transport within the Golgi stack, whereas COPII-coated are involved in transfer from the ER to the Golgi. In contrast, clathrin coated vesicles are the main form of transport carriers in the endocytic and recycling pathways, from the plasma membrane to the lysosome or TGN

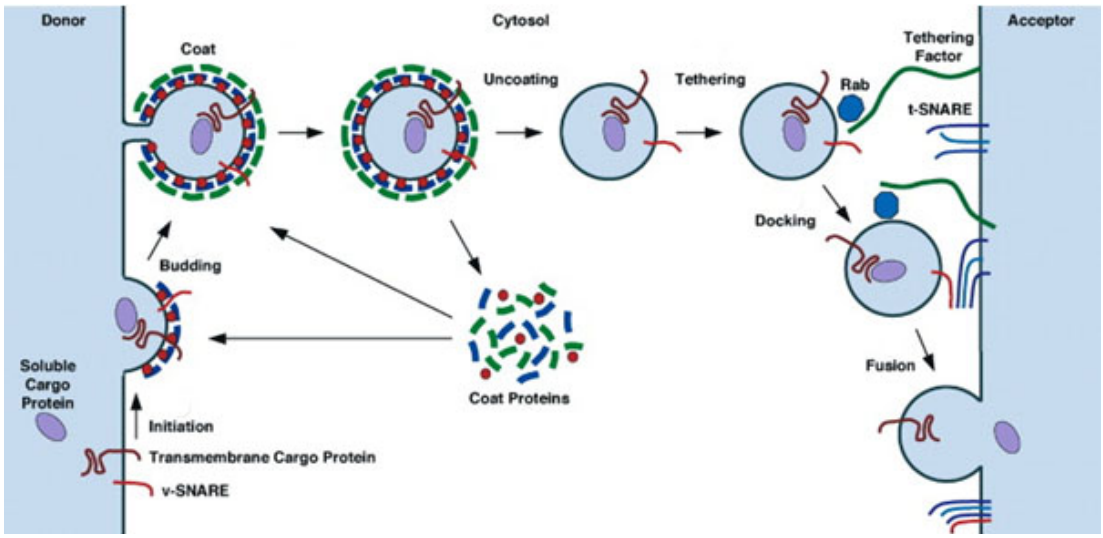

Figure 1.4 Vesicle transport from donor to acceptor compartments. Adapted from Bonifacino & Glick, 2004**.** Coat proteins are recruited to the donor compartment and recruit and sort cargo. Coat complexes then polymerise into a scaffold and induce membrane curvature, concentrating cargo and forming the bud. Eventually the link between the bud and the donor compartment is severed, either by accessory proteins or the coat proteins themselves. As the vesicle nears the donor compartment, it is uncoated, and coat proteins are recycled back to the donor compartment for further budding. Tethering factors and Rab proteins initiate contact between the vesicle and the acceptor compartment, and bring the v-SNAREs on the vesicle in contact with the t-SNAREs on the acceptor compartment. This allows the SNAREs to form a *trans*-SNARE complex, promoting fusion of the vesicle and compartment membranes, and subsequent delivery of the cargo.

(McMahon & Mills, 2004). Once budded, vesicles are targeted by the presence of SNAP (Soluble N-ethylamide factor attachment protein) receptors (SNAREs) on both the vesicle (v-SNARE), and acceptor (t-SNARE) membranes (Südhof & Rothman, 2009). SNARES are promiscuous and can interact with multiple other SNARES. In addition, these targeting proteins are recycled, and so the same SNARES are found on both anterograde, and retrograde vesicles. Therefore, additional factors are required to ensure specific vesicle targeting. Tethering factors, such as the exocyst and the Golgi associated retrograde pathway (GARP) complex, are protein complexes which mediate the initial contact between a vesicle and its acceptor compartment, before v- and t-SNAREs form complexes known as SNAREpins, which bring the membranes together and initiate fusion (Südhof & Rothman, 2009; Chia & Gleeson, 2011). Tethering factors are a large and varied family, consisting of multiple subclasses, each of which deals with a different vesicle transport route. One of the first tethering factors discovered was p115, a type of tethering factor now known as a golgin, which facilitates vesicular transport between Golgi cisternae (Waters *et al.,* 1992; Yu & Hughson, 2010). Golgins are members of the long coiled-coil tethering factor family, one of the two main classes of tethering factors. In the other class are the heteromeric multi-subunit tethering complexes (MTCs), and include

such tethering factors as the HOPS complex. The HOPS (homotypic fusion and vacuole protein sorting)/class C Vps (vacuolar protein sorting) complex, and its variant the class C core vacuole/endosome tethering (CORVET) complex tether vesicles between early endosomes and lysosomes, and are both composed of four vacuolar protein sorting proteins; Vps11, Vps16, Vps18 and Vps33, as well as two additional subunits which differ between the two complexes. (Yu & Hughson, 2010). Like HOPS and CORVERT, the aforementioned GARP complex is composed of four Vps proteins, Vps51, Vps52, Vps53 and Vps54. However, GARP is a member of the CATCHR (complex associated with tethering containing helical rods) subclass, and is responsible for tethering vesicles from endosomes back to the TGN, a route of transport known as the retrograde pathway (Bonifacino & Hierro, 2011).

Trafficking is also co-ordinated by Rab GTPases, which reversibly interact with membranes by the ability to 'switch' between GDP and GTP binding. In the GTP-bound 'on' state Rab GTPases act as recruiters for transport components such as tethering factor and sorting adaptors, thereby mediating vesicle docking and fusion (Stenmark, 2009).

1.3.1.2 The retrograde transport pathway

As previously described, retrograde transport is required to recycle vesicles and cargo back from endosomes to the Golgi, in order to maintain homeostasis in the cell. Retrograde transport consists of multiple pathways from the early endosomal to Golgi compartments: via the late endosome, via the recycling endosome, or directly to the TGN (Johannes & Popoff, 2008). Distinct SNAREs, GTPases and tethering factors direct the action of retrograde transport, many of which have not been observed in anterograde trafficking. One such example is a retrograde SNARE complex required for early endosome and late endosome to TGN transport. This SNARE complex is composed of endosomal t-SNAREs Syntaxin 6, Syntaxin 16 and Vti1a and the v-SNARE vesicle associated membrane protein 4 (VAMP4), and interacts with Rab GTPase Rab6a. (Mallard *et al*., 2002). In addition to Rab6, several more GTPases, including Rab9 are involved in endosome to TGN transport; as Rab9 localises to late endosomes for membrane fusion (Lombardi *et al.,* 1993; Carroll *et al.,* 2001).

An increasing number of proteins are seen to be trafficked back to the Golgi, both endogenous and exogenous. One such endogenous protein is the mannose-6-phosphate receptor (MPR). MPRs chaperone mannose-6-phosphate-modified hydrolases from the TGN to lysosomes, but then must be recycled back to the TGN via the late endosome for further chaperoning, and so can be used as a marker for retrograde transport function (Mallard *et al.,* 1998; Pérez-Victoria *et al.,*2008). The B-subunit of *Shigella dysenteriae* and haemorrhagic *Escherichia coli* toxin Shiga toxin (STxB) also uses retrograde transport, though it uses a separate retrograde pathway to MPR (Mallard *et al.,* 1998). STxB enters cells via clathrin mediated endocytosis, and hijacks early and recycling endosomes, where it accumulates before being rapidly transferred to the TGN and on to the Golgi (Mallard *et al.,* 1998).

Despite travelling by separate pathways, both MPR and STxB are dependent on the retromer complex for transport (McKenzie *et al.,* 2013). Retromer is a coat complex localised to recycling endosomes, and is comprised of two distinct subcomplexes: one containing sorting nexins (SNX)1/2 and SNX 5/6 and one containing Vps26, Vps29 and Vps35 (Carlton *et al.,* 2004). Cation independent-MPR (CI-MPR) is thought to bind Vps35, while Vps26 is required for STxB transport (McKenzie *et al.,* 2013). The fact that retromer straddles two completely distinct retrograde transport pathways identifies it as a central component in endosome to TGN trafficking.

1.3.2. The GARP complex

The GARP complex is a member of the quatrefoil family of tethering factors, and is involved in endosome, particularly early and late endosome, to TGN retrograde transport (Conibear *et al.,* 2003; Bonifacino & Hierro, 2011). GARP was initially discovered in the yeast *Saccharomyces cerevisiae* as a trimer of three large proteins: Vps52p, Vps53p and Vps54p which localised to the TGN and were involved in carboxy peptidase Y (CPY) trafficking, a pathway analogous to MPR recycling (Conibear & Stevens, 2000). Further investigation showed that mutation of any of the three Vps proteins resulted in the same slow growth phenotype, destabilisation of late Golgi membrane proteins, and mis-trafficking of CPY pathway components, confirming their role in retrograde transport (Conibear & Stevens, 2000). Additionally, none of the three GARP components are known to exist as monomers, and all three are required for complex stability (Conibear & Stevens, 2000).

In order to further classify the GARP trimer, its interactions with other transport components were investigated in *S. cerevisiae*. Subsequently, the active form of the Rab6 *S. cerevisiae* homologue, Ypt6p, was seen to recruit the GARP complex to the Golgi for protein recycling, by binding to Vps52p (Siniossoglou & Pelham, 2001; Siniossoglou & Pelham 2002). This interaction then triggered the recruitment of late Golgi SNARE Tlg1p, for recycling from early endosomal membranes to the Golgi (Siniossoglou & Pelham, 2001). However, none of the three known GARP components directly bound to Tlg1p, prompting further research into GARP associated proteins and the discovery of a fourth protein in the complex, Vps51p. It is Vps51p that binds the SNARE Tlg1p via its N-terminal (Siniossoglou & Pelham, 2002; Conibear *et al.,* 2003). Although VPS51p was initially highlighted in the original screen for components of vesicular transport machinery, it did not appear to have the identical mutant phenotype or role as Vps52p, VPs53p and Vps54p and so was not originally considered part of the complex (Conibear & Stevens, 2000). Indeed, Vps51p is not essential for GARP formation, or targeting to the Golgi membrane, and its mutation results in a milder slow-growth phenotype than Vps52p, Vps53p or Vps54p mutation (Siniossoglou & Pelham, 2002; Conibear *et al.,* 2003).

In 2005, the human homologue of GARP was first characterised by Liewen *et al.,* but again, it was thought to consist of only human Vps52, Vps53 and Vps54. Vps51, originally known as Another new gene 2 (Ang2), was not identified as the fourth component until several years later, when it was identified on a yeast 2-hybrid screen of GARP interactors, and was seen to bind Vps52, Vps53 and Vps54, in a complex of 1:1:1:1 stoichiometry (Pérez-Victoria *et al.,* 2010a).

In humans, GARP localises predominantly with the TGN and Golgi, but also exhibits a dispersed vesicular distribution (Liewen *et al.,* 2005). The dispersal seen in location is caused by recruitment of GARP to endosomes involved in the retrograde pathway before vesicle budding, so that when the transport vesicle does bud and travels to the acceptor compartment, it is already ready to dock without needing to recruit extra factors (Quenneville *et al.,* 2006). The most well-studied cargo that human GARP facilitates is CI-MPR, which is recycled back to the TGN after chaperoning mannose-6-phosphate-modified hydrolases such as cathepsin D (CatD) to lysosomes for degradation (Pérez-Victoria *et al.,* 2008). Rab9 and TIP47 (Tail interacting protein of 47kDa) are required for CI-MPR

retrieval from late endosomes, but cannot complete the cycle without GARP action. GARP loss results in reduced levels of CatD, due to a precursor being mis-sorted into lysosomes rather than the fully formed protein (Pérez-Victoria *et al.,* 2008). GARP depletion shows similar effects to retromer loss, as it blocks STxB transport to the TGN, and results in reduced and more diffuse staining of TGN marker TGN46 (Mallard *et al.,* 1998; Pérez-Victoria *et al.,*2008). In addition to its role in tethering retrograde transport intermediates, GARP is also able to interact with individual SNAREs, particularly t-SNARES syntaxin 6, syntaxin 16, Vti1a and v-SNARE VAMP4 in order to promote assembly of retrograde trafficking SNARE complex (Pérez-Victoria and Bonifacino*,* 2009).

The GARP complex is relatively large, and three of the four components, Vps52, Vps53 and Vps54 range from 700-1700 amino acid residues in size (Bonifacino & Hierro, 2011) The fourth component, Vps51 is far smaller, at 125-320 residues, but still exhibits the conserved amphipathic coiled-coil domain found at the C-terminus of all four components; which is responsible for complex assembly and stabilisation (Siniossoglou & Pelham 2002; Quenneville *et al.,* 2006; Bonifacino & Hierro, 2011). As GARP is a heteromeric complex, each of the four components play distinct roles in the tethering action. The complex is assembled by the interaction of coiled-coil domains at the C-terminals of each component. Therefore, the N-terminal domains, which extend from the centre of the complex, are responsible for complex function (Conibear *et al.,* 2003; Siniossoglou & Pelham 2002). Vps51 links GARP to syntaxin 6, the mammalian homologue of Tlg1p, and sytaxin 10 via binding between the conserved syntaxin HabC motif and a short α-helix containing a di-tyrosine motif in the N-terminal of Vps51 (Pérez-Victoria *et al.,* 2010b; Abascal-Palacio *et al.,* 2016). This interaction with syntaxin 6 contributes to the formation of the retrograde SNARE complex for endosome to TGN trafficking. However, as Vps51 also interacts with syntaxin 10 in the same manner, this suggests that GARP engages in a second SNARE interaction at the TGN, as simultaneous binding is not possible (Abascal-Palacio *et al.,* 2016). Vps52 colocalises with the GTPase Rab6 for vesicle delivery to the late Golgi, and has also been seen to interact with syntaxin 10 (Liewen *et al.,* 2005). Vps53 and Vps52 are both able to recruit syntaxin 16 and Vti1a, while Vps53 and Vps54 interact with the v-SNARE VAMP4 for SNARE complex assembly (Pérez-Victoria *et al.,* 2009; Luo *et al.,* 2011). Vps53 also binds to retrograde transport intermediates for tethering function (Pérez-Victoria *et al.,* 2009). Vps54 however, is perhaps the most important member of the complex, as it is not only solely responsible for GARP

recruitment to the early endosomal compartment, but also for localisation to the TGN, and is essential for both the beginning and end of this retrograde transport pathway (Quenneville *et al.,* 2006).

While GARP plays a clear and direct role in eukaryotic retrograde transport from early and late endosomes back to the TGN, it has also been indicated as indirectly affecting a number of other processes, emphasising the impact that retrograde transport has on multiple cellular mechanisms. For example, as a complex, GARP affects gene regulation in *Caenorhabditis elegans* as GARP depletion compromises the miRNA pathway, possibly due to loss of a membrane related miRNA process (Vasquez-Rifo *et al.,* 2013).

Mutations in specific components of the GARP complex have been reported to have effects in a wide range of species. The *UNH-1* mutation in the Vps51 homolog *UNHINGED* in the plant group *Arabidopsis* confers a deformed leaf phenotype, as GARP may be responsible for recycling of proteins essential for leaf development (Pahari *et al.,* 2014). The spontaneous hypomorphic *wobbler* mutation in Vps54 results in destabilisation of the entire GARP complex, and motor neurone disease similar to amyotrophic lateral sclerosis (ALS) in humans, as well as infertility in mice (Duchen *et al.,* 1968; Schmitt-John *et al.,* 2005), suggesting that GARP plays a key role in neuronal development and maintenance. This is further supported by the discovery that heterozygous mutations in Vps53 have been identified as the cause of progressive cerebello-cerebral atrophy type 2, which causes progressive microcephally, spasticity and epilepsy in humans (Feinstein *et al.,* 2014).

Vps52 is the only component of the complex which has, so far been implicated in a GARP-independent role. Interestingly, a mutation in Vps52 during embryonic development, t^{w5}, which results in severe gastrulation defects and embryonic death at 6.5 days into development (E6.5) in mice, occurs while Vps52 is not complexed in GARP, or indeed even expressed in the same embryonic tissues as Vps53 and Vps54 (Sugimoto *et al.,* 2012). This implies that Vps52 is the only GARP component so far to have a role outside of the complex, especially as the homozygous mutation results in much earlier embryonic lethality than that of homozygous Vps54 mutations at E11 days (Karlsson *et al.,* 2013).

1.3.3. Retrograde transport and infection

As an important cellular pathway to traffic cargo into the heart of the cell, endosome-Golgi retrograde transport pathways (EGRTP) is an ideal target for hijack by invading pathogens, and has been implicated in the pathogenicity of multiple bacterial and viral infections and intoxications. Several toxins, particularly bacterial toxins featuring the A/B subunit conformation, such as STx, cholera toxin (CTx), and *Pseudomonas* toxin (PEx) all utilise the retrograde transport pathway to reach the ER, where they shut down host protein production (Spooner *et al.,* 2006; Mukhopadhyay & Linstedt, 2013). The plant toxin ricin also exploits EGRTP in a similar fashion to reach the ER. (Wesche, 2002). Cellular factors involved in the mechanisms of transport differ from toxin to toxin, despite the common destination. For example, STx and PEx rely on a Rab6 dependent pathway to reach the ER, but neither ricin nor CTx interact with Rab6 at all (Spooner *et al.,* 2006; Morikawa *et al.,* 2009), again highlighting the complexity of EGRTP.

In addition to bacterial toxins, there are several species of bacteria which directly affect the mechanisms of retrograde transport, without secreting endotoxins. Rather than hitching a ride on the retrograde pathway, *Legionella pneumophila,* the causative agent of Legionnaire's disease, translocates its RidL protein, which binds to the retromer component Vps29. This interaction diverts the retromer complex to the *Legionella*-containing vacuole, disrupting retrograde transport, and promoting bacterial growth (Finsel *et al.,* 2013). In a similar mechanism, the Q fever pathogen *Coxiella burnetii* also subverts EGRTP by recruitment of retromer in order to promote bacterial growth (McDonough *et al.,* 2013; Personnic *et al.,* 2016).

Use of EGRTP is not limited to bacteria and toxins. Several viruses have been shown to interact with retromer to promote their own growth. Retromer is exploited in the retrograde trafficking of the key envelope glycoprotein (Env) of human immunodeficiency virus (HIV)-1. However, rather than entry, Env uses EGRTP for facilitating virion morphogenesis. Env is initially trafficked by the anterograde transport pathway to the peripheral site of virion formation. If Env is not incorporated into a novel virion, it is transported back to the Golgi in a retromer-dependent manner. Loss of retromer therefore results in excess levels of Env incorporated into virions (Groppelli *et al.,* 2014).

Although a conclusive linking of VACV with specific components of EGRTP had not been seen at the time of this investigation, a substantial amount of evidence existed to suggest that successful VACV growth involves the retrograde transport system. During IEV fusion with the plasma membrane and EEV egress, some B5 from the IEV outer membrane remains on the cell surface. Evidence collected by Ward & Moss (2000) and Husain and Moss (2005) indicates that this B5 may be recycled back from the cell surface to the Golgi network via the retrograde transport pathway, as the cytoplasmic tail domain contains a tyrosine residue at position 310, and two leucine residues at 315 and 316, a motif which has been implicated in several proteins as a regulator for endocytosis (Marks *et al.,* 1996). These motifs may be involved in signalling for inclusion in clathrin coated vesicles for retrieval from the plasma membrane back to the Golgi network, as deletion of any of the residues results in reduced rates of retrograde transportation, as seen by the rate of antibody uptake, and far higher levels of staining on the cell surface than the Golgi area (Ward & Moss, 2000). Additionally, expression of EH21, a known inhibitor of endocytic function resulted in a significant reduction in B5 uptake from the surface, a significant increase in the surface staining of B5, F13 and A36, and a reduction of EEV in the extracellular media (Husain & Moss, 2005). F13 also shows evidence of being recycled from the cell surface back to the TGN. F13 has been seen to colocalise with both endocytic marker FM64 in punctate structures in the cell periphery, and clathrin-coated pit marker Texas-red conjugated transferrin (TR-tfn). Late endosome marker LAMP2 and F13 were also seen to associate (Husain & Moss, 2003) Taken together, these imply retrieval of F13 from the cell surface in late endosomes via clathrin-mediated recycling, a hypothesis confirmed by the blocking of F13 retrieval by endocytosis inhibitors such as EH21 (Husain & Moss, 2003; Husain & Moss 2005). This recycling of individual IEV proteins, including B5, F13 and A36 may occur in order to maximise IEV formation at the viral wrapping station, if EV proteins have limited production, or to decrease the visibility of infected cells to immune responders (Ward & Moss, 2000; Husain and Moss, 2005), though neither has been conclusively proved as yet.

1.4. Aims and Objectives

The aim of this thesis is to investigate the roles of two proteins: MKK3 and Vps52 in the replication and spread of VACV. By using several methods of inhibiting gene expression, such as siRNA transfection, mutation and pharmaceutical inhibition, we can determine the roles of these proteins in the VACV replication cycle, and examine the effects of their loss. By attaining greater understanding of the complex VACV life cycle and how it interacts with the host cell, new methods of anti-poxviral treatment, or biomedical applications may be revealed. The aims of this project are as follows:

1. To inhibit expression of MKK3 both *in vitro* and *in vivo*, and examine the effects of this loss on VACV replication. Furthermore, identify which stage of the VACV replication cycle MKK3 influences (Chapter 3)
2. To inhibit expression of Vps52 and the GARP complex by siRNA transfection and mutation, and examine the effects of this loss on VACV replication. Furthermore, identify which stage of the VACV replication cycle Vps52 and GARP influence (Chapter 4 & 5).
3. To detail the cellular components of the EGRTP that are required for VACV morphogenesis, specifically the effects of retromer loss, and Retro-2 treatment (Chapter 5).

2 Materials and Methods

2.1. Cell lines and viruses

2.1.1. Cell lines

Dulbecco's modified Eagle's medium (DMEM) (Life Technologies), containing 50µg/ml streptomycin, 50µg/ml penicillin (pen/strep) (Sigma) and 10% foetal bovine serum (FBS) (Life Technologies) was used to grow the following cell lines: rabbit kidney epithelial cells (RK-13), African green monkey kidney epithelial cells (BS-C-1 and Vero), and human cervix carcinoma epithelial cells (HeLa). All cell lines were passaged regularly to maintain viability. Cells were washed in phosphate buffered saline (PBS) and lifted off the flask using 0.5% Trypsin EDTA (Life Technologies) before transfer to a fresh tissue culture flask. Wild type (WT) mouse embryonic fibroblasts (MEFs) and mutant (MU) *Wobbler (Wob)* MEFswere kindly provided by Professor Thomas Schmitt-John (Aarhus University, Denmark) and were grown in pyruvate-free DMEM (Life Technologies), containing 50µg/ml penicillin, 50µg/ml streptomycin (Sigma), and 20% FBS (Life Technologies). *Wob* MEFs contain a leucine to glutamine substitution at position 967 in Vps54, which decreases the half –life of both Vps54 and the entire GARP complex (Schmitt-John *et al.,* 2005; Pérez-Victoria *et al.,* 2010a) MEFs were received as primary cells and were immortalised through their crisis stage by repeated 1:1 passages every 72 hours until cells became permissible for growth in tissue culture flasks. Once immortalised, MEF cells were passaged regularly for maintenance as described above. All cells were grown at 37^{o}C, 5% CO_2 and 95% humidity.

2.1.2. Viruses

Vaccinia virus Western Reserve (VACV-WR) and VACV-A5-enhanced green fluorescent protein (VACV-A5-EGFP) were provided by Professor Geoffrey L Smith (University of Cambridge). Viruses used in all experiments were sucrose cushion-purified VACV-WR and VACV-A5-EGFP.

2.1.3. Preparation of viral stocks

RK-13 cells were grown to confluency in ten 175cm^2 tissue culture flasks and infected with VACV-WR at a multiplicity of infection (MOI) of 0.1 in DMEM containing 2.5% FBS and pen/strep and incubated for 48h at 37^{o}C and 5% CO_2. Once the majority of the cells showed a cytopathic effect,

cells were scraped down in the media, centrifuged at 3000g for 10min and the supernatant discarded. Cells were re-suspended in 10ml 10mM Tris-HCl, pH 9, and incubated on ice for 15min before being dounce homogenised on ice for 25 strokes. The dounced pellet was then centrifuged at 2000g for 5min and the supernatant layered on top of 18ml 36% sucrose in 10mM Tris-HCl (pH 9). Tubes were filled to capacity on top of the viral supernatant with additional 10mM Tris-HCl (pH 9), and centrifuged in an ultra-centrifuge (XL-90, Beckman) rotor SW28 for 80min at 13500rpm. Finally, the supernatant was discarded and the pellet re-suspended in 1ml Tris-HCl (pH9), and stored at -70^{o}C.

2.2. siRNA transfection

HeLa cells ($1.5x10^5$ cells per well for a 6 well plate and $4x10^3$ cells per well for a 96 well plate) were incubated at 37^{o}C, 5% CO_2 for 24h to approximately 75% confluency. siRNA (Table 1) was prepared from 20µM stocks stored at -70^{o}C to dilutions of 5µM for a 6 well plate transfection and 250nM for a 96 well plate, in 1x siRNA buffer (Thermo Scientific).

For a 6 well plate transfection, 5µM siRNA stocks were further diluted to a concentration of 0.25µM in serum free, antibiotic free DMEM. Transfection reagent Dharmafect 1 (Dharmacon) was diluted in serum free, antibiotic free DMEM to a final concentration of 1%. For the mock transfected negative control, siRNA was replaced with 1x siRNA buffer. Dharmafect and siRNA were incubated separately for 5min at room temperature (RT), mixed at a 1:1 ratio and incubated for a further 20min at RT. After incubation, media was removed from the previously prepared HeLa cells and 400µl siRNA Dharmafect mix was added to each well, along with 1600µl 5% FBS, antibiotic free DMEM. Plates were incubated at 37^{o}C, 5% CO_2 for 48h.

For a 96 well plate transfection, Dharmafect 1 was diluted in serum-free, antibiotic-free DMEM to a final concentration of 0.15% and incubated at RT for 5min. siRNA and Dharmafect 1 were combined in a 1:1 ratio and incubated at RT for 20min. Media was removed from the prepared HeLa cells in the 96 well plate and replaced with 80µl DMEM supplemented with 5% FBS only, and 20µl appropriate siRNA/Dharmafect 1 mix. The siRNA/Dharmafect 1 mix was replaced with 20µl siRNA buffer for the mock transfected control. Cells were incubated for 48h at 37^{o}C, 5% CO_2.

Table 2.1 Sequences of siRNAs used for transfections

siRNA	Sequence
VP16	GGGCGAAGUUGGACUCGUAUU
Rab1A (SMARTpool)	GAACAAUCACCUCCAGUUA; CAAUCAAGCUUCAAAUAUG; GGAAACCAGUGCUAAGAAU; CAGCAUGAAUCCCGAAUAU
PLK1 (SMARTpool)	CAACCAAAGUCGAAUAUGA; CAAGAAGAAUGAAUACAGU; GAAGAUGUCCAUGGAAAUA; CAACACGCCUCAUCCUCUA
MKK3 (SMARTpool)	GGUGGAGGCUGAUGACUUG; CCGCAGAGCGUAUGAGCUA CCAAUGUCCUUAUCAACAA; GGAGAUUGCUGUGUCUAUC
Vps51	GCUAUUCUCUGAAGCUAUU
Vps52 (SMARTpool)	CGAAAGAGGCAGUAAGGAA; GAUCACACCCACAAUGAAA GGCAAUGUCUCCACGGCAA; CCAGAUGAUGGUUGAACAU
Vps53	GGAUGUAAGUCUGAUUGAAUU
Vps54	UCACGAUGUUUGCAGUUAAUU
Vps26 (SMARTpool)	GCUAGAACACCAAGGAAUU; UAAAGUGACAAUAGUGAGA UGAGAUCGAUAUUGUUCUU; CCACCUAUCCUGAUGUUAA
Vps35 (SMARTpool)	GAACAUAUUGCUACCAGUA; GAAAGAGCAUGAGUUGUUA GUUGUAAACUGUAGGGAUG; GAACAAAUUUGGUGCGCCU

2.3. Western blotting

2.3.1. Protein collection and protein concentration calculation

Adherent cells were washed twice with ice-cold PBS, then lysed in protein lysate buffer (50 mM Tris-Cl pH 7.5, 100 mM NaCl, 1% (w/v) NP40) and 1:7 protease inhibitor (Complete tablets, Roche) on ice for 30min before storage at -70^{o}C. After thawing, lysates were centrifuged at 16,100 g for 5 min and the pellet discarded. A BCA (Bicinchoninic acid) Protein Assay Kit (Thermo Scientific Pierce) was used to calculate protein concentrations according manufacturer's instructions, in a 96 well plate. The plate was the incubated for 30min at 37^{o}C and the absorbance was determined on a FluoStar Optima plate reader at 562nm.

2.3.2. Sodium dodecyl sulphate – polyacrylamide gel electrophoresis (SDS-PAGE) and western blotting

Protein samples were mixed in a 1:1 ratio with 2x Laemmli sample buffer (Biorad) with added β-mercaptoethanol at a final concentration of 355mM. Samples were then boiled at 98^{o}C for 5mins before being separated, along with a SeeBlue plus 2 prestained standard ladder (Invitrogen), by SDS-PAGE on either a 10% or 15% polyacrylamide resolving gel. The resolving gels were layered with 5% stacking gels, and electrophoresis was performed in TRIS running buffer (final concentrations: 192mM glycine, 25mM tris base, 3mM SDS, pH adjusted to 8.3) at 90-120v for 2-3h. Either a semi-dry or a wet blotting technique was used to transfer samples onto nitrocellulose (Maniatis) or PVDF membranes (Merck Millipore). Nitrocellulose membranes were equilibrated in transfer buffer (Final concentrations: 39mM glycine, 48mM trisbase, 1.3mM SDS, 20% (v/v) methanol). PVDF membranes were first activated by submersion in methanol, then distilled water, and finally briefly equilibrated in transfer buffer. Semi-dry blot gels were blotted at 15V for 30min while wet blot gels were blotted at 100v for 1h. Following protein transfer, membranes were blocked in Odyssey blocking buffer (Li-Cor), diluted 1:1 in PBS, for 1h at RT. Membranes were then incubated with primary antibodies at 4^{o}C overnight, then fluorescent secondary antibodies for 1h at RT. Blots were scanned in a Li-Cor Odyssey scanner and quantified using Image Studio Lite version 3.1.

Table 2.2 Antibodies used for western blotting

Antibody	Specifications	Dilution	Supplier	Catalogue number
Primary antibodies				
Anti-Actin (loading control	Mouse monoclonal	1:1000	Abcam	3700S
Anti-Actin (loading control)	Rabbit polyclonal	1:1000	Cell signalling	4967
Anti-MKK3	Rabbit polyclonal	1:1000	Cell Signalling	5674
Anti-p38	Rabbit polyclonal	1:500	Cell Signalling	9212
Anti-Phosphorylated p38	Mouse monoclonal	1:500	Cell Signalling	9216
Anti-Vps51 (Anti-C11orf2)	Rabbit polyclonal	1:500	GeneTex	GTX105644
Anti-Vps52	Rabbit polyclonal	1:500	Aviva Systems Biology	ARP57644 _P050
Anti-Vps53	Rabbit polyclonal	1:500	Novus Biologicals	NBP1-76901
Anti-Vps54	Rabbit polyclonal	1:500	Aviva Systems Biology	OAAB09222
Anti-E3	Mouse monoclonal	1:500	BEI Resources	NR-4547
Anti-D8	Mouse monoclonal	1:1000	Gift from Professor Geoffrey Smith, University of Cambridge	
Anti-Vps26	Rabbit polyclonal	1:1000	Abcam	ab23892
Anti-Vps35	Mouse monoclonal	1:500	Abcam	ab57632
Secondary Antibodies				
Li-Cor Anti-mouse IgG (DyLight 680	Goat polyclonal	1:15000	Cell Signalling	5470
Li-Cor Anti-mouse IgG (DyLight 800 4X	Goat polyclonal	1:15000	Cell Signalling	5151
Li-Cor Anti-rabbit IgG (DyLight 680	Goat polyclonal	1:15000	Cell Signalling	5366
Li-Cor Anti-rabbit IgG (DyLight 800 4X	Goat polyclonal	1:15000	Cell Signalling	5151

2.4. Growth curves

2.4.1. Fluorescent growth curves

Cells were infected with VACV-A5-EGFP at a multiplicity of infection (MOI) of 0.05 for multistep growth curves and MOI of 5 for single step growth curves. Viral stocks were diluted in complete DMEM containing 2.5% FBS. For *Wob* MEF cells, pyruvate-negative DMEM, containing 2.5% FBS and pen/strep antibiotics was used to dilute the viral stocks. Cells were incubated with viral inoculum for 1hr at 37^{o}C, 5% CO_2. Inoculum was removed, cells were washed with medium and incubated with 2.5% DMEM. This was considered the 0 hours post infection (hpi) time point. Fluorescence of EGFP was measured as an indicator of viral growth, using a Synergy HT Multi-Mode Microplate 123 Reader (BioTek), with excitation set to 485nm, and emission at 528nm. For a multi-step growth curve, fluorescence was measured at 0, 12, 24, 36 and 48hpi, and at 0, 4, 8, 12 and 24hpi for a single step growth curve.

2.4.2. Plaque assay growth curve

Cells were infected as described above for either a single- or a multi-step growth curve. For multistep growth curves, cells were scraped down into the media and viral titres present determined by plaque assay on confluent BS-C-1 cells. Viral samples were frozen and thawed three times and sonicated at level 2 in a Misonix 3000 sonicator. Samples were serially diluted in complete DMEM containing 2.5% FBS and pen/strep. For titrations involving *wobbler* MEF cells, complete DMEM was substituted for pyruvate negative DMEM. BS-C-1 cells were inoculated with 1ml per well of viral dilutions for 1h at 37^{o}C and 5% CO_2, then removed and replaced with a 1:1 solution of 2xDMEM containing 5% FBS and pen/strep and 1.5% carboxymethylcellulose (CMC) (Sigma), before incubation for 72h at 37^{o}C and 5% CO_2. After 72h, the DMEM/CMC overlay was replaced with 0.1% crystal violet (Sigma-Aldrich) solution made up in 15% methanol for 1hr to allow plaque counting.

In a single-step growth curve, supernatants were removed from wells at each time point and centrifuged to remove cell debris. Anti-L1 antibody (BEI Resources, 1:500 dilution) was then added to the supernatants at a ratio of 1:500, and incubated for 1hr at 37^{o}C to inactivate IMVs. Viral titres in the supernatants were determined immediately by plaque assay. Cell monolayers were scraped down into the medium and titre also determined by plaque assay, as previously described.

2.4.3. Staining and counting cells

Cells from siRNA transfections and fluorescent growth curves were fixed in 96 well plates by addition of 100µl formalin for 30min. Formalin was then discarded and replaced with 50µl of 25µg/ml Hoechst 33342 solution diluted in ice cold, serum- and antibiotic-free DMEM. Plates were incubated for 30min in the dark at RT. Images were taken in 2 channels using a Zeiss Cell Observer microscope and the Zen 2012 (Carl Zeiss Microscopy) program. Cells were then counted using Image J software and a macro written by Dr Charlotte Bell (The Roslin Institute). Fluorescence per cell was calculated using the data from single- and multi- step fluorescent growth curves.

Cell death was also determined using CellTiter Blue Cell Viability Assay (Promega). 20µl reagent was added to each well of a growth curve plate and incubated for 1-4h at 37^{o}C. Fluorescence was then determined on a Synergy HT Multi-Mode Microplate 123 Reader (BioTek) at 590nm.

2.5. MKK3 *In vivo* experiments

2.5.1. In vivo VACV infection time course in MKK3 knockout and wild type mice

Wild type (WT) and MKK3 knockout C57Bl6 ;129S1-*Map2k3*^{tm1Flv}/J (MKK3$^{-/-}$) mice were kindly donated by Dr J. Kenneth Baillie, and bred by Dr Sara Clohisey (The Roslin Institute), after having originally been obtained from The Jackson Laboratory. Mice were infected intranasally with 4x10^{5} pfu VACV-WR in a PBS vehicle. Control mice were inoculated with PBS only. Clinical scores and weights were recorded daily. Mice were scored on the severity of clinical symptoms on a 0-3 scale according to severity, where 0 indicated no symptoms, and 3 indicated severe signs. Clinical signs included: reduced spontaneous activity, ruffled fur, and hunched posture as well as weight loss. Any mice falling below 75% of the starting body weight or scoring higher than 3 for clinical symptoms were euthanized. All mice were euthanized day 7 post infection, and their lungs, liver, brain and spleen collected for tissue analysis. Lungs were also collected for staining and fixing for histological examination. The experiment was covered by appropriate Home Office personal and project licences and approved by the local ethics committee. All live animal work, post mortem examinations and histopathology were carried out by Dr. Pip Beard, under the Home Office Project Licence PPL60/3777, in accordance with the Animal (Scientific Procedures) Act, 1986.

2.5.2. Viral titration from mouse tissues

Mouse tissues were lysed before titration by adding 1ml DMEM with 2.5% FBS and pen/strep antibiotics to safe-lock Eppendorf tubes (Eppendorf) along with one 5mm stainless steel bead (Qiagen). Mouse organ samples were then layered on top of the DMEM. Tubes were lysed at 28,000Hz for 2min in a Qiagen tissue lyser. Sample blocks were rotated and lysed again at 28,000Hz for a further 2 minutes to ensure thorough lysis. Supernatants were collected and centrifuged for 5min at 3000rpm in a tabletop centrifuge. The resulting pellets were discarded, and the viral titres in the remaining supernatants were assessed by plaque assay as previously described.

2.5.3. Histopathology of mouse tissues

Lungs collected from the mice in section 2.5.1 were inflated and immersed in 10% neutral buffered formalin (Sigma-Aldrich UK) until fixed, then processed using routine methods, and embedded in paraffin blocks. 5µm thin sections were cut and stained with haemotoxylin and eosin for histological examination. The sections were then assessed blind by a veterinary pathologist (Dr Pip Beard), before being unblinded and groups analysed.

2.5.4. Cytokine array of mouse tissues

An R&D Systems Proteome Profiler Array Kit – Mouse Cytokine Array Panel A was used to examine the levels of cytokines in mouse tissues. Triton-X 100 was added to 400µl previously homogenised mouse lung tissue to a final concentration of 1%. Samples were freeze-thawed and centrifuged at 10,000g for 30min for immediate assay. The manufacturer's protocol was followed, with the exception that bound cytokines were detected using LiCor Odyssey. Array membranes were incubated for 30min at RT in IRDye 800 Strepavidin antibody (LiCor catalogue #926-32230) diluted at a ratio of 1:200 in array buffer 6. Membranes were washed 3 times in 1x wash buffer for 10min and then read on a LiCor Odyssey scanner.

2.6. Immunofluorescence

Table 2.3 Antibodies for immunofluorescence

Antibody	Specifications	Dilution	Supplier	Catalogue number
Primary antibodies				
Anti-TGN46	Sheep polyclonal	1:500	AbD Serotec	AHP500
Anti-LC3B	Rabbit polyclonal	1:200	Cell Signalling	3868
Anti-Giantin	Rabbit polyclonal	1:250	Biolegend	924302
Anti-B5	Mouse monoclonal	1:500	BEI Resources	NR-556
Anti-B5	Rabbit polyclonal	1:500	BEI Resources	NR-629
Anti-F13	Rabbit polyclonal	1:500	Gift from Dr Geoffrey Smith, University of Cambridge	
Secondary Antibodies				
Anti-rabbit secondary Ab, Alexa Fluor 488	Goat polyclonal	1:500	Life Technologies (Molecular Probes)	A11034
Anti-rabbit secondary Ab, Alexa Fluor 568	Goat polyclonal	1:500	Life Technologies (Molecular Probes)	A11011
Anti-mouse secondary Ab, Alexa Fluor 568	Goat polyclonal	1:500	Life Technologies (Molecular Probes)	A11004
Alexa Fluor 594 Anti-Sheep IgG (H / L)	Donkey polyclonal	1:500	Life Technologies	A11016

2.6.1. Immunofluorescence

Cells were seeded onto 20mm x 20mm coverslips (SLS) in six well plates at a density of $1.5x10^5$ cells for HeLa cells, and $2x10^5$ cells per well for MEF cells. If VACV infection was being examined, cells were infected at an MOI of 5 for 8h. Cells were fixed with 2ml of formalin for 30min, washed with PBS, then permeabilsed in 0.2% Triton-X100 for 5min at RT, and washed 3 times in PBS. Primary antibody was diluted in PBS + 2% FBS, and was incubated on cells in a humidity chamber for 1h at RT. Coverslips were washed three times in PBS + 2% FBS before addition of secondary antibody,

also diluted in PBS+ 2% FBS, and fluorescently labelled phalloidin (Alexa Fluor 633, Molecular Probes). Cells were incubated with secondary antibody for a further 1h at RT, then washed three times in PBS and once in distilled water. ProLong Gold mounting media containing DAPI (4-,6-diamidino-2-phenylindole) (Cell Signalling) was used to mount the coverslips on slides, which were then allowed to dry at 4^{o}C overnight. Slides were then examined on a Zeiss 710 confocal microscope.

2.6.2. IMARIS image analysis

Two- dimensional Z –stacks were taken on a Zeiss 710 confocal microscope. These Z-stacks were then rendered into three-dimensional (3D) images, and analysis was performed with IMARIS image analysis software (IMARIS, version 8.2; Bitplane AG, Switzerland). Z-stacks were rendered into three dimensions and the IMARISCell module was used to segments the nucleus, cell, and B5 labelled vesicles. Images of vesicles were exported to spots and filtered for association with EGFP representing VACV cores, or AlexaFluor 488 representing VACV F13. These vesicles were then quantified in order to analyse number of B5-labelled vesicles, their diameter, and the percentage of B5 –labelled vesicles associating with other labelling of interest.

2.7. Retro-2-based assays

2.7.1. Shiga toxin survival assay

Vero cells were seeded into a 96 well plate at a density of 1x10^{5} cells per well and incubated at 37^{o}C and 5% CO_2 for 24h to confluency. Retro-2 (Sigma, or kindly donated by Dr Daniel Gillet at French Atomic Energy Commission (CEA) Saclay) was re-suspended in dimethyl sulphoxide (DMSO), then diluted to a range of concentrations in FBS-free, antibiotic-free DMEM. Appropriate dilutions were added to each well and cells incubated for 2h at 37^{o}C, 5% CO_2. Shiga toxin 2 (STx-2) (lot #111108V2 Toxin Technology, Inc) was serially diluted from the stock concentration of 500µg/ml in serum- free and antibiotic-free DMEM, to a range of concentrations and added to appropriate wells. Cells were then incubated for 48h, in the continued presence of STx-2 and Retro-2. At 48h post intoxication, cell viability was determined using CellTiter Blue, as described in 2.4.3.

2.7.2. Retro-2 growth curve assays

HeLa cells were seeded into a 96 well plate at a density of $5x10^4$ cells per well and incubated at 37°C and 5% CO_2 for 24h to confluency. Retro-2 and the related compounds – Retro-1, VP184 or Retro-2.1 (kindly donated by Dr Daniel Gillet at CEA Saclay) were re-suspended in DMSO to a range of concentrations in FBS-free, antibiotic-free DMEM and the appropriate dilution was added to each well. Plates were incubated for 2h at 37°C, 5% CO_2. Cells were then infected with VACV-A5-EGFP at an MOI of 0.05 for a multi-cycle based growth curve as described in section 2.4.1 and 2.4.2, or an MOI 5 for a single cycle growth curve, as described in 2.4.2. The drugs remained present for the duration of the assays.

2.7.3. *In vivo* VACV infection time course in Retro-2 treated mice

Retro-2 was re-suspended in DMSO at a concentration 66.6mg/ml (210mM). Groups of 6 female BALB/c mice (aged 6-8 weeks) were injected intraperitoneally with 270µl PBS containing 30µl (10% v/v) DMSO alone as a negative control, or 30µl Retro-2 solution. Mice were also intranasally inoculated with VACV-WR at a concentration of $1x10^4$ pfu diluted in 20µl PBS, or sham infected with just the PBS vehicle, while lightly anaesthetised with isofluorane. Mice were injected with the Retro-2 or control solution at either days -1 and 1 post infection, or days 1 and 2 post infection. Mice were observed daily and scored for clinical signs of disease (ruffled fur, hunched posture, reduced activity), and measured daily for weight loss. Any mice falling below 75% of the starting body weight were euthanized. All animal experiments were carried out under a UK Home Office Licence and assessed by the local Animals Ethics and Welfare Committee. After the experiment's conclusion, 7 days post infection, all mice were euthanized and lungs were taken and titred for virus according to the protocol in section 2.4.2. All live animal work and post mortem examinations were carried out by Dr Pip Beard, under the Home Office Project Licence PPL 70/8483, in accordance with the Animal (Scientific Procedures) Act, 1986.

3 The cellular MAPK Kinase protein MKK3 is not required for VACV growth *in vitro* or *in vivo*

3.1. Introduction

A 2014 high throughput loss of function screen of cellular factors influencing VACV replication (Beard *et al.,* 2014*.)* identified p38 activator MKK3 as a pro-viral factor in a successful VACV infection. This chapter focuses on examining the role of MKK3 in VACV growth and replication, by siRNA knockdown of the MKK3 gene *in vitro*, and through the use of MKK3 knockout mice.

The extracellular environment is constantly changing, and cells must be able to react appropriately to stimuli such as UV radiation, inflammation, heat shock and osmotic stress. MAP kinase pathways trigger and mediate responses to these stimuli, and the subsequent expression of required genes. Currently, there are four known MAPK families: ERK, JNK, p38 and ERK5/BMK1 (Raman & Cobb, 2003; Wang & Tournier, 2006). Although the specific kinase cascades vary from family to family, all the MAPK families have a conserved core cascade consisting of three layers. In this core, MAP3Ks activate MAP2Ks by dual phosphorylation of Ser and Thr residues, and these MAP2Ks then go on to activate the final layer, MAPKs, by dual phosphorylation of specific Thr and Tyr residues (Raman & Cobb, 2003). In most cases, MAP3Ks exhibit a certain level of promiscuity and can activate downstream components in more than one cascade, such as MEKK1, which is involved in both the JNK and the ERK5 pathway (Davis, 2000; Wang & Tournier, 2006). In comparison, MAP2Ks are far more specific, and in general, only activate the MAPK from one family. However, exceptions do exist, such as MKK4, which phosphorylates both JNK and p38, though while it is an essential component of the JNK cascade, it is not a strong activator of the p38 pathway (Derijard *et al.,* 1995; Yang *et al.,* 1997).

The p38 MAPK pathway was first identified through its response to LPS stimulation, and is now known to be activated by a wide range of stimuli, including UV radiation, heat shock, osmotic changes, growth factors and certain families of cytokines (Han *et al.,* 1993; Zarubin & Han*,* 2005). Multiple MAP3Ks are involved in the p38 cascade, including MLK1, MEKK1 and TGF-β-activated kinase (TAK)1. Several of these MAP3Ks are also part of the JNK cascade, meaning that activating

these kinases can result in either specific, or simultaneous p38 and JNK activation, depending on the nature of the stimuli (Zarubin & Han, 2005). At the MAP2K stage of the cascade, only 3 kinases are able to phosphorylate p38 at the Thr180 and Tyr182 residues: MKK3, MKK4 and MKK6 (Raingeaud *et al.,* 1995; Derijard *et al.,* 1995; Han *et al.,* 1996; Moriguch *et al.,* 1996; Raingeaud *et al.,*1996). Of the two MAP2Ks specific to the p38 cascade, MKK3, (also known as MAP2K3), is activated by dual phosphorylation of Ser189 and Thr193 residues, and MKK6 by dual phosphorylation of Ser151 and Thr157 (Han *et al.,* 1996). Although the majority of p38 activation involves MKK3, 4 or 6, there exists an MKK-independent method of p38 phosphorylation, mediated by transforming growth factor β-activated protein kinase (TAK)- binding protein 1 (TAB1). When p38 is expressed with TAB1, it induces auto-phosphorylation of p38 at a level of activation similar to MKK6 (Ge *et al.,* 2002). Once the cascade is completed and p38 activated, it triggers a range of biological processes, including inflammation and cytokine production, apoptosis, cell cycle progression and tumour suppression (Zarubin & Han, 2005).

As the cascade is fairly simple, and culminates in only one MAPK, multiple mechanisms of regulation exist in order to ensure that the correct final substrate is activated. One such method of ensuring specificity is the presence of multiple isoforms of both p38. p38 exists in four different isoforms p38α, p38β, p38γ and p38δ, and the isoform activated depends both on the stimuli present and the MAP2K involved (Enslen *et al.,* 2000). MKK6 can phosphorylate all four of the p38 isoforms, while MKK3 activates p38α, p38γ and p38δ, and MKK4 is able to only significantly activate the p38α isoform, though it can also weakly activate p38γ and p38δ (Enslen *et al.,* 1998; Enslen *et al.,* 2000; Remy *et al.,* 2010). Specificity of end product production is also obtained by differential activation of MAP2Ks and subsequent p38 isoforms according to the nature of the triggering stimuli. For example, MKK3 is the dominant activator of p38δ by UV radiation, osmotic shock and TNF-α (Remy *et al.,* 2010). With regards to other isoforms, many forms of environmental stress except TNF-α binding activate p38β, while p38α is responsive to a wide range of stresses and cytokines, but not growth factors (Remy *et al.,* 2010).

Optimal activation of p38 in the presence of TNF-α or TGF-β activity requires MKK3 (Wang *et al.,* 2002; Branch *et al.,* 2003). Although MKK6 is non-essential for TNF-α-induced p38 activation,

MKK3 and MKK6 double knockout mice display lower levels of TNF-α-induced p38 stimulation compared to MKK3 single knockout animals. This, along with the similarity of the MKK3 and MKK6 *in vivo* knockout phenotypes, and the fact that loss of one MAP2K does not entirely remove p38 phosphorylation, shows that the two kinases are somewhat redundant, and are able to compensate for each other in the event of expression inhibition (Raingeaud *et al.,* 1996; Brancho *at al.,* 2003; Ma *et al.,* 2007).

As previously mentioned, p38 is activated by stimulation by the key inflammatory mediators TNF-α and TGF-β, meaning that p38, and specifically MKK3 play an important role in the inflammatory response and cytokine production. TGF-β selectively activates the p38α and δ isoforms via MKK3 in order to mediate the formation of extracellular matrixes (Wang *et al.,* 2002). TNF-α also acts via MKK3, stimulating p38 in order to induce the production of cytokines including IL-1 and IL-6, but also a wide range of other cytokines, including IL-5, IL-12(p70), IL-17, eotaxin and GM-CSF (Wysk *et al.,* 1999; Srivastiava *et al.,* 2015). Interferons have been linked to p38 in both the innate and the adaptive immune responses. Both MKK3 and MKK6 are recruited by type 1 interferons during the innate immune response for rapid p38 activation and production of ISGs (Li *et al.,* 2005), while IFN-γ expression by $CD4^+$ and $CD8^+$ T-cells is up-regulated following p38 activation (Conze *et al.,* 2000). The pathology of several viruses are thought to involve p38 in some form, including development of neuronal injury in HIV-1, interferon release and T cell regulation in influenza A virus, and vascular leakage in Dengue virus (Conze *et al.,* 2000; Medders & Kaul, 2011; Börgeling *et al.,* 2014; Fu *et al.,* 2014).

Previous research has shown that VACV is able to interact with not only the p38 pathway but several of the MAPK cascades in a variety of ways. VACV releases a protein, Vaccinia growth factor (VGF) which has sequence homology to the mammalian epidermal growth factor (EGF). The main role of VGF is to modulate host defences and evade the inflammatory response. It also activates the ERK1/2 pathway at early stages of infection (Magalhães *et al.,*2001; Andrade *et al.,* 2004). This activation is then sustained for the duration of VACV replication cycle, and is required for optimal viral DNA replication, as well as anti-apoptotic signals which prevent cell death while the virus replicates (Andrade *et al.,* 2004).

The early VACV protein E3 antagonises protein kinase R (PKR) activity, and subsequently PKR-dependent activation of p38. One of the substrates of p38 in the context of an infection is NF-κB, a transcription factor that mediates cytokine expression. E3 therefore suppresses p38 and NF-κB in order to inhibit the expression of a wide array of anti-viral cytokines, including multiple members of the IFN, IL, TNF and TGF families (Myskiw *et al.,* 2009). Conversely, the VACV protein A52 interacts with TRAF6 in order to activate the p38 pathway and NF-κB activation, resulting in upregulation of the anti-inflammatory cytokine IL-10 production. The interaction of A52 with TRAF6 induces non-classical p38 activation, stimulating TRAF6 oligomerisation and subsequent phosphorylation of MAP3K TAK1. TAK1 is then able to phosphorylate p38 via TAB1, independently of MKK3 or MKK6 (Ge *et al.,* 2002; Maloney *et al.,*2005; Stack *et al.,* 2013). Simultaneously, A52 also inhibits p38-induced NF-κB through differential regulation, and interaction with the interleukin receptor associated kinase 2 (IRAK2), inhibiting the production of cytokines IL-8 and RANTES (Maloney *et al.,* 2005).

These opposing interactions of p38 with VACV exhibits the important role that differential regulation plays in p38 activation and activity. The activation of the p38 pathway by VACV proteins E3 and A52 occurs through non-classical mechanisms: E3 via RIG-I-like receptor signalling (Zhang *et al.,* 2009), and A52 via TAK1, TAB1 and IRAK2 (Maloney *et al.,*2005; Stack *et al.,* 2013). Neither of these mechanisms have shown signs of classical p38 activation involving the major p38 activators MKK3 or MKK6. However, a high throughput loss of function screen of cellular factors influencing VACV replication highlighted MKK3 as having a pro-viral role in VACV growth (Beard *et al.,* 2014). This was the first study to examine the effects of the p38 pathway on VACV growth, rather than the effects of VACV on the p38 cascade and related cellular mechanisms. Therefore, this chapter focuses on examining the role of MKK3 in VACV growth and replication, by siRNA knockdown of the MKK3 gene *in vitro*, and through the use of MKK3 knockout mice.

3.2. Aims

1. To investigate the effect of knockdown of the MKK3 protein by MKK3-targeting siRNA on VACV replication.
2. To examine the *in vivo* effects of MKK3 loss.
3. To identify the stage of the VACV replication cycle that is influenced by MKK3 knockdown.

3.3. Results

3.3.1. Transfection of HeLa cells with MKK3-targeting siRNA inhibits protein expression

In order to investigate the impact of MKK3-loss on VACV spread and replication, MKK3 was knocked down by transfection of specific MKK3-targeting siRNA. A previous study has identified MKK3 as a strong pro-viral host factor, and showed that MKK3 loss resulted in a significant reduction in VACV-induced fluorescence (Beard *et al.,* 2014). Initial experiments in this chapter set out to replicate this finding. In order to investigate the impact of MKK3-loss on VACV spread and replication in vitro, MKK3 expression was inhibited ("knocked down") by transfection of specific MKK3 targeting siRNA. HeLa cells were transfected with either a non-targeting control siRNA directed at the HSV-1 protein VP16 (NT), or a SMARTpool of four individual siRNAs targeting different sequences within the MKK3 gene. A SMARTpool was used rather than one single siRNA to enhance the specificity and magnitude of the siRNA knockdown, and reduce the chances of off-target effects obscuring the true outcome of MKK3 knockdown on VACV growth. At 48h post transfection, cells were collected and MKK3 expression was examined using western blotting. Transfection of cells with the MKK3-targeting siRNA SMARTpool resulted in a 55% significant reduction in protein expression compared to MKK3 levels in the non-targeting control (Figure 3.1A,B)

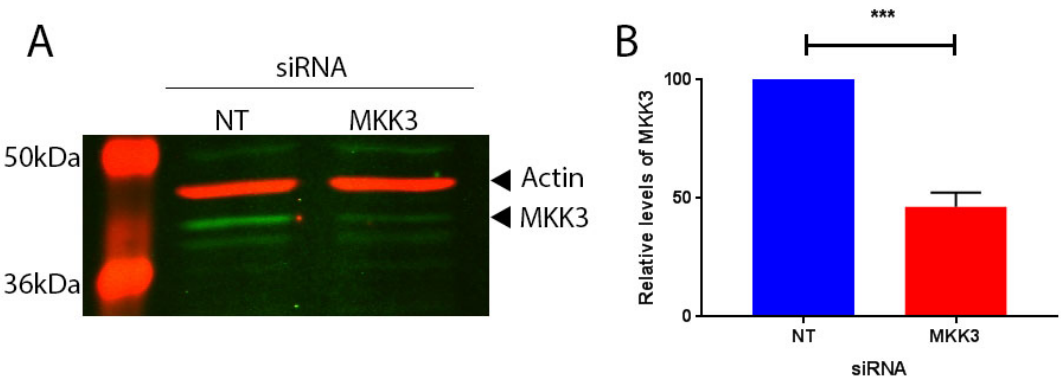

Figure 3.1 MKK3 expression is reduced by siRNA knockdown. (A) HeLa cells were transfected with either a non-targeting siRNA (NT), or a SMARTpool composed of 4 siRNAs targeting MKK3. After 48h, cells were collected and proteins separated by SDS-PAGE, then probed using anti-MKK3 (green) and anti-actin (red) antibodies and visualised using fluorescent secondary antibodies and direct infra-red fluorescence (Li-Cor) on an Odyssey scanner. (B) Levels of MKK3 compared to actin were quantified in MKK3 knockdown cells and the NT control in Image Studio Lite. Data represents means and SEMs of 2 biological repeats. ***,$p<0.001$.

3.3.2. MKK3 knockdown reduces VACV growth as measured by fluorescence

Once the siRNA was shown to successfully reduce MKK3 levels, MKK3 knockdown cells were infected with VACV in order to determine the effect of MKK3 depletion on VACV replication and spread. Here, replication refers to the production of infectious virions, including replication of the viral genome, protein production and morphogenesis of IMVs over the course of one replication cycle. 'Spread' refers to the maturation of IMVs to IEVs, their transport to the cell surface, egress as CEVs or EEVs, and their ability to travel to and infect other cells. Collectively, spread and replication will here be referred to as growth. Firstly, a multi-cycle growth curve was used to examine the growth (incorporating replication and spread) of the virus. In a multi-cycle growth curve, cells are infected at a low MOI, and measurements are taken up to 48h post infection (hpi). Not all cells are infected on inoculation, enabling multiple replication cycles to occur. In these initial studies, a strain of VACV containing the fluorescent protein enhanced green fluorescent protein (EGFP) attached to the A5 capsid protein was used (VACV-A5-EGFP). The EGFP tag allowed fluorescence intensity to be measured as a proxy of viral growth (Carter *et al.,* 2003). HeLa cells were transfected with either an NT siRNA as a negative control, or siRNA targeting the known pro-VACV host factor Rab1A as a positive control. Rab1A is a small GTPase localised to the ER-Golgi membrane, and has been shown to play a key role in VACV growth (Pechenick-Jowers *et al*., 2015; Liu *et al.,* 2016), making it an ideal positive control for VACV growth curves. A third cohort of HeLa cells were transfected with the siRNA SMARTpool targeting MKK3. After 48h of transfection, cells were infected with VACV-A5-EGFP at an MOI of 0.05, and fluorescence was measured at 12h intervals up to 48hpi. The fluorescence levels in all 3 samples remained around 1600 units for the first 36hpi (Figure 3.2A). However, after this time point, the NT siRNA-transfected cells began to exhibit an increase in fluorescence, with levels eventually increasing by 40% compared to background levels present at 0hpi. In comparison, the cells transfected with the Rab1A positive control siRNA exhibited an increase in viral fluorescence of just 2% compared to the 0hpi background levels over the course of the growth curve, confirming the inhibitory effect that Rab1A loss has on VACV fluoresence. Loss of MKK3 only resulted in only a 20% increase in fluorescence over the course of the experiment, a significant reduction compared to the negative control. Therefore, the results shown here are in

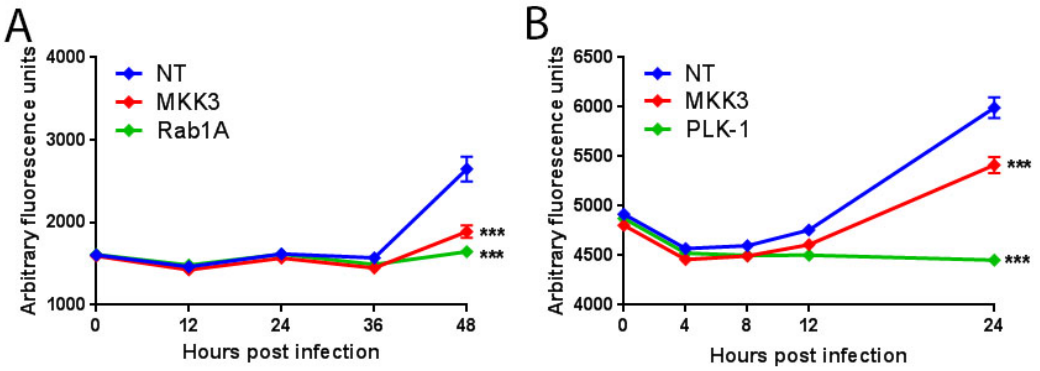

Figure 3.2 MKK3 knockdown inhibits VACV growth in both multi- and single-step growth curves, as measured by fluorescence. (A) HeLa cells were transfected with either a SMARTpool targeting MKK3, NT siRNA as a negative control, or siRNA targeting known cytotoxic gene Rab1A as a positive control. After 48h, transfected cells were infected with VACV-A5-EGFP at an MOI of 0.05, and fluorescence was measured every 12h for 48h. Results show the means and SEMs of five technical repeats and are representative of 2 biological repeats. Statistical analysis was performed using a one-way analysis of variance (ANOVA) with multiple comparisons at the 48 hpi time point. ***, $p<0.001$. (B) HeLa cells were transfected with a SMARTpool targeting MKK3. NT siRNA was used a negative control, while siRNA targeting PLK-1 was used as a positive control. After 48h, transfected cells were infected with VACV-A5-EGFP at an MOI of 5, and fluorescence was measured at 0, 4, 8, 12 and 24h post infection. Results show the means and SEMs of five technical repeats and are representative of 2 biological repeats. Statistical analysis was performed using a one-way analysis of variance (ANOVA) with multiple comparisons at the 48 hpi tie point. ***, $p<0.001$

agreement with those seen in the previously published Beard *et al* study, that MKK3 is a proviral host protein.

Viral replication was also measured via fluorescence over the course of a single step growth curve, in order to examine the effect of MKK3 knockdown on viral replication. HeLa cells were siRNA transfected as described above. After 48h, cells were then infected with VACV-A5-EGFP at an MOI of 5. This high MOI ensures that all cells are infected at the 0h time point, and allows intracellular virion replication to be examined by EGFP fluorescence over the course of one 24h replication cycle. Fluorescence readings were taken every 4h, up till 12hpi, then a final reading was taken at 24h. While NT siRNA was used as a negative control, the serine/threonine protein kinase polo-like kinase (PLK)-1 was used as a positive control rather than Rab1A, as Rab1A affects VACV spread, rather than replication (Pechenick-Jowers *et al*., 2015). PLK-1 is a host cell protein essential for mitosis and cell survival, and inhibition of PLK-1 expression is lethal (Lu *et al.,* 2008). Therefore, transfection of siRNA targeting PLK-1 results in cell death, and subsequently prevents EGFP expression. In cells treated with the NT siRNA, fluorescence signal initially decreased but began to increase again at

12hpi and reached levels clearly above background at 24hpi (Figure 3.2B), consistent with the expected VACV replication kinetics. PLK-1 loss resulted in a significant reduction in viral replication compared to the NT negative control at 24hpi, confirming the efficacy of siRNA transfections (Figure 3.2B). Depletion of MKK3 gave an intermediate phenotype in which the cells clearly supported detectable levels of viral EGFP expression, but to significantly lower levels than the NT control cells. Taken together, these results suggest that MKK3 knockdown significantly inhibits both the replication and spread of VACV, when measured via levels of fluorescence

3.3.3. MKK3 knockdown does not influence production of infectious virions

In order to directly assess the effects of MKK3 loss on the formation of infectious virions, the multi-cycle and single-cycle growth curves were repeated, however virus growth was assessed using a plaque assay rather than measuring A5-linked fluorescence. HeLa cells were transfected with either siRNA targeting the NT negative control, the Rab1A positive control, or the SMARTpool targeting MKK3. After 48h, cells were infected with VACV-WR at low MOI of 0.05, and then were collected, and virus titrated at 12h intervals until 48hpi. Although a reduction of approximately 0.5 $\log_{10}$ in viral titre was seen at 48hpi in the positive control compared to the negative control (Figure 3.3), this result did not reach significance, due to high levels of inter-experiment variance. At 48hpi, there was no difference in viral titre seen between MKK3 knockdown cells and the NT control, and this result was seen consistently across all repeats. Accordingly, in order to examine the effect of MKK3 loss on specific stages of the VACV life cycle, a single-step, titrated growth curve was also performed. At each time point, the supernatant of infected samples was collected separately from the cell monolayers

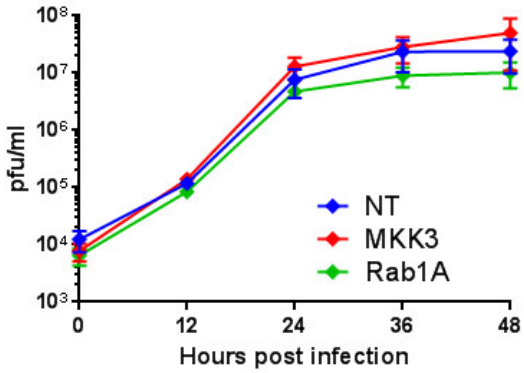

Figure 3.3 Loss of MKK3 does not affect viral titre. HeLa cells were transfected with either a SMARTpool targeting MKK3, NT siRNA, or siRNA targeting known proviral host factor Rab1A. After 48h, transfected cells were infected with VACV-WR at an MOI of 0.05. Cells were collected and titrated for plaque assay at 12h intervals post infection, up to 48hpi. Data is a collation of 3 biological repeats.

in order to measure both extracellular (EEV) and intracellular (IMV, IEV and CEV) production. As described in Materials and Methods, the supernatant was treated with an antibody targeting the early VACV IMV protein L1, thereby neutralising any IMVs present, and ensuring that only the levels of EEVs were examined in the supernatant fraction. The cellular fraction was also collected and titred separately, in order to measure the levels of cell-associated virus (CAV) present, thereby allowing the effects of host protein loss on individual parts of the life cycle to be determined. HeLa cells were

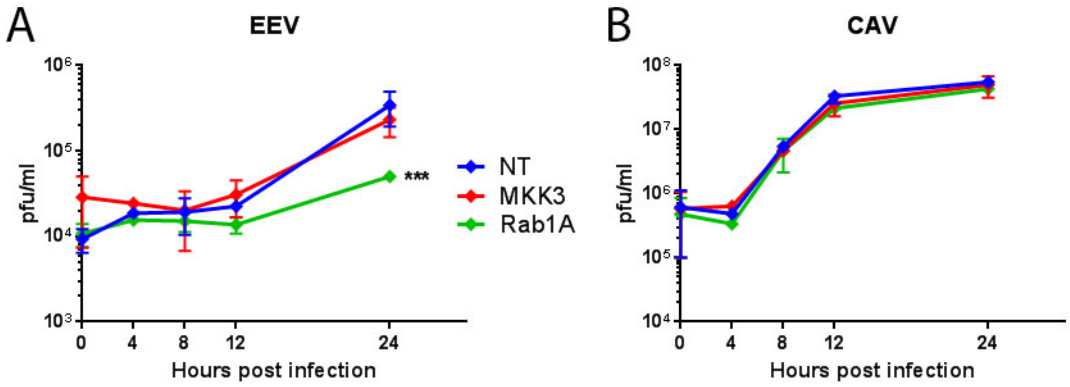

Figure 3.4 Effects of MKK3 loss are not evident in a viral titre in a single replication cycle (A and B) HeLa cells were transfected with either a SMARTpool targeting MKK3, NT siRNA or siRNA targeting Rab1A. After 48 h, transfected cells were infected with VACV-WR at an MOI of 5. At 0, 4, 8, 12 and 24 h post infection, supernatant (A) was removed, neutralised for IMVs using anti-L1 antibody and titrated. Cell monolayers (B) were also collected and titrated. Data represents the means and SEMs of 2 biological repeats. ***, $p<0.001$

transfected with siRNA as described above, and at 48h post transfection, cells were infected with VACV-WR at a high MOI of 5. Supernatant and cells were collected and titred separately at intervals up to 24hpi. At the final time point, Rab1A knockdown had significantly reduced EEV titre in the extracellular fraction compared to the NT negative control (Figure 3.4A). The EEV present in the supernatant of Rab1A knockdown cells increased from $1x10^4$ pfu/ml to $5x10^4$, whereas the cells treated with the NT siRNA control increased from $1x10^4$ pfu/ml to $2x10^5$ pfu/ml, four fold higher than the positive control. This result was consistent with previously published data, as Rab1A is known to affect the wrapping stage of the VACV life cycle, and its depletion detrimentally affects the levels of EEV released (Pechenick-Jowers *et al*., 2015). However, no difference in viral titre in the supernatant was seen when comparing the samples transfected with siRNA targeting MKK3 and the negative control. In the cellular fraction, loss of Rab1A had no effect on viral titre compared to the negative

control, a result which was again in agreement with previous data, as Rab1A does not affect the formation of IMVs, only EEVs (Pechenick-Jowers *et al*., 2015). In addition, no difference in IMV titre was seen in the MKK3 knockdown cells compared to the NT control, in fact the NT-, MKK3- and Rab1A- knockdown cells all demonstrated very similar titres of IMV production at all time points over the course of the experiment (Figure 3.4). Taken together, these results suggest that knockdown of MKK3 has no effect on viral growth when growth is measured directly by titre. However, cell culture does not always accurately reflect the effects of gene knockdown *in vivo*. Therefore, the effect of MKK3 loss *in vivo* was examined.

3.3.4. MKK3 loss does not affect VACV infection *in vivo*

A murine model of VACV disease was used in order to further investigate the relationship between MKK3 and VACV. Pharmaceutical inhibition of MAPK p38 has previously been shown to have protective effects during *in vivo* infection with a number of other viruses, such as influenza A virus and dengue virus (Börgeling *et al.,*2014; Fu *et al.,* 2014). Mice containing an MKK3 null mutation were already available at the Roslin Institute for an influenza project, and were kindly donated by Dr Kenneth Baillie. All mouse work was performed by Dr Pip Beard. Wild type (WT) and MKK3 knockout mice ($MKK3^{-/-}$) were either given an intranasal inoculation of $1x10^4$ pfu VACV-WR, or mock infected with the PBS vehicle. Body weights and clinical symptoms were then recorded daily over the course of a 7d infection. Clinical symptoms included ruffled fur, weight loss, hunched posture and reduced activity, and were scored on a 0-3 scale according to severity, where 0 indicated no symptoms, and 3 indicated severe signs. Uninfected mice, both WT and $MKK3^{-/-}$ maintained their body weight over the course of the infection (Figure 3.5A), while infected mice, of both phenotypes exhibited weight loss of up 25% of their starting weight by 7days post infection (dpi). There was no difference between the weight loss seen in infected, WT mice and in infected $MKK3^{-/-}$ mice. A similar trend was seen in the scoring of clinical symptoms recorded during the infection (Figure 3.5B). Uninfected mice of both phenotypes showed no clinical signs as expected, and though clinical symptoms appeared a day earlier in $MKK3^{-/-}$ mice than in the WT animals, by the end of the experiment, both groups exhibited the same levels of symptoms. These results show that loss of MKK3 does not greatly influence the severity of VACV disease in mice.

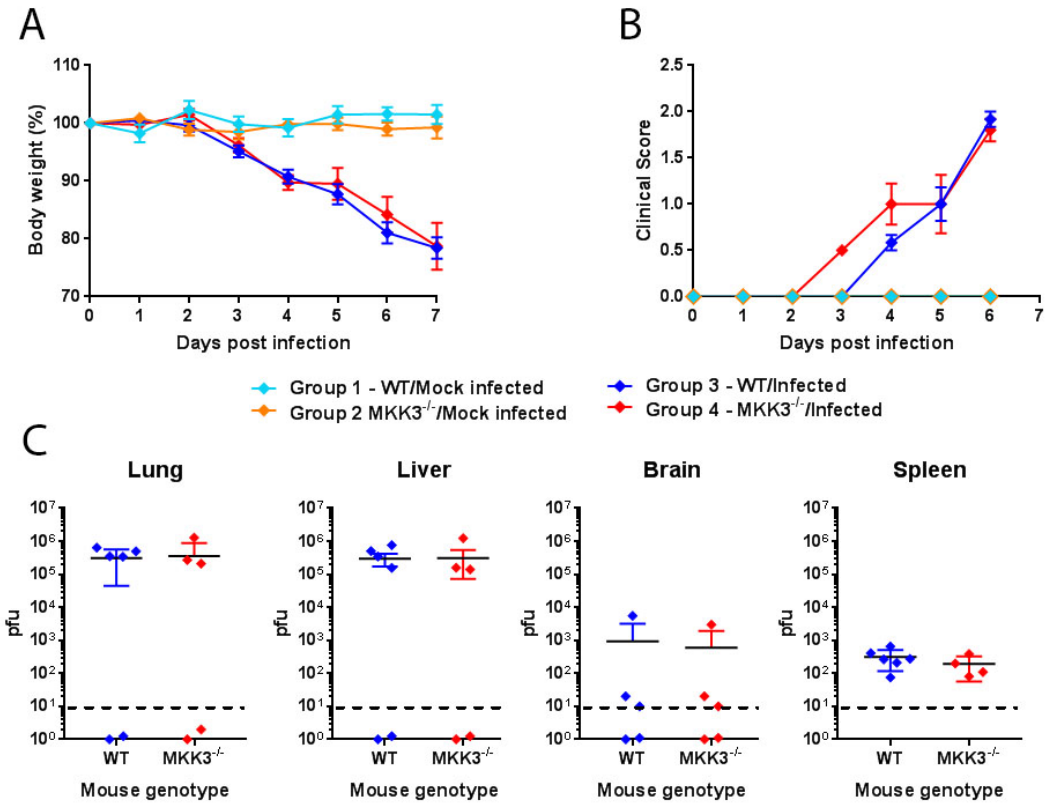

Figure 3.5 MKK3 loss does not affect viral growth or disease in a murine model of VACV *in vivo*. WT C57BL/6 mice and C57BL/6 with an MKK3 null mutation ($MKK3^{-/-}$) were originally obtained from The Jackson Laboratory, and donated to this project by Dr Kenneth Baillie. Animals were randomly sorted into groups of 6, and one group of 5. Group 1 were WT mice, mock infected with PBS. Group 2 were mock infected, $MKK3^{-/-}$ knockouts. Group 3 were WT mice were inoculated intranasally (i.n.) with $1x10^4$ PFU of purified VACV-WR on day 0. Group 4 were $MKK3^{-/-}$ knockout mice infected on day 0 as described (group of 5). All mice were examined daily for weight loss (A), and clinical symptoms (B). At 7dpi, the experiment was terminated and viral loads were assessed (C). Lungs, livers, brains and spleens were collected from all infected mice and processed for viral titration using plaque assay. Mean titre and SEM are also shown. Dashed line on scatter plots represents the limits of detection.

At the conclusion of the experiment, lungs, liver, brains and spleen were collected from infected mice, and lysed and titred for virus. In all four organs examined: brain. lung, liver and spleen, there were no significant differences in viral titre between the WT and $MKK3^{-/-}$ mice (Figure 3.5C). Although the brains, lungs and livers of several individuals exhibited viral titres below the limits of detection, equal numbers of these 'titre-negative' mice were seen in both phenotypes in each organ, therefore resulting in no overall difference in viral titre. Interestingly, the individuals seen to have undetectable viral titres in one organ did not necessarily have undetectable levels of virus in other organs. Overall, these show that MKK3 loss has no effect on viral titre in a variety of organs *in vivo*.

In order to further investigate the course of VACV infection in an MKK3 knockout mouse, histological analysis was performed on the lung, liver brain and spleen tissue of infected mice. All sections for histology were examined by Dr Pip Beard, a trained veterinary pathologist. The tissue sections were fixed in neutral buffered formalin and stained according to standard haematoxylin and eosin protocols, before being examined blinded (Figure 3.6). After examination, slides were unblinded and each group analysed. In the lung tissue, neither WT nor MKK3$^{-/-}$, mock infected mice exhibited any significant lesions, as expected. 4 of the 6 infected WT mice, and 2 of the 5 infected MKK3$^{-/-}$ mice exhibited moderate levels of pathology characterised by multifocal, subacute, fibrinonecrotic bronchopneumonia with rare intracytoplasmic eosinophilic inclusions in the lung tissue. The remaining 2 infected WT mice and 3 MKK3$^{-/-}$ mice displayed milder changes characterised by mild to moderate perivascular inflammation (neutrophils, lymphocytes and macrophages). Overall, there was

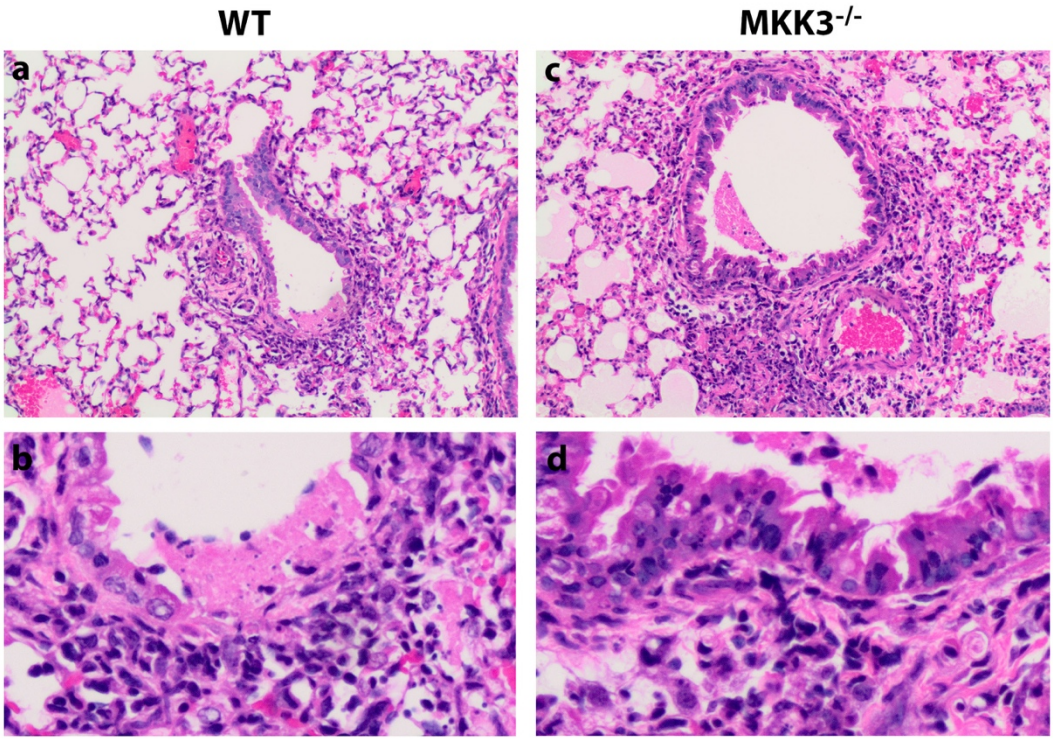

Figure 3.6. MKK3 loss does not affect VACV-induced tissue pathology. Lung tissue was collected at necropsy from the WT (a and b) and MKK3$^{-/-}$ (C and d) mice used in Figure 3.5. Tissue sections were fixed in neutral buffered formalin and stained according to standard haematoxylin and eosin protocols. Slides were examined blind, by light microscopy, for signs of disease. Slides were later unblinded and each group analysed. All histopathology carried out by Dr Pip Beard.

no histopathological evidence present that suggested that MKK3 loss affected disease *in vivo,* as the pathological changes identified and severity of lesions did not correlate with genotype. In addition, no significant pathology was identified in the liver, spleen or brains of any mice involved in the experiment (data not shown).

3.3.5. MKK3-dependent cytokine expression is not essential for VACV clearance *in vivo*

As loss of MKK3 had no effect on the overall course of VACV infection in the mouse model, we examined the *in vivo* effects of MKK3 loss on cytokine levels in mouse tissue to determine if MKK3 gene deletion resulted in any changes in immune response during infection. In order to do this, a cytokine array was performed on tissues collected from the mouse experiment described in 3.3.4. Previous studies have shown that MKK3-dependent p38 activation is essential for the expression of a wide range of cytokines, including multiple members of the IL, and IFN families, eotaxin, GM-CSF, macrophage inflammatory protein (MIP-1), and TNF-α (Wysk *et al.,* 1999; Lia *et al.,* 2005; Srivastiava *et al.,* 2015). The clearance of a VACV infection is also dependent on a number of cytokines, several of which overlap with those dependent on MKK3 activation for expression; including type I and type II interferons, IL-1β, IL-10, IL-12p40 and TNF-α (Haga & Bowie, 2005; Ryan *et al.,* 2009). The cytokine array aimed to examine the cytokine response to VACV infection, and determine if MKK3 loss results in any changes in immune response to VACV infection, that could be too subtle to be seen using body weight, clinical signs, or histopathology. Lung tissues from infected WT and MKK3$^{-/-}$ mice were pooled and analysed using a mouse cytokine array panel, consisting of immobilised capture antibodies for 40 different cytokines in duplicate on a nitrocellulose membrane. Clarified tissue was incubated with the membranes to allow binding, and fluorescent detection reagents were used to produce a signal proportionate to the amount of cytokine present. A PBS negative control was also used, which exhibited a relative fluorescent level of 0, and a reference spot provided by the kit was used as a positive control, which gave a relative level of 100. Only 10 cytokines showed a significant difference in expression between WT and MKK3$^{-/-}$ lung tissue lysates: I-309, eoxtaxin, IL-1β, IP-10 (CXCL10), MCP-5 (CCL12), MIG (CXCL9), MIP-1α (CCL3), MIP-1β (CCL4), TIMP-1 and TREM-1. The level of significance varied from $p< 0.05$ to $p<0.001$ (Figure 3.7). All the significant changes identified showed a decrease in cytokine/chemokine expression in the MKK3$^{-/-}$ compared to the WT samples, with the exception of TREM-1, which exhibited a higher level

of expression in the MKK3$^{-/-}$ samples. Of the 10 differentially expressed cytokines, IL-1β, eotaxin, MIP-1α, MIP-1β, exhibit a direct dependence on MKK3-induced p38 activation for their expression (Srivastiava *et al.,* 2015). IP-10, TIMP-1 and TREM-1 are dependent on general p38 signalling (Tibbles *et al.,* 2002; Tong *et al.,* 2004; Murakami *et al.,* 2007) while I-309, MIG and MCP-5 have only been loosely linked to p38 (Wang *et al.,* 2006; Kanda *et al.,* 2007; Huang *et al.,* 2010). The reduction of expression levels of these cytokines and chemokines indicates that the p38 pathway is affected by MKK3 loss, but that this loss is not significant enough to impact viral growth. In conclusion, loss of MKK3 *in vivo* results in an inhibition in the cytokine response to infection, but this inhibition is not sufficient to alter the course of VACV disease as a whole. When considered together, the results of the cytokine array, *in vivo* experiment and direct measurement of viral growth indicate that MKK3 loss, whether by siRNA knockdown, or genetic mutation, is not sufficient to inhibit VACV growth in cells or mice.

Figure 3.7 (facing page) MKK3 is not essential for an overall effective cytokine response. Levels of cytokines present the mice used in Fig3.5 were analysed using an R&D systems mouse cytokine array panel, according to the protocol provided in the kit. Cytokine levels were visualised using fluorescent secondary antibodies and a LiCor Odyssey. Data shows means and SEMs of 2 technical repeats. Multiple T-tests were used for statistical analysis. *,$p<0.05$; **,$p<0.01$; ***,$p<0.001$.

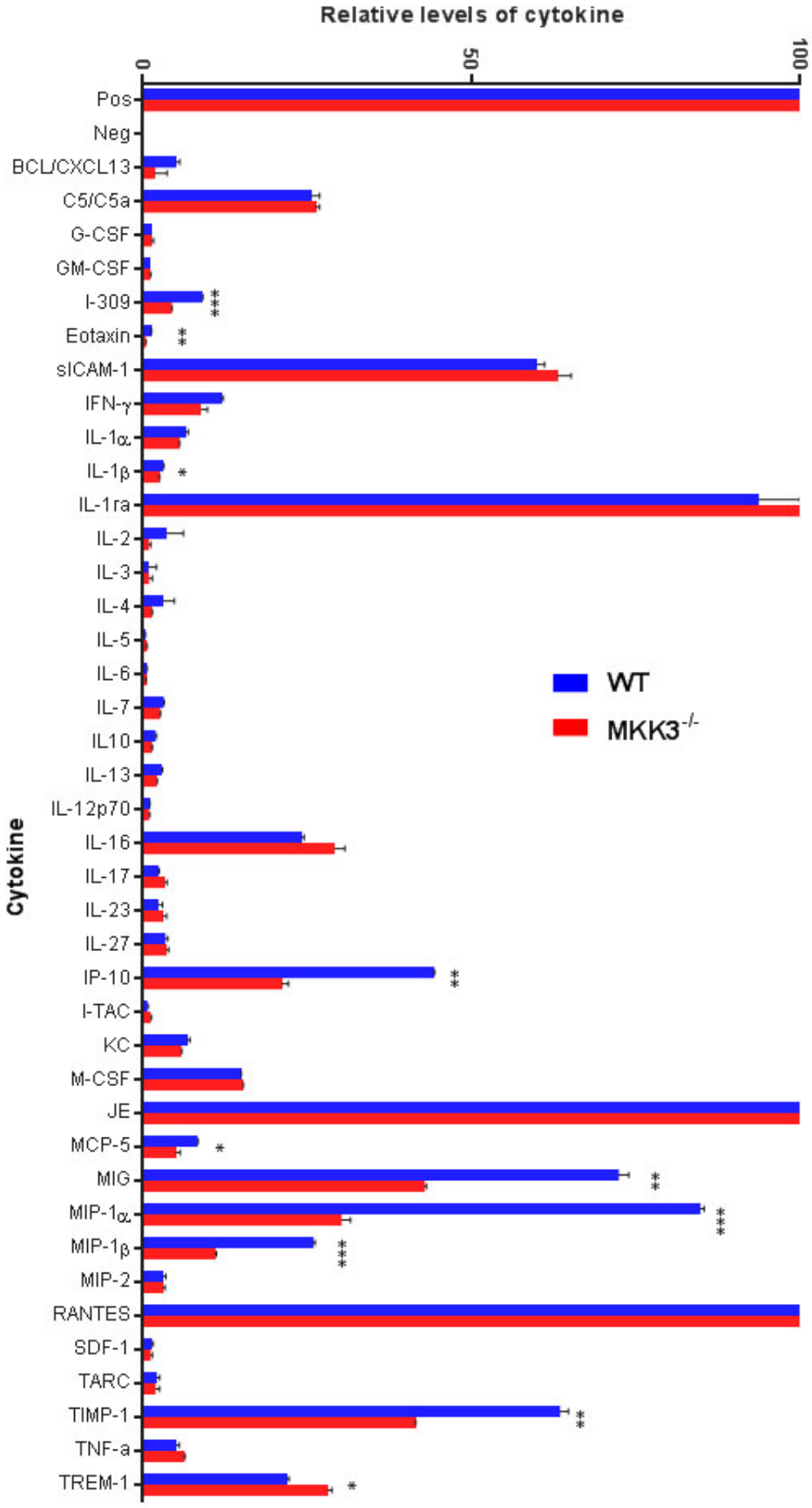
Relative levels of cytokine
0
50
100
Cytokine
Pos
Neg
BCL/CXCL13
C5/C5a
G-CSF
GM-CSF
I-309
Eotaxin
sICAM-1
IFN-γ
IL-1α
IL-1β
IL-1ra
IL-2
IL-3
IL-4
IL-5
IL-6
IL-7
IL10
IL-13
IL-12p70
IL-16
IL-17
IL-23
IL-27
IP-10
I-TAC
KC
M-CSF
JE
MCP-5
MIG
MIP-1α
MIP-1β
MIP-2
RANTES
SDF-1
TARC
TIMP-1
TNF-a
TREM-1
WT
MKK3-/-

3.3.6. MKK3 knockdown does not reduce total or phosphorylated p38 levels

Despite the results demonstrating that alteration of MKK3 expression levels does not affect production of infectious virions *in vitro* or *in vivo*, or alter disease course in mice, there still remains the apparent reduction in VACV growth in MKK3 knockdown cells when measured via fluorescence of EGFP tagged to the A5 capsid protein. The final section of this work concentrated on determining the reason for the apparent reduction in A5 production (Figure 3.2). Initially, levels of p38 and phosphorylated p38 (Pp38) were examined in control and MKK3 knockdown cells. MKK3 is one of the three MAP2Ks responsible for activating the MAPK p38, along with MKK6, and to a lesser extent, MKK4 (Raingeaud *et al.,* 1994; Derijard *et al.,* 1995; Han *et al.,* 1996; Moriguch *et al.,* 1996; Raingeaud *et al.,*1996). Therefore, MKK3 knockdown may not be sufficient to impact overall Pp38 levels. HeLa cells were transfected with either the NT negative control siRNA, or an siRNA SMARTpool targeting MKK3. After a 48h transfection, cells were either infected with VACV-WR at an MOI of 5, or mock infected. At 0, 1 and 2hpi, cells were collected and examined for levels of p38 and Pp38 by Western blotting. With some fluctuations, levels of p38 in the Western blot appeared consistent across the 2h in uninfected and infected cells, and in both NT control and MKK3 knockdown conditions (Figure 3.8A). Pp38 levels in both infected, WT and MKK3 knockdown cells also appeared relatively consistent, though again fluctuations were seen (Figure 3.8C & D). In uninfected MKK3 knockdown cells, Pp38 appeared to decrease over the course of the experiment, though no consistent trend was seen in NT-transfected cells. Overall, these results suggest that knockdown of MKK3 does not consistently affect the expression of p38, or its activation, compared to NT cells. However, these results represent only one biological repeat and therefore further repeats would need to be performed in order to performs statistics and draw any definitive conclusions.

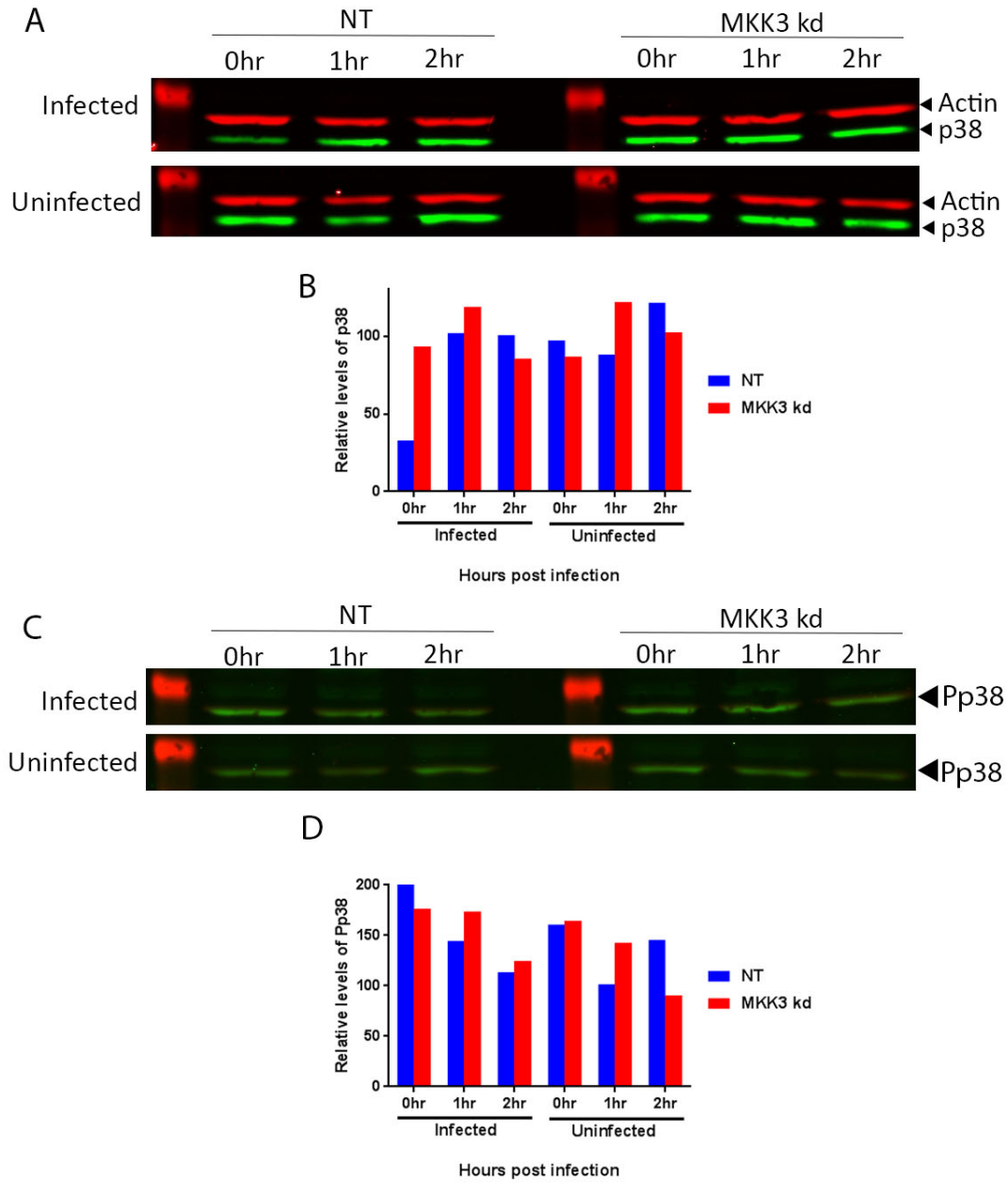

Figure 3.8 MKK3 knockdown does not reduce total or phosphorylated p38 levels. HeLa cells were transfected with either a non-targeting siRNA (NT), or a SMARTpool composed of 4 siRNAs targeting MKK3. After 48h, cells were infected with VACV-WR at MOI 5, or mock infected as an uninfected control. At 0, 1 and 2h post infection, cells lysed and proteins separated by SDS-PAGE, then probed using anti-p38 (A) or anti-phosphorylated p38 (C) and anti-actin antibodies, and visualised using fluorescent secondary antibodies and direct infra-red fluorescence (Li-Cor) on an Odyssey scanner. Image Studio Lite was used to quantify the total p38 (B) and phosphorylated p38 (D) blots. The actin loading control bands were used to normalise the quantification of p38 and Pp38. Data represents one biological repeat.

3.3.7. MKK3 loss affects production of VACV proteins

As levels of p38 nor Pp38 were not consistently affected in the MKK3 deficient cells compared to the control cells, levels of viral proteins were examined in the knockdown cells in order to further investigate the role that MKK3 apparently plays in the generation of fluorescence during VACV infection. Ultimately, a fluorescent growth curve, using the VACV-A5-EGFP strain does not directly measure viral production. Instead, production of the tagged A5 protein is being measured (Carter *et al.,* 2003). Therefore, we considered the possibility that MKK3 loss was affecting viral protein production rather than whole virion replication. The early IMV protein E3, and the late protein D8 were selected to investigate the levels of viral protein over the course of one replication cycle to see if A5 production was specifically affected, or if a there was a more global effect on viral protein production. Early proteins such as E3 are transcribed immediately upon virion uncoating and viral mRNA may be produced as early as 12 minutes post infection (Kates & McAuslan, 1967; Munyon et al., 1967; Wright *et al.,* 2001). In contrast D8 is a late protein, and so is not transcribed until late in the replication cycle after DNA replication has occurred (Keck & Moss, 1990) astranscription factors for late proteins are typically activated at approximately 4.5hpi.

HeLa cells were transfected with either the NT control siRNA, or the siRNA SMARTpool targeting MKK3. After 48h transfection, cells were infected with VACV-WR at a high MOI of 5. At 2h intervals, up to 8h post infection, cells were collected and the levels of E3 and D8 were examined by Western blotting (Figure 3.9A). MKK3 levels were also included, to test that the siRNA knockdown had worked. Actin was used as a loading control. Visualisation of the SDS-PAGE gel showed a clear reduction in MKK3 expression in the cells transfected with MKK3-targeting siRNA compared to the NT control (Figure 3.9A). Quantification of these bands relative to the actin loading control confirmed an average reduction in MKK3 expression of 50% throughout the infection (Figure 3.9B), consistent with the 55% reduction seen in Figure 3.1

Levels of the early VACV capsid protein E3 increased over the course of the full 8h infection in both control and MKK3 knockdown cell types as expected. However, the MKK3-deficient cells showed a reduction in E3 expression compared to the NT negative control transfected cells (Figure 3.9A). This was confirmed by quantification of the bands visualised in the western blot (Figure 3.9) which showed

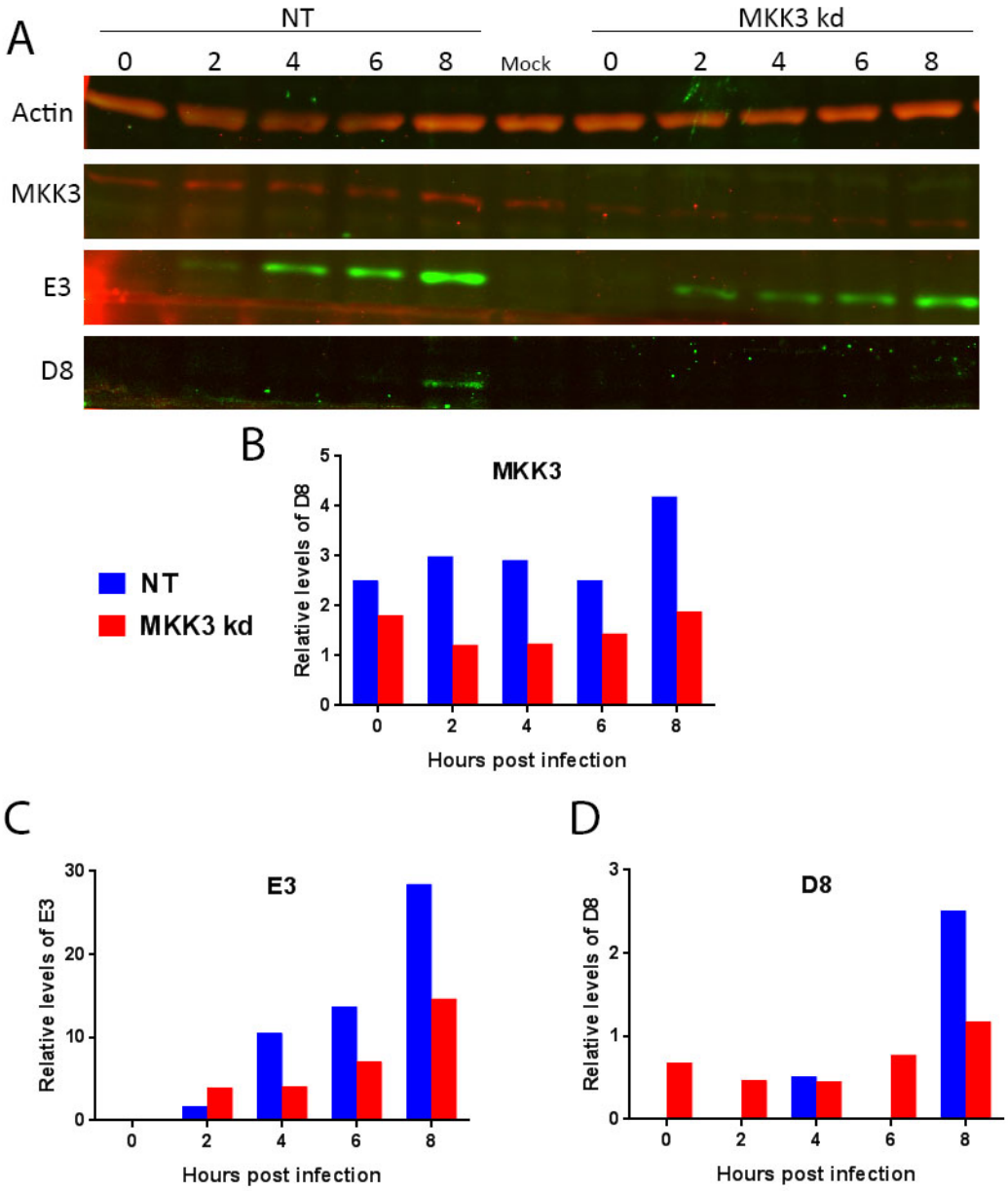

Figure 3.9. MKK3 loss affects production of VACV proteins. HeLa cells were transfected with either a non-targeting siRNA (NT), or a SMARTpool composed of 4 siRNAs targeting MKK3. After 48h cells were infected with VACV-WR at MOI 5, or mock infected as an uninfected. At 0, 2, 4, 6 and 8h post infection, cells were were lysed and proteins separated by SDS-PAGE, and then probed using antibodies raised against MKK3, early VACV protein E3, or late VACV protein D8. Anti-actin antibodies were used as a loading control (A). Bands were visualised using fluorescent secondary antibodies and direct infra-red fluorescence (Li-Cor) on an Odyssey scanner, and were normalised according to the actin loading control. Image Studio Lite was used to quantify the levels of MKK3 (B), E3 (C) and D8 (D). Data represents one biological repeat.

that E3 expression in MKK3 knockdown cells was inhibited by approximately 50% by MKK3 depletion compared to the NT control at 4, 6 and 8hpi. Levels of D8 expression were far lower overall (Figure 3.9A). Minimal levels of protein were detected in NT and MKK3 knockdown cells from 0-6h, possibly from input virus. Quantification showed that D8 was not expressed in control cells until

8hpi (Figure 3.9D). At 8hpi, MKK3 loss resulted in an approximate two-fold reduction in D8 expression compared to the NT-transfected control cells. Together, these reductions in both early and late protein production in MKK3 knockdown cells indicate that MKK3 loss impairs viral protein production, possibly in a p38-independent manner.

3.4. Discussion

The main focus of this chapter was to examine the effect of MKK3 loss on VACV growth through siRNA transfection *in vitro,* and genetic mutation *in vivo,* and to subsequently characterise this interaction. A potential pro-VACV role for MKK3 was first highlighted during a high-throughput siRNA-based screen for host factors involved in VACV infection, in which MKK3 appeared as a positive hit (Beard *et al.,* 2014). MKK3 is a MAP2K which, along with MKK6 and to a lesser extent, MKK4, initiate dual phosphorylation, and activation of the MAPK p38 in order to then activate genes involved in a wide range of cellular mechanisms, including apoptosis, cell differentiation and immune response (Raingeaud *et al.,* 1994; Derijard *et al.,* 1995; Han *et al.,* 1996; Moriguch *et al.,* 1996; Raingeaud *et al.,*1996).

For the *in vitro* investigations, a SMARTpool of four siRNAs was used to knockdown MKK3, resulting in approximately a 55% reduction in gene expression. Initially, these knockdown cells were used to investigate the effect of MKK3 loss on VACV growth and replication, using a strain of VACV containing EGFP bound to the VACV A5 capsid protein. This virus allows EGFP fluorescence to be used as a surrogate measure of viral growth (Carter *et al.,* 2003). Viral replication and spread, i.e. the completion of several sequential life cycles, was measured using a multicycle growth curve. Viral replication was measured using a single-cycle growth curve. The observed reduction in MKK3 expression significantly reduced EGFP fluorescence when compared to the non-targeting siRNA control. However, when viral load was measured directly by titre, rather than indirectly by fluorescence, no significant difference was seen either in multi-cycle growth or the EEV and IMV fractions of a single replication cycle. This result was also translated to the *in vivo* investigations. WT and MKK3$^{-/-}$ C57BL/6 mice infected with VACV-WR and observed over the course of 7 days showed no differences in clinical symptoms, weight loss or disease progression. In addition, no difference in viral load or histopathology was identified.The levels of 40 key cytokines in the lungs of the mice from the *in vivo* time course were examined, and although 10 cytokines which have previously been implicated as interacting with MKK3 were significantly reduced in the MKK3$^{-/-}$ animals, the overall all change in cytokine response was not sufficient to alter the course of disease.

The final experiments in this programme of work concentrated on the discrepancy between the two methods of assessing viral growth – the levels of VACV-A5-EGFP fluorescence in MKK3 knockdown cells was reduced compared to the negative control, however viral titres were unchanged. When the levels of p38 and phosphorylated p38 were examined in infected and uninfected cells, no differences were seen in total p38 levels in MKK3 deficient cells compared to negative control cells. Phosphorylated p38 appeared to decrease over the course of the experiment in both infected and uninfected cells. Finally, levels of VACV IMV proteins were examined over an 8h infection. Levels of both the early protein selected, E3, and the late IMV protein D8 were reduced in MKK3 knockdown cells, suggesting MKK3 promotes viral protein production.

While the Beard *et al.* siRNA screen identified MKK3 in particular as a pro-viral host factor, the p38 pathway has previously been linked to VACV infection. However, previous work has not examined the effect of p38 on VACV growth, but instead focused on the effects of VACV on the p38 pathway. Early VACV IMV protein E3 inhibits PKR-dependent p38 activation in order to suppress NF-κB and the production of inflammatory cytokines (Myskiw *et al.,* 2009). Another VACV protein, A52 deliberately activates p38 via TRAF6 and TAK1 in order to upregulate NF-κB and the production of anti-inflammatory cytokine IL-10, and simultaneously inhibits IRAK2-induced p38 to suppress NF-κB and cytokines IL-8 and RANTES (Maloney *et al.,* 2005; Stack *et al.,* 2013). However, none of these interactions are known to occur via the classical p38 activation pathway, involving MKK3 or MKK6. The identification of MKK3 as a proviral host factor in the 2014 high-throughput screening (Beard *et al.*) is the first time that VACV has been linked to the p38 pathway via one of the classical, and most significant MAP2Ks, MKK3. The initial results in this chapter, replicated the effects of MKK3 loss seen in the high-throughput screen, as the validation of the MKK3 knockdown was also performed using the fluorescent virus, rather than titre (Beard *et al.,* 2014). However, further investigation showed that the direct growth of VACV was not affected, either *in vitro* or *in vivo*, by MKK3 knockdown or MKK3 null mutation.

The discrepancy between the two methods of viral growth measurement identified in this work highlights the importance of careful analysis of results seen in high throughput screens. During high-throughput screens large numbers of samples must be examined therefore a fast, cheap and relatively

easy method of measuring virus growth is required such as the use of fluorescently labelled VACV. However, this chapter demonstrates that fluorescent assays are not necessarily equivalent to viral titre, as fluorescence measures levels of expression of a viral protein, not production of infectious virion. It is important that any positive results obtained from these screens are validated using direct methods of viral growth measurement.

Loss of MKK3 *in vivo* did not have any significant effects of disease course, body weight, or viral load. Histopathology of the lungs of infected mice also showed no difference in $MKK3^{-/-}$ compared to knockout. However, a cytokine panel array performed on the lung tissue of infected mice showed significant differences in the expression of ten cytokines: I-309, eoxtaxin, IL-1β, IP-10 (CXCL10), MCP-5 (CCL12), MIG (CXCL9), MIP-1α (CCL3), MIP-1β (CCL4), TIMP-1 and TREM-1. All 10 of these cytokines have previously been linked to the p38 pathway (Srivastiava *et al.,* 2015; Tibbles *et al.,* 2002; Tong *et al.,* 2004; Murakami *et al.,* 2007; Wang *et al.,* 2006; Kanda *et al.,* 2007; Huang *et al.,* 2010). The reduction in expression of these cytokines indicates that the p38 pathway is inhibited by the loss of MKK3 in mice. However, several other cytokines/chemokines that are suggested to rely on MKK3 signalling, such as IFN-γ, GM-CSF and IL-17 did not exhibit any significant changes in expression in the $MKK3^{-/-}$ samples, which may be due to the ability of MKK6 to compensate for MKK3 loss, but only for certain pathways, triggers or downstream activators. (Raingeaud *et al.,* 1996; Brancho *at al.,* 2003; Ma *et al.,*2007).

Of these ten cytokines/chemokines, IL-1β, IP-10, I-309, eotaxin, MCP-5, MIG and MIP-1α are known to be part of the innate immune response to successfully clear a VACV infection (Perera *et al.,* 2001; Reading *et al.,* 2003; Haga & Bowie, 2005; Krathwohl *et al.,* 2006; Delaloye *et al.,* 2009; Ryan *et al.,* 2009; Hickman *et al.,* 2015). No evidence exists in the literature of VACV interacting with, or triggering the expression of TIMP-1 or TREM-1. However, as the reduction of these cytokines did not affect disease progression in the $MKK3^{-/-}$ mice, this suggests that they may not essential for the VACV-specific immune response, or can be compensated for by other immune components. Alternatively, the suppression of cytokine response in $MKK3^{-/-}$ mice was not of a great enough magnitude to an effect on the overall disease. For example, IL-1β expression was inhibited only by 19% in the $MKK3^{-/-}$ mice. Aside from IL-1β, few of the cytokines which are considered key to an

anti-VACV immune response such as IFNs or TNF-α, were affected by MKK3 loss, which may explain why no overall change was seen in disease progression *in vivo* (Haga & Bowie, 2005; Ryan *et al.,* 2009). Furthermore, cytokine levels were only examined in lung tissue, and it is possible that other organs or tissues expressed different levels of cytokines, and showed different effects to MKK3 loss.

When VACV infects a cell, it shuts down translation of host proteins, in order to prioritise the expression of its own genes. The virus then specifically removes the translational repressor, eIF4E binding protein (4E-BP) of the key eukaryotic translation initiation factor 4F (eIF4F), and promotes activation of this initiation factor, thereby increasing viral replication and gene expression (Walsh *et al.,* 2008). This critical component of translation is rapidly activated by the MAP kinase-interacting kinase 1 (Mnk1), which in turn is activated by the MAPKs p38, and ERK. It has been shown that stimulation of Mnk1 further increases viral replication and protein expression (Waskiewicz *et al.,* 1997; Walsh *et al.,* 2008). MKK3 loss may alter p38 phosphorylation, leading to lower levels of Mnk1 activation, and subsequently reduced activation of eIF4F and viral protein production. However, as discussed previously, further examination of the levels of Pp38 in MKK3 knockdown cells would be required to confirm this hypothesis. Examination of eIF4F and Mnk1 levels would also help to determine if the role of MKK3 in VACV protein production is as a part of the p38 cascade, or if it is a secondary, p38 independent role, as well as determining if VACV utilises the p38 pathway only through non-classical routes such as TAK1 and IRAK2.

Levels of phosphorylated, and therefore activated p38 did not appear to be reduced as expected in MKK3 cells, potentially due to the ability of MKK6 to compensate to a certain extent for its fellow MAP2K (Raingeaud *et al.,* 1996; Brancho *at al.,* 2003; Ma *et al.,*2007). Titres of VACV both *in vivo* and *in vitro* are unaffected by MKK3 loss, as is clinical disease, despite the clear effect on viral protein production. This indicates that although viral protein production is significantly impaired, this inhibition is not sufficient to effect viral replication as a whole, and therefore suggests that during infection VACV produces an excess of capsid proteins. VACV is not currently known to produce any excesses of early or late proteins, though this phenomenon has been observed in other viruses, such as

hepatitis B (HBV). Excess proteins produced by HBV multimerise in the ER and are released as non-infectious subviral particles (Churin *et al.,* 2015).

Despite the evidence presented here, further investigation would be required to fully elucidate the role of MKK3 in VACV infection. The first and foremost task for extended investigation of this topic would be the repetition of the total p38 and Pp38 western blots, as well as the VACV protein production western blots, in order to generate statistics and be able to make reliable conclusions. Viral titrations could be performed with VACV-EGFP, to allow direct comparison between fluorescence assays and plaque assays, by using the same virus. Aside from these current weaknesses, there are multiple areas that could be further characterised. For example, another avenue of investigation would be to examine the effects of MKK6 loss, as MKK3 and MKK6 are closely related and share 79% of their genetic identity (Moriguchi *et al.,* 1996). Effects of MKK6 loss on fluorescence assays and titre would be examined both alone, and as a double knockdown with MKK3, to determine the presence of any synergistic effects. There also exist blanket p38 inhibitors such as SB203580, which has been shown to reduce EGFP expression in monocytes infected with VACV-EGFP (Hu *et al.,* 2007), and SB202190, which inhibits growth of an EGFP-tagged strain of monkeypox virus (Kindrachuk *et al.,* 2011). Both these studies used EGFP as a measure of viral growth, so the next step would be to treat cells with these p38 inhibitors, then directly examine formation of infectious virions by a plaque-assay based growth, as well as examining viral protein levels. This would determine if it is still only protein production that is affected during complete p38 inhibition, or if the effect is great enough that virion formation is also affected. p38 exists as multiple isoforms – p38α, p38β, p38γ and p38δ, and MKK3 activates only p38α, p38γ and p38δ, and MKK6 is able to activate all 4 isoforms (Enslen *et al.,* 1997; Brancho *et al.,* 2000; Remy *et al.,* 2010). Therefore, even when MKK3 is knocked down by siRNA or the gene mutated, MKK6 is still able to activate p38, and compensate for the loss of the closely related MKK3. Use of p38 inhibitors to block the kinase cascade would therefore ensure a more universal effect, by blocking all p38 isoforms, and potentially amplify the effects of p38 inhibition compared to just targeting MKK3.

The link between VACV and cellular translation could be further examined by measuring the levels of phosphorylated Mnk1, or activated eIF4F during VACV infection and MKK3 deficiency.

Additionally, it is always good scientific practice to examine the effects of gene loss knockdown in more than one cell line, especially when established lab strains such as HeLa cells have been used, as they are no longer comparable to primary cell-derived lines, and so the loss of MKK3 may elicit a different response in different cells.

Overall, this chapter shows that removing a key activator of the p38 pathway, MKK3, does alter susceptibility of mice to VACV disease. Neither does it affect virion production, however it does impair viral protein expression. Further studies are required to determine if this is via a p38-dependent or independent mechanism. Additionally, while this chapter successfully shows that MKK3 can be successfully knocked down by siRNA targeting, and that MKK3 has a highly specific effect on the VACV life cycle, it also highlights the pitfalls of using high-throughput screens.

4 Blocking cellular retrograde transport by destabilising the GARP complex inhibits VACV morphogenesis

4.1. Introduction

Retrograde transport refers to the recycling of proteins from endosomes back to the TGN, in order to maintain homeostasis in the cell. The general mechanism of retrograde transport is the same as anterograde transport. Selected donor compartment proteins are sorted into a budding vesicle for release. Vesicle coat proteins such as clathrin initiate budding and sorting by the formation of curvature-inducing scaffolding on the donor surface (McMahon & Mills, 2004). V-SNAREs on vesicle membranes and t-SNAREs on acceptor compartments then target transport vesicles to the correct acceptor compartment, where tethering factors and Rab GTPases facilitate membrane binding and fusion, completing cargo delivery (Bonifacino & Glick, 2004). Although retrograde transport can occur via a number of different pathways, some of these pathways overlap, and it is possible for cargo to utilise more than one pathway. For example, CI-MPR can travel both by retromer-dependent transport in HeLaM cells via the recycling endosomes, and by GARP-dependent transport in HeLa cells, via early and late endosomes (Carlton *et al.,* 2004; Pérez-Victoria *et al.,* 2008). The retrograde transport system can be hijacked by microbial invaders such as the recruitment of EGRTP components by *L. pneumophila* to the *Legionella*- containing vacuole in order to promote bacterial growth (Finsel *et al.,* 2013). The enterohaemorrhagic *E. coli* (EHEC) shiga toxin (STx) B subunit uses clathrin mediated endocytosis to enter cells then is able to travel via retrograde transport pathways from endosomes to TGN and eventually to the endoplasmic reticulum where it inhibits protein synthesis. Like CI-MPR, STxB is able to interact with both early and recycling endosomes, and therefore utilises more than one retrograde transport pathway (Mallard *et al.,* 1998).

The GARP complex is a tethering factor of the quatrefoil family that is specific to retrograde transport cargo, and is comprised of four large proteins, Vps51, Vps52, Vps53 and Vps54 (Conibear *et al.,* 2003; Vasan *et al.,* 2010). In both yeast and human cells, Vps51 was discovered significantly later than the other three components due to its smaller size and milder mutation phenotype (Siniossoglou & Pelham, 2002; Pérez-Victoria *et al.,* 2010b). GARP localises predominantly to the TGN, but is also

recruited to early and late endosomal transport vesicles (Liewen *et al.,* 2005; Quenneville *et al.,* 2006). At the TGN, GARP binds the components of the retrograde transport SNARE, consisting of t-SNAREs syntaxin 6, syntaxin 16 and Vti1a, and v-SNARE VAMP4 (Pérez-Victoria *et al.,* 2009).

The GARP complex and the effects of its loss are difficult to study in mammalian cells, as null mutation of the components results in embryonic lethality at around E12 (Schmitt-John *et al.,* 2005; Karlsson *et al.,* 2013). An alternative to null mutations of GARP components is a hypomorphic mutation of Vps54 known as *Wobbler (Wob*), which reduces the stability of Vps54, in turn increasing the rate of degradation of the entire complex (Schmitt-John *et al.,* 2005). *Wob* was originally observed when it arose spontaneously in C57 BL/Fa mice, leaving homozygous individuals with neuronal symptoms such as poor growth, infertility, progressive weakness, ataxia and muscle wasting (Duchen *et al.,* 1968). The source of the mutation was later identified as a leucine to glutamine substitution at position 967 in Vps54, a domain critical for stability and maintaining folding and GARP interaction, but not functionality. Therefore, this substitution decreases the stability and half-life of both Vps54 and the whole of GARP, without affecting the pre-degradation functional activity (Schmitt-John *et al.,* 2005; Pérez-Victoria *et al.,* 2010a). A reduction in trafficking and resultant mislocalisation for both StxB and CI-MPR in *Wob* mouse embryonic fibroblasts (MEFs) show that this mutation can be used as a method to examine the effects of GARP loss on retrograde trafficking (Karlsson *et al.,* 2013)

It has been suggested in previous research that VACV is able to utilise the retrograde transport pathway to aid morphogenesis. The IEV proteins B5, F13, A33 and A36 are recycled under permissible conditions from the plasma membrane to the TGN, and accumulate at the cell membrane when endocytosis is inhibited (Husain & Moss, 2005). F13 has been shown to colocalise with markers for clathrin-mediated endocytosis (Husain & Moss, 2003). Additionally, both F13 and B5 have been shown to contain potential motifs for internalisation, interaction with clathrin coated vesicles and retrograde transport. A tyrosine residue at position 310, and two leucine residues at 315 and 316 are characteristic of this motif, and it is hypothesised that A33 and A36 may contain similar sequences (Ward & Moss 2000; Huasin & Moss, 2005). Another route of investigation showed that VACV infection in RK_{13} cells increases the rate of endocytosis, as shown by a rapid increase in transport of endocytosis marker horseradish peroxidase (HRP) (Schmelz *et al.,* 1994). Taken together, this

evidence supports a hypothesis that VACV stimulates retrograde transport in order to recycle key IEV proteins. However, the evidence is not conclusive, and mechanistic details are lacking.

Two recent high-throughput, siRNA based screens designed to highlight cellular proteins involved in VACV replication and spread identified both Vps52 and Vps54 as proviral host factors, further supporting a role for retrograde transport in VACV infection (Sivan *et al.,* 2013; Beard *et al.,* 2014) This chapter focuses on using various methods of GARP inhibition, in particular Vps52 and Vps54 depletion to study the effects of GARP loss on VACV replication. Over the course of the chapter, the exact stage of VACV morphogenesis for which GARP is required is investigated.

4.2. Aims

The main aims of the present chapter are as follows:

1. To characterise the impact of Vps52-targeting siRNA on cellular retrograde transport pathways and VACV replication.
2. To investigate the effects of the *Wobbler* mutation on VACV replication.
3. To identify which stage of the VACV replication cycle GARP is involved in.

4.3. Results

4.3.1. siRNA targeting Vps52 reduces the levels of Vps52 in HeLa cells

In order to investigate the impact of Vps52-loss on VACV growth and retrograde transport, Vps52 was knocked down by transfection of specific siRNA. GARP is a complex which relies on the presence of all four components, Vps51, Vps52, Vps53 and Vps54 for stability and complete function. Knockdown of any of the four components destabilises the complex and increases the rate of its degradation (Conibear & Stevens, 2000; Pérez-Victoria *et al.*, 2010a). Vps52 was identified as a strong pro-viral host factor, and previous findings show that depletion of Vps52 by siRNA gene silencing resulted in a five-fold reduction in VACV fluorescence (Beard *et al.,* 2014). To replicate this finding, HeLa cells were transfected with either a non-targeting control siRNA targeting herpes simplex virus 1 protein VP16, or with a SMARTpool consisting of four distinct siRNAs all targeting Vps52. The SMARTpool rather than one individual Vps52-targeting siRNA was used in order to enhance the magnitude and specificity of gene knockdown, and reduce the possibility of off-target effects. 48h post transfection, cells were harvested and the level of Vps52 expression was assessed using western blotting. Cells transfected with the Vps52 targeting siRNA SMARTpool exhibited 40% less Vps52 protein than those transfected with the non-targeting control (Figure 4.1A & B). This indicates that the SMARTpool was effective at reducing the level of Vps52.

The levels of autophagosome protein LC3-II (microtubule-associated protein 1A/1B-light chain 3)-II were determined in order to verify that Vps52 was functionally inhibited by the siRNA treatment. The LC3 protein associates with the autophagosome once autophagy is induced. Increased levels in LC3 in a non-autophagic cell can indicate a block in autophagosomal degradation or lysosome function, and has previously been linked to loss of GARP function (Renna *et al.,* 2010; Pérez-Victoria *et al.,* 2010b). Again, HeLa cells were transfected with the non-targeting siRNA, or the Vps52 targeting SMARTpool. After 48 hours of transfection, cells were fixed and labelled with DAPI and fluorescent antibodies targeting the LC3B isoform of LC3 (Figure 4.1C). Vps52 cells transfected with siRNA transfected with siRNA targeting Vps52 displayed elevated levels of bright LC3B puncta compared to the control transfected cells, indicating that the reduction in Vps52 expression impairs retrograde transport.

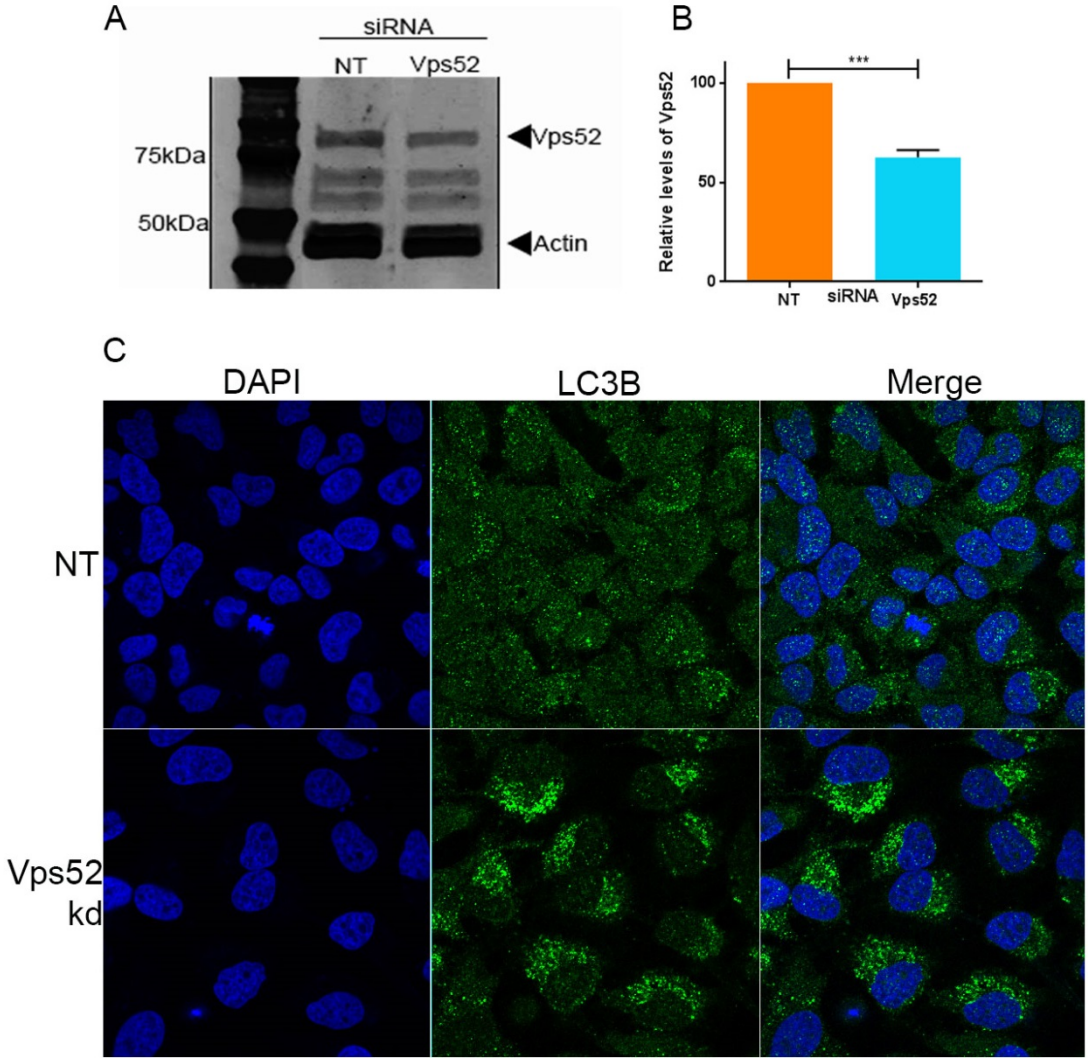

Figure 4.1 Vps52 Targeting siRNA reduces levels of Vps52 in HeLa cells. (A) HeLa cells were transfected with either a non-targeting siRNA (NT), or a SMARTpool composed of 4 siRNAs targeting Vps52. After 48h, cells were collected and lysates separated by SDS-PAGE, transferred to nitrocellulose and then probed using anti-Vps52 and anti-actin antibodies and visualised using fluorescent secondary antibodies and direct infra-red fluorescence (Li-Cor) on an Odyssey scanner. Molecular mass markers are shown on the left, and polypeptide species of interest are indicated and labelled with arrows. (B) Levels of Vps52 compared to actin were quantified in Vps52 knockdown cells and the NT control in Image Studio Lite. Data collated from three biological repeats, SEM calculated and displayed as error bars. ***, $p < 0.001$. (C) HeLa cells were seeded onto coverslips and were transfected with either a NT siRNA or the Vps52 SMARTpool. After 48h, cells were fixed and labelled using an antibody targeting GARP depletion marker, LC3B, and DAPI. Cells were visualised on a Zeiss confocal microscope, and single optical sections taken.

4.3.2. Vps52 knockdown affects retrograde transport, but not Golgi morphology

The impact of Vps52 knockdown on cellular function was further investigated using markers for the TGN and Golgi network. The Golgi network protein TGN46 is recycled between endosomes and the trans-Golgi network, and previous studies have shown it to be mislocalised when components of the retrograde transport pathway are knocked down (Pérez-Victoria *et al.,* 2008; Nonnenmacher *et al.,* 2015). Therefore, it was used here as a marker of retrograde transport function in Vps52 knockdown cells. HeLa cells were transfected with either the non-targeting VP16 negative control, or the Vps52-targeting siRNA SMARTpool, or were mock-transfected with the siRNA buffer alone. After 48h of transfection, cells were fixed and labelled with anti-TGN46 antibodies. In addition, DNA was stained with DAPI, and actin was stained with phalloidin (Figure 4.2A). In mock-transfected, or VP16 transfected cells, TGN46 consistently labelled a distinct, peri-nuclear location with a speckled pattern, consistent with the expected location of the TGN. However, in Vps52 knockdown HeLa cells, the TGN46 exhibited a far more focal, juxta-nuclear staining,often of lower intensity, consistent with previous studies (Perez-Victoria *et al.,* 2008). The number of cells exhibiting unaffected, or "diffuse" staining and cells containing mislocalised or "focal" labelling was quantified (Figure 4.2B). There were significantly more cells exhibiting mislocalised TGN46 when Vps52 was depleted, compared to the control cells, showing that Vps52 knockdown elicited a disruption of retrograde transport. In order to ensure that the mislocalisation of TGN46 was indeed in response to Vps52 depletion and not due to Golgi disruption, the Golgi marker giantin was also examined (Figure 4.2C). HeLa cells were transfected with the non-targeting VP16 siRNA negative control, the Vps52-targeting siRNA SMARTpool, or a siRNA targeting Rab1A. Rab1A is an isoform of the small GTPase Rab1 which localises to the ER-Golgi membrane and is involved in Golgi stability (Liu *et al.,* 2016) characteristics making Rab1A knockdown an ideal positive control for Golgi structure changes. Giantin distribution in both the non-targeting siRNA transfected negative control and the Vps52 knockdown cells appeared as focal, peri-nuclear accumulations consistent with the location of the Golgi body. In comparison, in the Rab1A depleted positive control, giantin staining appeared to be disorganised and covered a greater area than seen in the negative control. Taken together, the results of both the TGN46 and giantin staining suggest that loss of Vps52 impairs the retrograde transport pathway, but that these effects are specific, and not a result of complete Golgi disruption.

Figure 4.2 (facing page) Vps52 knockdown affects retrograde transport but not Golgi morphology. (A) HeLa cells were seeded onto coverslips and were either mock transfected, or transfected with a NT siRNA or an siRNA SMARTpool targeting Vps52. After 48, cells were fixed and labelled using an antibody targeting retrograde transport marker TGN46, phalloidin, and DAPI. Cells were visualised on a Zeiss confocal microscope and cross section images taken. (B) Approximately 100 cells were selected at random from each of the mock, NT and Vps52 knockdown slides, and the distribution of TGN46 was visually qualified as diffuse or focal. This analysis was then quantified as a percentage of the total number of cells. Data representative of 3 collated biological repeats. ***, $p<0.001$. (C) HeLa CELLs were seeded onto coverslips were transfected with either a NT siRNA, an siRNA SMARTpool targeting Vps52 or an siRNA targeting known Golgi stabiliser, Rab1A. After 48, cells were fixed and labelled using an antibody targeting the Golgi marker giantin, and DAPI. Cells were visualised on a Zeiss confocal microscope, and single optical sections taken.

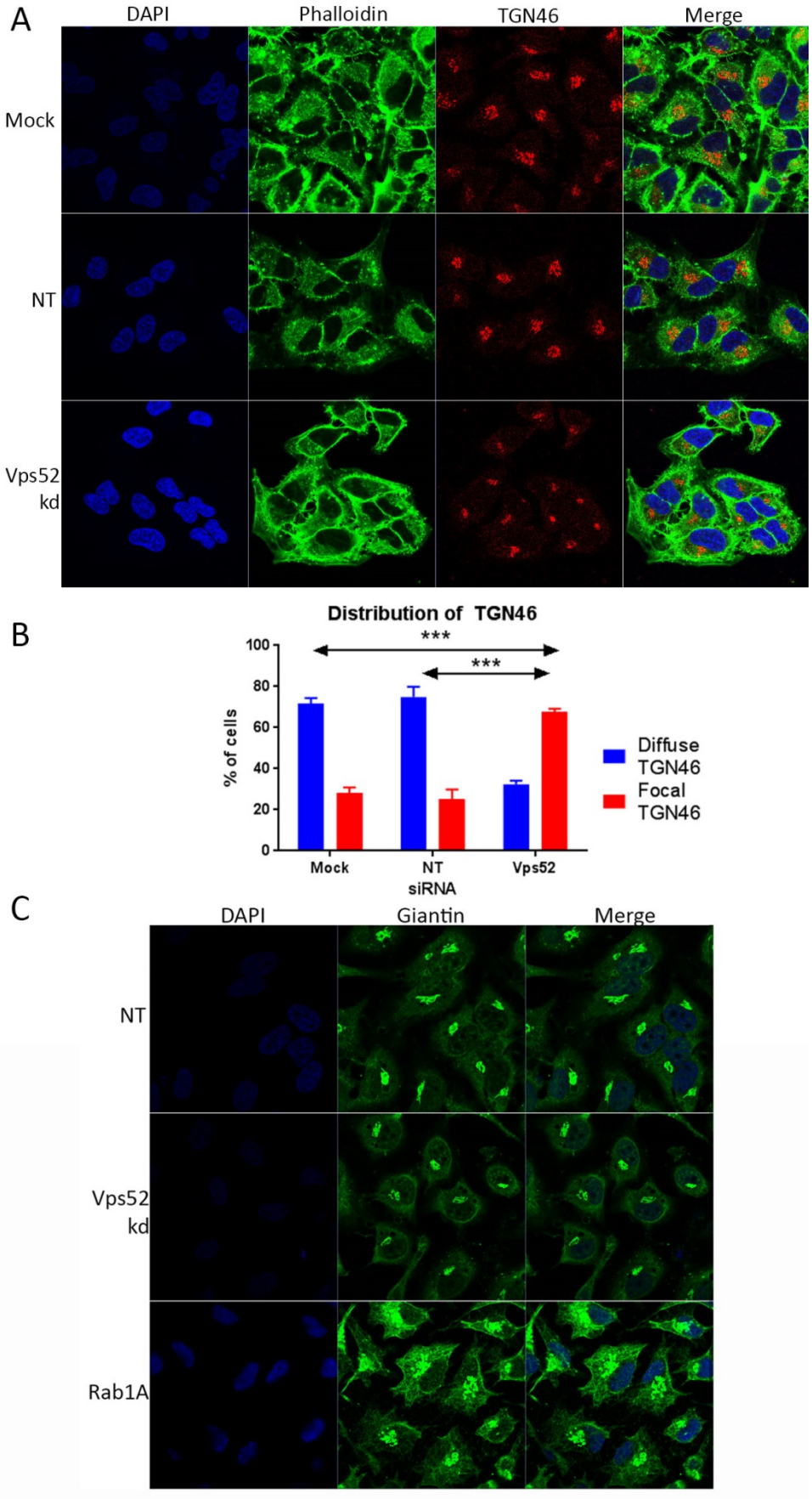
A
DAPI
Phalloidin
TGN46
Merge
Mock
NT
Vps52
kd
B
Distribution of TGN46
***
***
% of cells
100
80
60
40
20
0
Mock
NT
siRNA
Vps52
Diffuse
TGN46
Focal
TGN46
C
DAPI
Giantin
Merge
NT
Vps52
kd
Rab1A

4.3.3. Knockdown of Vps52 inhibits VACV infection

Given that Vps52 depletion detrimentally affects the endosome to Golgi retrograde transport pathway (EGRTP), the impact of this loss on VACV replication and spread was examined. A strain of VACV containing EGFP tagged to the viral A5 capsid protein (VACV-A5-EGFP) was used which allowed fluorescence readings to be used as an indicator of viral growth (Carter *et al.,* 2003). For negative controls, HeLa cells were either mock transfected with siRNA buffer alone, or transfected with the nontargeting siRNA. Rab1A-targeting siRNA was used as a positive control, as this small GTPase has previously been shown to be essential for optimal growth of VACV (Pechenick-Jowers *et al.,* 2015). The Vps52 targeting siRNA was transfected into cells both as a SMARTpool and as the four deconvoluted component siRNAs. At 48h, cells were infected with VACV-A5-EGFP at an MOI of 0.05 plaque forming units (pfu) per cell. A low MOI was used so that not all cells were infected at time point 0, and virus was able to spread through the cell monolayer via a series of replication cycles. Fluorescence was used as a surrogate of viral growth, and readings were taken every 12hpi from 0 to 48hpi (Figure 4.3A**).** As expected, levels of fluorescence in the two negative controls increased exponentially over time. However, fluorescence in cells transfected with the Vps52 SMARTpool, as well as all four of the deconvoluted siRNAs increased only slightly, in line with the Rab1A transfected positive control. By the 48hpi end point of the experiment, all the Vps52 knockdown cells, both SMARTpool and deconvoluted, and the Rab1A depleted cells exhibited significantly less EGFP signal than the negative controls.

In order to assess the level of toxicity associated with the siRNA, cells remaining at the final 48h time point were fixed and stained with Hoechst 33342 to identify live cells (data not shown). Fluorescence per cell was then calculated; to ensure that reduction in fluorescence seen in Figure 4.3A did indeed represent a reduction in viral replication and spread, rather than off target cytotoxicity (Figure 4.3B). This data showed that two out of the four deconvoluted Vps52 siRNAs significantly reduced virus-linked fluorescence per cell compared to both the negative controls, and a third one reduced fluorescence per cell compared to the mock transfected negative control. In addition, both the Vps52 SMARTpool and the Rab1A positive control showed significant reduction in viral growth per cell compared to both the non-targeting and the mock transfected negative controls. These results indicate

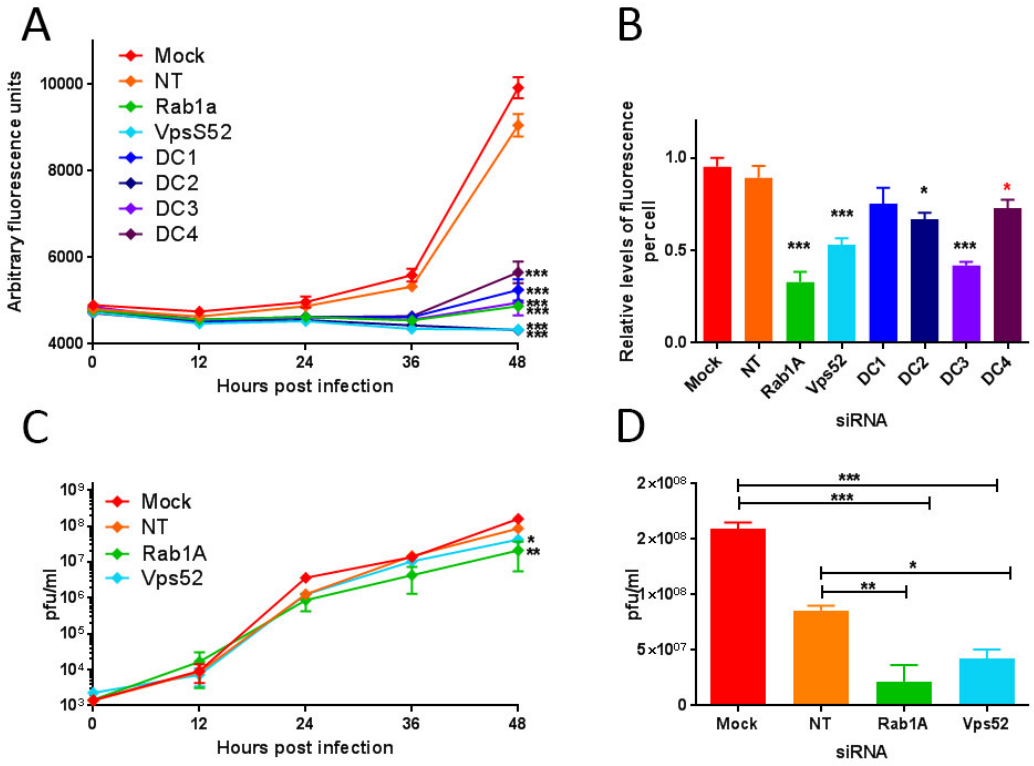

Figure 4.3 Vps52 knockdown inhibits VACV replication. (A) HeLa cells were transfected with either a SMARTpool targeting Vps52, or one of four individual deconvoluted components of the Vps52 SMARTpool (DC 1-4). Mock transfection, or NT siRNA were used as negative controls, and Rab1A siRNA was the positive control. After 48h, cells were infected with VACV-A5-EGFP at an MOI of 0.05, and fluorescence was measured every 12h for 48h. Results show the means and SEMs of six technical repeats and are representative of 3 biological repeats. (B) Cells from (A) were fixed using formalin, and stained with ice-cold Hoechst 33342 solution. Images were taken using a Zeiss Cell observer microscope and counted using Image J. GFP fluorescence per cell was then calculated to normalise for cell loss. Data represents the means and SEMs of 6 technical repeats. Statistical analysis for (A) and (B) were performed using a one-way ANOVAs, comparing test samples to the Mock and NT negative controls. *, $p<0.05$; ***, $p<0.001$. (C) HeLa cells were transfected as described in (A). 48 hours, transfected cells were infected with VACV-WR at an MOI of 0.05. Cells were collected and titrated for plaque assay at 12h intervals for 48hpi. Data represents a collation of 2 biological repeats, error bars are SEMs. (D) Viral titres of the data produced in (C) were statistically analysed at 48hpi, using a one-way ANOVA with multiple comparisons. *, $p<0.05$; ***, $p<0.001$.

that the reduction in EGFP fluorescence seen in Figure 4.3A was due to on-target effects, and not cell loss.

To more directly assess the effect of Vps52 loss on viral replication, the experiment described above was repeated, with VACV replication measured by viral titration (Figure 4.3C) HeLa cells were transfected as described above, with non-targeting, Vps52 or Rab1A targeting siRNA, or mock transfected. 48h after transfection, cells were infected with VACV-WR at a low MOI of 0.05. Viral samples were collected and titrated from 0 to 48 hpi at 12h intervals. At 48 hpi, there was a significant mean reduction of 1-$\log_{10}$ in viral growth in the positive control Rab1A knockdown cells, compared to

the negative controls, which is consistent with results seen previously (Pechenick-Jowers *et al.,* 2015). In Vps52 knockdown cells, the reduction in viral growth compared to the negative controls was smaller, at approximately 0.5 $\log_{10}$ plaque forming units, but still significant. This was seen more clearly when just the 48 hour time points were examined, in Figure 4.3D. Therefore, both fluorescent measurements and viral titre support the results of the previous study (Beard *et al.,* 2014), that Vps52 is required for optimal and effective growth and replication of VACV.

4.3.4. Knockdown of any GARP component inhibits replication of VACV

The effect of the knockdown of each individual GARP component on VACV replication was examined, in order to determine if only Vps52 or the whole GARP complex is required by VACV. GARP is a heteromeric complex also consisting of three other components in addition to Vps52: Vps51, Vps53 and Vps54. All four components are required for full stability of the complex (Conibear *et al.,* 2003; Siniossoglou & Pelham 2002, and Vps54 loss was also seen to affect VACV growth in a high-throughput siRNA based screen (Sivan *et al.,* 2013). Firstly, the stability of GARP was examined during the loss of individual components. HeLa cells were transfected with the non-targeting siRNA control, or with siRNAs targeting one of the GARP components – Vps51, Vps52, Vps53 or Vps54. 48h post transfection, cells were collected, lysed and a Western blot was performed to examine the levels of Vps52 in each sample (Figure 4.4A). Targeting of the four Vps GARP components resulted in 40-50% reduction of Vps52 expression (Figure 4.4B). This indicates that the whole complex is required for stability, and that loss of any one component also decreases expression of the other proteins, and is in agreement with previous investigations into GARP stability (Conibear *et al.,* 2003; Siniossoglou & Pelham 2002). Ideally, expression of Vps51, Vps53 and Vps54 would have also been examined during component knockdown, however, numerous attempts to detect Vps51, Vps53 and Vp54 using antibodies targeting these three proteins were not successful (data not shown). In order to determine if siRNA depletion of any GARP component affected VACV growth, a fluorescence-based multi-step growth curve was performed on siRNA knockdown cells. HeLa cells were mock transfected, or transfected with non-targeting, VP16 siRNA as a negative control, as previously described. Again, siRNA targeting known pro-viral cellular factor Rab1A was used as a positive control. Remaining cells were transfected with either the Vps52-targeting siRNA SMARTpool, or single siRNAs targeting Vps51, Vps53 or Vps54. A final set of cells was transfected

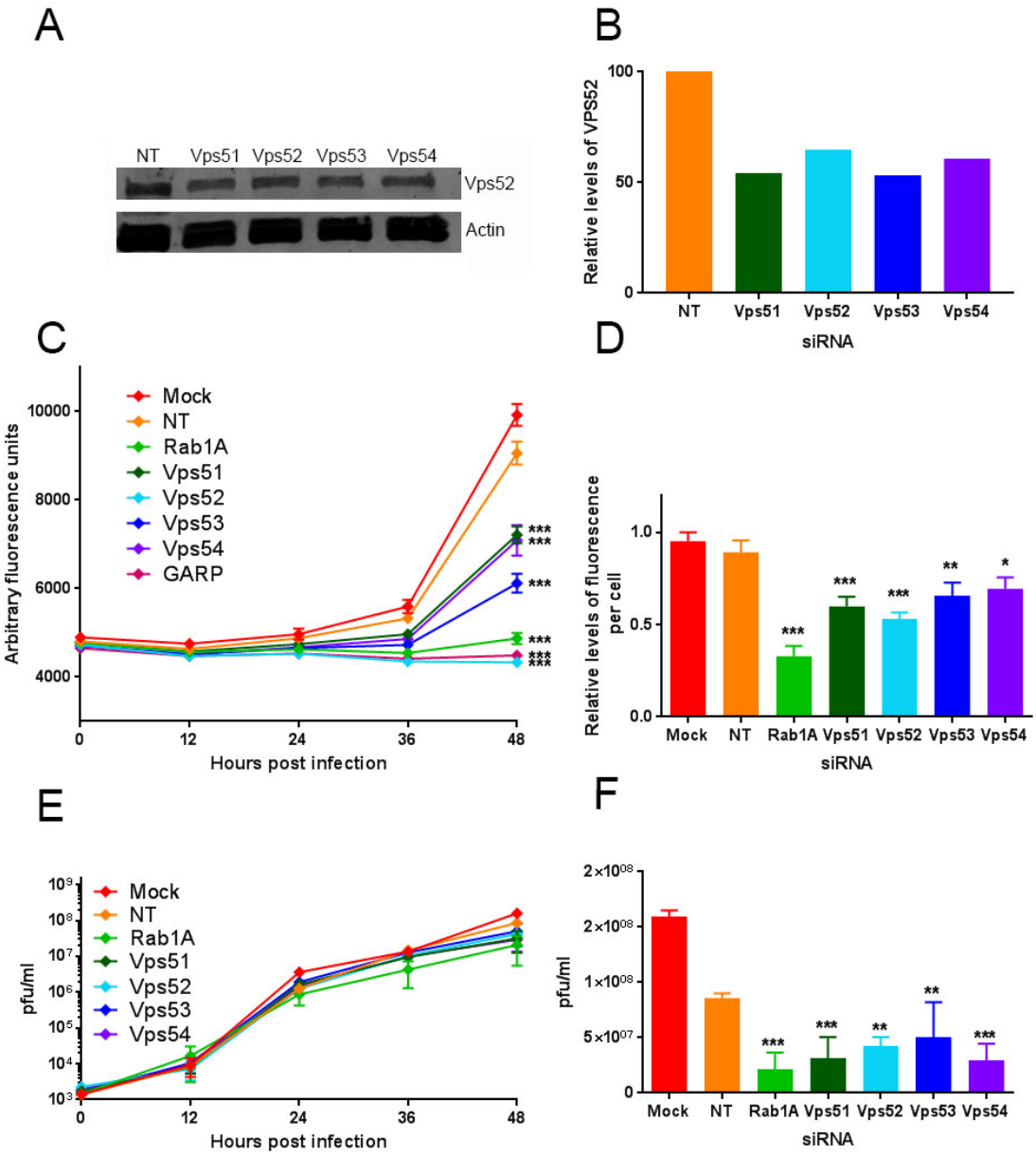

Figure 4.4 Knockdown of any GARP component inhibits replication of VACV. (A) HeLa cells were transfected with either a SMARTpool targeting Vps52, an siRNA targeting Vps51, Vps53, Vps54 or negative control NT siRNA. After 48 hours, cells were collected and run on an SDS-PAGE gel, then probed using anti-Vps52 and anti-actin antibodies and visualised using fluorescent secondary antibodies and direct infra-red fluorescence (Li-Cor) on an Odyssey scanner. (B) Levels of Vps52 compared to actin were quantified in GARP component knockdown cells and the NT control in Image Studio Lite. (C) HeLa cells were transfected as described in (A), along with an extra mock transfected negative control, Rab1A as a positive control and a combination of all the GARP components. After 48h, transfected cells were infected with VACV-A5-EGFP at an MOI of 0.05, and fluorescence measured every 12h for 48h. Results show the means and SEMs of six technical repeats and are representative of 2 biological repeats. Statistical analysis was performed using a one-way ANOVA with multiple comparisons at the 48hpi time point. ***, $p<0.001$. (D) Normalisation for cell death was performed as described in Figure 4.3D *, $p<0.05$; **,$p<0.01$. (E) HeLa cells were transfected and infected with VACV-WR as described in Figure 4.4C. Cells were collected and titrated for plaque assay every 12h, up to 48hpi. Data represents a collation of 2 biological repeats, error bars are SEMs. (F) Viral titres of the data produced in (E) were statistically analysed at 48hpi, using a one-way ANOVA with multiple comparisons. *, $p<0.05$; **, $p<0.01$ ***, $p<0.001$.

with siRNA targeting all four of the GARP components. After 48h, cells were infected with VACV-A5-EGFP at a low MOI of 0.05, and fluorescence was measured as an indicator of viral growth over 48hpi (Figure 4.4C). Very little or no increase in fluorescence was seen in the Rab1A knockdown, positive control cells, Vps52 depleted cells or the GARP depleted cells. The levels of fluorescence in the Vps53 knockdown cells showed less of a decrease in fluorescence than the the positive control. Vps51 and Vps54 knockdown showed similar levels of EGFP inhibition, but had the least impact. Depletion of any GARP component, as well as depletion of the complete complex resulted in a significant reduction in viral growth when compared to both negative controls. The greatest impact on virus-induced fluorescence was seen in Vps52 knockdown and would suggest that Vps52 is the most important member of GARP in terms of VACV interaction. However, this could be due to the fact that only Vps52 was knocked down with a SMARTpool of four distinct siRNAs, rather than just one individual siRNA, and so received a more efficient knockdown than the other components.
At the final 48hpi time point, cells were fixed and DNA stained in order to perform a cell count. Fluorescence per cell was then calculated for each sample, in order to confirm that reduction in fluorescence was not due to off target, cytotoxic siRNA effects (Figure 4.4D). All GARP components displayed significant reduction in viral fluorescence per cell compared to both the mock transfected and non-targeting negative controls, confirming that the effects of all transfected siRNAs were not through cytotoxic effects.

Further to using fluorescence as a measure of viral growth, the effects of GARP component depletion was examined by measuring infectious virion production by plaque assay. HeLa cells were transfected with the controls or GARP components as described above, and after 48h, were infected with VACV-WR at a low MOI of 0.05, for multi-cycle growth. Viral titrations were then performed over 48hpi. As seen in previous results (Figure 4.3 C&D) and Pechenick Jowers et al., 2015), Rab1A knockdown reduced the level of VACV plaque forming units by approximately 1 $\log_{10}$ (Figure 4.4E). All the GARP components, when knocked down individually, showed a significant reduction, varying from 0.5 to 0.75 $\log_{10}$ pfu/ml, in infectious virions, compared to the mock transfected control at 48hpi. This was seen more clearly when looking at the 48hpi time point alone (Figure 4.4F).

4.3.5. Vps52 loss affects extracellular enveloped virion production

In order to determine which stage of the VACV life cycle Vps52 affects, the titres of the supernatant- and cell-associated virus (CAV) were calculated in a single step growth curve. In a single step growth curve the supernatants from infected cell cultures contain EEVs, and are separated from the cell associated fraction which contains all other forms of virion, but are predominantly IMVs. As before, HeLa cells were transfected with non-targeting, Vps52 or Rab1A siRNA. Rab1A was once again used as a control as it has previously been shown to specifically affect the production of EEVs in VACV replication, but not CAV (Pechenick Jowers *et al.,* 2015). 48h after transfection, cells were infected at a high MOI of 5 with VACV-WR, and viral titres were calculated over the course of 24h. Supernatants were separated from the CAV, and any contaminating IMVs in the supernatant were neutralised prior to titration with an antibody targeting IMV protein L1, to ensure that only EEVs released from cells were titred. When the EEVs present in the supernatant wwere titred (Figure 4.5A) a 1-$\log_{10}$ reduction in live virus was seen in the positive control compared to the non-targeting control, and approximately a 1/3 of a $\log_{10}$ reduction of VACV in Vps52 knockdown cells compared to the non-targeting control. However, the titre of cell-associated virus (Figure 4.5B) reached over $1x10^7$ pfu/ml in all three samples, and showed no significant difference between the non-targeting negative control and the Rab1A knockdown positive control, or when the Vps52 depleted cell titre was

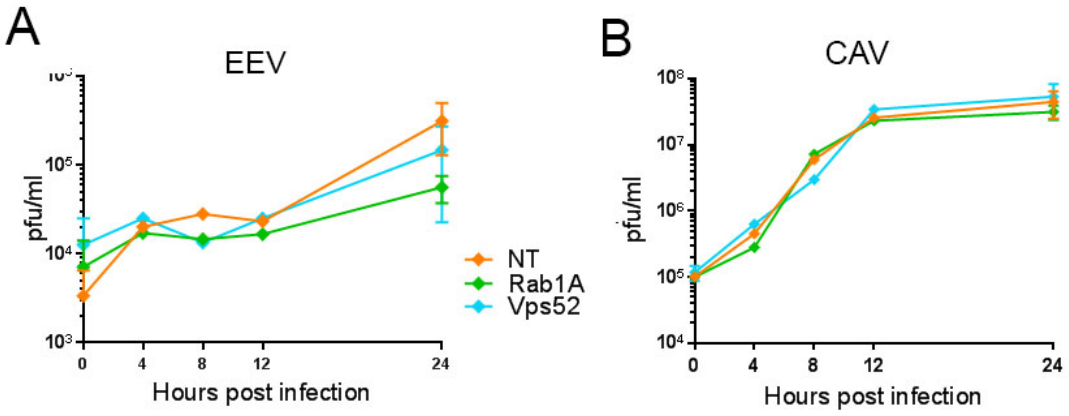

Figure 4.5 Vps52 loss affects VACV EEV production. (A and B) HeLa cells were transfected with a SMARTpool targeting Vps52, NT siRNA or siRNA targeting Rab1a as a positive control. After 48h, transfected cells were infected with VACV-WR at an MOI of 5. At 0, 4, 8, 12 and 24hpi, supernatant (A) was removed, neutralised for IMVs using anti-L1 antibody and titrated for a plaque assay. Cell monolayers (B) were also collected and titrated. Data represents the means and SEMs of 3 biological repeats. Statistical analysis was performed using a one-way ANOVA on the 24h time point data. $p>0.05$.

compared to the negative control. The reduction in EEV production was consistent across 3 biological replicates in cells deficient in Vps52, however, a high degree of inter-experimental variance resulted in $p>0.05$, and therefore no formal statistical significance. This suggests that loss of Vps52 may not affect production of IMVs, but suggests that Vps52 does affect VACV morphogenesis after the IMV stage of the life cycle, impairing IEV production or EEV release.

Overall, these results show that Vps52 is required for optimal function of the EGRTP, and the optimal replication of VACV. In addition, the presence of all four GARP components is required for complex stability, since knockdown of any one component significantly reduces viral growth, and knockdown of any component inhibits the expression of Vps52. Finally, the results of the single step growth curve indicate that Vps52 knockdown specifically affects the production of EEVs, but not IMVs. However, these results have also highlighted two drawbacks of using siRNA to inhibit cellular gene expression. The quantification of retrograde transport disruption in Figure 4.2A shows that 25% of the population of cells transfected with Vps52 targeting siRNA retained normal TGN46 distribution, indicating that transfection was not a completely efficient method of impairing EGRT. In addition, Hoechst staining revealed moderate cytotoxic effects of the Vps52 targeting siRNA. While this could be controlled by measuring fluorescence per cell, it restricted the use of this model. Another method of protein depletion was therefore employed to validate the findings obtained by siRNA transfection.

4.3.6. Expression of GARP complex is reduced in *Wobbler* MEFs

As another method of protein depletion was required to investigate GARP loss, the growth of VACV in *Wobbler* MEF cells was characterised. The *Wobbler* (*Wob*) mutation is a hypomorphic missense mutation, converting leucine to glutamine at codon 967 in the Vps54 subunit of GARP, and was originally characterised in C57BL/6J mice (Schmitt-John *et al.,* 2005). The mutation occurs in an area of the protein required for complex assembly, so although the Vps54 is still produced, it is unstable, with a shortened half-life. Consequently, as the presence of the entire complex is required for full function and stability, overall GARP levels in *Wob* cells are reduced, and a partial loss of function is seen, including missorting of proteins involved in the EGRTP such as CI-MPR (Perez-Victoria *et al.,* 2010a; Karlsson *et al.,* 2013). This makes the *Wob* mutation a useful tool for studying GARP

depletion, and more suitable than homozygous null mutants of any GARP subunit, which are embryonic lethal, and exceptionally difficult to work with (Karlsson *et al.,* 2013).

Primary wild type (WT) and *Wobbler* (MU) mouse embryonic fibroblasts (MEF) cells were kindly donated by Dr Schmitt-John of Aarhus University, Denmark from a parental C57BL/6J mouse strain. Cells were then immortalised through repeated serial passaging, resulting in two independently derived WT and two MU cell lines. Immortalisation was achieved by splitting primary cells into as many 25cm^2 flasks as possible before the crisis stage occurred at approximately passage 10, and cells began to die, due to not being adapted to growth in the tissue culture environment. During the crisis

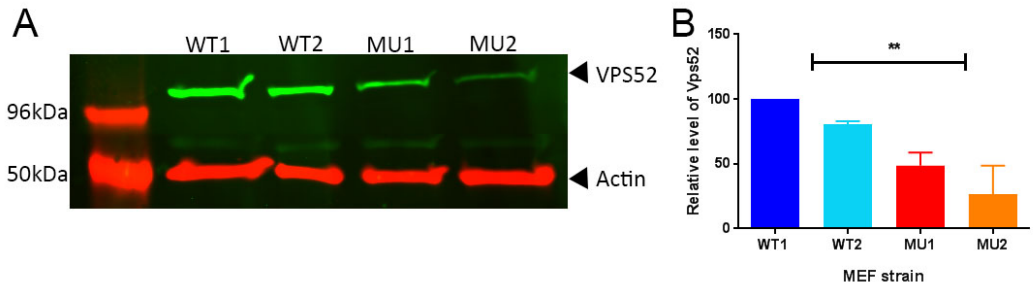

Figure 4.6. Expression of GARP complex is reduced in *Wobbler* MEFs, as is VACV replication. (A) Reduction in Vps52 expression in WT and *Wobbler (Wob*) cells. Cell lysates from two independently immortalised strains of wild type (WT) MEF cells, and two strains of mutant (MU) *Wob* MEF cells were analysed by SDS-PAGE and Western blotting. The membrane was probed with anti-Vps52 and anti-actin antibodies and visualised using fluorescent secondary antibodies and direct infra-red fluorescence (Li-Cor) on an Odyssey scanner. (B) Levels of Vps52 compared to actin were quantified in WT and MU cells in Image Studio Lite. Results are means and SEMs of three collated biological repeats, normalised to actin levels. Statistical analysis was performed using a one-way ANOVA, comparing means of MU strains to means of WT cell lines. **, $p<0.01$.

stage, flasks were passaged at a ratio of 1:1 every three days, until a small proportion of cells underwent presumed survival mutations and began to grow to confluence again. The immortalisation process took approximately six months. Two independently derived lines of WT and two independently derived lines of MU were immortalised and included in future experiments order to rule out the possibility that spontaneous mutations acquired during immortalisation caused the phenotypes seen. The two WT cell lines both required 38 passages before immortalisation and confluency was achieved, and the two MU cell lines, MU1 and MU2 required 54 and 37 passages respectively.

In order to confirm that the *Wob* mutation destabilises the GARP complex, levels of Vps52 were examined in cell lysates. Vps51, Vps53 and Vps54 levels were investigated, but the available

antibodies did not work, and could not be optimised (data not shown). Immortalised WT and MU MEFs were collected, and protein levels in cell lysates determined by western blotting. Figure 4.6A shows a reduction in Vps52 expression in both of the MU MEF cell lines compared to WT. The amount of Vps52 was quantified (Figure 4.6B), and revealed that the *Wob* mutation significantly reduced Vps52 expression by an average of 52%: therefore showing a greater impact than siRNA transfection.

4.3.7. The *Wob* MEF mutation reduces VACV replication through inhibition of EEV production

Following confirmation that the *Wob* mutation reduced levels of GARP, specifically Vps52, multi-cycle growth curves were performed in order to determine the effect of this depletion on VACV replication and spread. WT and MU MEFs were infected with VACV-A5-EGFP at a low MOI of 0.05, and fluorescence readings were taken as an indicator of viral growth up to 48hpi. Differences in viral fluorescence between WT and MU cells were seen as early as 24hpi (Figure 4.7A), while EGFP levels in both MU cell lines retained background levels until after 36hpi. Virus-induced fluorescence levels were highly similar in both MU cell lines, and both MU cell lines showed a 69% reduction in EGFP compared to the WT1 cell line, and a 50% reduction compared to WT2 cells, both of which differences were highly significant.

Levels of infectious virions in MU and WT cells were then compared by plaque assay. WT and MU MEF cells were infected with VACV-WR at a low MOI of 0.05 to investigate multicycle growth. Cells and supernatants were collected together and titrated up to 48hpi. Figure 4.7B shows that a difference of 1 $\log_{10}$ in infectious virions in MU cells compared to WT was seen as early as 12 hpi. This reduction of viral growth in MU cells was maintained throughout the experiment, but decreased to 0.5 $\log_{10}$ at 48hpi, as virus production plateaued. Again, this results shows that GARP is required for optimal VACV replication.

Following this, a single-cycle growth curve was performed, to determine if the reduction EEV in production seen in Vps52-targeting siRNA knockdown cells was also present in the MEFs. WT and MU cells were infected with VACV-WR at a high MOI of 5 pfu/cell, and viral titrations performed over 24h. At each time point, supernatant was separated from cells and any extracellular IMVs present

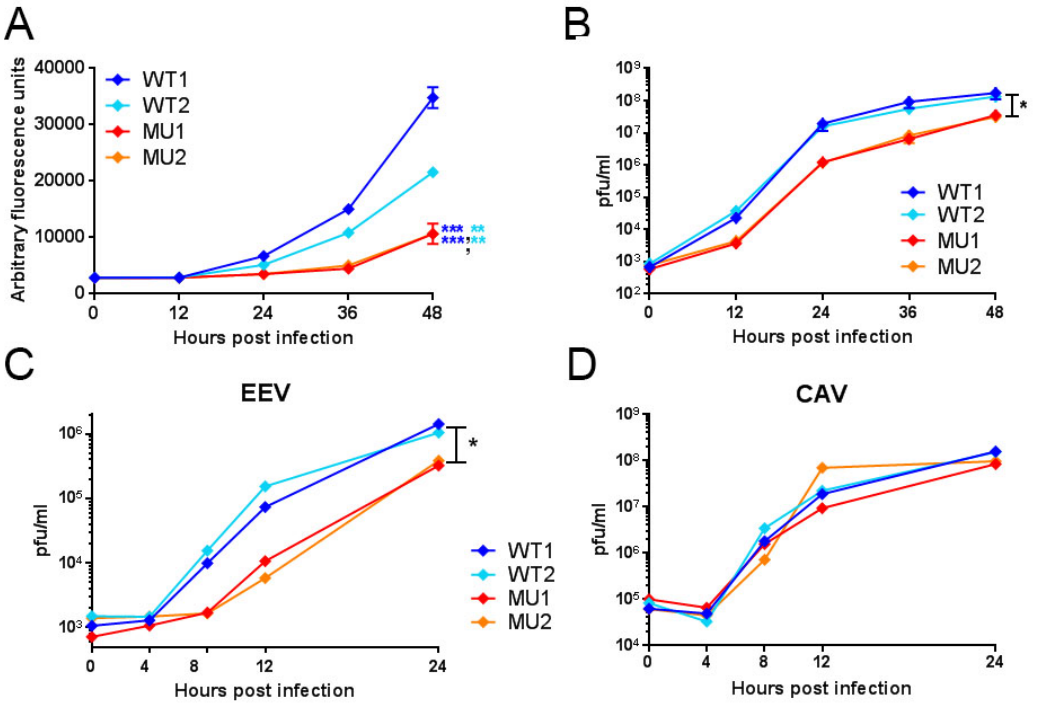

Figure 4.7 Wob MEF mutation inhibits VACV replication. (A) Two strains each of immortalised WT and MU MEF cells were infected with VACV-A5-EGFP, MOI 0.05. Fluorescence was measured at 12h intervals up to 48hpi. Results represent the means and SEMs of three collated biological repeats. Statistical analysis was performed using a one-way ANOVA, with multiple comparisons at 48hpi. **, $p<0.01$; ***, $p<0.001$. (B) Two strains each of WT and MU MEF cells were VACV-WR, MOI 0.05. At 12h intervals, up to 48hpi, cells were collected and titred for plaque assay. Results represent the means and SEMs of three collated biological repeats. Statistical analysis was performed using a one-way ANOVA, with multiple comparisons. *, $p<0.05$. (C and D) Two strains each of WT and MU MEF cells were infected with VACV-WR at an MOI of 5. At 0, 4, 8, 12 and 24hpi, supernatant (C) was removed and titrated for a plaque assay. Cell monolayers (D) were also collected and titrated. Data representative of 4 biological repeats. Statistical analysis was performed using a one-way ANOVA, with multiple comparisons. *, $p<0.05$.

in the supernatant fraction were neutralised with an antibody targeting IMV protein L1. Supernatant and cell-associated virus levels were then assessed independently. A reduction of up to 1 $\log_{10}$ infectious virions was seen in the supernatant at 8, 12 and 24 hpi (Figure 4.7C), indicating that GARP loss impacts the production or release of EEVs from cells. In comparison, no significant differences in titre were seen at any time point in the cell-associated fraction (Figure 4.7D) indicating that the early stages of VACV replication, namely IMV formation, were not affected by GARP loss. This result also confirms, by independent method and cell type, that GARP is required specifically for optimal EEV production and/or release. The results of this experiment concur with the results seen in Figure 4.5, and show that, by two independent methods of protein depletion GARP is required for IEV

morphogenesis, but not IMV production. The results seen in the MEFs were far more consistent than those seen in siRNA transfected cells, therefore the MEFs were used for all following work.

4.3.8. Loss of GARP Affects IEV production and produces aberrant B5-containing vesicles

In order to identify more specifically the point of EEV production at which GARP is involved, the levels and distribution of IEVs in WT and MU MEFs were compared and examined using immunofluorescent microscopy. WT and MU MEFs were infected with VACV-A5-EGFP at a high MOI of 5 pfu/cell. After 8h, cells were fixed, permeabilised and labelled with an antibody targeting the VACV IEV/EEV membrane protein B5. Maximum intensity projections taken through WT cells showed that the EGFP-labelled VACV IMVs were distributed as expected, in large, perinuclear viral factories, as well as small punctate labelling throughout the cytoplasm, representing individual virions (Figure 4.8A, left panel). B5 labelling in WT cells revealed accumulations close to the viral factories, known as wrapping stations. The majority of the EGFP puncta also showed labelling for B5, indicating that they were either IEVs in the cytoplasm of the cell, or CEVs on the cell surface. A small number of the dispersed, cytoplasmic EGFP puncta did not co-localise with B5, representing unwrapped IMVs. The distribution of the EGFP-labelled VACV cores were not altered in MU cells, as large EGFP-labelled perinuclear viral factories and dispersed cytoplasmic puncta were still seen (Figure 4.8A, right panel). However, B5 staining showed a different pattern. In the GARP depleted cells, the wrapping station was still evident, but there were fewer B5-labelled puncta in the cell periphery and cytoplasm (Figure 4.8A right panel), indicating that GARP depletion resulted in fewer IEVs/CEVs. In addition, higher magnification image Z-stacks (Figure 4.8B) showed that fewer B5 puncta colocalised with the VACV-EGFP that would identify them as IEVs/CEVs, but that there werealso accumulations of B5, that were not associated with EGFP signal at all, suggestive of "empty" IEVs lacking a central virion core. For further investigation and quantification, multiple infected *Wob* MEFs were imaged and analysed. Z-stacks were taken of 25 WT cells and 24 MU cells randomly selected from three independent experiments. IMARIS software was then used to quantify B5-positive puncta. IMARIS is an image analysis software that creates 3D images of cells from confocal microscopy data. The nucleus, cytoskeleton, and various structures such as vesicles are segmented, labelled and measured. The software allows associations between labelled objects to be

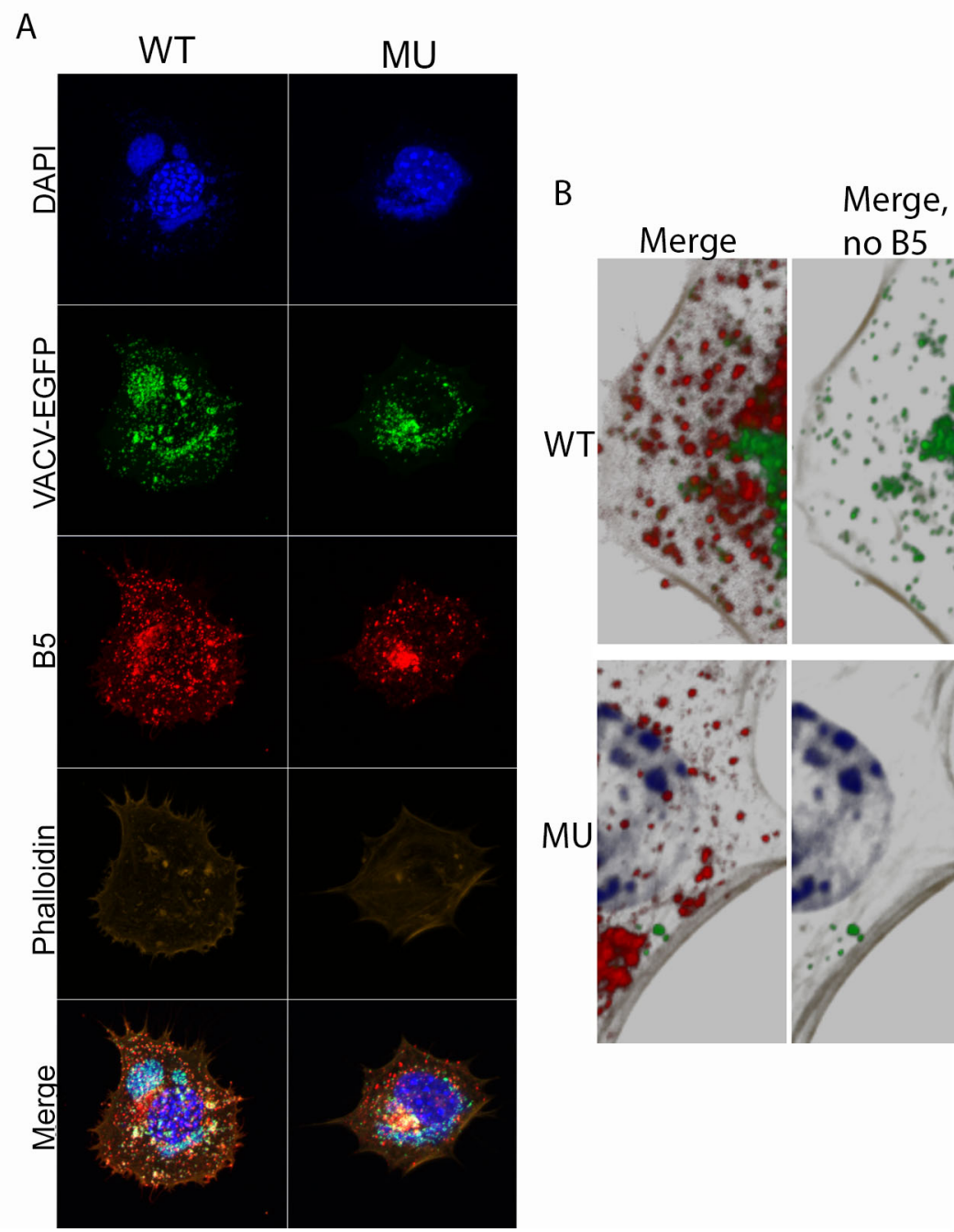

Figure 4.8 Loss of GARP Affects IEV production and produces aberrant B5-containing vesicles. (A) WT and MU MEFs were infected with VACV-A5-EGFP, MOI 5. At 8hpi, cells were fixed and labelled using an antibody targeting VACV EEV protein B5. Phalloidin actin staining and DAPI were also used. Cells were visualised on a Zeiss confocal microscope, and maximum intensity projections taken. (B) Serial optical sections were taken at ~6μm intervals throughout the depth of the cell, and then processed by Zeiss Zen Black software and visualised as a Z stack.

determined. Firstly, the number of IEV/CEVs in the cytoplasm of each of the cells was calculated (Figure 4.9A) by quantifying the number of B5-labelled puncta. MU cells showed a highly significant ($p<0.001$), 2-fold reduction in the overall number of IEV/CEVs, compared to WT cells. The next step was to calculate the proportion of B5 puncta co-localising with EGFP-labelling, which would determine the number of "empty", i.e. not associating with an EGFP-labelled capsid, IEVs. The amount of B5-positive puncta associating with EGFP-labelled virions also showed a statistically significant reduction; from over 90% association in WT cells to approximately 60% in MU cells (Figure 4.9B). However, the diameter of these B5 puncta were also significantly larger in MU cells than WT (Figure 4.9C), increasing from 0.96 µm in WT cells to 1.08 µm in MU cells. Further differences were seen when comparing the IEVs/CEV population present in MU cells with the B5 puncta lacking a VACV capsid. These "free" B5-positive puncta were significantly larger in terms of

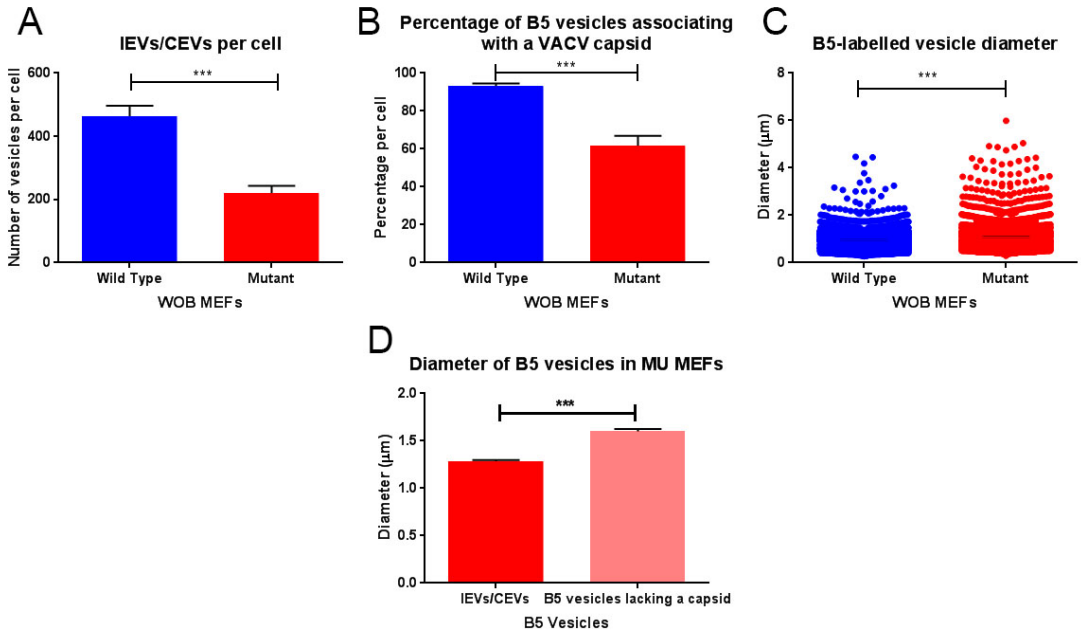

Figure 4.9 Depletion of GARP through mutation disrupts IEV wrapping and results in aberrant B5 accumulations. Imaris image analysis software (Bitplane) was used to create 3D images and analyse images of WT and MU MEF cells labelled for B5 and infected with VACV-A5-EGFP. (A) The total number of B5 puncta per cell. (B) The percentage of B5-containing vesicles per cell that were also associated with an EGFP tagged viral capsid. (C) The diameter of B5 puncta in WT cells compared to those in MU cells. Data represents the means and SEMs of 49 individual cells (24 WT and 25 MU) from 3 independent repeats. Data were statistically analysed using a Student T-test, *, $p<0.05$; ***, $p<0.001$. (D) The diameters of B5 puncta in MU MEF cells associated with EGFP labelled capsids compared to those vesicles independent of capsids. Data represents means and SEMs of 25 individual MU cells from 3 independent repeats. Data were statistically analysed using a Student T-test, ***, $p<0.001$.

diameter (Figure 4.9D) than their VACV-capsid associated counterparts. Consequently, these results suggest that GARP deficiency disrupts the process of wrapping IMVs to become IEVs, resulting in "empty" B5-containing vesicles which are not associated with a VACV capsid.

4.4. Discussion

The primary aim of this chapter was to determine the role of EGRTP on VACV replication and spread. The work focused on the GARP complex because of the results of the previously performed high-throughput siRNA-based screens which identified Vps52 (Beard *et al.,* 2014), and Vps54 (Sivan *et al.,* 2013) as pro-viral host factors during VACV infection. Vps52 and Vps54 are components of the GARP complex, along with Vps53 and Vps51. GARP acts as a tethering factor at the TGN in the EGRTP, interacting with Rab GTPases such as Rab6, and SNAREs such as syntaxin 6 to ensure tethering, and later attachment of transport vesicles to specific acceptor compartments in the TGN (Liewen *et al.,* 2005; Pérez-Victoria *et al.,* 2010b).

In this chapter, GARP expression was reduced by two methods. The first method, transfection of a Vps52-targeting SMARTpool of siRNAs, reduced Vps52 protein expression by approximately 40%, which was sufficient to impair the function of the GARP complex, as shown by the increase in levels of autophagy marker LC3, and altered distribution of TGN46. The knockdown of Vps52, and indeed knockdown of any GARP component resulted in an average of 2-fold reduction in VACV-associated fluorescence, and a 0.5 $\log_{10}$ reduction in infectious virions. A single step growth curve was then performed in order to determine which part of the VACV life cycle GARP loss was affecting. Separate titration of cell-associated virions and extracellular virions showed no change in IMV production in the Vps52 knockdown cells compared to the NT and mock transfected controls, but a 0.2 $\log_{10}$ reduction in EEV titre. *Wobbler* MEF cells, containing a hypomorphic mutation in the Vps54 protein which decreases overall GARP levels, were also used to examine the effects of GARP loss on VACV infection. An average reduction of 60% VACV growth was seen in MU MEFs, compared to the WT cells in terms of titration. Reductions in viral growth of up to 1 $\log_{10}$ were also seen in EEV replication in MU cells over a single replication cycle, while IMV levels were unaffected, confirming the results obtained using Vps52-targeting siRNA. Overall, these findings revealed that GARP is required for optimal VACV growth. The next aim in this chapter was to further identify the roles that GARP and retrograde transport play in IEV production. Immunofluorescent labelling of VACV and the IEV protein B5 in WT and MU MEF cells and the use of image analysis software revealed a reduction in IEV/CEV production as well as large aberrant accumulations of B5, which were

independent of VACV capsids in the MU MEFs, suggesting that GARP is required for the wrapping of IEVs.

Vps52 knockdown using an siRNA SMARTpool resulted in an average 2-fold reduction in VACV growth as measured by fluorescence. However, depletion of the positive control, Rab1A also showed an approximate 2-fold reduction in VACV fluorescence. In the initial siRNA screen which highlighted Vps52 as a pro-viral factor, siRNA transfection saw a greater reduction in Vps52 expression, and induced a five-fold reduction in VACV replication (Beard *et al.,* 2014), while the level of fluorescence reduction in Rab1A knockdown cells was consistent with previous studies (Pechenick-Jowers *et al.,* 2015). The differences between the VACV inhibition by Vps52 depletion seen in the fluorescent growth curve compared to the titration highlight the importance of confirming results seen in fluorescence assays with live virus counts, as discussed in the previous chapter.

VACV infection has been previously been linked to retrograde transport in several different ways, including recycling of IEV proteins B5, F13, A36 and A33 remaining at the cell surface after EEV egress back to the TGN by endocytosis (Husain & Moss, 2005). It was also independently shown that VACV infection resulted in increased rates of endocytosis (Schmelz *et al.,* 1994). However, no previous study has characterised the exact route that VACV utilises, or why IEV proteins are retrieved from the cell surface after EEV/CEV release. Based on the increase in endocytosis in VACV infected cells, and evidence of the retrieval of IEV proteins from the cell surface, along with identification of Vps52 and Vps54 as pro-viral cellular factors, we hypothesised that GARP is involved in the recycling of peripheral IEV proteins from endosomes back to the TGN. Given that IEV production peaks earlier in infection than IMV production, suggesting a limited number of IEV wrapping proteins (Tsutsui, 1983; Ulaeto *et al.,* 1996) it is possible that GARP facilitates the recycling of these IEV proteins, to allow the production of further IEVs. This model supports the hypothesis that the TGN is the most likely site for the IEV wrapping station (Ichihashi *et al.,* 1971; Hiller & Weber, 1985; Schmelz *et al.,* 1994),

With the effect of GARP deficiency confirmed by two separate methods, and IEV/EEV production highlighted as the life cycle stage requiring retrograde transport, next aim of this chapter was to further elucidate the role EGRTP in IEV/EEV production. Several IEV proteins including B5 and

F13, remain on the cell surface after EEV egress, and are then recycled back to a juxta-nuclear area in a retrograde transport dependent manner (Ward & Moss, 2000; Husain & Moss, 2005) This, along with the drop in EEV production during GARP depletion suggests a model in which GARP tethers vesicles containing IEV proteins traveling from the cell surface back to the TGN for wrapping of new IEVs. The presence of B5 accumulations seen not associated with the green fluorescent viral cores in MU cells suggest that in the absence of GARP, these accumulations have not been correctly tethered to the wrapping station. However, the results shown here do not rule out the possibility that GARP is not involved directly in IEV protein transport, but is responsible for the trafficking of an unknown host protein which is required for wrapping. In this model, it is likely that the aberrant B5 puncta would be empty IEV membranes which were unable to wrap IMVs. This hypothesis is supported by a study performed by Van Eijl *et al.* (2002) which showed that IEV proteins B5 and F12 are transported to the cell periphery even in the event of a morphogenesis block after IMV formation.

Despite the results obtained so far, deeper investigation is required to completely define the role of GARP and EGRTP in VACV infection. For example, the localisation of other IEV proteins could be examined in the event of GARP deficiency. F13 would be of particular interest here as, like B5, it is deposited on the cell surface during EEV/CEV egress, and is thought to contain a motif for internalisation and recycling (Ward & Moss 2000; Huasin & Moss, 2005). Whether or not B5 and F13 co-localise in GARP deficient cells would shed further light on the identity of the aberrant B5 puncta seen in the MU *Wob* MEFs. A different avenue of investigation would be to examine the effects of the loss of other EGRTP components, such as retromer, on VACV infection. This would determine if VACV requires only GARP for morphogenesis, or utilises a complete retrograde pathway. siRNA could again be used to knockdown other EGRTP components, or a third method of EGRTP block could be investigated, such as pharmacological agent, again to further clarify the role of retrograde transport in IEV/EEV production.

In conclusion, the data in this chapter not only validates the results of the previous high-throughput screens, but are also the first to confirm a link between a specific component of the retrograde transport pathway, GARP, and EEV production. The nature of this link, and whether VACV interacts with any other EGRTP components requires further experimentation and will be investigated in the next chapter.

5 VACV uses retromer-independent, Retro-2 susceptible retrograde transport to facilitate IEV wrapping

5.1. Introduction

Many infectious agents and toxins utilise the retrograde transport system in order to enter cells, such as the bacterial toxin StxB (Spooner *et al.,* 2006). Most of these cases show the endosome to Golgi transport pathway being used as a method to reach the Golgi and ER. It is far less common to see the retrograde transport system used to facilitate viral morphogenesis and release, as has been show in Chapter 4. This chapter focuses on the nature of GARP's role in VACV morphogenesis, and other potential components of the VACV retrograde pathway, in order to further elucidate the method by which VACV engages the EGRTP.

The IEV/EEV membrane protein F13 typically composes 5-7% of the total EEV protein levels, and is required for VACV spread and plaque formation (Hirt *et al.,* 1986; Vliegen *et al.,* 2012). F13 is located on the inside of the IEV membrane, in the space between the IEV double membranes. Consequently, once the EEV exits the cell, F13 is found on the cytosolic face of the host plasma membrane (Schmutz *et al.,* 1995). F13 is often seen to associate with B5, and both proteins are still correctly trafficked to the Golgi even when expressed in absence of virions (Payne, 1992; Lorenzo *et al.,* 2000). F13 contains a motif which conveys phospholipase activity, and it is thought that this domain is responsible for preventing F13 accumulation at the Golgi, and potentially for triggering trafficking of IEVs from the wrapping station to the cell surface (Sung *et al.,* 1997). Additionally, F13 may be the trigger for VACV associated retrograde transportation, as the formation of endocytic vesicles required for recycling of IEV proteins is reliant on phospholipase activity (Husain & Moss, 2003).

One of the major components of retrograde transport is retromer, a coat complex localised to early and recycling endosomes. Coat protein complexes are recruited to the donor compartment during vesicle transport, and form a scaffold on the outside of the donor compartment which induces membrane curvature, initiating vesicle formation (McMahon & Mills, 2004). Once budded from the donor compartment, vesicles are targeted by SNARE complexes on the vesicle and acceptor compartment to

the correct location, where tethering factors such as GARP initiate interaction and binding between the SNARE complexes and vesicles, allowing delivery of the cargo (McMahon & Mills, 2004; Chia & Gleeson, 2011). Much like GARP, retromer was initially discovered in *S. cerevisiae*, as two subcomplexes: one consisting of Vps26, Vps29, Vps35, and the other of Vps5 and Vps17, which associate through the interaction of Vps35 and Vps5. Disruption of Vps29 or Vps35 expression was shown to result in mislocalisation of CPY and Vps10, two yeast proteins known to be reliant on retrograde trafficking for proper sorting. This indicated a role for retromer in endosome to Golgi transport (Seaman *et al.,* 1998). Highly conserved orthologues of the yeast retromer were later discovered in mammalian cells. Vps35 was shown to form the core of the complex, binding Vps26 at its N-terminus, and Vps29 at its C-terminus, as well as exhibiting multiple binding sites for the other retromer subcomplex, composed of sorting nexin 1/2 (SNX1/SNX2) and SNX5/SNX6, the mammalian orthologues of Vps5 and Vps17 respectively. (Haft *et al.,* 2000; Trousdale & Kim, 2015).

Formation of the retromer complex is facilitated by Vps26, but it is the SNX subcomplex that targets

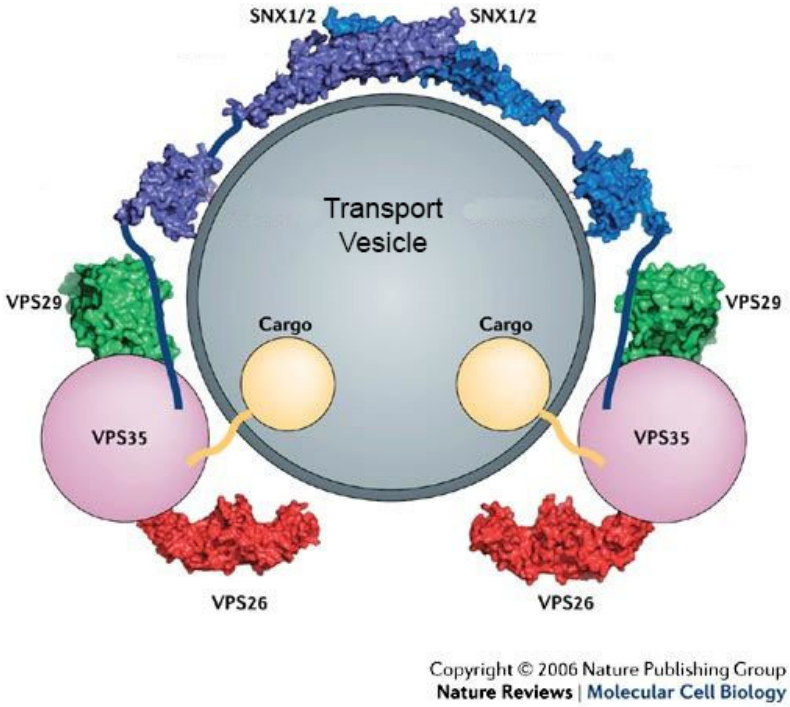

Figure 5.1 The retromer complex. Adapted from Bonifacino & Rojas, 2006. Retromer is a coat complex that is recruited to, and forms a scaffold on the outside of transport vesicles. The SNX subunits of retromer form dimers and bind endosomes. This SNX subcomplex is also bound to Vps35, the core of the Vps subcomplex. The Vps subcomplex, consisting of Vps26, Vps29 and Vps35 is responsible for binding the cargo and including it in the transport vesicle.

retromer to the endosomal membrane, via the interaction of a Phox homology domain in SNX with specific lipids on the endosomal surface (Arighi *et al.,* 2004; Carlton *et al.,* 2004). The SNX subcomplex is also responsible for the formation of tubular organelles at the surface of endosomes for cargo sorting, though it is the Vps subcomplex that binds the necessary cargo for inclusion in transport vesicles (Carlton *et al.,* 2004; Trousdale & Kim, 2015).

Retromer is required not only for the correct sorting of endogenous cargo such as CI-MPR, but is also appropriated by several pathogens and toxins (Arighi *et al.,* 2004; Trousdale & Kim, 2015). Most of these utilise the retrograde transport pathway, and therefore retromer, as a method of entry into cells, and a route to the endoplasmic reticulum. For example, both Shiga toxin and human papillomavirus (HPV) 16 rely on direct binding with retromer for exit from the early endosomal compartment before further trafficking to the TGN (McKenzie *et al.,* 2013; Popa *et al.,*2015). However, HIV-1 was shown by Groppelli *et al.,* (2014) to exploit retromer and the EGRTP for correct targeting of its envelope glycoprotein (Env), in the first instance of retromer facilitating pathogen morphogenesis rather than entry. HIV-1 is assembled at the cell surface, and Env, a key protein for infectivity, is transported out to the site of virion formation by the anterograde transport pathway. Once there, it is either incorporated into virions, or is retrieved back to the Golgi, for recycling. Loss of retromer results in increased levels of Env incorporation into virions, and mis-targeting of the protein that is still endocytosed (Groppelli *et al.,* 2014).

The retrograde transport system is a highly conserved system and is utilised by a number of different pathogens and toxins. Both of these factors make the EGRTP an attractive potential target for pharmacological intervention during disease. One such EGRTP inhibitor is Retro-2, a small molecule dihydroquinazolinone which was discovered during a high-throughput screen to identify compounds pharmacologically active against ricin and shiga toxin (STx) (Stechmann *et al.,* 2010). Ricin is derived from the seeds of the castor oil plant, and is not only highly toxic, but is also considered a bioterror risk. STx is produced by *Shigella dysenteriae* and enterohemorrhagic *Escherichia coli*, and causes severe disease, including kidney failure. Ricin and STx have similar mechanisms, as they are both composed of a catalytic A chain, bound non-covalently to receptor-binding B chain, though the structures differ (Johannes & Römer, 2010; Spooner & Lord, 2015). The B-chains bind glycolipids

on cell surfaces, then enter by endocytosis, and are trafficked via EGRTPs to the Golgi, and then on to the ER. STx binds only to the Gb3 glycosphingolipid, whereas ricin is far more promiscuous, though both toxins can enter in clathrin-dependent, and –independent manners (Sandvig *et al.,* 2013). Once at the ER, the toxins' A-subunits inhibit protein biosynthesis by inactivating ribosomes. (Johannes & Römer, 2010; Spooner & Lord, 2015). The ability of Retro-2 to inhibit the action of both ricin and STx both *in vivo* and *in vitro* in multiple cell lines indicates that these toxins share use of at least one part of the retrograde transport pathway, or that Retro-2 inhibits more than one part of EGRTP (Stechmann *et al.,* 2010; Secher *et al.,* 2015), although the mechanism of Retro-2 is not yet fully understood.

Retro-2 and related compound Retro-1, which was also discovered in the initial high-throughput screen performed by Stechmann *et al.,* (2010) spontaneously convert from an achiral to a cyclical state for stability. The two compounds have no additional or synergistic effects when administered together, indicating that they have the same target (Stechmann *et al.,* 2010; Park *et al.,* 2012.) A Retro-2 derived compound, Retro-2.1 was later discovered as another pharmacologically active agent against toxins, but with a 500-fold higher inhibitory effect on Stx, and a 1000-fold higher inhibitory effect against ricin than Retro-2 (Gupta *et al.,* 2013).

Investigations into the mechanism of Retro-2 action have shown that it is extremely specific in its effect. Treatment of cells with the compound does not affect endocytosis, protein degradation, the late endosomal pathway, transport from early or recycling endosomes or anterograde transport (Stechmann *et al.,* 2010). However, syntaxin 5, a t-SNARE found in SNARE complexes associated with endosome to Golgi transport, is strongly displaced, but not degraded or inhibited on Retro-2 treatment. This finding was further supported by the discovery that Retro-2, and Retro-2.1 pre-treatment of cells inhibits the transduction of adeno-associated virus 2 (AAV2). AAV2 utilises a non-classical route to the TGN of which syntaxin 5 is an essential component, but which bypasses many of the classical retrograde pathway markers, such as retromer, Rab7 and Rab9. However, the mechanism of syntaxin 5 has not yet been discovered (Stechmann *et al.,* 2010; Nonnenmacher *et al.,* 2015). In addition to ricin and Stx, Retro-2 has been shown to inhibit the progress of several viral and

parasitical diseases, including *Leishmaniasis amazonesis* (Canton & Kima, 2012), polyomaviruses and papillomaviruses (Nelson *et al.,* 2013; Carney *et al.,* 2014).

The fact that Retro-2 targets a cellular pathway rather than pathogens, and in EHEC infections inhibits toxin action rather than bacterial growth, makes it less likely that resistance to the compound will develop as quickly as resistance to conventional antimicrobials (Secher *et al.,* 2015). This, along with its low level of toxicity and effect on a wide range of pathogens, makes Retro-2 an attractive potential pharmaceutical for further development.

The previous chapter showed that disruption of EGRTP by both siRNA knockdown and genetic mutation of the GARP complex, resulted in a reduction in VACV growth, specifically by the inhibition of EEV production, and the failure to correctly wrap IEVs. This chapter aims to further elucidate the role of retrograde transport in VACV infection, and determine the identity of the aberrant B5 vesicles seen in MU *Wob* MEF cells. As F13 is, like B5, an IEV/EEV protein which is deposited at the cell surface on EEV release (Smith *et al.,* 2002), defining the localisation of this protein in MU *Wob* MEFs may aid the identification of the aberrant B5 vesicles also seen in these cells. Retromer is a key component of classical retrograde transport from early and recycling endosomes to the TGN (Carlton *et al.,* 2004). Like the GARP complex, it is essential for the correct trafficking of EGRTP marker CI-MPR, and knockdown of either complex results in severe mislocalisation and disrupted downstream events of this protein (McKenzie *et al.,* 2013; Pérez-Victoria *et al.,* 2008). As GARP is directly involved in VACV growth, it may be possible that retromer is also involved, as EGRTP is not just one route, but a complex set of overlapping pathways.

A recent RNAi screen to investigate the genetic requirements for ricin intoxication implicated GARP components Vps53 and Vps54 as essential factors, not only for ricin effect, but also as essential for the function of Pseudomonas exotoxin (PEx), the toxin secreted by *Pseudomonas aeruginosa.* Retromer was also highlighted in this study as a required cellular factor for ricin and PEx intoxication (Moreau *et al.,* 2011). Taken together, this evidence suggests that Retro-2 may be a potential third way of inhibiting VACV growth by EGRTP disruption, as well as a potential anti-viral treatment for *in vivo* VACV infection.

5.2. Aims

The main aims of this chapter are as follows:

1. To characterise the aberrant B5 vesicles seen MU *Wob* MEFs
2. To detail the cellular components of the EGRTP that are required for VACV morphogenesis
    a. Investigate the impact of retromer knockdown
    b. Investigate the impact of Retro-2 treatment on VACV replication, spread and pathogenesis.

5.3. Results

5.3.1. B5 and F13 colocalise independently of VACV capsids in GARP deficient cells

In order to determine further the identity of the aberrant B5 vesicles seen in VACV-infected MU *Wob* MEF cells (Figure 4.8), B5 and F13 were simultaneously labelled to examine levels of colocalisation in *Wob* MEF cells. WT and MU cells were infected with VACV-WR at a high MOI of 5 pfu/cell. After an 8h infection, cells were fixed, permeabilsed and labelled with antibodies targeting the VACV IEV/EEV membrane proteins B5 and F13. Maximum intensity projections were taken of 10 WT and 10 MU cells for visual examination, along with Z-stacks for IMARIS image analysis. IMARIS software created 3D images of these cells, which were then segmented and analysed. IMARIS analysis confirmed that there were three-fold fewer B5 labelled vesicles in the MU MEF cells than in the WT cells, confirming the results seen in Figure 4.8 (data not shown). Vesicles where B5 colocalised with F13 were also counted, and their diameter measured. B5 and F13 labelling in both WT and MU MEF cells showed overlapping red B5 and green F13 puncta (Figure 5.2A). Approximately 90% of these B5-labelled vesicles in both WT and MU MEF cells were also associated with F13 puncta (Figure 5.2B). The vesicles labelled with both B5 and F13 were significantly larger in the MU MEFS (Figure 5.2C & D) compared to the WT MEFs. As the VACV capsids were not labelled, these puncta could not be differentiated into true IEV/CEVs or the aberrant vesicles seen in Figure 4.8. Five colour fluorescence, including VACV-A3-YFP was trialled (results not shown), but there was too much overlap between the green and yellow channels meaning a virus with a fluorescently labelled capsid could not be incorporated into these experiments. However, these results suggest that a considerable percentage of B5/F13 labelled-puncta – most likely the corresponding 30% seen in Figure 4.9 - were not associated with a capsid, as both figures 4.8 and 4.9 in the previous chapter show that B5 puncta not associating with a VACV capsid were also significantly larger. Negative controls labelled anti-B5 antibody only, anti-F13 antibody only or no primary antibodies were performed and showed no background fluorescence (data not shown).

Taken together, these results suggest that the aberrant B5 vesicles seen in MU *Wob* MEFs also contain F13. The identity of these vesicles is still unknown, but the evidence here gives rise to two theories. Either the vesicles seen may be complete, “empty” IEV membranes which have not been correctly

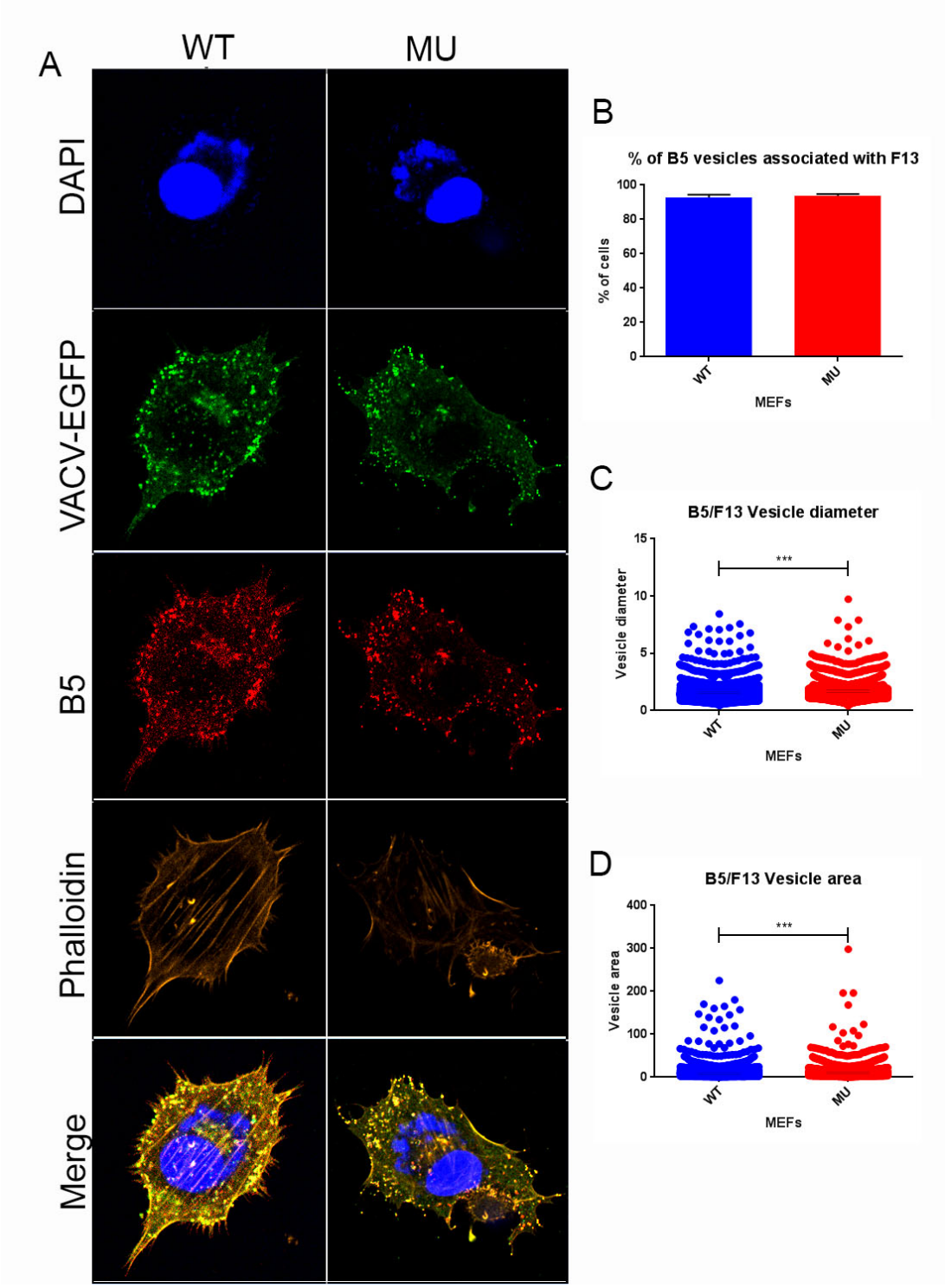

Figure 5.2 B5 and F13 colocalise independently of VACV capsids in GARP deficient cells. (A) *Wob* MEF cells were infected with VACV-WR at MOI 5. After an 8h infection, cells were fixed and labelled with antibodies targeting EEV proteins B5 and F13, as well as staining with DAPI and phalloidin. Cells were visualised using fluorescent secondary antibodies and an LSM 710 Zeiss confocal microscope, and single optical sections were taken. Imaris software was used to quantify these images, examining the total number of B5 puncta per cell in WT compared to MU cells (B); the percentage of B5 puncta colocalising with F13 labelled puncta (C); and the surface area of these B5/F13 containing vesicles in WT and MU cells (D). Data represents means and SEM from 10 individual cells from 1 biological repeat, and a student t-test was used for statistical analysis. ***, $p<0.001$.

wrapped around an IMV, or they are vesicles containing CEV/EEV proteins deposited at the plasma membrane during virus egress which cannot be recycled back to the TGN and wrapping station.

5.3.2. Retromer knockdown does not affect VACV growth

GARP functions at the end of the retrograde transport pathway, tethering vesicles to acceptor compartments at the TGN. In order to determine if VACV also utilises the donor compartment end of EGRTP, the role of the coat complex retromer in VACV infection was examined, by siRNA knockdown of retromer components. Retromer is composed of two sub-complexes, the SNX1/2-SNX5/6 targeting complex, and the Vps26-Vps35-Vps29 cargo binding complex (Trousdale & Kim, 2015). Previous studies have shown that siRNA knockdown of Vps26 or Vps35 can successfully inhibit the function of the whole complex and impair retrograde transport of retromer dependent cargo (Gokool *et al.,* 2007; Popoff *et al.,* 2007; Groppelli *et al.,* 2014). Therefore, siRNAs targeting these genes were used. HeLa cells were transfected with siRNA SMARTpools targeting Vps26 or Vps35. SMARTpools of four individual siRNAs were used to knockdown Vps26 and Vps35 rather than one single siRNA for each gene in order to enhance the magnitude of reduction and reduce the effect of any off-target effects. Cells were infected with a non-targeting siRNA to HSV1 protein VP16 or mock transfected as negative controls. After 48h of transfection, cells were lysed and the levels of Vps26 and Vps35 were assessed using western blotting. Cells transfected with the Vps26 siRNA SMARTpool exhibited a 50% reduction in Vps26 expression compared to the negative controls (Figure 5.3A, B). Vps35 protein was reduced by 60% compared to the non-targeting and mock-transfected controls (Figure 5.3C, D).

The function of the EGRTP in cells with reduced levels of Vps26 or Vps35 was then examined by TGN46 staining. TGN46 is a TGN marker known to display mislocalisation and reduced expression when retrograde transport is inhibited (Perez-Victoria *et al.,* 2008). HeLa cells were mock transfected, or transfected with NT siRNA, or SMARTpools targeting Vps26 or Vps35. After 48h of transfection, cells were fixed and labelled with an anti-TGN46 antibody. In the negative control cells, TGN46 appeared as intense peri-nuclear accumulations, consistent with the expected site of the TGN (Figure 5.3E). In both Vps26 and Vps35 knockdown cells, less juxta nuclear staining was seen, with very little TGN46 visible at all in the Vps26 cells, and dispersed, weak staining of Vps35 seen throughout the

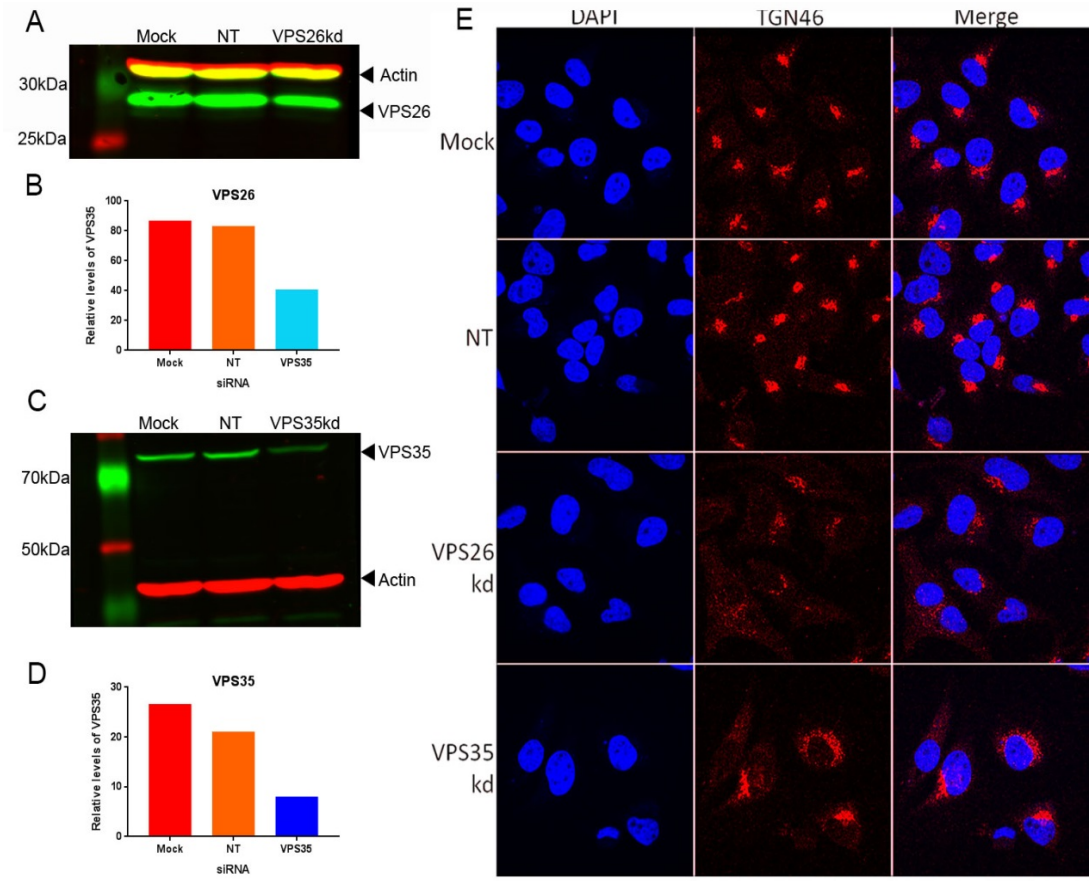

Figure 5.3. Retromer knockdown inhibits retrograde transport. (A) HeLa cells were transfected with an siRNA SMARTpool targeting Vps26. Negative controls were either mock transfected or transfected NT siRNA. After 48h cells were collected and lysed for protein separation on an SDS-PAGE gel, before transfer to a PVDF membrane by western blotting. Antibodies targeting Vps26 and loading control actin, and proteins were visualised using fluorescent secondary antibodies and a Li-Cor Odyssey. (B) Protein levels from (A) were quantified using Image Studio Lite, and normalised to each lane's actin control. The yellow band seen is an off-target background band at the same size of the actin band. (C) HeLa cells were transfected with an siRNA SMARTpool targeting Vps35. Controls and western blotting was performed as described in (A). Antibodies targeting Vps35 and loading control actin, and proteins were visualised using fluorescent secondary antibodies and a Li-Cor Odyssey. (D) Protein levels from (E) were quantified using Image Studio Lite. (E) Retromer depletion alters trafficking of retrograde transport marker TGN46. HeLa cells were transfected with siRNA targeting a retromer component, Vps26 or Vps35. Mock transfection or transfection with an NT siRNA were used for negative controls. After 48h cells were fixed and labelled with antibodies targeting retrograde transport marker TGN46, and labelled with DAPI, then visualised on a Zeiss LSM 710 confocal microscope.

cells in addition to the juxta-nuclear location seen in the positive control. These results indicated that the Vps26 and Vps35 targeting SMARTpools reduce protein expression sufficiently to impair retrograde transport.

With this confirmation, the next step was to examine the effect of Vps26 or Vps35 depletion on VACV infection *in vitro*. HeLa cells were transfected with the VP16 non-targeting siRNA, or mock-

transfected with siRNA buffer as negative controls. A siRNA targeting 5'-AMP-activated protein kinase subunit beta-1 (PRK-AB1) was used as a positive control, as this is the human orthologue of *Drosophila* gene AMPKβ, which is a known pro-VACV cellular gene (Moser *et al.,* 2010). The SMARTpools targeting Vps26 and Vps35 were also transfected into cells, and all wells were incubated for 48h. After this transfection period, cells were infected with VACV-A5-EGFP at an MOI of 0.05 and fluorescence measured as an indicator of viral growth and spread up to 48hpi (Carter *et al.,* 2003). Over the course of 48hpi, the virus-induced fluorescence in Mock and the NT negative controls increased by around two-fold from the initial background levels. The positive control PRK-AB1 knockdown cells exhibited significantly reduced EGFP fluorescence in comparison to these negative controls. However, VACV-linked fluorescence was not affected in the retromer knockdown cells (Figure 5.4A). Very little difference was seen in the Vps26 or Vps35 knockdown HeLa cells compared to the negative control, any changes seen were not significant ($p>0.05$). In order to ensure that the transfected siRNAs were not inducing cytoxicity, a cell death assay was performed using the CellTiter Blue cell viability assay at the final 48hpi time point. The assay consists of redox dye resazurin, which live, viable cells are able to convert to the fluorescent resorufin, while non-viable cells produce no fluorescence. Cells were incubated for 1-4 hours, and then the fluorescent signal was

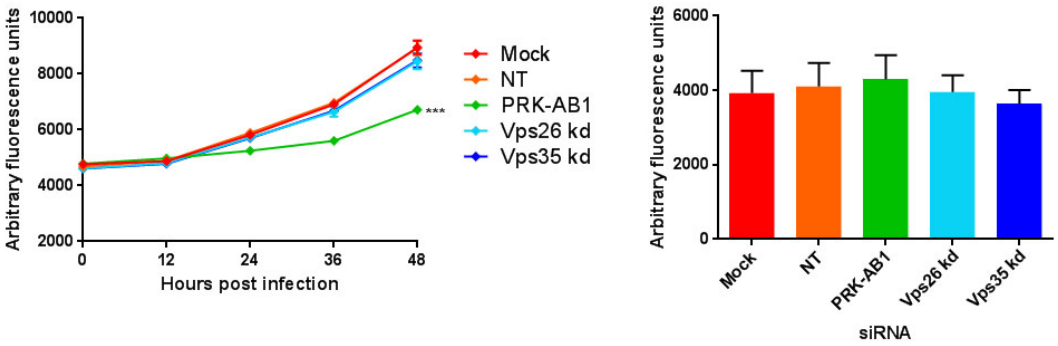

Figure 5.4. Retromer knockdown does not affect VACV growth. (A) HeLa cells were transfected with siRNA targeting retromer components Vps26 or Vps35. Controls were transfected either with siRNA buffer alone (mock), NT siRNA, or, as a positive control, the siRNA targeting PRK-AB1. After 48h, cells were infected with VACV-A5-EGFP at an MOI of 0.05, and fluorescence was measured at 12h intervals up to 48hpi. Data represents the means and SEMs of 6 technical repeats collated from 2 biological repeats. Statistical analysis was performed using a one-way ANOVA at 48hpi, with multiple comparisons. ***, $p<0.001$. (B) At the final time point in the multi-step growth curve described in (A), cells were fixed and stained with Celltiter Blue and read at 590nm. Data represents the means and SEMs of 6 technical repeats collated from 2 biological repeats. Statistical analysis was performed using a one-way ANOVA at 48hpi, with multiple comparisons. $p>0.05$

read as a measure of cell viability. No differences in cytotoxicity were seen when comparing any of the transfected cells to the mock transfected cells (Figure 5.4B). The results of these two experiments show that although retromer was successfully knocked down by transfection of siRNAs targeting Vps26 and Vps35, and retrograde transport was subsequently inhibited, this did not affect VACV production. Therefore, VACV does not require retromer for optimal growth and spread.

5.3.3. Retro-2 inhibits VACV growth

5.3.3.1 Retro-2 treatment protects against shiga toxin-2 by blocking retrograde transport

In order to further characterise the retrograde transport pathway used by VACV, chemical inhibition of EGRT was used. Retro-2 and the related Retro-1 are dihydroquinazolines that were originally discovered in a high throughput screen for pharmacological inhibitors of ricin and STx, two toxins known to hijack the EGRTP for successful intoxication (Stechmann *et al.,* 2010; Park *et al.,* 2012). Retro-2 treatment results in the extremely specific displacement of retrograde transport-associated t-SNARE syntaxin 5, without affecting other processes such as anterograde transport, endocytosis or protein degradation. However, the exact mechanism of action is unknown (Stechmann *et al.,* 2010). Retro-2 and its derivatives were an attractive method for inhibiting retrograde transport in VACV and examining the impact of this compound on growth of the virus. Retro-2 and the related compounds: Retro-1, VP184, and Retro-2.1 were kindly donated by Dr. Daniel Gillet at CEA Saclay, France.

To test the activity of Retro-2, a cell death assay was performed using Shiga toxin 2 (STx-2). Vero cells were pre-treated with concentrations of Retro-2, ranging from 25μM to 200μM. As DMSO had been used to resuspend and dilute the Retro-2, this was used as a negative control. STx2 from EHEC was serially diluted in media from 100ng/ml to 32pg/ml and used to intoxicate the cells after 2h of Retro-2 pre-treatment. Retro-2 was not removed, and was present throughout the intoxication. At 48h post intoxication, cells were fixed and stained with CellTiter Blue in order to measure cell viability. Cells treated with STx-2, but not Retro-2 (dark blue bars) exhibited a dose-dependent decrease in cell viability, with approximately 50% of cells dead at the highest Stx2 concentration, compared to cells treated with media alone (Figure 5.5). Even at the lowest concentration of STx2, 32pg/ml, an average 4 fold reduction in cell survival was seen between the intoxicated and the media only cells, indicating that even at extremely low concentrations, this batch of Stx2 (lot #111108V2, Toxin Technology, Inc) was still extremely toxic.

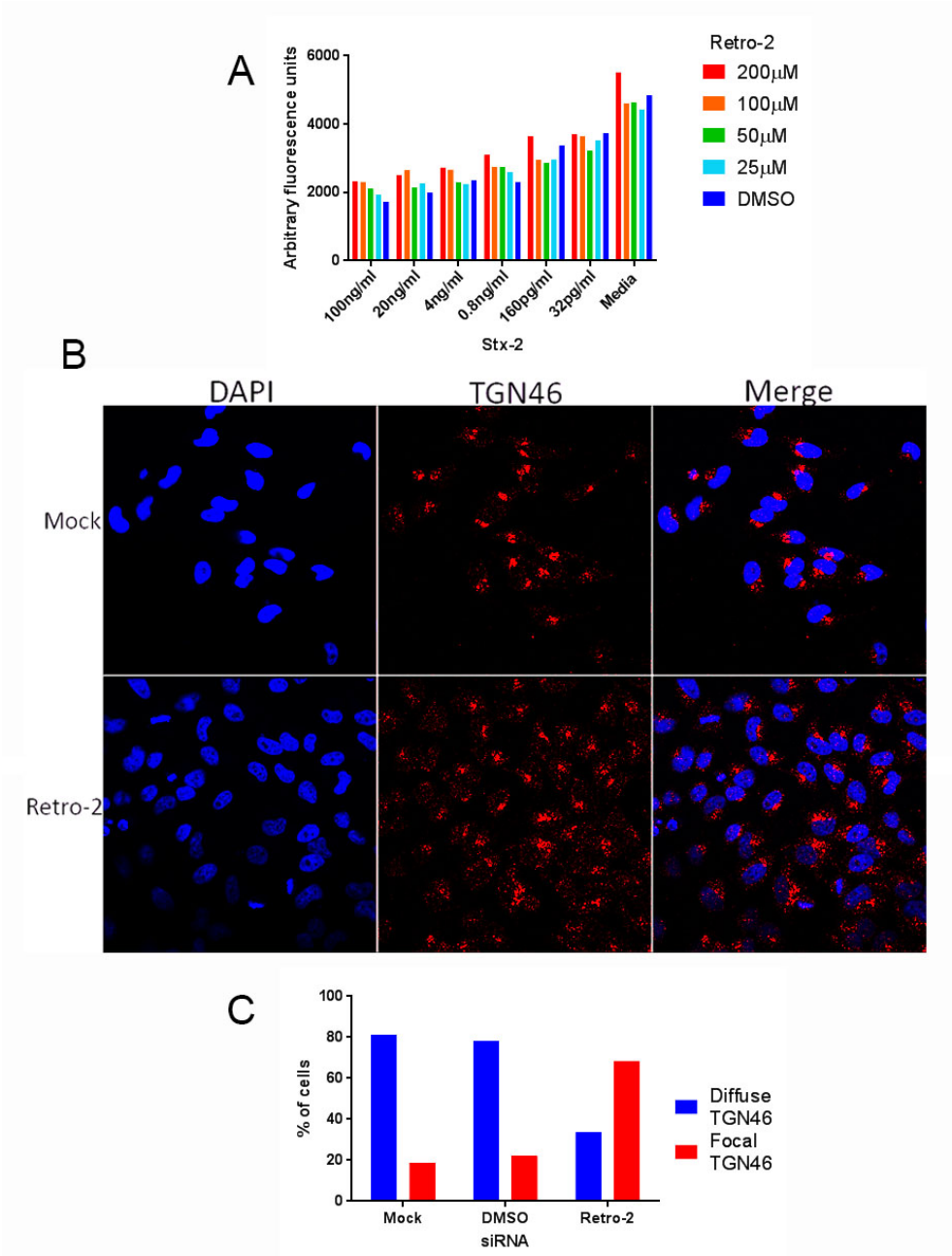

Figure 5.5. Retro-2 treatment protects against STx by blocking retrograde transport. (A) Vero cells were treated with varying concentrations of Retro-2 resuspended in DMSO, from 200μM-25μM, or DMSO alone as a negative control. After a 2h incubation, cells were treated with STx2 of concentrations ranging from 100ng/ml to 32pg/ml, or media alone as a negative control. Retro-2 concentrations were reapplied, so as to be present throughout. At 48hpi, cells were fixed with CellTiter Blue and fluorescence was read to assay cell viability represented by arbitrary fluorescent units. Representative of 5 biological repeats. (B) HeLa cells were treated with Retro-2 at a working concentration of 30μM. After an 8h incubation, cells were fixed and labelled with an anti-TGN46 antibody, and stained with DAPI. Cells were then visualised using a Zeiss LSM 710 confocal microscope. (C) Approximately 250 cells were selected at random from each of the mock and Retro-2 knockdown slides, and the distribution of TGN46 was visually qualified as diffuse or focal. This analysis was then quantified as a percentage of the total number of cells. Data representative of one biological repeat.

Despite the strong effect of STtx2, pre-treatment with 200μM Retro-2 was still able to partially inhibit STx2 action and increase cell viability, again in a dose-dependent manner. Even at the highest concentrations of STx2, treatment with 200μM Retro-2 increased cell survival by 25% compared to the cells treated with the DMSO control.

The ability of Retro-2 to inhibit retrograde transport was also examined using the retrograde transport marker TGN46. HeLa cells were mock-treated with DMSO, or treated with Retro-2 at the 30μM working concentration of Retro-2, as used by Stechmann *et al.,* (2010). After an 8h incubation, cells were fixed and labelled with an anti-TGN46 antibody and a fluorescent secondary antibody for visualisation with confocal microscopy. In mock treated cells, TGN46 was seen as expected, in intense, perinuclear accumulations consistent with the expected location of the TGN (Figure 5.5B, top). In comparison, Retro-2 treatment resulted in more dispersed and less intense staining (Figure 5.5B, bottom). Quantification of these results (Figure 5.5C) exhibited a clear decrease in the number of cells with focal TGN46 after Retro-2 treatment compared to the mock treated control, indicating that a concentration of 30μM was sufficient to disrupt the retrograde transport pathway, even though higher concentrations were required to make an impact on STx2 intoxication.

5.3.3.2 Retro-2 treatment inhibits VACV growth

In order to determine whether Retro-2 inhibits VACV growth, a multi-cycle growth curve was performed. HeLa cells were treated with a range of Retro-2 concentrations from 1nM to 100μM. Although the working concentration of Retro-2 is 30μM, a full range of concentrations were used to ensure that VACV inhibition did not require a different concentration of the compound, as it had not been previously tested on this virus. Control cells were mock treated with DMSO, or received only media. After a 2h pre-treatment, cells were infected with VACV-A5-EGFP at an MOI of 0.05, in the continued presence of Retro-2, and fluorescence was measured as an indicator of viral growth and spread up to 48 hpi. The cells treated only with DMSO, and those cells treated with the lower concentrations of Retro-2: (1μM, 100nM, 10nM and 1nM), showed at least 100% increase in EGFP expression over background fluorescence levels by 48hpi In comparison, fluorescence in 100μM and 10μM treated cells increased by only 25% and 40% respectively from infection to 48hpi (Figure

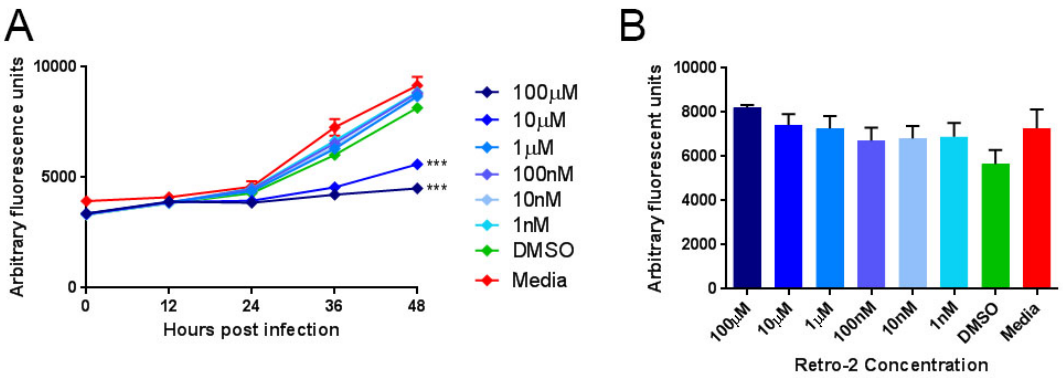

Figure 5.6 Retro-2 treatment inhibits VACV growth. (A) HeLa cells were incubated for 2h with Retro-2 at concentrations ranging from 100μM to 1nM, or DMSO or media alone for negative controls. Cells were infected with VACV-A5-EGFP at an MOI of 0.05 in the continued presence of Retro-2, and fluorescence was measured every 12h up to 48hpi. Data represents means and SEMs of six technical repeats, and is representative of five independent biological repeats. Statistical analysis was performed using a one-way ANOVA at 48hpi with multiple comparisons ***, $p<0.001$. (B) After the 48h infection, cells pretreated with Retro-2 were fixed and stained with CellTiter Blue to assess cell viability. Data shows the mean and SEM of six technical repeats, representative of 5 biological repeats. $p>0.05$.

5.6A), indicating inhibition of viral replication. The effect of Retro-2 treatment was apparent from 24hpi, and by 48hpi, cells treated with 100μM or 10μM Retro-2 exhibited highly significant inhibition of VACV growth ($p<0.001$) compared to both the negative controls. The IC_{50} Retro-2 was calculated as 6.10μM. At 48hpi, all cells were fixed and stained with CellTiter Blue to ensure that Retro-2 had not had a cytotoxic effect at the higher concentrations of treatment. Figure 5.6B shows that not only were 100μM and 10μM concentrations non-toxic, but they appeared to slightly increase cell survival compared to the DMSO control. This was most likely due to the reduced viral growth in these cells resulting in less virus-induced cell lysis, rather than any direct protective effect on the cell itself. The result verifies that the reduction in viral fluorescence seen in 100μM and 10μM Retro-2 treated cells in Figure 5.6A was not due to Retro-2-induced cell death.

5.3.3.3 Retro-2 related compounds also inhibit VACV growth

In addition to Retro-2, three related compounds were also available: Retro-1, VP184 and the far more efficient derivative of Retro-2, Retro-2.1 (Gupta *et al.,* 2013). These compounds were also tested for their effect on VACV infection. As described above, HeLa cells were pre-treated for 2 hours with a range of concentrations, from 1nM to 10μM for each compound, then infected with VACV-A5-EGFP at an MOI of0.05. 100μM was not used for any of the three compounds, as unlike Retro-2, Retro-1,

VP184 and Retro-2.1 all showed significant cytotoxic effects at the highest concentration (data not shown). Over the course of 48h, fluorescence was measured at regular intervals, and at the conclusion of the experiment cells were stained with CellTiter Blue to determine cell viability. Retro-1 treatment resulted in a significant reduction of VACV–linked fluorescence at 10μM and 100nM (Figure 5.7A), exhibiting a 44% and 18% reduction in final fluorescence levels respectively. Despite seeing an inhibitory effect at 100nM, no effect was seen at 1μM Retro-1. However, the Retro-1 IC_{50} was calculated at 7.59μM. The cell viability assay showed minimal cytotoxicity at all concentrations of compound used in the growth assay, once again confirming that the highly significant reduction seen at 10μM Retro-1 was due to loss of viral EGFP expression as opposed to increased cell death.

In VP184 treated cells, only treatments of 10μM and 1μM exerted significant inhibitory effects on EGFP expression compared to the negative controls (Figure 5.7B), resulting in a 49% and 24% respective reduction in final fluorescence levels. All other concentrations of the compound showed levels of virus-linkedfluoresence very similar to those seen in the controls, indicating that these concentrations were too low to have any effect. The IC_{50} of VP184 was calculated at 1.75μM, indicating a higher efficacy than Retro-2 and Retro-1. Once again, no significant cytotoxic effects were recorded in cells treated even with the highest concentrations of VP184 (Figure 5.7B).

Of the four compounds tested, Retro-2.1 was by far the most effective, as concentrations of 10μM, 1μM and 100nM were all extremely inhibitory, preventing almost all fluorescence increase in the treated cells (Figure 5.7C). In keeping with this, the IC_{50} calculated at 27.6nM, a far lower concentration than the other three compounds. This is consistent with previous studies that showed that Retro-2.1 was 500-fold more effective than Retro-2 in STx intoxication, and 1000-fold more effective during ricin intoxication (Gupta *et al.,* 2013). In VACV infection, Retro-2.1 is 100-fold more effective than Retro-2, as 10μM is the lowest concentration at which Retro-2 is effective, and the IC_{50} of Retro-2.1 is 100-fold lower than that of Retro-2. However, this increased efficiency is coupled with slight cytoxicity (Figure 5.7C) at 10μM and 1μM compared to lower concentrations, though the decrease in cell survival is still not a significant effect when compared to the survival of the control treated cells. 100nM appears to be the optimum working concentration for Retro-2.1, as it exerts a similar level of inhibition as the higher concentrations, but has no cytotoxic effects.

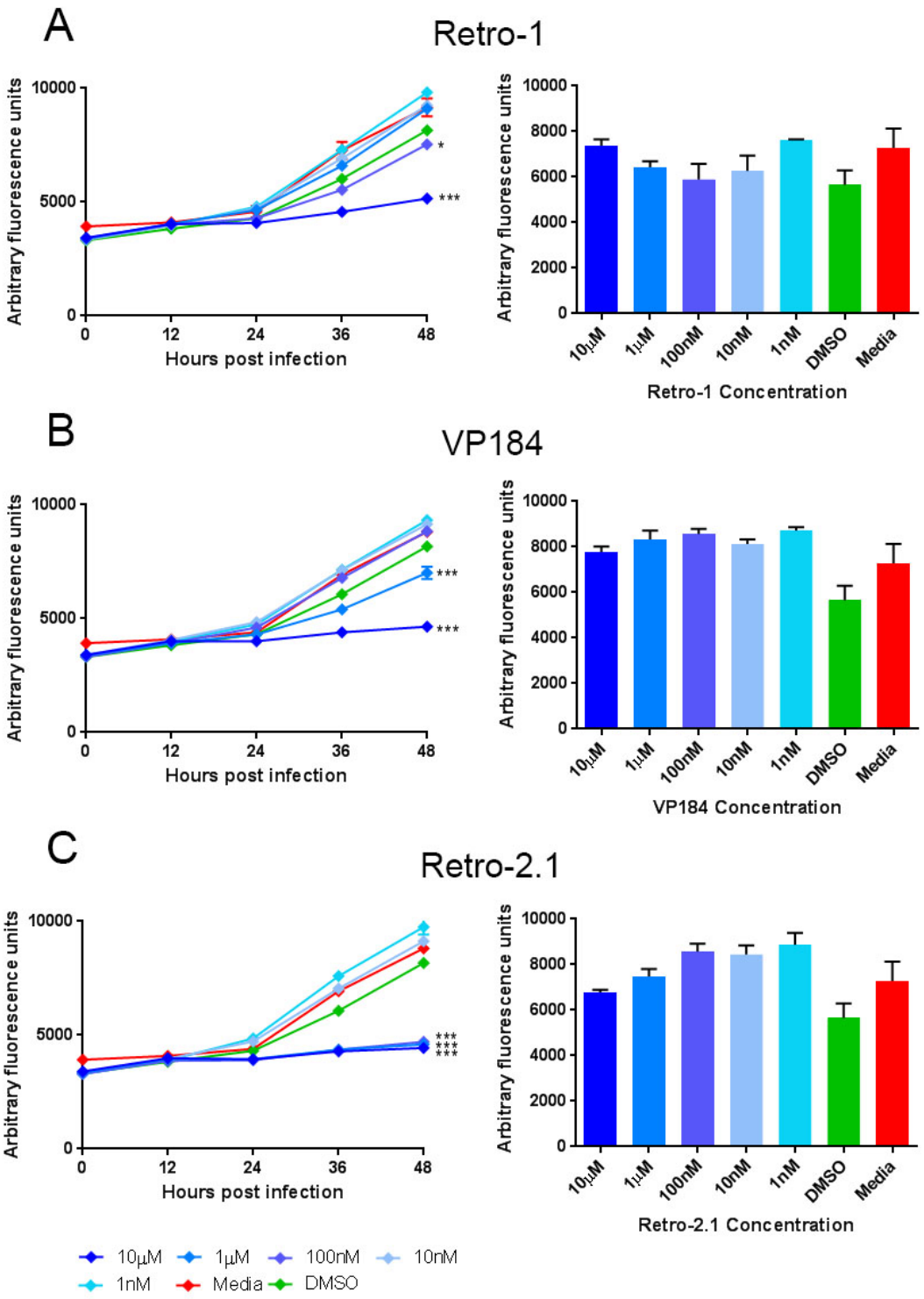

Figure 5.7 Retro-2 related compounds also inhibit VACV growth. HeLa cells were incubated for 2h with either Retro-1 (A),VP184 (B), or Retro-2.1(C) at concentrations ranging from 10μM to 1nM, or DMSO or media alone for negative controls. Cells were infected with VACV-A5-EGFP at and MOI of 0.05 in the continued presence of the small molecule compounds, and fluorescence was measured every 12h up to 48hpi . Data represent means and SEMs of six technical repeats. Statistical analysis was performed using a one-way ANOVA, at 48hpi with multiple comparisons *, $p<0.05$; ***, $p<0.001$. After the 48h infection, cells pretreated with the small molecule compounds were fixed and stained with CellTiter Blue to assess cell viability. Data shows the mean and SEM of six technical

5.3.3.4 Retro-2 and related compounds inhibit EEV production

As all four of the tested compounds significantly inhibited VACV growth, the next step was to determine at which stage of the VACV life cycle the compounds exerted their effects. To this end, a single-step growth curve was performed to allow the separate calculation of CAVs and EEVs in the supernatant. HeLa cells were pre-treated with one of the four compounds at the final working concentrations, which were derived from Figure 5.6 and Figure 5.7. After 2h of treatment, cells were infected with VACV-WR at a high MOI of 5 pfu per cell, in the continued presence of the compounds, and viral titres were examined at 0 and 24hpi. Supernatants were separated from the cell

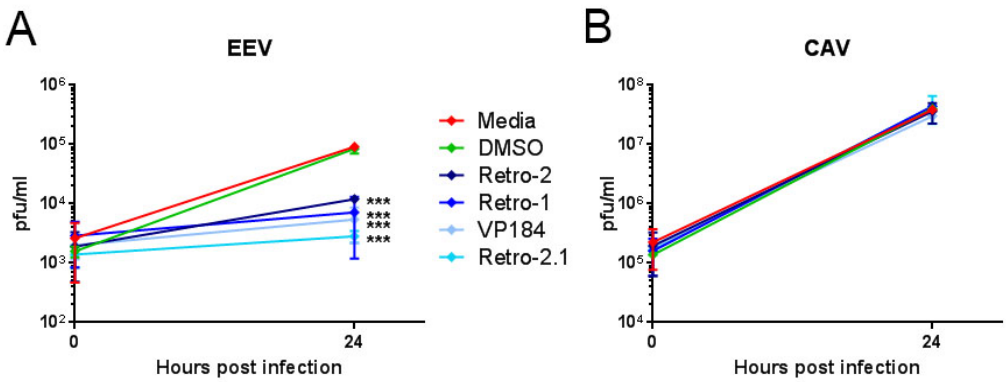

Figure 5.8 Retro-2 and related compounds inhibit EEV production. (A and B) HeLa cells were treated with Retro-2 or a related small molecule compound at the appropriate working concentration. After a 2h incubation, cells were infected with VACV-WR at MOI of 5, in the continued presence of the compounds. At 0 (to measure residual inoculum) and 24hpi, supernatant (A) was removed, neutralised for IMVs using anti-L1 antibody and titrated for a plaque assay. Cell monolayers (B) were also collected and titrated. Data represents the means and SEMs of 2 individual biological repeats. Statistical analysis was performed using a one-way ANOVA with multiple comparisons. ***, $p<0.001$

associated virus, and IMVs in the supernatant were neutralised prior to titration with an antibody targeting IMV protein L1, to ensure that only EEVs released from cells were titred.

At 24h, levels of EEV increased by 1.6 $\log_{10}$ pfu/ml in the mock and DMSO samples, but by only 0.3-0.7 $\log_{10}$ in the compound treated cells. Therefore, treatment of cells with any of the compounds resulted in highly significant ($p<0.001$) reductions in EEV titre by the final 24hpi time point, compared to the DMSO mock-treated and media only treated cells (Figure 5.8A). The inhibition of EEV release was greatest in Retro-2.1 treated cells, which again confirmed that Retro-2.1 was a more

efficient than Retro-2. In comparison, levels of cell associated virus in all cells, both treated and mock treated, exhibited a 2 $\log_{10}$ increase over the residual inoculum by 24hpi. This increase in viral titre indicated normal IMV production, and revealed that none of the compounds exerted any effect on the levels of cell associated virus when compared to the negative controls (Figure 5.8B). These data show that as with siRNA knockdown of VPS52 and the *Wob* mutation, the production and release of EEVs is affected by Retro-2 induced EGRT inhibition.

5.3.3.5 Retro-2 treatment displays additional effects on VACV to the *Wob* mutation

A growth curve involving both Retro-2 and the *Wob* mutation was used in order to determine if the combination of EGRTP inhibition methods resulted in any additional or synergistic effects. Retro-2 treatment results in the dispersal of Golgi SNARE syntaxin-5 (Stechmann *et al.,* 2010), though the exact mechanism is still unknown. A yeast 2-hybrid screen of *Caenorhabditis elegans* cells by Luo *et al.* (2011) showed an interaction between the syntaxin 5 and GARP component Vps54. However, this interaction has not been further investigated, or seen in mammalian cells. WT and MU MEF cells were incubated for 2h with 30μM of Retro-2, after which cells were infected with VACV-A5-EGFP at a low MOI of 0.05 pfu per cell, in the continued presence of Retro-2. Virus-linked Fluorescence was measured over 48h, before end point cell viability was determined using the CellTiter Blue assay. By 48hpi, both WT MEF cells pretreated with media alone, and those pretreated with the DMSO carrier exhibited a 24000 unit increase in fluorescence, showing that the DMSO carrier had no effect on EGFP expression (Figure 5.9A). Pre-treatment of WT cells with Retro-2 resulted in a significant, 33% reduction in EGFP expression to 13000 fluorescence units, compared to the mock and DMSO treated WT cells. This inhibition mirrors the result seen in HeLa cells pretreated with Retro-2, and confirmed the effects of Retro-2 on viral EGFP expression in different cell lines (Figure 5.6). VACV-linked fluorescence in MU MEFs mock treated with media or treated with the DMSO carrier alone exhibited lower levels of EGFP expression than the WT control cells, as expected. Finally, treatment of MU *Wob* MEF cells with Retro-2 further inhibited VACV growth, with a 48hpi reading of just 6000 fluorescent units. This was a 62% reduction in VACV fluorescence compared to the MU control cells, and a 64% reduction compared to the WT, Retro-2 treated cells, indicating that combining the *Wob* mutation and Retro-2 treatment had an additive effect on VACV growth, as measured by

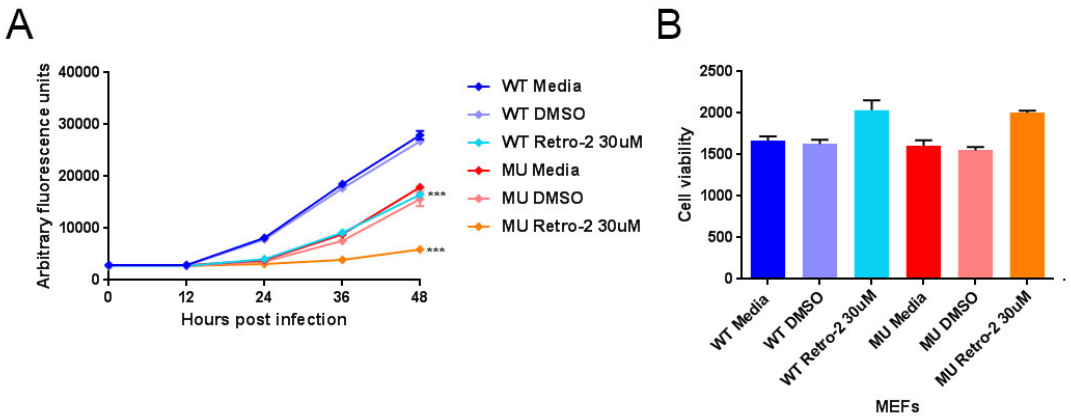

Figure 5.9 Retro-2 treatment displays additional effects on VACV to the Wob mutation. (A) WT and MU *Wob* MEF cells were treated with 30μM Retro-2, DMSO alone or media for 2h before infection with VACV-A5-EGFP. Presence of Retro-2 was maintained throughout the course of the growth curve. Fluorescence was measured every 12h up to 48hpi. Data shows the means and SEMs of three technical repeats, representative of four biological repeats. Statistical analysis was performed using a one-way ANOVA with multiple comparisons, to allow comparison of treated cells compared to non-treated cells, as well as WT to MU. ***, $p<0.001$. (B) After the 48h infection, cells were fixed and stained with CellTiter Blue to assess cell viability. Data shows the mean and SEM of three technical repeats, representative of 5 biological repeats.

fluorescence. The inhibition of viral growth in all cells was confirmed as not due to cell death by a cell viability assay (Figure 5.9B). As seen in previous assays, Retro-2 treatment actually increased cell survival in infected cells compared to the corresponding control treated cell, though again this is most likely due to reduced virus-induced cell lysis due to lower levels of virus in the Retro-2 treated cells. This additional reduction in viral growth in Retro-2 treated *Wob* MEF cells indicates these two methods of inhibiting VACV growth are non-redundant. It also suggests that VACV is dependent on both the GARP complex and syntaxin 5 function for optimal growth, but potentially uses these cellular factors in separate pathways.

5.3.3.6 Retro-2 treatment affects IEV production and causes formation of aberrant B5 vesicles

One of the key findings of VACV infection in GARP deficient *Wob* MEFs was the appearance of aberrant B5 puncta in the MU MEFs, which were independent of a VACV capsid (Figure 4.8). An immunofluorescence assay to show the distribution of IEV/EEV protein B5 in Retro-2 treated cells was therefore performed in order to determine if pharmacological inhibition of EGRTP also resulted in capsid-independent accumulations of B5. HeLa cells were pre-treated with Retro-2, or mock treated with DMSO for 2h before cells were infected at a high MOI of 5 pfu per cell, using VACV-A5-EGFP

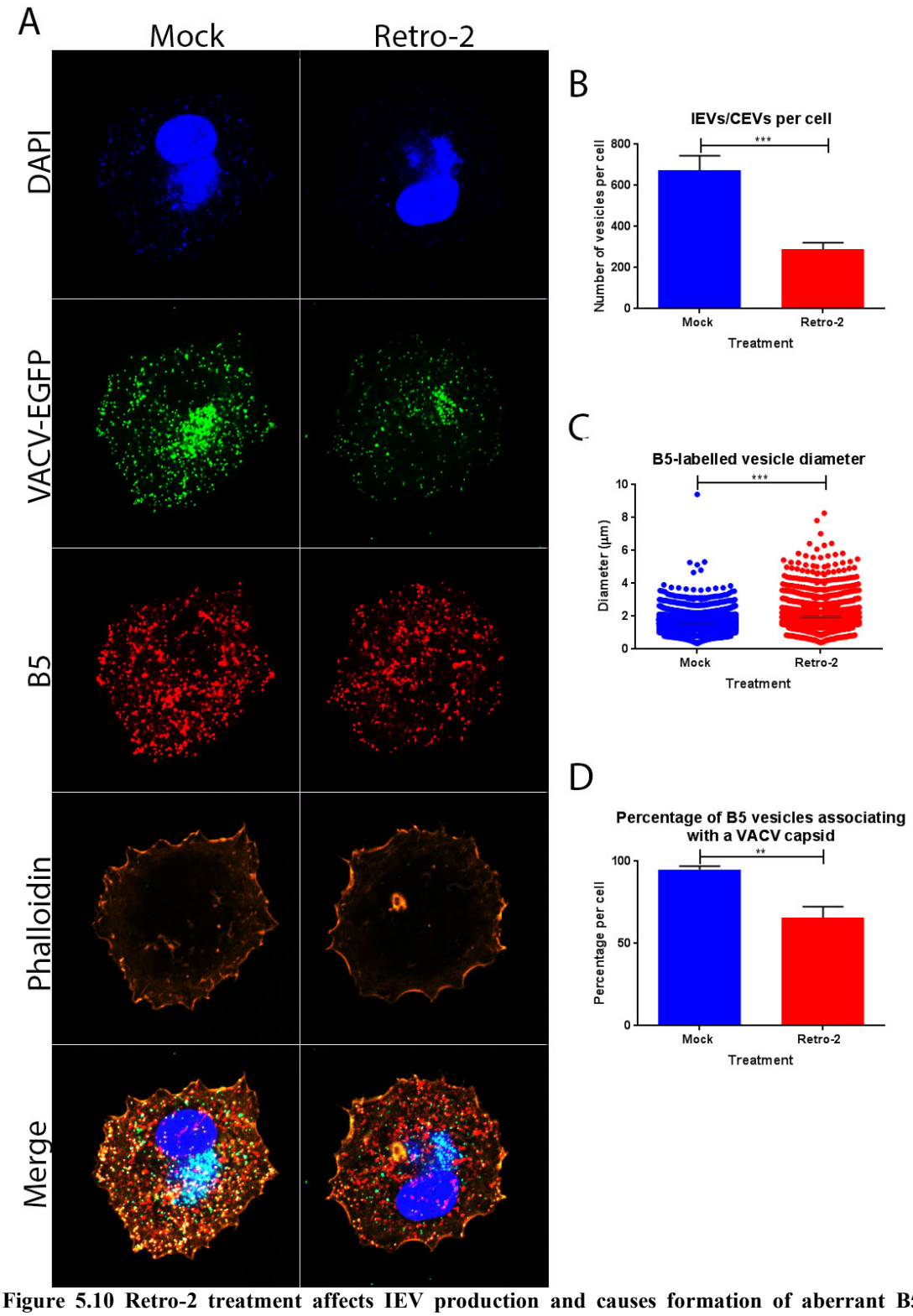

Figure 5.10 Retro-2 treatment affects IEV production and causes formation of aberrant B5 vesicles (A) HeLa cells were treated with Retro-2 at 30µM for 2h, then infected with VACV-A5-EGFP, MOI 5 in the continued presence of Retro-2. At 8hpi, cells were fixed and labelled using an anti-B5 antibody, and phalloidin, and DAPI were stained. Cells were visualised on a Zeiss confocal microscope, and single optical sections taken. (B-D) Z-stacks were taken and used to create 3D images of the cells on IMARIS software. The total number of B5 puncta per cell in mock compared to Retro-2 treated cells (B); diameter of these puncta (C); the percentage of B5 puncta colocalising with VACV-EGFP capsids (D). Data represents means and SEM from 13 individual cells from 1 biological repeat, and a student t-test was used for statistical analysis. **, $p<0.01$, ***, $p<0.001$.

in the continued presence of Retro-2. At 8hpi, cells were fixed, permeabilised and labelled with an antibody targeting the IEV/EEV membrane protein B5, and a fluorescent secondary antibody.

Maximum intensity projections taken through the mock-treated cells showed a juxta-nuclear viral factory, indicated by the presence of VACV-EGFP accumulation, and DAPI DNA staining (Figure 5.10A, left panel). Further examination showed high numbers of yellow colocalised staining of green VACV and red B5 puncta in the periphery of mock-treated cells, indicating the presence of IEVs/CEVs. Retro-2 treatment did not alter the distribution of VACV-EGFP; however it did result in the appearance of fewer B5 puncta in the HeLa cells. Additionally, there was a reduction in the levels of B5-labelled puncta colocalising with VACV-EGFP, indicating fewer IEVs/CEVs in Retro-2 treated cells (Figure 5.10A, right panel). These observations were quantified by taking Z stacks of randomly selected mock- and Retro-2-treated cells, which were recreated into 3D images using Bitplane IMARIS software. B5-labelled puncta were identified and counted, and numbers in control treated cells were compared to those in the treated cells. Retro-2 treatment resulted in a highly significant, 2-fold reduction in B5-positive puncta in the cell cytoplasm (Figure 5.10B), compared to the cells treated only with DMSO. The percentage of these B5-labelled vesicles associating with a VACV capsid was also significantly reduced (Figure 5.10D), from 95% association in the mock treated cells, to 66% in the Retro-2 treated cells. This indicated not only a reduction in IEV production, but also matches the presence of the same capsid-independent, aberrant B5 puncta seen in the *Wob* MEFs (Figures 4.8, 4.9). In further support of this, measurement of the diameters of the B5 puncta showed a significant, 20% increase in vesicle size in the Retro-2 treated cells (Figure 5.10D). Taken together, these results indicate that impairment of EGRTP through Retro-2 treatment inhibits the correct wrapping of IMVs to form IEVs/EEVs, in a similar mechanism to the inhibition seen in the *Wob* MEFs.

5.3.4. Retro-2 treatment prior to infection inhibits VACV growth, and alleviates systemic disease symptoms *in vivo*

Retro-2 has been shown in previous studies to protect against ricin, EHEC and *Leishmania* species *in vivo* (Stechmann *et al.,* 2010; Secher *et al.,* 2015; Canton *et al.,* 2012). In animal models of VACV infection, EEVs are responsible for the long-range spread of VACV around the body, and the

initiation of systemic disease (Payne, 1980), and as Retro-2 pre-treatment strongly inhibited EEV formation and release *in vitro* (Figure 5.8, Figure 5.10) suggesting that it might protect against systemic VACV disease. In order to investigate this hypothesis, the effect of Retro-2 in an *in vivo* model of VACV was investigated. Retro-2 was resuspended in a DMSO carrier at a concentration of 210mM [67.3mg/ml]. Although Retro-2.1 proved more effective *in vitro,* there were solubility issues which rendered this compound unsuitable for *in vivo* use. On two separate occasions, mice were injected intraperitoneally with 100mg Retro-2 per kg body weight. One group received treatment 24h before and 24h after infection with VACV-WR, and a second group were treated 24h and 48h post infection. For the infection, mice were lightly anaesthetised with isofluorane, then VACV was delivered by intranasal injection at a dose of $1x10^4$ pfu , diluted in a PBS vehicle. Control groups were either treated but not infected, infected and treated only with the DMSO vehicle, or both mock treated and mock infected. Uninfected mice, both Retro-2 treated and mock-treated, maintained their body weight throughout the course of the experiment, with no difference seen between mice receiving injection of Retro-2, and those receiving only the vehicle (Figure 5.11A, groups 1, 5 and 6). These results are consistent with previous *in vivo* assays showing no toxicity or side effects in Retro-2 treatment (Stechmann *et al.,* 2010; Secher *et al.,* 2015; Canton & Kima, 2012). In comparison, mice infected with VACV, and mock-treated (group 2) rapidly lost weight from day 3 post infection onwards, and displayed all the expected symptoms of systemic VACV infection, including ruffled fur, a hunched posture, and reduced activity. Of the six mice in this group, 3 reached the humane endpoint, and were euthanized before the conclusion of the experiment. Similar results were seen in those mice receiving Retro-2 treatment only after VACV infection (group 4), at 24 and 48hpi; rapid weight loss and increasing signs of disease, and one instance of euthanasia (Figure 5.11B). However, the mice that received pre-treatment of Retro-2 24h before and 24h after VACV infection lost less weight than their group 2 and group 4 counterparts, and showed less severe disease symptoms. Although the difference in weight loss did not reach overall significance, a significant reduction in weight loss was seen at day 5 in the mice pretreated with Retro-2 compared to the sham treated animals. By 7dpi, the mice pretreated with Retro-2 showed a significant reduction in clinical symptoms compared to the group 2 and group 4 animals (Figure 5.11B), and none of the mice in this group reached the humane end point.

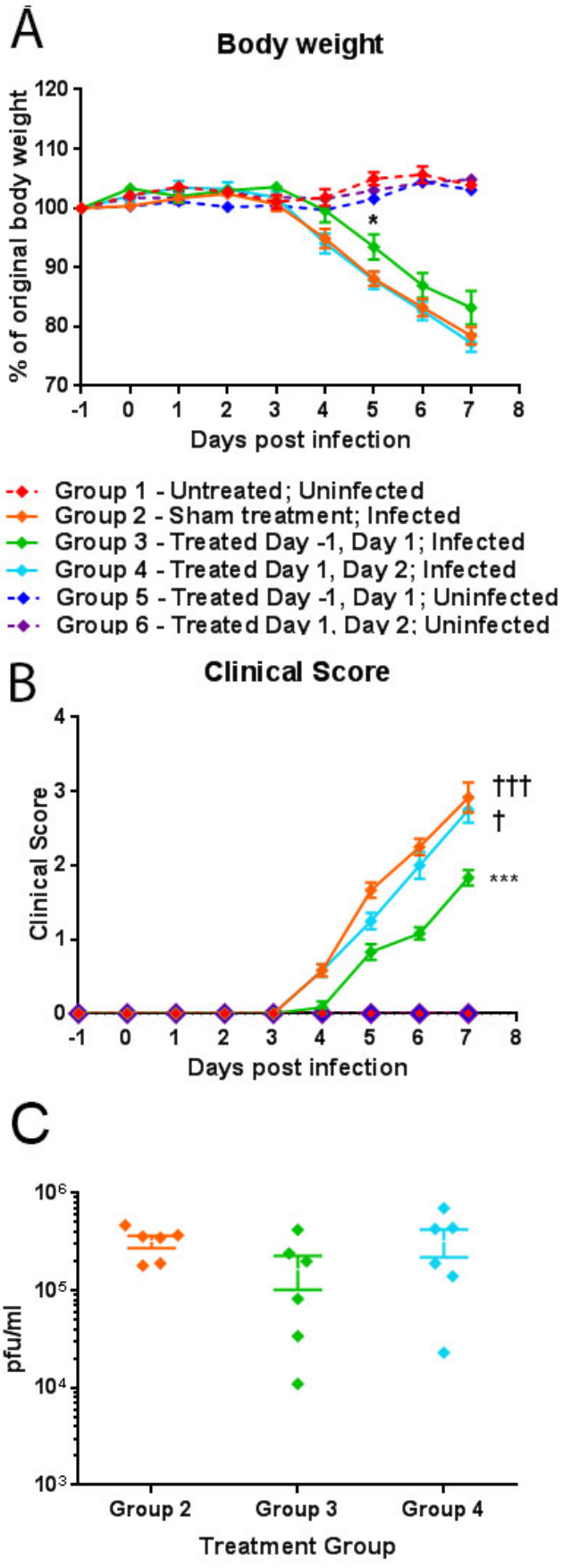

Figure 5.11. Retro-2 treatment prior to infection inhibits VACV growth *in vivo*. BALB/c female mice were randomly assigned into 6 groups of 6 mice each. Group 1 were untreated, uninfected controls. Group 2 were inoculated intranasally (i.n.) with $1x10^4$ PFU of purified VACV-WR on day 0, and sham treated with 300µl 10% DMSO in PBS on day 1 and 2 post infection. Group 3 were infected on day 0 as described and treated with 100mg/kg Retro-2 in PBS on day -1 and +1. Group 4 were infected on day 0 as described and treated with 100mg/kg Retro-2 in PBS on day +1 and +2 post infection. Group 5 were uninfected and treated with 100mg/kg Retro-2 in PBS on day -1 and +1. Group 6 were uninfected and treated with 100mg/kg Retro-2 in PBS on day +1 and +2 post infection. All mice were examined daily for weight loss (A), and clinical symptoms (B) Crucifixes represent the number of animals that reached the human end point before the conclusion of the experiment. At 7 days post infection, the experiment was terminated and viral loads were assessed in all infected mice – groups 2, 3 and 4 by collection and lysing of lung tissue and standard plaque assay (C). Error bars represent SEMs of six individual animals. Statistical analysis was performed using a one-way ANOVA with multiple comparisons, and student T-tests. *, $p<0.05$; ***, $p<0.001$

These results indicate that Retro-2 can significantly alleviate systemic disease, but only when given prior to infection.

After the infection course, lungs were collected from the mice and the titre of VACV in infected groups (groups 2, 3 and 4) was determined by plaque assay (Figure 5.11C). This revealed that pre-treatment of mice with Retro-2 24h before infection (group 3) on average reduced the titre of VACV in the lungs compared to groups 2 and 4 – sham treated and treated only post infection, though this result did not quite reach significance (p=0.07). Overall however, these results indicate that Retro-2 has a protective effect on VACV infection in a mouse model, when used as a pre-treatment, before infection.

5.4. Discussion

5.4.1. F13 and B5

The focus of this chapter was to characterise the interaction between the EGRTP and VACV. The localisation of B5vesicles in *Wob* MEFs was compared with that of another IEV/EEV protein, F13. Almost all the B5 seen colocalised with F13 in vesicles which although fewer in number were, on average, significantly larger in the MU MEFs than those seen in the WT cells. Although a proportion of the puncta in MU MEF cells are likely to be IEVs/CEVs, the mean increase in diameter is consistent with the aberrant B5-labelled vesicles seen in Figure 4.8 and 4.9, and suggests that these same capsid-independent vesicles were present, and also contain F13.

Both B5 and F13 are essential for VACV growth, and key components of the IEV/EEV membrane, as deletion of B5 results in a small plaque phenotype and a loss of comet formation (Wolffe *et al.,* 1993), and loss of F13 results in an inability to form plaques at all (Blasco & Moss, 1991). As VACV IEVs exit from the cell, several envelope proteins, including F13 and B5 are deposited on the cell surface after fusion of the plasma and virus membranes (Smith et al., 2002). Previous studies have shown that B5 left at the plasma membrane is recycled back to the TGN, due to a motif in the protein's cytoplasmic tail which has been implicated as a regulator for endocytosis (Ward & Moss (2000) and Husain and Moss (2005). Additionally, F13 has been implicated in clathrin-mediated endocytosis, as VACV-infected cells treated with the endocytosis inhibiting drug chlorpromazine exhibit accumulations of F13, and TR-tfn, a marker of clathrin–dependent internalisation, under the plasma membrane (Husain & Moss, 2003). Together, these results showing colocalisation of B5 and F12 support a model whereby IEV/CEV proteins deposited at the plasma membrane on viral egress cannot be retrieved and recycled back to the wrapping station for further IEV membrane production in the absence of GARP. However, there is also the possibility of an alternative model in which GARP is required for the correct sorting of an as-yet-unidentified cellular protein required for wrapping and IEV formation. In this model, the B5/F13-labelled puncta would represent IEV membranes which could not be correctly tethered to the wrapping station, or enveloped round the IMVs. This model is supported by the evidence that B5 and another IEV protein, F12, are still transported to the cell periphery, even when morphogenesis is inhibited after IMV formation (Van Eijl *et al.,* 2002), and

both B5 and F13 are correctly targeted to the Golgi area, even when expressed in the absence of VACV infection or other IEV proteins (Lorenzo *et al.,* 2000). A similar situation is seen in HSV-1, with the production of non-infectious L particles (Szilágyi & Cunningham, 1991).

In comparison, Sivan *et al,* (2016), showed that when retrograde transport is blocked by the small, pharmacologically active molecule Retro-2, IEV/EEV formation is blocked, and F13 accumulates in vesicles in the cell periphery. However, no colocalisation was seen between F13 and B5. Sivan *et al.,* suggested that F13 localises in early endosomes before being trafficked through the retrograde transport pathway to associate with B5 in IEV membrane precursors at the TGN. However, as a different method of EGRTP impairment was used, targeting a different component of the retrograde transport pathway, it is likely that the effects seen on F13 transport in Retro-2 treated cells are due to these differences. It may be that Retro-2 interferes with the initial trafficking of F13 to the wrapping station, while GARP affects the recycling of IEV proteins back to the wrapping station after an initial incorporation into a VACV enveloped virion membrane.

In order to determine whether the B5/F13 puncta in the MU *Wob* MEFs are whole membranes unable to correctly wrap IMVs, or are membranes deposited at the cell surface which cannot be recycled back to the wrapping station due to the block in retrograde transport, a number of experiments could be performed. Initially, localisation of other IEV/EEV proteins in *Wob* MEFs could be examined, such as A36 and F12, and their level of association with B5, F13 and each other in the absence of optimal GARP levels. Should all the IEV/EEV proteins associate with each other, this would support the model that IEV membranes are assembled in GARP deficient cells, but cannot be correctly wrapped around IMVs. The nature of the puncta themselves could also be examined. The B5 and F12 structures seen when these proteins are expressed alone co-stain with the fluid phase endocytosis marker HRP, indicating that they are contained in endosomes (Van Eijl *et al.,* 2002). Similar staining could be performed in *Wob* MEFs to examine if the B5/F13 labelled puncta seen in the mutant cells are contained in endosomes, and if so, which kind of endosomes: early, late or recycling. If these experiments showed positive results it, would support the model that GARP loss prevents recycling of plasma membrane-deposited IEV/EEV proteins.

5.4.2. Retromer

Another focus of this chapter was investigation into other components of EGRTP that are involved in optimal VACV growth. This focused firstly on the siRNA knockdown of retromer components Vps26 and Vps35. Retromer is a coat complex which associates with early and recycling endosomes, and is required for the correct retrograde transport of both endogenous cargo, and several pathogens and toxins (Trousdale & Kim, 2015). The hydrolase chaperone CI-MPR is a well characterised cargo of EGRTP, and relies on both retromer and GARP for its correct sorting and trafficking in HeLa cells (Arighi *et al.,* 2004; Pérez-Victoria, *et al.,* 2008). As GARP is required for optimal VACV growth, we hypothesised that retromer is also involved in EEV production. Transfection of siRNA SMARTpools targeting retromer complex components Vps26 and Vps35 successfully reduced expression of these proteins and disrupted EGRTP as demonstrated by TGN46 trafficking. However, despite this successful reduction in protein levels, VACV growth was not affected, disproving the hypothesis and indicating the presence of a non-classical, retromer-independent retrograde transport pathway. This finding highlights the complexity of these cellular pathways. There are two main retrograde transport routes which have been characterised, one from early endosomes to the TGN, often via recycling endosomes, and one from late endosomes to the TGN. Despite requiring different GTPases, tethering factors and SNARE proteins for their function, both routes have been shown to be reliant on retromer for initial cargo sorting (Ganley *et al.,* 2008; McKenzie *et al.,* 2013), and revealing the role of retromer as a key component in EGRTP. Retromer is required for the correct localisation of multiple endogenous genes, such as CI-MPR (McKenzie *et al.,* 2013), as well as successful trafficking of several toxins and pathogens, including exit from the early endosomal compartment of the STxB subunit, and HPV16 (Mallard *et al.,* 1998; Popa *et al.,* 2015), and sorting of HIV-1 protein Env (Groppelli *et al.,* 2014). However, examples of non-classical, retromer-independent retrograde transport have been observed. One such endogenous example is the retromer-independent, Rab9-dependent recycling of the endopeptidase furin from late endosomes to the TGN (Chia *et al.,* 2011). Non-classical, retromer-independent retrograde transport has also been exhibited by adeno-associated virus 2 (AAV2), for transduction of its genome to the nucleus. AAV2 utilises a retrograde pathway independent of retromer, as well as late and recycling endosomes, and the syntaxins 6 and 16, key components of the retrograde transport SNARE complex. This evidence, along with the results

achieved here, support the presence of a non-classical retrograde pathway, used by endogenous and exogenous cargo. (Nonnenmacher *et al.,* 2015) Further steps in this line of investigation would be to examine the effects of the loss of other suspected components in this non-classical, retromer-independent pathway on VACV infection.

5.4.3. Retro-2

As syntaxin 5 had been implicated in the non-classical EGRTP, as an essential requirement for AAV2 transduction (Nonnenmacher *et al.,* 2015), this SNARE was knocked down using siRNA transfection. Here however, the siRNA proved highly cytotoxic, hampering interpretation of the experiment (results not shown). Another method of syntaxin 5 disruption was therefore used, in the form of Retro-2, a small molecule inhibitor of the retrograde transport pathway (Stechmann *et al.,* 2010). Retro-2 impairs retrograde transport by causing displacement of t-SNARE syntaxin 5, though the exact mechanism is unknown (Stechmann *et al.,* 2010). Initially, TGN46 trafficking assay and an STxB cell death assay showed that Retro-2 successfully inhibited retrograde transport. Following this, single and multi-cycle VACV growth curves examined the effect of Retro-2 and related compounds Retro-1, VP184 and Retro-2.1 on VACV growth. All the compounds tested showed significant inhibition of VACV growth, specifically EEV production, indicating that VACV also requires syntaxin 5 as well as GARP for IEV wrapping. Treatment with Retro-2 also resulted in the aberrant, large, capsid-independent B5-labelled vesicles as seen in the mutant *Wob* MEF cells. This model of VACV inhibition also translated to an *in vivo* mouse model, as Retro-2 pre-treatment of mice infected with VACV-WR reduced viral titres and clinical signs of disease.

There are two well-characterised anti-poxvirus drugs already in circulation which, like Retro-2, also target the IEV wrapping process. The first of these, IMCBH was initially discovered to inhibit VACV growth and release in 1968, and was later found to selectively target the IEV/EEV protein F13. However, this drug is ineffective both *in vivo*, and against any other poxvirus, and so is not a target for further development as a therapeutic agent (Kato *et al.,* 1968; Schmutz *et al.* 1991). The more recently characterised anti-poxvirus drug, ST-246 is a small molecule compound active against multiple poxviruses, which again targets the F13 IEV/EEV protein (Yang *et al.,* 2005). Retro-2 and ST-246 show similar effects, in they both reduce EEV production 5-10 fold in single-step growth curves,

which is enough to almost completely block VACV multi-cycle growth. Additionally, neither drug affects IMV production (Yang *et al.,* 2005, this work). However, each drug holds advantages over the other. ST-246 is susceptible to resistance by substitution or insertion mutations in the F13 gene, rendering it ineffective (Duraffour *et al.,* 2015). In this aspect, Retro-2 is the superior choice for therapeutic development, as targets not only a cellular factor which is a far lower mutation/resistance risk than a viral protein, but is extremely specific, and inhibits only one component of EGRTP. Despite this, while ST-246 successfully protects against VACV inoculation *in vivo* when administered post infection (Yang *et al.,* 2005), Retro-2 only protects against VACV when administered as a pre-treatment, when administered at days -1 and +1 either side of infection, and does not have an effect when administered only as a post-infection treatment, and so requires further development in this area. In comparison, when used as a treatment for *Leishmaniasis amazonesis* and EHEC, Retro-2 exerted a protective effect when administered up to 3 weeks or 26 hours post infection respectively (Canton & Kima, 2012; Secher *et al.,*2015). Taken along with the results seen here, this evidence indicates that Retro-2, with development, could eventually have potential not only as an anti-poxvirus drug, but to supplement poxvirus vaccination in the event of an outbreak or bioterror incident.

As the difference in viral titres seen here from the *in vivo* experiment did not quite reach significance, additional work in this area would begin with a biological repeat of the infection time course and lung titre, administering Retro-2 several hours before the VACV infection was performed, rather than one day, as seen in the Stechmann *et al.* protocol (2010). Retro-2.1 could also be tested against VACV *in vivo*, as it is known to have a far higher efficiency than Retro-2; including 1000-fold greater inhibition of ricin intoxication (Gupta *et al.,* 2013), and 100-fold greater inhibitory affect against VACV. With regards to further elucidating the mechanism of Retro-2 action on VACV growth, several more *in vitro* studies could be performed. Other researchers have shown that when Retro-2 is used as the method of retrograde transport inhibition, B5 fails to associate with VACV capsids, which is consistent with the results obtained here, but B5 and F13 do not colocalise, as discussed earlier (Sivan *et al.,* 2016). Further development of this project would certainly require the re-examination of B5 and F13 colocalisation, as these two proteins have high levels of association in retrograde-deficient *Wob* MEF cells. Should the results of the Sivan *et al* paper be confirmed, this may suggest that VACV uses at least two separate, non-classical retrograde pathways.

Overall, the results of this chapter show that VACV utilises a retromer-independent, non-classical retrograde transport pathway to correctly wrap IEVs. This pathway involves GARP and syntaxin 5, and loss of these components results in one of two possible models: either retrograde transport is required to recycle EEV/CEV proteins deposited on the cell surface after virus egress, or this pathway is required for the correct trafficking of an as-yet-unknown cellular factor which is required for IEV membrane envelopment of the IMV at the wrapping station. Additionally, Retro-2 has been shown to be a potential candidate as an anti-poxvirus prophylactic.

6. General Discussion

6.1. Thesis aims and overview.

The aim of this thesis was to investigate the role of two cellular proteins during VACV infection: MKK3 and Vps52. siRNA knockdown, genetic mutation and pharmaceutical agents were used to inhibit expression of the proteins of interest both *in vitro* and *in vivo* in order to determine the effects of MKK3 and Vps52 on VACV infection. In addition to its role as the prototypic poxvirus, VACV has many applications as a vaccine vector and as a tool to investigate cellular mechanisms. However, the replication cycle of VACV is complex and poorly understood. By examining the interactions of VACV with cellular proteins and pathways, the mechanisms of VACV replication and growth can be further elucidated.

6.2. Conclusions and implications

A high-throughput, siRNA based screen performed by Beard *et al.* (2014) identified multiple novel pro-viral cellular factors required for optimum VACV growth and replication, two of which are the proteins of interest here: MKK3 and Vps52. Both proteins exhibited significant pro-viral effects in the original screen, and validation with a fluorescence-based growth assay showed that knockdown of these proteins significantly affected viral-linked fluorescence. As the two proteins were unrelated, they were investigated separately, but using similar techniques.

6.2.1. MKK3

Transfection of HeLa cells with an siRNA SMARTpool targeting MKK3 was able to not only substantially knock down MKK3 expression, but also significantly inhibit the expression of viral linkedEGFP in both multi-and single-cycle growth assays. However, this inhibition did not translate to viral titre in cell culture or disease severity in a murine model of VACV disease. While virion production was not altered by loss of MKK3, production of VACV early and late proteins was substantially inhibited by 50% compared to the negative control. This result, along with the reduction in A5-tagged fluorescence indicates that MKK3 is required for optimal viral protein production.

One of the key roles of the p38 pathway is the production of cytokines during the inflammatory response, with expression of appropriate cytokines occurring by differential activation of the pathway. As a consequence of this, p38 has been linked to both the pathology of a number of infectious diseases, including influenza A and dengue fever (Börgeling *et al.,* 2014; Fu *et al.,* 2014). Use of SB203580 during dengue virus infection suppresses the dengue-induced over-production of pro-inflammatory cytokines such as TNF-α and IL-8 which can lead to severe dengue fever (Fu *et al.,* 2014). Highly pathogenic avian influenza is also able to over-induce p38 activation, leading to increased pro-inflammatory cytokine expression and viral pathogenicity (Börgeling *et al.,* 2014). In comparison, VACV both activates and inhibits the p38 pathway, and subsequently, the expression of downstream genes; upregulating the production of anti-inflammatory cytokines, and down-regulating inflammatory mediators in order to promote its own survival (Myskiw *et al.,* 2009; Maloney *et al.,* 2005).

Although previous studies have shown that the MKK3 and the p38 pathway are required for optimal EGFP expression in cells infected with fluorescently tagged VACV (Hu *et al.,* 2007; Beard *et al.,* 2014), the direct effect of MKK3 inhibition on viral titre had not been examined. Investigation here showed that loss of MKK3 had no discernible effect on viral titre *in vivo* or *in vitro*, despite a reduction in the production of early, late and IMV proteins in HeLa cells. The lack of effect on direct measurements of growth such as viral titre suggests a model in which VACV produces an excess of proteins, meaning that inhibiting protein expression by MKK3 loss is not enough of an effect to also inhibit virion formation or morphogenesis. This occurrence of protein levels exceeding the amount required for virion production has been seen in other viruses, such as Hepatitis B virus (Churin *et al.,* 2015), where overproduced proteins are multimerised and formed into non-infectious sub-viral particles. However, this protein excess has never been seen before in VACV, and the model outlined here also suggests a role for MKK3 in regulating viral protein production. Although MKK3 specifically has not been previously linked to viral protein production, the p38 and ERK-activated kinase Mnk1 has been shown to activate cellular translation initiation factor eIF4F, at the control of VACV. As VACV shuts down translation of cellular genes in favour of its own, this activation of eIF4F substantially increases viral gene expression and replication (Waskiewicz *et al.,* 1997; Walsh *et al.,* 2008) In the Walsh *et al.* study, cells deficient in Mnk1 exhibited not only a reduction in VACV

protein expression, but also a reduction in production of plaque forming units a result which was not seen here. This is likely due to the fact that Mnk1 is activated by the ERK pathway as well as the p38 cascade (Waskiewicz *et al.,* 1997), and so direct loss of Mnk1 has a greater effect on VACV translation than only inhibiting one part of the p38 pathway by MKK3 knockdown. Therefore, the results of this thesis suggest that in this signalling cascade, p38 may be activated specifically by MKK3 in order to promote the production of viral proteins. However, while p38 may be important in VACV pathogenesis, the role of MKK3 specifically is not essential, as although viral protein production was effected by loss of MKK3, the impact was not sufficient to affect replication.

6.2.2. Vps52

The host protein Vps52 was knocked down using siRNA SMARTpool transfection, as well as using the *Wobbler* genetic mutation in MEFs. Both methods significantly reduced expression of the Vps52 protein, and resulted in a significant inhibition of VACV-A5-EGFP growth. Direct measurement of infectious virions produced during Vps52 loss showed significant reductions in viral titre compared to the corresponding controls in both siRNA transfected cells and *Wob* mutated cells. Separate examination of the cellular and supernatant fractions of single step growth curves showed that both Vps52-targeting siRNA transfection and the *Wob* mutation had the same effect: a reduction specifically in EEV production, but no difference in IMV production compared to the corresponding controls. This indicated that Vps52 and the GARP complex affect wrapping of IMVs to form IEVs, or a later process in virion morphogenesis such as EEV release. Immunofluorescent labelling of VACV and IEV proteins in *Wob* MEF cells confirmed the IEV/EEV reduction shown in the single cycle growth curve, and also revealed large, aberrant, accumulations consisting of B5 and F13, but existing independently of VACV capsids.

Having identified the GARP complex as required for IEV production, we expanded our study to identify other components of EGRTP involved in infection. The retromer complex, despite being one of the key components of many retrograde transport pathways was shown to not be required for VACV growth as transfection of siRNA targeting two of the components of the complex, Vps26 and Vps35 did not alter VACV growth compared to the negative control. Although retromer is not required by VACV, the t-SNARE syntaxin 5 is essential for optimal growth, as pharmacological

inhibition of this protein by small molecule compound Retro-2, and several related compounds not only successfully disrupted EGRTP, but also inhibited both multi-cycle VACV growth and EEV production, as seen in *Wob* MEFs and siRNA knockdown of Vps52. Again mirroring the results seen in *Wob* MEFs, treatment of cells with Retro-2 also produced large, aberrant accumulations of IEV/EEV protein B5, which were seen to exist independently of a VACV capsid. These effects also translated into a mouse model, as treatment of mice with Retro-2 prior to VACV infection reduced viral titres and inhibited clinical symptoms, weight loss and disease progression, though only marginally

Several studies have previously suggested that retrograde transport may play a role in VACV infection, as cells infected with VACV exhibit increased rates of endocytosis, and increased activity of the endosome to TGN pathway (Schmelz *et al.,* 1994), and several IEV proteins, such as B5 and F13, deposited on the cells surface after EEV egress are thought to be recycled back to the TGN (Husain & Moss, 2004). However, this is the first time that the exact retrograde components and pathway required for optimal VACV growth have been investigated. Taking into account the increase in endocytosis in VACV infected cells, the recycling of IEV proteins from the cell surface and the identification of Vps52 and Vps54 of pro-viral cellular factors in two independent screens (Schmelz *et al.,* 1994; Husain & Moss, 2005; Sivan *et al.,* 2013; Beard *et al.,* 2014), we hypothesised that GARP is involved in retrieving deposited IEV proteins from the cell surface, and recycling them back to the TGN-located wrapping station.

As previously mentioned, several IEV proteins including B5 and F13, remain on the cell surface after EV egress, and are then recycled back to a juxta-nuclear area in a retrograde transport dependent manner (Ward & Moss, 2000; Husain & Moss, 2005) This, along with the drop in EEV production during GARP depletion, suggests a model in which GARP tethers vesicles containing IEV proteins traveling from the cell surface back to the TGN for wrapping of new IEVs. The presence of accumulations containing B5 and F13 that were not associated with the green fluorescent viral cores in MU cells suggest that in the absence of GARP, these accumulations have not been correctly tethered to the wrapping station, or as recycled membrane components from the cell surface unable to dock to the site of IEV production. However, the results shown here do not rule out the possibility that

GARP is not involved directly in IEV protein transport, but is responsible for the trafficking of an unknown host protein which is required for wrapping. In this model, it is likely that the aberrant B5 puncta would be empty IEV membranes which were unable to wrap IMVs. This hypothesis is supported by a study performed by Van Eijl *et al.* (2002) which showed that IEV proteins B5 and F12 are transported to the cell periphery even in the event of a morphogenesis block after IMV formation. In the van Eijl study, treatment of cells with IMCBH, which inhibits IEV wrapping showed aggregates of B5 accumulating in vesicles in the cytoplasm, similar to the B5 puncta we observed when retrograde transport was impaired by both GARP mutation and Retro-2 treatment. Additionally, co-localisation of B5 and F12 in capsid-independent puntca was seen under these conditions, supporting the colocalisation of capsid-independent B5 and F13 seen in this thesis, and again supporting the theory that loss of GARP results in empty IEV membranes that cannot be correctly tethered to the wrapping station.

VACV infection has been shown to increase the rates of cellular endocytosis (Schmelz *et al.,* 1994), and the IEV/EEV protein F13 has been linked to clathrin-mediated endocytosis, as blockage of this endocytic pathway with chlorpromazine resulted in F13 accumulation under the plasma membrane (Husain & Moss, 2003). However, the reduction in IEV/CEV and EEV production seen in retrograde transport inhibition is independent of endocytosis. Examination of fluid phase endocytosis in *Wobbler* MEFs showed no difference in rates of endocytosis between WT and mutant cells, indicating that the effect of MEFs is limited to endosome to TGN transport (Karlsson *et al.,* 2013). Nor does Retro-2 affect endocytosis, as treatment of cells with the compound did not inhibit clathrin-mediated uptake of endocytosis marker transferrin (Stechmann *et al.,* 2010). Additionally, inhibition of endocytosis using a strain of VACV expressing a dominant negative clathrin-coated endocytosis adaptor protein did not affect levels of IEV/CEV production, suggesting that endocytosis is not essential (Husain & Moss, 2005). However, in this paper, IEV/CEV production was counted using electron microscopy, with greatly varying virion numbers between sections, calling into question the accuracy of such a technique. Therefore, this work shows that inhibition specifically of the retrograde transport pathway reduces IMV wrapping, but we cannot make any conclusions about the impact of inhibition of endocytosis, as the first step in the pathway returning viral proteins from cell surface to the TGN.

We also hypothesised that GARP was not the only cellular EGRTP component involved in recycling of VACV IEV proteins back to the TGN. Retromer is a key component in the correct retrograde trafficking of a wide variety of cargo both endogenous, such as CI-MPR (Arighi *et al.,* 2004) and invasive, such as the HIV Env protein (Groppelli *et al.,* 2014). Given its involvement in transporting pathogen components, and its role in sorting and binding cargo at endosomal compartments (Carlton *et al.,* 2004; Kim *et al.,* 2015), we proposed a model in which retromer played a role in recycling IEV proteins for further use at the TGN wrapping station. However, this hypothesis was disproved when results showed that loss of retromer subunits Vps26 and the complex core Vps35, did not alter VACV growth compared to the negative controls. This lack of effect was maintained, despite the fact that retromer knockdown was able to disrupt trafficking of retrograde transport marker TGN46, therefore showing that siRNA knockdown of Vps35 and Vps26 was successful. Since retromer is a core component of EGRTP, this suggested that VACV utilises a non-classical pathway, as the two main retrograde transport routes, one originating from early endosomes and one from late endosomes both rely on retromer for initial cargo sorting, despite being otherwise largely independent of each other (Ganley *et al.,* 2008; McKenzie *et al.,* 2013). Although retromer is involved in trafficking many different retrograde cargoes, the evidence presented is not the first instance that retromer-independent, non-classical retrograde transport has been observed, and supports the findings of previous studies such as Nonnenmacher *et al.,* (2015) which, through siRNA transfection targeting various retrograde components, showed that transduction of AAV2 does not require retromer, or the several key components of the retrograde SNARE complex such as syntaxin 6 and syntaxin 16.

The final route of investigation into retrograde transport and VACV infection was the pharmacological inhibitor of retrograde transport, Retro-2. In addition, Retro-2 is thought to disrupt retrograde transport by altering the distribution of syntaxin 5, a SNARE required for the non-classical, retromer-independent transduction of AAV2. This requirement was shown by both siRNA targeting of syntaxin, and treatment with Retro-2 (Stechmann *et al.,* 2010; Nonnenmacher *et al.,* 2015). These links suggested that Retro-2 treatment may constitute a third method of disrupting EGRTP in order to inhibit VACV growth, as well as a potential VACV anti-viral. Retro-2, along with related compounds Retro-1, VP184 and Retro-2.1 all significantly impacted overall VACV growth and EEV production, a similar effect to the anti-poxvirus drug ST-246. However, while ST-246 directly targets the virus via

the F13 IEV protein, Retro-2 targets the cell, and inhibits VACV growth by disrupting syntaxin 5 distribution, and therefore the retrograde transport pathway, meaning that Retro-2 treatment poses a lower risk of resistance mutations (Yang *et al.,* 2005; Stechmann *et al.,* 2010). Although the results presented here indicate that only pre-treatment with Retro-2 is protective against VACV infection *in vivo*, investigations with other pathogens have shown that Retro-2 can exert a protective effect several hours or days after infection, as systemic treatment with the drug can successfully reduce weight loss and improve survival of mice intoxicated with EHEC strain O104:04 (Secher *et al.,* 2015). This, along with the fact that cellular factors are far less susceptible to functional mutations than viral proteins, indicates that if further development, Retro-2 could have potential as anti-poxvirus prophylactic.

6.3. Overall Discussion

Although the two hits from the original screen, MKK3 and Vps52 appear to play very different roles in VACV infection, examining the results from the three chapters together presents some interesting perspectives. Although they only constitute a small percentage of virions production of IEVs/EEVs during VACV is a process of much controversy and debate. The origin of the IEV double membrane, and the location of the IEV wrapping station has been proposed as the ER/Golgi network intermediate compartment (Sodeik *et al.,* 1993; Van Eijl *et al.,* 2002); the TGN (Ichihashi *et al.,* 1971; Hiller & Weber, 1985; Schmelz *et al.,* 1994); or endosomal compartments (Van Eijl *et al.,* 2002). The results presented here do not add any new evidence to the arguments for IEV membrane origin, they do support the theory that the IEV wrapping station is situated at, or closely associated with, the TGN. While GARP acts as a tethering factor at early and late endosomes, it localises predominantly at the Golgi, as seen by colocalisation of Vps52, Vps53 and Vps53 with Golgi marker GM130 (Liewen *et al.,* 2005). Syntaxin 5 is also found localised to the TGN, and is displaced from this positioning following treatment with Retro-2 (Stechmann *et al.,* 2010). Therefore, the two retrograde components found here to be essential for IEV production are both localised to the TGN, implying that this is where wrapping of IEVs occurs.

Two potential models are proposed here for the involvement of retrograde transport in VACV IEV/EEV production. One model suggests that GARP tethers vesicles containing IEV proteins at the

TGN wrapping station as they are recycled back from the cell surface, while the other suggests that loss of GARP results in an inability for formed IEV membranes to wrap IMVs.

Syntaxin 5 has previously been linked to retrograde transport, and as the part of a SNARE complex also including GS28, Ykt6 and GS15, is required for the endosome to Golgi transport of STxB and the mannose-6-phophate receptor (Tai *et al.,* 2004; Amessou *et al.,* 2007). Specific RNAi knockdown of syntaxin 5 resulted in a significant block in StxB transport, an effect similar to that caused by syntaxin 16 knockdown (Amessou *et al.,* 2007). As syntaxin 5 and syntaxin 16 are known to function in two independent SNARE complexes, this suggests the existence of a separate, syntaxin 5 dependent retrograde transport route. The main SNARE complex that GARP is thought to interact with is the late-Golgi complex containing syntaxin 6 and syntaxin 16 (Pérez-Victoria & Bonifacino, 2009). However, not only does the *C. elegans* GARP complex interact with the syntaxin 5 orthologue, SYX-5 in a yeast two-hybrid system, but the Vps54 orthologue has been shown to bind directly to *C. elegans* SYX-5 (Luo *et al.,* 2011), indicating that GARP does not interact exclusively with the syntaxin 16 containing SNARE complex . The evidence presented here and in previous studies indicates that in the context of VACV infection, GARP interacts with the syntaxin 5 SNARE complex at the TGN as well as the syntaxin 6 and syntaxin 16 SNARE complex, most likely to ensure correct targeting of its cargo.

While these results shed more light on the specific components of the retrograde pathway that VACV utilises for IEV production; they does not support either of the proposed mechanisms over the other. Determining which of these models is correct would require more investigation. For example, a yeast two-hybrid screen could be conducted for proteins that interact with GARP, and the hits from this examined for their effect on VACV growth. Any proteins not directly part of EGRTP may be a candidate for the unknown cellular protein that may be responsible for IEV wrapping, which also requires GARP for correct targeting. In another route of investigation, the identity of the aberrant accumulations of B5 and F13 in GARP deficient and Retro-2 treated cells could be further investigated. If the IEV proteins are seen to colocalise with markers of early, late or recycling endosomes, this would support the model that GARP is required for tethering vesicles containing recycled proteins from the cell surface. If, however, the proteins were not contained inside an

endosome, but the complete repertoire of IEV proteins were present, this would support the 'empty membrane' model.

Another method of determining which of the proposed models is correct would be an antibody uptake, or 'antibody gobbling' experiment. In such an experiment, *Wob* MEF cells would be infected with VACV-EGFP at a high MOI, and infected for 6h, before being chilled on ice with a high concentration of anti-B5 antibody, to stall progression of the infection. A cohort of cells would be fixed and levels of surface B5 examined after this incubation, while another cohort would subsequently be incubated at 37^{o}C for 2h to reactivate morphogenesis, and allow uptake and trafficking. Levels of internalised B5 staining could then be examined and compared to the previously fixed control, and as well as comparing levels between WT and MU cells. Co-staining with a TGN marker such as TGN46, or a Golgi marker such as giantin would also indicate if internalised B5 had been recycled back to the TGN/wrapping station. Previous studies have used a similar protocol to follow the route of retrograde transported cargo, such as Groppelli *et al.* (2013), which utilised an antibody feeding assay to track the movement of HIV-1 protein Env, and showed that if this protein is not incorporated into new virions at the site of morphogenesis near the cell surface, it is recycled back to the Golgi, in a retromer-pathway. Seaman *et al.* (2004) also used this protocol to show that CI-MPR cannot be recycled back to the Golgi in absence of retromer, and later in 2007 to demonstrate that the retrograde trafficking of CI-MPR is specifically dependent on a sorting motif in the CI-MPR tail. We obtained preliminary data from an antibody gobbling experiment which showed that MU *Wob* MEF cells exhibit lower levels of internalised B5 after a 2h 37^{o}C reactivation incubation. However, lack of time meant we were unable to complete colocalisation staining, or quantification of B5 levels on the surface post anti-body addition on ice and pre-incubation, meaning that we were unable to draw any conclusions from this experiment (data not shown).

The proteins examined here, MKK3 and Vps52 are involved in very different aspects of the VACV life cycle; MKK3 in viral protein production, and Vps52 in IEV wrapping. However, the results show that the role of MKK3 in protein production is not significant enough to impact virion formation in MKK3 deficient cells, suggesting that IMV and non-structural proteins are produced in excess. Conversely, the requirement of Vps52 and EGRTP in recycling IEV/EEV proteins back from the cell

surface to the wrapping station suggests that IEV envelope proteins are produced at a deficiency, especially as blocking retrograde transport so significantly impacts IEV production. Considering that EEVs are key for the long range dissemination and spread of VACV (Appleyard *et al*, 1971; Payne, 1980), this difference between levels of IEV proteins and other viral proteins is an interesting revelation that warrants further investigation, including the effect of MKK3 loss on IEV protein levels, and the subsequent effect on IEV production. It could also be argued that the effects of MKK3 and Vps52 knockdown have shown that the overall amount of viral proteins is not important, but the location of viral proteins are key for optimal growth.

Overall, this thesis highlights the pitfalls of carrying out high-throughput genetic screens in transformed cell lines, and measuring a representative of viral growth rather than directly examining virion formation. However, the work presented here also demonstrates the power of high-throughput genetic screens to identify novel features of virus-cell interactions, and aid in the understanding of viral infection cycles and the role of the host cell in VACV infection. This is particularly important in VACV as it has multiple applications in molecular biology and vaccine development, but a highly complex life cycle, many features of which are still poorly understood, such as the process of wrapping IEVs. In addition, we have identified a potential druggable target in the retrograde transport system, which with future development, may make Retro-2 and its derivatives successful pharmaceutical agents for anti-poxviral intervention.

Bibliography

- Abascal-Palacios, G., Schindler, C., Rojas, A.L., Bonifacino, J.S. and Hierro, A., 2013. Structural basis for the interaction of the Golgi-Associated Retrograde Protein Complex with the t-SNARE Syntaxin 6. *Structure*, *21*(9), pp.1698-1706.
- Ahn, B.Y. and Moss, B., 1992. RNA polymerase-associated transcription specificity factor encoded by vaccinia virus. *Proceedings of the National Academy of Sciences*, *89*(8), pp.3536-3540.
- Alcamí, A. and Smith, G.L., 1996. Receptors for gamma-interferon encoded by poxviruses: implications for the unknown origin of vaccinia virus. *Trends in microbiology*, *4*(8), pp.321-326.
- Alessi, D.R., Saito, Y., Campbell, D.G., Cohen, P., Sithanandam, G., Rapp, U., Ashworth, A., Marshall, C.J. and Cowley, S., 1994. Identification of the sites in MAP kinase kinase-1 phosphorylated by p74raf-1. *The EMBO journal*, *13*(7), p.1610.
- Altenburger, W., Süter, C.P. and Altenburger, J., 1989. Partial deletion of the human host range gene in the attenuated vaccinia virus MVA. *Archives of Virology*, *105*(1-2), pp.15-27.
- Amessou, M., Fradagrada, A., Falguières, T., Lord, J.M., Smith, D.C., Roberts, L.M., Lamaze, C. and Johannes, L., 2007. Syntaxin 16 and syntaxin 5 are required for efficient retrograde transport of several exogenous and endogenous cargo proteins. *Journal of Cell Science*, *120*(8), pp.1457-1468.
- Andrade, A.A., Silva, P.N., Pereira, A.C., de SOUSA, L.P., Ferreira, P.C., Gazzinelli, R.T., Kroon, E.G., Ropert, C. and Bonjardim, C.A., 2004. The vaccinia virus-stimulated mitogen-activated protein kinase (MAPK) pathway is required for virus multiplication. *Biochemical Journal*, *381*(2), pp.437-446.
- Appleyard, G., Hapel, A.J. and Boulter, E.A., 1971. An antigenic difference between intracellular and extracellular rabbitpox virus. *Journal of General Virology*, *13*(1), pp.9-17.
- Arighi, C.N., Hartnell, L.M., Aguilar, R.C., Haft, C.R. and Bonifacino, J.S., 2004. Role of the mammalian retromer in sorting of the cation-independent mannose 6-phosphate receptor. *Journal of Cell Biology*, *165*(1), pp.123-133.

- Armstrong, J.A., Metz, D.H. and Young, M.R., 1973. The mode of entry of vaccinia virus into L cells. *Journal of General Virology*, *21*(3), pp.533-537.
- Baek, S.H., Kwak, J.Y., Lee, S.H., Lee, T., Ryu, S.H., Uhlinger, D.J. and Lambeth, J.D., 1997. Lipase activities of p37, the major envelope protein of vaccinia virus. *Journal of Biological Chemistry*, *272*(51), pp.32042-32049.
- Baxby, D., 1977. The origins of vaccinia virus. *The Journal of Infectious Diseases*, *136*(3), pp.453-455.
- Beard, P.M., Griffiths, S.J., Gonzalez, O., Haga, I.R., Jowers, T.P., Reynolds, D.K., Wildenhain, J., Tekotte, H., Auer, M., Tyers, M. and Ghazal, P., 2014. A loss of function analysis of host factors influencing vaccinia virus replication by RNA interference. *PloS One*, *9*(6), p.e98431.
- Bedson, H.S. and Dumbell, K.R., 1964. Hybrids derived from the viruses of variola major and cowpox. *Journal of Hygiene*, *62*(02), pp.147-158.
- Bisht, H., Weisberg, A.S., Szajner, P. and Moss, B., 2009. Assembly and disassembly of the capsid-like external scaffold of immature virions during vaccinia virus morphogenesis. *Journal of Virology*, *83*(18), pp.9140-9150.
- Black, E.P. and Condit, R.C., 1996. Phenotypic characterization of mutants in vaccinia virus gene G2R, a putative transcription elongation factor. *Journal of Virology*, *70*(1), pp.47-54.
- Blanchard, T.J., Alcami, A., Andrea, P. and Smith, G.L., 1998. Modified vaccinia virus Ankara undergoes limited replication in human cells and lacks several immunomodulatory proteins: implications for use as a human vaccine. *Journal of General Virology*, *79*(5), pp.1159-1167.
- Blasco, R. and Moss, B., 1992. Role of cell-associated enveloped vaccinia virus in cell-to-cell spread. *Journal of Virology*, *66*(7), pp.4170-4179.
- Blasco, R., Sisler, J.R. and Moss, B., 1993. Dissociation of progeny vaccinia virus from the cell membrane is regulated by a viral envelope glycoprotein: effect of a point mutation in the lectin homology domain of the A34R gene. *Journal of Virology*, *67*(6), pp.3319-3325.
- Bonifacino, J.S. and Glick, B.S., 2004. The mechanisms of vesicle budding and fusion. *Cell*, *116*(2), pp.153-166.

- Bonifacino, J.S. and Hierro, A., 2011. Transport according to GARP: receiving retrograde cargo at the trans-Golgi network. *Trends in Cell Biology*, *21*(3), pp.159-167.
- Bonifacino, J.S. and Rojas, R., 2006. Retrograde transport from endosomes to the trans-Golgi network. *Nature reviews Molecular cell biology*, *7*(8), pp.568-579.
- Börgeling, Y., Schmolke, M., Viemann, D., Nordhoff, C., Roth, J. and Ludwig, S., 2014. Inhibition of p38 mitogen-activated protein kinase impairs influenza virus-induced primary and secondary host gene responses and protects mice from lethal H5N1 infection. *Journal of Biological Chemistry*, *289*(1), pp.13-27.
- Brancho, D., Tanaka, N., Jaeschke, A., Ventura, J.J., Kelkar, N., Tanaka, Y., Kyuuma, M., Takeshita, T., Flavell, R.A. and Davis, R.J., 2003. Mechanism of p38 MAP kinase activation in vivo. *Genes & Development*, *17*(16), pp.1969-1978.
- Bray, M., 2003. Pathogenesis and potential antiviral therapy of complications of smallpox vaccination. *Antiviral Research*, *58*(2), pp.101-114.
- Bray, M. and Wright, M.E., 2003. Progressive vaccinia. *Clinical Infectious Diseases*, *36*(6), pp.766-774.
- Breathnach, C.C., Rudersdorf, R. and Lunn, D.P., 2004. Use of recombinant modified vaccinia Ankara viral vectors for equine influenza vaccination. *Veterinary Immunology and Immunopathology*, *98*(3), pp.127-136.
- Breiman, A., Carpentier, D.C., Ewles, H.A. and Smith, G.L., 2013. Transport and stability of the vaccinia virus A34 protein is affected by the A33 protein. *Journal of General Virology*, *94*(4), pp.720-725.
- Broyles, S.S., 2003. Vaccinia virus transcription. *Journal of General Virology*, *84*(9), pp.2293-2303.
- Broyles, S.S. and Fesler, B.S., 1990. Vaccinia virus gene encoding a component of the viral early transcription factor. *Journal of Virology*, *64*(4), pp.1523-1529.
- Broyles, S.S., Yuen, L., Shuman, S. and Moss, B., 1988. Purification of a factor required for transcription of vaccinia virus early genes. *Journal of Biological Chemistry*, *263*(22), pp.10754-10760.

- Canton, J. and Kima, P.E., 2012. Targeting host syntaxin-5 preferentially blocks Leishmania parasitophorous vacuole development in infected cells and limits experimental Leishmania infections. *The American Journal of Pathology*, *181*(4), pp.1348-1355.
- Carlton, J., Bujny, M., Peter, B.J., Oorschot, V.M., Rutherford, A., Mellor, H., Klumperman, J., McMahon, H.T. and Cullen, P.J., 2004. Sorting nexin-1 mediates tubular endosome-to-TGN transport through coincidence sensing of high-curvature membranes and 3-phosphoinositides. *Current Biology*, *14*(20), pp.1791-1800.
- Carney, D.W., Nelson, C.D., Ferris, B.D., Stevens, J.P., Lipovsky, A., Kazakov, T., DiMaio, D., Atwood, W.J. and Sello, J.K., 2014. Structural optimization of a retrograde trafficking inhibitor that protects cells from infections by human polyoma-and papillomaviruses. *Bioorganic & Medicinal Chemistry*, *22*(17), pp.4836-4847.
- Carroll, K.S., Hanna, J., Simon, I., Krise, J., Barbero, P. and Pfeffer, S.R., 2001. Role of Rab9 GTPase in facilitating receptor recruitment by TIP47. *Science*, *292*(5520), pp.1373-1376.
- Carter, G.C., Law, M., Hollinshead, M. and Smith, G.L., 2005. Entry of the vaccinia virus intracellular mature virion and its interactions with glycosaminoglycans. *Journal of General Virology*, *86*(5), pp.1279-1290.
- Carter, G.C., Rodger, G., Murphy, B.J., Law, M., Krauss, O., Hollinshead, M. and Smith, G.L., 2003. Vaccinia virus cores are transported on microtubules. *Journal of General Virology*, *84*(9), pp.2443-2458.
- Cepeda, V. and Esteban, M., 2014. Novel insights on the progression of intermediate viral forms in the morphogenesis of vaccinia virus. *Virus research*, *183*, pp.23-29.
- Chan, W.M. and Ward, B.M., 2010. There is an A33-dependent mechanism for the incorporation of B5-GFP into vaccinia virus extracellular enveloped virions. *Virology*, *402*(1), pp.83-93.
- Chang, C.I., Xu, B.E., Akella, R., Cobb, M.H. and Goldsmith, E.J., 2002. Crystal structures of MAP kinase p38 complexed to the docking sites on its nuclear substrate MEF2A and activator MKK3b. *Molecular Cell*, *9*(6), pp.1241-1249.

- Chia, P.Z.C., Gasnereau, I., Lieu, Z.Z. and Gleeson, P.A., 2011. Rab9-dependent retrograde transport and endosomal sorting of the endopeptidase furin. *Journal of Cell Science*, *124*(14), pp.2401-2413.
- Chia, P.Z.C. and Gleeson, P.A., 2011. The Regulation of Endosome-to-Golgi Retrograde Transport by Tethers and Scaffolds. *Traffic*, *12*(8), pp.939-947.
- Choi, M.S., Heo, J., Yi, C.M., Ban, J., Lee, N.J., Lee, N.R., Kim, S.W., Kim, N.J. and Inn, K.S., 2016. A novel p38 mitogen activated protein kinase (MAPK) specific inhibitor suppresses respiratory syncytial virus and influenza A virus replication by inhibiting virus-induced p38 MAPK activation. *Biochemical and Biophysical Research Communications*, *477*(3), pp.311-316.
- Chung, C.S., Hsiao, J.C., Chang, Y.S. and Chang, W., 1998. A27L protein mediates vaccinia virus interaction with cell surface heparan sulfate. *Journal of Virology*, *72*(2), pp.1577-1585.
- Churin, Y., Roderfeld, M. and Roeb, E., 2015. Hepatitis B virus large surface protein: function and fame. *Hepatobiliary Surgery and Nutrition*, *4*(1), p.1-10.
- Condit, R.C., Xiang, Y. and Lewis, J.I., 1996. Mutation of vaccinia virus gene G2R causes suppression of gene A18R ts mutants: implications for control of transcription. *Virology*, *220*(1), pp.10-19.
- Conibear, E., Cleck, J.N. and Stevens, T.H., 2003. Vps51p mediates the association of the GARP (Vps52/53/54) complex with the late Golgi t-SNARE Tlg1p. *Molecular Biology of the Cell*, *14*(4), pp.1610-1623.
- Conibear, E. and Stevens, T.H., 2000. Vps52p, Vps53p, and Vps54p form a novel multisubunit complex required for protein sorting at the yeast late Golgi. *Molecular Biology of the Cell*, *11*(1), pp.305-323.
- Cono, J., Casey, C.G., Bell, D.M. and Centers for Disease Control and Prevention, 2003. Smallpox vaccination and adverse reactions. *Morbidity and Mortality Weekly Report: Recommendations and Reports,*, *52*, pp.1-28.
- Conze, D., Lumsden, J., Enslen, H., Davis, R.J., Le Gros, G. and Rincón, M., 2000. Activation of p38 MAP kinase in T cells facilitates the immune response to the influenza virus. *Molecular Immunology*, *37*(9), pp.503-513.

- Cudmore, S., Cossart, P., Griffiths, G. and Way, M., 1995. Actin-based motility of vaccinia virus. *Nature*, *378*(6557), p.636.
- Cudmore, S., Reckmann, I., Griffiths, G. and Way, M., 1996. Vaccinia virus: a model system for actin-membrane interactions. *Journal of Cell Science*, *109*(7), pp.1739-1747.
- Dales, S. and Mosbach, E.H., 1968. Vaccinia as a model for membrane biogenesis. *Virology*, *35*(4), pp.564-583.
- Dales, S. and Siminovitch, L., 1961. The development of vaccinia virus in Earle's L strain cells as examined by electron microscopy. *The Journal of Biophysical and Biochemical Cytology*, *10*(4), pp.475-503.
- Davis, R.J., 2000. Signal transduction by the JNK group of MAP kinases. *Cell*, *103*(2), pp.239-252.
- DeHaven, B.C., Gupta, K. and Isaacs, S.N., 2011. The vaccinia virus A56 protein: a multifunctional transmembrane glycoprotein that anchors two secreted viral proteins. *Journal of General Virology*, *92*(9), pp.1971-1980.
- Delaloye, J., Roger, T., Steiner-Tardivel, Q.G., Le Roy, D., Reymond, M.K., Akira, S., Petrilli, V., Gomez, C.E., Perdiguero, B., Tschopp, J. and Pantaleo, G., 2009. Innate immune sensing of modified vaccinia virus Ankara (MVA) is mediated by TLR2-TLR6, MDA-5 and the NALP3 inflammasome. *PLoS Pathogens*, *5*(6), p.e1000480.
- Dellis, S., Strickland, K.C., McCrary, W.J., Patel, A., Stocum, E. and Wright, C.F., 2004. Protein interactions among the vaccinia virus late transcription factors. *Virology*, *329*(2), pp.328-336.
- Derijard, B., Raingeaud, J., Barrett, T. and Wu, I.H., 1995. Independent human MAP kinase signal transduction pathways defined by MEK and MKK isoforms. *Science*, *267*(5198), p.682.
- Doceul, V., Hollinshead, M., van der Linden, L. and Smith, G.L., 2010. Repulsion of superinfecting virions: a mechanism for rapid virus spread. *Science*, *327*(5967), pp.873-876.
- Duchen, L.W. and Strich, S.J., 1968. An hereditary motor neurone disease with progressive denervation of muscle in the mouse: the mutant'wobbler'. *Journal of Neurology, Neurosurgery & Psychiatry*, *31*(6), pp.535-542.

- Duncan, S.A. and Smith, G.L., 1992. Identification and characterization of an extracellular envelope glycoprotein affecting vaccinia virus egress. *Journal of Virology*, *66*(3), pp.1610-1621.
- Duraffour, S., Lorenzo, M.M., Zöller, G., Topalis, D., Grosenbach, D., Hruby, D.E., Andrei, G., Blasco, R., Meyer, H. and Snoeck, R., 2015. ST-246 is a key antiviral to inhibit the viral F13L phospholipase, one of the essential proteins for orthopoxvirus wrapping. *Journal of Antimicrobial Chemotherapy*, p.dku545.
- Earl, P.L., Americo, J.L., Wyatt, L.S., Eller, L.A., Whitbeck, J.C., Cohen, G.H., Eisenberg, R.J., Hartmann, C.J., Jackson, D.L., Kulesh, D.A. and Martinez, M.J., 2004. Immunogenicity of a highly attenuated MVA smallpox vaccine and protection against monkeypox. *Nature*, *428*(6979), pp.182-185.
- Engelman, J.A., Lisanti, M.P. and Scherer, P.E., 1998. Specific inhibitors of p38 mitogen-activated protein kinase block 3T3-L1 adipogenesis. *Journal of Biological Chemistry*, *273*(48), pp.32111-32120.
- Engelstad, M., Howard, S.T. and Smith, G.L., 1992. A constitutively expressed vaccinia gene encodes a 42-kDa glycoprotein related to complement control factors that forms part of the extracellular virus envelope. *Virology*, *188*(2), pp.801-810.
- Engelstad, M. and Smith, G.L., 1993. The vaccinia virus 42-kDa envelope protein is required for the envelopment and egress of extracellular virus and for virus virulence. *Virology*, *194*(2), pp.627-637.
- Enslen, H., Brancho, D.M. and Davis, R.J., 2000. Molecular determinants that mediate selective activation of p38 MAP kinase isoforms. *The EMBO Journal*, *19*(6), pp.1301-1311.
- Enslen, H., Raingeaud, J. and Davis, R.J., 1998. Selective activation of p38 mitogen-activated protein (MAP) kinase isoforms by the MAP kinase kinases MKK3 and MKK6. *Journal of Biological Chemistry*, *273*(3), pp.1741-1748.
- Feinstein, M., Flusser, H., Lerman-Sagie, T., Ben-Zeev, B., Lev, D., Agamy, O., Cohen, I., Kadir, R., Sivan, S., Leshinsky-Silver, E. and Markus, B., 2014. VPS53 mutations cause progressive cerebello-cerebral atrophy type 2 (PCCA2). *Journal of Medical Genetics*, *51*(5), pp.303-308.

- Finsel, I., Ragaz, C., Hoffmann, C., Harrison, C.F., Weber, S., van Rahden, V.A., Johannes, L. and Hilbi, H., 2013. The Legionella effector RidL inhibits retrograde trafficking to promote intracellular replication. *Cell Host & Microbe*, *14*(1), pp.38-50.
- Frischknecht, F., Moreau, V., Röttger, S., Gonfloni, S., Reckmann, I., Superti-Furga, G. and Way, M., 1999. Actin-based motility of vaccinia virus mimics receptor tyrosine kinase signalling. *Nature*, *401*(6756), pp.926-929.
- Fu, Y., Yip, A., Seah, P.G., Blasco, F., Shi, P.Y. and Hervé, M., 2014. Modulation of inflammation and pathology during dengue virus infection by p38 MAPK inhibitor SB203580. *Antiviral Research*, *110*, pp.151-157.
- Ganley, I.G., Espinosa, E. and Pfeffer, S.R., 2008. A syntaxin 10–SNARE complex distinguishes two distinct transport routes from endosomes to the trans-Golgi in human cells. *The Journal of Cell Biology*, *180*(1), pp.159-172.
- Ge, B., Xiong, X., Jing, Q., Mosley, J.L., Filose, A., Bian, D., Huang, S. and Han, J., 2002. TAB1β, a novel splicing variant of TAB1 that interacts with p38α but not TAK1. *Journal of Biological Chemistry*.
- Gershon, P.D. and Moss, B., 1990. Early transcription factor subunits are encoded by vaccinia virus late genes. *Proceedings of the National Academy of Sciences*, *87*(11), pp.4401-4405.
- Gibson, W.A. and Langsten, R.E., 2004. Generalized vaccinia in a deployed military member. *The Journal of Emergency Medicine*, *27*(2), pp.127-131.
- Gokool, S., Tattersall, D. and Seaman, M.N., 2007. EHD1 Interacts with Retromer to stabilize SNX1 tubules and facilitate endosome-to-Golgi retrieval. *Traffic*, *8*(12), pp.1873-1886.
- Goldstein, J.A., Neff, J.M., Lane, J.M. and Koplan, J.P., 1975. Smallpox vaccination reactions, prophylaxis, and therapy of complications. *Pediatrics*, *55*(3), pp.342-347.
- Gonzalez, F.A., Raden, D.L. and Davis, R.J., 1991. Identification of substrate recognition determinants for human ERK1 and ERK2 protein kinases. *Journal of Biological Chemistry*, *266*(33), pp.22159-22163.

- Groppelli, E., Len, A.C., Granger, L.A. and Jolly, C., 2014. Retromer regulates HIV-1 envelope glycoprotein trafficking and incorporation into virions. *PLoS Pathogens*, *10*(11), p.e1004518.
- Gupta, N., Pons, V., Noël, R., Buisson, D.A., Michau, A., Johannes, L., Gillet, D., Barbier, J. and Cintrat, J.C., 2013. (S)-N-Methyldihydroquinazolinones are the active enantiomers of Retro-2 derived compounds against toxins. *ACS Medicinal Chemistry Letters*, *5*(1), pp.94-97.
- Haft, C.R., de la Luz Sierra, M., Bafford, R., Lesniak, M.A., Barr, V.A. and Taylor, S.I., 2000. Human orthologs of yeast vacuolar protein sorting proteins Vps26, 29, and 35: assembly into multimeric complexes. *Molecular Biology of the Cell*, *11*(12), pp.4105-4116.
- Haga, I.R. and Bowie, A.G., 2005. Evasion of innate immunity by vaccinia virus. *Parasitology*, *130*(S1), pp.S11-S25.
- Hammaker, D., Boyle, D.L., Topolewski, K. and Firestein, G.S., 2014. Differential regulation of anti-inflammatory genes by p38 MAP kinase and MAP kinase kinase 6. *Journal of Inflammation*, *11*(1), p.14.
- Han, J., Lee, J.D., Bibbs, L. and Ulevitch, R.J., 1994. A MAP kinase targeted by endotoxin and hyperosmolarity in mammalian cells. *Science-AAAS-Weekly Paper Edition*, *265*(5173), pp.808-810.
- Han, J., Lee, J.D., Jiang, Y., Li, Z., Feng, L. and Ulevitch, R.J., 1996. Characterization of the structure and function of a novel MAP kinase kinase (MKK6). *Journal of Biological Chemistry*, *271*(6), pp.2886-2891.
- Han, J., Lee, J.D., Tobias, P.S. and Ulevitch, R.J., 1993. Endotoxin induces rapid protein tyrosine phosphorylation in 70Z/3 cells expressing CD14. *Journal of Biological Chemistry*, *268*(33), pp.25009-25014.
- Hashizume, S.C., 1975. Special edition future of vaccination: Everything about attenuated vaccines. Basics of new attenuated vaccine strain LC16m8. *Clinical Virus*, *3*, pp.229-35.
- Heidenreich, K.A. and Kummer, J.L., 1996. Inhibition of p38 mitogen-activated protein kinase by insulin in cultured fetal neurons. *Journal of Biological Chemistry*, *271*(17), pp.9891-9894.

- Herrera, E., del Mar Lorenzo, M., Blasco, R. and Isaacs, S.N., 1998. Functional analysis of vaccinia virus B5R protein: essential role in virus envelopment is independent of a large portion of the extracellular domain. *Journal of Virology*, *72*(1), pp.294-302.
- Herrero-Martinez, E., Roberts, K.L., Hollinshead, M. and Smith, G.L., 2005. Vaccinia virus intracellular enveloped virions move to the cell periphery on microtubules in the absence of the A36R protein. *Journal of General Virology*, *86*(11), pp.2961-2968.
- Heuser, J., 2005. Deep-etch EM reveals that the early poxvirus envelope is a single membrane bilayer stabilized by a geodetic "honeycomb" surface coat. *The Journal of Cell Biology*, *169*(2), pp.269-283.
- Hickman, H.D., Reynoso, G.V., Ngudiankama, B.F., Cush, S.S., Gibbs, J., Bennink, J.R. and Yewdell, J.W., 2015. CXCR3 chemokine receptor enables local CD8+ T cell migration for the destruction of virus-infected cells. *Immunity*, *42*(3), pp.524-537.
- Hiller, G., Eibl, H. and Weber, K., 1981. Characterization of intracellular and extracellular vaccinia virus variants: N1-isonicotinoyl-N2-3-methyl-4-chlorobenzoylhydrazine interferes with cytoplasmic virus dissemination and release. *Journal of Virology*, *39*(3), pp.903-913.
- Hiller, G. and Weber, K., 1985. Golgi-derived membranes that contain an acylated viral polypeptide are used for vaccinia virus envelopment. *Journal of Virology*, *55*(3), pp.651-659.
- Hirt, P., Hiller, G. and Wittek, R., 1986. Localization and fine structure of a vaccinia virus gene encoding an envelope antigen. *Journal of Virology*, *58*(3), pp.757-764.
- Hollinshead, M., Vanderplasschen, A., Smith, G.L. and Vaux, D.J., 1999. Vaccinia virus intracellular mature virions contain only one lipid membrane. *Journal of Virology*, *73*(2), pp.1503-1517.
- Holzer, G.W. and Falkner, F.G., 1997. Construction of a vaccinia virus deficient in the essential DNA repair enzyme uracil DNA glycosylase by a complementing cell line. *Journal of Virology*, *71*(7), pp.4997-5002.
- Horsington, J., Lynn, H., Turnbull, L., Cheng, D., Braet, F., Diefenbach, R.J., Whitchurch, C.B., Karupiah, G. and Newsome, T.P., 2013. A36-dependent actin filament nucleation promotes release of vaccinia virus. *PLoS Pathogens*, *9*(3), p.e1003239.

- Hsiao, J.C., Chung, C.S. and Chang, W., 1999. Vaccinia virus envelope D8L protein binds to cell surface chondroitin sulfate and mediates the adsorption of intracellular mature virions to cells. *Journal of Virology*, *73*(10), pp.8750-8761.
- Hu, N., Shikuma, C., Shiramizu, B., Koo, R. and Yewdell, J.W., 2007. Signaling pathways involved in foreign antigen expression by a recombinant vaccinia virus (89.38). *The Journal of Immunology*, *178*(1 Supplement), pp.S156-S156.
- Huang, C.H., Chu, Y.T., Kuo, C.H., Wang, W.L., Hua, Y.M., Lee, M.S. and Hung, C.H., 2010. Effect of procaterol on Th2-related chemokines production in human monocyte and bronchial epithelial cells. *Pediatric Pulmonology*, *45*(10), pp.977-984.
- Huang, C.Y., Lu, T.Y., Bair, C.H., Chang, Y.S., Jwo, J.K. and Chang, W., 2008. A novel cellular protein, VPEF, facilitates vaccinia virus penetration into HeLa cells through fluid phase endocytosis. *Journal of Virology*, *82*(16), pp.7988-7999.
- Hubbs, A.E. and Wright, C.F., 1996. The A2L intermediate gene product is required for in vitro transcription from a vaccinia virus late promoter. *Journal of Virology*, *70*(1), pp.327-331.
- Husain, M. and Moss, B., 2002. Similarities in the induction of post-Golgi vesicles by the vaccinia virus F13L protein and phospholipase D. *Journal of Virology*, *76*(15), pp.7777-7789.
- Husain, M. and Moss, B., 2003. Intracellular trafficking of a palmitoylated membrane-associated protein component of enveloped vaccinia virus. *Journal of Virology*, *77*(16), pp.9008-9019.
- Husain, M. and Moss, B., 2005. Role of receptor-mediated endocytosis in the formation of vaccinia virus extracellular enveloped particles. *Journal of Virology*, *79*(7), pp.4080-4089.
- Ichihashi, Y., 1996. Extracellular enveloped vaccinia virus escapes neutralization. *Virology*, *217*(2), pp.478-485.
- Ichihashi, Y., Matsumoto, S. and Dales, S., 1971. Biogenesis of poxviruses: role of A-type inclusions and host cell membranes in virus dissemination. *Virology*, *46*(3), pp.507-532.

- Ishii, K. and Moss, B., 2001. Role of vaccinia virus A20R protein in DNA replication: construction and characterization of temperature-sensitive mutants. *Journal of Virology*, *75*(4), pp.1656-1663.
- Jiang, Y., Chen, C., Li, Z., Guo, W., Gegner, J.A., Lin, S. and Han, J., 1996. Characterization of the structure and function of a new mitogen-activated protein kinase (p38β). *Journal of Biological Chemistry*, *271*(30), pp.17920-17926.
- Jiang, Y., Gram, H., Zhao, M., New, L., Gu, J., Feng, L., Di Padova, F., Ulevitch, R.J. and Han, J., 1997. Characterization of the structure and function of the fourth member of p38 group mitogen-activated protein kinases, p38δ. *Journal of Biological Chemistry*, *272*(48), pp.30122-30128.
- Johannes, L. and Popoff, V., 2008. Tracing the retrograde route in protein trafficking. *Cell*, *135*(7), pp.1175-1187.
- Johannes, L. and Römer, W., 2010. Shiga toxins—from cell biology to biomedical applications. *Nature Reviews Microbiology*, *8*(2), pp.105-116.
- Johnson, B.F., Kanatani, Y., Fujii, T., Saito, T., Yokote, H. and Smith, G.L., 2011. Serological responses in humans to the smallpox vaccine LC16m8. *Journal of General Virology*, *92*(10), pp.2405-2410.
- Johnston, S.C. and Ward, B.M., 2009. Vaccinia virus protein F12 associates with intracellular enveloped virions through an interaction with A36. *Journal of Virology*, *83*(4), pp.1708-1717.
- Jonak, C., Heberle-Bors, E. and Hirt, H., 1994. MAP kinases: universalmulti-purpose signaling tools. *Plant Molecular Biology*, *24*(3), pp.407-416.
- Kanda, N., Shimizu, T., Tada, Y. and Watanabe, S., 2007. IL-18 enhances IFN-γ-induced production of CXCL9, CXCL10, and CXCL11 in human keratinocytes. *European Journal of Immunology*, *37*(2), pp.338-350.
- Karlsson, P., Droce, A., Moser, J.M., Cuhlmann, S., Padilla, C.O., Heimann, P., Bartsch, J.W., Füchtbauer, A., Füchtbauer, E.M. and Schmitt-John, T., 2013. Loss of vps54 function leads to vesicle traffic impairment, protein mis-sorting and embryonic lethality. *International Journal of Molecular Sciences*, *14*(6), pp.10908-10925.

- Kates, J.R. and McAuslan, B.R., 1967. Poxvirus DNA-dependent RNA polymerase. *Proceedings of the National Academy of Sciences*, *58*(1), pp.134-141.
- Kato, N., Eggers, H.J. and Rolly, H., 1969. Inhibition of release of vaccinia virus by N1-isonicotinoyl-N2-3-methyl-4-chlorobenzoylhydrazine. *The Journal of experimental medicine*, *129*(4), p.795.
- Katsafanas, G.C. and Moss, B., 2004. Vaccinia virus intermediate stage transcription is complemented by Ras-GTPase-activating protein SH3 domain-binding protein (G3BP) and cytoplasmic activation/proliferation-associated protein (p137) individually or as a heterodimer. *Journal of Biological Chemistry*, *279*(50), pp.52210-52217.
- Katsafanas, G.C. and Moss, B., 2007. Colocalization of transcription and translation within cytoplasmic poxvirus factories coordinates viral expression and subjugates host functions. *Cell Host & Microbe*, *2*(4), pp.221-228.
- Katz, E., Wolffe, E.J. and Moss, B., 1997. The cytoplasmic and transmembrane domains of the vaccinia virus B5R protein target a chimeric human immunodeficiency virus type 1 glycoprotein to the outer envelope of nascent vaccinia virions. *Journal of virology*, *71*(4), pp.3178-3187.
- Keck, J.G., Baldick, C.J. and Moss, B., 1990. Role of DNA replication in vaccinia virus gene expression: a naked template is required for transcription of three late trans-activator genes. *Cell*, *61*(5), pp.801-809.
- Kidokoro, M., Tashiro, M. and Shida, H., 2005. Genetically stable and fully effective smallpox vaccine strain constructed from highly attenuated vaccinia LC16m8. *Proceedings of the National Academy of Sciences of the United States of America*, *102*(11), pp.4152-4157.
- Kindrachuk, J., Arsenault, R., Kusalik, A., Kindrachuk, K.N., Trost, B., Napper, S., Jahrling, P.B. and Blaney, J.E., 2012. Systems kinomics demonstrates Congo Basin monkeypox virus infection selectively modulates host cell signaling responses as compared to West African monkeypox virus. *Molecular & Cellular Proteomics*, *11*(6), pp.M111-015701.
- Krathwohl, M.D. and Anderson, J.L., 2006. Chemokine CXCL10 (IP-10) is sufficient to trigger an immune response to injected antigens in a mouse model. *Vaccine*, *24*(15), pp.2987-2993.

- Law, M., Carter, G.C., Roberts, K.L., Hollinshead, M. and Smith, G.L., 2006. Ligand-induced and nonfusogenic dissolution of a viral membrane. *Proceedings of the National Academy of Sciences*, *103*(15), pp.5989-5994.
- Lederman, E.R., Davidson, W., Groff, H.L., Smith, S.K., Warkentien, T., Li, Y., Wilkins, K.A., Karem, K.L., Akondy, R.S., Ahmed, R. and Frace, M., 2012. Progressive vaccinia: case description and laboratory-guided therapy with vaccinia immune globulin, ST-246, and CMX001. *Journal of Infectious Diseases*, *206*(9), pp.1372-1385.
- Li, Z., Jiang, Y., Ulevitch, R.J. and Han, J., 1996. The primary structure of p38γ: a new member of p38 group of MAP kinases. *Biochemical and Biophysical Research Communications*, *228*(2), pp.334-340.
- Li, Y., Batra, S., Sassano, A., Majchrzak, B., Levy, D.E., Gaestel, M., Fish, E.N., Davis, R.J. and Platanias, L.C., 2005. Activation of mitogen-activated protein kinase kinase (MKK) 3 and MKK6 by type I interferons. *Journal of Biological Chemistry*, *280*(11), pp.10001-10010.
- Liewen, H., Meinhold-Heerlein, I., Oliveira, V., Schwarzenbacher, R., Luo, G., Wadle, A., Jung, M., Pfreundschuh, M. and Stenner-Liewen, F., 2005. Characterization of the human GARP (Golgi associated retrograde protein) complex. *Experimental Cell Research*, *306*(1), pp.24-34.
- Liu, X., Wang, Z., Yang, Y., Li, Q., Zeng, R., Kang, J. and Wu, J., 2016. Rab1A mediates proinsulin to insulin conversion in β-cells by maintaining Golgi stability through interactions with golgin-84. *Protein & Cell*, *7*(9), pp.692-696.
- Lo, Y.Y., Wong, J.M. and Cruz, T.F., 1996. Reactive oxygen species mediate cytokine activation of c-Jun NH2-terminal kinases. *Journal of Biological Chemistry*, *271*(26), pp.15703-15707.
- Locker, J.K., Kuehn, A., Schleich, S., Rutter, G., Hohenberg, H., Wepf, R. and Griffiths, G., 2000. Entry of the two infectious forms of vaccinia virus at the plasma membrane is signaling-dependent for the IMV but not the EEV. *Molecular Biology of the Cell*, *11*(7), pp.2497-2511.

- Lombardi, D., Soldati, T., Riederer, M.A., Goda, Y., Zerial, M. and Pfeffer, S.R., 1993. Rab9 functions in transport between late endosomes and the trans Golgi network. *The EMBO Journal*, *12*(2), p.677.
- Lorenzo, M.M., Galindo, I., Griffiths, G. and Blasco, R., 2000. Intracellular localization of vaccinia virus extracellular enveloped virus envelope proteins individually expressed using a Semliki Forest virus replicon. *Journal of Virology*, *74*(22), pp.10535-10550.
- Lu, L.Y., Wood, J.L., Minter-Dykhouse, K., Ye, L., Saunders, T.L., Yu, X. and Chen, J., 2008. Polo-like kinase 1 is essential for early embryonic development and tumor suppression. *Molecular and Cellular Biology*, *28*(22), pp.6870-6876.
- Luo, L., Hannemann, M., Koenig, S., Hegermann, J., Ailion, M., Cho, M.K., Sasidharan, N., Zweckstetter, M., Rensing, S.A. and Eimer, S., 2011. The Caenorhabditis elegans GARP complex contains the conserved Vps51 subunit and is required to maintain lysosomal morphology. *Molecular Biology of the Cell*, *22*(14), pp.2564-2578.
- Ma, F.Y., Tesch, G.H., Flavell, R.A., Davis, R.J. and Nikolic-Paterson, D.J., 2007. MKK3-p38 signaling promotes apoptosis and the early inflammatory response in the obstructed mouse kidney. *American Journal of Physiology-Renal Physiology*, *293*(5), pp.F1556-F1563.
- Magalhães, J.C., Andrade, A.A., Silva, P.N., Sousa, L.P., Ropert, C., Ferreira, P.C., Kroon, E.G., Gazzinelli, R.T. and Bonjardim, C.A., 2001. A mitogenic signal triggered at an early stage of Vaccinia virus infection: implication of MEK/ERK and PKA in virus multiplication. *Journal of Biological Chemistry*.
- Mallard, F., Antony, C., Tenza, D., Salamero, J., Goud, B. and Johannes, L., 1998. Direct pathway from early/recycling endosomes to the Golgi apparatus revealed through the study of shiga toxin B-fragment transport. *The Journal of Cell Biology*, *143*(4), pp.973-990.
- Mallard, F., Tang, B.L., Galli, T., Tenza, D., Saint-Pol, A., Yue, X., Antony, C., Hong, W., Goud, B. and Johannes, L., 2002. Early/recycling endosomes-to-TGN transport involves two SNARE complexes and a Rab6 isoform. *The Journal of Cell Biology*, *156*(4), pp.653-664.
- Maloney, G., Schröder, M. and Bowie, A.G., 2005. Vaccinia virus protein A52R activates p38 mitogen-activated protein kinase and potentiates lipopolysaccharide-induced interleukin-10. *Journal of Biological Chemistry*, *280*(35), pp.30838-30844.

- Marks, M.S., Woodruff, L., Ohno, H. and Bonifacino, J.S., 1996. Protein targeting by tyrosine-and di-leucine-based signals: evidence for distinct saturable components. *The Journal of Cell Biology*, *135*(2), pp.341-354.
- Mathew, E., Sanderson, C.M., Hollinshead, M. and Smith, G.L., 1998. The extracellular domain of vaccinia virus protein B5R affects plaque phenotype, extracellular enveloped virus release, and intracellular actin tail formation. *Journal of Virology*, *72*(3), pp.2429-2438.
- Mayr, A., Bavarian Nordic A/S, 2004. *Altered strain of the modified vaccinia virus Ankara (MVA)*. U.S. Patent 6,682,743.
- McCart, J.A., Ward, J.M., Lee, J., Hu, Y., Alexander, H.R., Libutti, S.K., Moss, B. and Bartlett, D.L., 2001. Systemic cancer therapy with a tumor-selective vaccinia virus mutant lacking thymidine kinase and vaccinia growth factor genes. *Cancer Research*, *61*(24), pp.8751-8757.
- McCurdy, L.H., Rutigliano, J.A., Johnson, T.R., Chen, M. and Graham, B.S., 2004. Modified vaccinia virus Ankara immunization protects against lethal challenge with recombinant vaccinia virus expressing murine interleukin-4. *Journal of Virology*, *78*(22), pp.12471-12479.
- McDonough, J.A., Newton, H.J., Klum, S., Swiss, R., Agaisse, H. and Roy, C.R., 2013. Host pathways important for Coxiella burnetii infection revealed by genome-wide RNA interference screening. *Molecular Biology*, *4*(1), pp.e00606-12.
- McIntosh, A.A. and Smith, G.L., 1996. Vaccinia virus glycoprotein A34R is required for infectivity of extracellular enveloped virus. *Journal of Virology*, *70*(1), pp.272-281.
- McKenzie, J.E., Raisley, B., Zhou, X., Naslavsky, N., Taguchi, T., Caplan, S. and Sheff, D., 2013. Retromer guides STxB and CD8-M6PR from early to recycling endosomes, EHD1 guides STxB from recycling endosome to golgi. *Traffic*, *13*(8), pp.1140-1159.
- McMahon, H.T. and Mills, I.G., 2004. COP and clathrin-coated vesicle budding: different pathways, common approaches. *Current Opinion in Cell Biology*, *16*(4), pp.379-391.
- Medaglia, M.L.G., Sá, N.M., Correa, I.A., Costa, L.J. and Damaso, C.R., 2015. One-step duplex polymerase chain reaction for the detection of swinepox and vaccinia viruses in skin

lesions of swine with poxvirus-related disease. *Journal of Virological Methods*, *219*, pp.10-13.

- Medders, K.E. and Kaul, M., 2011. Mitogen-activated protein kinase p38 in HIV infection and associated brain injury. *Journal of Neuroimmune Pharmacology*, *6*(2), pp.202-215.
- Meiser, A., Sancho, C. and Locker, J.K., 2003. Plasma membrane budding as an alternative release mechanism of the extracellular enveloped form of vaccinia virus from HeLa cells. *Journal of Virology*, *77*(18), pp.9931-9942.
- Meisinger-Henschel, C., Späth, M., Lukassen, S., Wolferstätter, M., Kachelriess, H., Baur, K., Dirmeier, U., Wagner, M., Chaplin, P., Suter, M. and Hausmann, J., 2010. Introduction of the six major genomic deletions of modified vaccinia virus Ankara (MVA) into the parental vaccinia virus is not sufficient to reproduce an MVA-like phenotype in cell culture and in mice. *Journal of Virology*, *84*(19), pp.9907-9919.
- Mercer, J. and Helenius, A., 2008. Vaccinia virus uses macropinocytosis and apoptotic mimicry to enter host cells. *Science*, *320*(5875), pp.531-535.
- Meyer, H. (2013). Summary report on first, second and third generation smallpox vaccines. [online] *World Health Organisation*. Available at: http://www.who.int/immunization/sage/meetings/2013/november/2_Smallpox_vaccine_review_updated_11_10_13.pdf [Accessed 20 Jun. 2017].
- Midgley, C.M., Putz, M.M., Weber, J.N. and Smith, G.L., 2008. Vaccinia virus strain NYVAC induces substantially lower and qualitatively different human antibody responses compared with strains Lister and Dryvax. *Journal of General Virology*, *89*(12), pp.2992-2997.
- Minnigan, H. and Moyer, R.W., 1985. Intracellular location of rabbit poxvirus nucleic acid within infected cells as determined by in situ hybridization. *Journal of Virology*, *55*(3), pp.634-643.
- Meng, X., Embry, A., Sochia, D. and Xiang, Y., 2007. Vaccinia virus A6L encodes a virion core protein required for formation of mature virion. *Journal of Virology*, *81*(3), pp.1433-1443.

- Mody, N., Campbell, D.G., Morrice, N., Peggie, M. and Cohen, P., 2003. An analysis of the phosphorylation and activation of extracellular-signal-regulated protein kinase 5 (ERK5) by mitogen-activated protein kinase kinase 5 (MKK5) in vitro. *Biochemical Journal*, *372*(2), pp.567-575.
- Moreau, D., Kumar, P., Wang, S.C., Chaumet, A., Chew, S.Y., Chevalley, H. and Bard, F., 2011. Genome-wide RNAi screens identify genes required for Ricin and PE intoxications. *Developmental Cell*, *21*(2), pp.231-244.
- Morgan, C., 1976. The insertion of DNA into vaccinia virus. *Science*, *193*(4253), pp.591-592.
- Morgan, G.W., Hollinshead, M., Ferguson, B.J., Murphy, B.J., Carpentier, D.C. and Smith, G.L., 2010. Vaccinia protein F12 has structural similarity to kinesin light chain and contains a motor binding motif required for virion export. *PLoS Pathogens*, *6*(2), p.e1000785.
- Moriguchi, T., Kuroyanagi, N., Yamaguchi, K., Gotoh, Y., Irie, K., Kano, T., Shirakabe, K., Muro, Y., Shibuya, H., Matsumoto, K. and Nishida, E., 1996. A novel kinase cascade mediated by mitogen-activated protein kinase kinase 6 and MKK3. *Journal of Biological Chemistry*, *271*(23), pp.13675-13679.
- Morikawa, R.K., Aoki, J., Kano, F., Murata, M., Yamamoto, A., Tsujimoto, M. and Arai, H., 2009. Intracellular phospholipase A1γ (iPLA1γ) is a novel factor involved in coat protein complex I-and Rab6-independent retrograde transport between the endoplasmic reticulum and the Golgi complex. *Journal of Biological Chemistry*, *284*(39), pp.26620-26630.
- Moser, T.S., Jones, R.G., Thompson, C.B., Coyne, C.B. and Cherry, S., 2010. A kinome RNAi screen identified AMPK as promoting poxvirus entry through the control of actin dynamics. *PLoS Pathogens*, *6*(6), p.e1000954.
- Moss, B., 1996. Genetically engineered poxviruses for recombinant gene expression, vaccination, and safety. *Proceedings of the National Academy of Sciences*, *93*(21), pp.11341-11348.
- Moss, B., 2013. Poxvirus DNA replication. *Cold Spring Harbor Perspectives in Biology*, *5*(9), p.a010199.
- Moss, B., 2015. Poxvirus membrane biogenesis. *Virology*, *479*, pp.619-626.

- Mukhopadhyay, S. and Linstedt, A.D., 2013. Retrograde trafficking of AB5 toxins: mechanisms to therapeutics. *Journal of Molecular Medicine*, *91*(10), pp.1131-1141.
- Mullin, J., Ahmed, M.S., Sharma, R., Upile, N., Beer, H., Achar, P., Puksuriwong, S., Ferrara, F., Temperton, N., McNamara, P. and Lambe, T., 2016. Activation of cross-reactive mucosal T and B cell responses in human nasopharynx-associated lymphoid tissue in vitro by Modified Vaccinia Ankara-vectored influenza vaccines. *Vaccine*, *34*(14), pp.1688-1695.
- Munyon, W., Paoletti, E. and Grace, J.T., 1967. RNA polymerase activity in purified infectious vaccinia virus. *Proceedings of the National Academy of Sciences*, *58*(6), pp.2280-2287.
- Murakami, Y., Kohsaka, H., Kitasato, H. and Akahoshi, T., 2007. Lipopolysaccharide-induced up-regulation of triggering receptor expressed on myeloid cells-1 expression on macrophages is regulated by endogenous prostaglandin E2. *The Journal of Immunology*, *178*(2), pp.1144-1150.
- Myskiw, C., Arsenio, J., van Bruggen, R., Deschambault, Y. and Cao, J., 2009. Vaccinia virus E3 suppresses expression of diverse cytokines through inhibition of the PKR, NF-κB, and IRF3 pathways. *Journal of Virology*, *83*(13), pp.6757-6768.
- Nelson, C.D., Carney, D.W., Derdowski, A., Lipovsky, A., Gee, G.V., O'Hara, B., Williard, P., DiMaio, D., Sello, J.K. and Atwood, W.J., 2013. A retrograde trafficking inhibitor of ricin and Shiga-like toxins inhibits infection of cells by human and monkey polyomaviruses. *Molecular Biology*, *4*(6), pp.e00729-13.
- Nonnenmacher, M.E., Cintrat, J.C., Gillet, D. and Weber, T., 2015. Syntaxin 5-dependent retrograde transport to the trans-Golgi network is required for adeno-associated virus transduction. *Journal of Virology*, *89*(3), pp.1673-1687.
- Ober, B.T., Brühl, P., Schmidt, M., Wieser, V., Gritschenberger, W., Coulibaly, S., Savidis-Dacho, H., Gerencer, M. and Falkner, F.G., 2002. Immunogenicity and safety of defective vaccinia virus lister: comparison with modified vaccinia virus Ankara. *Journal of Virology*, *76*(15), pp.7713-7723.

- Pahari, S., Cormark, R.D., Blackshaw, M.T., Liu, C., Erickson, J.L. and Schultz, E.A., 2014. Arabidopsis UNHINGED encodes a VPS51 homolog and reveals a role for the GARP complex in leaf shape and vein patterning. *Development*, *141*(9), pp.1894-1905.
- Park, J.G., Kahn, J.N., Tumer, N.E. and Pang, Y.P., 2012. Chemical structure of Retro-2, a compound that protects cells against ribosome-inactivating proteins. *Scientific Reports*, *2*, p.631.
- Parkinson, J.E. and Smith, G.L., 1994. Vaccinia virus gene A36R encodes a Mr 43-50 K protein on the surface of extracellular enveloped virus. *Virology*, *204*(1), pp.376-390.
- Payne, L.G., 1980. Significance of extracellular enveloped virus in the in vitro and in vivo dissemination of vaccinia. *Journal of General Virology*, *50*(1), pp.89-100.
- Payne, L.G., 1992. Characterization of vaccinia virus glycoproteins by monoclonal antibody precipitation. *Virology*, *187*(1), pp.251-260.
- Payne, L.G. and Kristenson, K., 1979. Mechanism of vaccinia virus release and its specific inhibition by N1-isonicotinoyl-N2-3-methyl-4-chlorobenzoylhydrazine. *Journal of Virology*, *32*(2), pp.614-622.
- Payne, L.G. and Norrby, E., 1976. Presence of haemagglutinin in the envelope of extracellular vaccinia virus particles. *Journal of General Virology*, *32*(1), pp.63-72.
- Payne, L.G. and Norrby, E., 1978. Adsorption and penetration of enveloped and naked vaccinia virus particles. *Journal of Virology*, *27*(1), pp.19-27.
- Pechenick-Jowers, T., Featherstone, R.J., Reynolds, D.K., Brown, H.K., James, J., Prescott, A., Haga, I.R. and Beard, P.M., 2015. RAB1A promotes Vaccinia virus replication by facilitating the production of intracellular enveloped virions. *Virology*, *475*, pp.66-73.
- Perdiguero, B. and Blasco, R., 2006. Interaction between vaccinia virus extracellular virus envelope A33 and B5 glycoproteins. *Journal of Virology*, *80*(17), pp.8763-8777.
- Perdiguero, B., Lorenzo, M.M. and Blasco, R., 2008. Vaccinia virus A34 glycoprotein determines the protein composition of the extracellular virus envelope. *Journal of Virology*, *82*(5), pp.2150-2160.

- Perera, L.P., Goldman, C.K. and Waldmann, T.A., 2001. Comparative assessment of virulence of recombinant vaccinia viruses expressing IL-2 and IL-15 in immunodeficient mice. *Proceedings of the National Academy of Sciences*, *98*(9), pp.5146-5151.
- Pérez-Victoria, F.J., Abascal-Palacios, G., Tascón, I., Kajava, A., Magadán, J.G., Pioro, E.P., Bonifacino, J.S. and Hierro, A., 2010a. Structural basis for the wobbler mouse neurodegenerative disorder caused by mutation in the Vps54 subunit of the GARP complex. *Proceedings of the National Academy of Sciences*, *107*(29), pp.12860-12865.
- Pérez-Victoria, F.J., Schindler, C., Magadán, J.G., Mardones, G.A., Delevoye, C., Romao, M., Raposo, G. and Bonifacino, J.S., 2010b. Ang2/fat-free is a conserved subunit of the Golgi-associated retrograde protein complex. *Molecular Biology of the Cell*, *21*(19), pp.3386-3395.
- Pérez-Victoria, F.J. and Bonifacino, J.S., 2009. Dual roles of the mammalian GARP complex in tethering and SNARE complex assembly at the trans-Golgi network. *Molecular and Cellular Biology*, *29*(19), pp.5251-5263.
- Pérez-Victoria, F.J., Mardones, G.A. and Bonifacino, J.S., 2008. Requirement of the human GARP complex for mannose 6-phosphate-receptor-dependent sorting of cathepsin D to lysosomes. *Molecular Biology of the Cell*, *19*(6), pp.2350-2362.
- Personnic, N., Bärlocher, K., Finsel, I. and Hilbi, H., 2016. Subversion of retrograde trafficking by translocated pathogen effectors. *Trends in Microbiology*, *24*(6), pp.450-462.
- Piacente, S., Christen, L., Dickerman, B., Mohamed, M.R. and Niles, E.G., 2008. Determinants of vaccinia virus early gene transcription termination. *Virology*, *376*(1), pp.211-224.
- Pogo, B.G., Berkowitz, E.M. and Dalest, S., 1984. Investigation of vaccinia virus DNA replication employing a conditional lethal mutant defective in DNA. *Virology*, *132*(2), pp.436-444.
- Popa, A., Zhang, W., Harrison, M.S., Goodner, K., Kazakov, T., Goodwin, E.C., Lipovsky, A., Burd, C.G. and DiMaio, D., 2015. Direct binding of retromer to human papillomavirus type 16 minor capsid protein L2 mediates endosome exit during viral infection. *PLoS Pathogens*, *11*(2), p.e1004699.

- Popoff, V., Mardones, G.A., Tenza, D., Rojas, R., Lamaze, C., Bonifacino, J.S., Raposo, G. and Johannes, L., 2007. The retromer complex and clathrin define an early endosomal retrograde exit site. *Journal of Cell Science*, *120*(12), pp.2022-2031.
- Qin, L., Upton, C., Hazes, B. and Evans, D.H., 2011. Genomic analysis of the vaccinia virus strain variants found in Dryvax vaccine. *Journal of Virology*, pp.JVI-05779.
- Quenneville, N.R., Chao, T.Y., McCaffery, J.M. and Conibear, E., 2006. Domains within the GARP subunit Vps54 confer separate functions in complex assembly and early endosome recognition. *Molecular Biology of the Cell*, *17*(4), pp.1859-1870.
- Raingeaud, J., Gupta, S., Rogers, J.S., Dickens, M., Han, J., Ulevitch, R.J. and Davis, R.J., 1995. Pro-inflammatory cytokines and environmental stress cause p38 mitogen-activated protein kinase activation by dual phosphorylation on tyrosine and threonine. *Journal of Biological Chemistry*, *270*(13), pp.7420-7426.
- Raingeaud, J., Whitmarsh, A.J., Barrett, T., Derijard, B. and Davis, R.J., 1996. MKK3-and MKK6-regulated gene expression is mediated by the p38 mitogen-activated protein kinase signal transduction pathway. *Molecular and Cellular Biology*, *16*(3), pp.1247-1255.
- Raman, M. and Cobb, M.H., 2003. MAP kinase modules: many roads home. *Current Biology*, *13*(22), pp.R886-R888.
- Reading, P.C., Symons, J.A. and Smith, G.L., 2003. A soluble chemokine-binding protein from vaccinia virus reduces virus virulence and the inflammatory response to infection. *The Journal of Immunology*, *170*(3), pp.1435-1442.
- Remy, G., Risco, A.M., Iñesta-Vaquera, F.A., González-Terán, B., Sabio, G., Davis, R.J. and Cuenda, A., 2010. Differential activation of p38 MAPK isoforms by MKK6 and MKK3. *Cellular Signalling*, *22*(4), pp.660-667.
- Renna, M., Jimenez-Sanchez, M., Sarkar, S. and Rubinsztein, D.C., 2010. Chemical inducers of autophagy that enhance the clearance of mutant proteins in neurodegenerative diseases. *Journal of Biological Chemistry*, *285*(15), pp.11061-11067.
- Roberts, K.L., Breiman, A., Carter, G.C., Ewles, H.A., Hollinshead, M., Law, M. and Smith, G.L., 2009. Acidic residues in the membrane-proximal stalk region of vaccinia virus protein

B5 are required for glycosaminoglycan-mediated disruption of the extracellular enveloped virus outer membrane. *Journal of General Virology*, *90*(7), pp.1582-1591.

- Roberts, K.L. and Smith, G.L., 2008. Vaccinia virus morphogenesis and dissemination. *Trends in Microbiology*, *16*(10), pp.472-479.
- Roper, R.L., Payne, L.G. and Moss, B., 1996. Extracellular vaccinia virus envelope glycoprotein encoded by the A33R gene. *Journal of Virology*, *70*(6), pp.3753-3762.
- Roper, R.L., Wolffe, E.J., Weisberg, A. and Moss, B., 1998. The envelope protein encoded by the A33R gene is required for formation of actin-containing microvilli and efficient cell-to-cell spread of vaccinia virus. *Journal of Virology*, *72*(5), pp.4192-4204.
- Rosales, R., Harris, N., Ahn, B.Y. and Moss, B., 1994a. Purification and identification of a vaccinia virus-encoded intermediate stage promoter-specific transcription factor that has homology to eukaryotic transcription factor SII (TFIIS) and an additional role as a viral RNA polymerase subunit. *Journal of Biological Chemistry*, *269*(19), pp.14260-14267.
- Rosales, R., Sutter, G. and Moss, B., 1994b. A cellular factor is required for transcription of vaccinia viral intermediate-stage genes. *Proceedings of the National Academy of Sciences*, *91*(9), pp.3794-3798.
- Rouse, J., Cohen, P., Trigon, S., Morange, M., Alonso-Llamazares, A., Zamanillo, D., Hunt, T. and Nebreda, A.R., 1994. A novel kinase cascade triggered by stress and heat shock that stimulates MAPKAP kinase-2 and phosphorylation of the small heat shock proteins. *Cell*, *78*(6), pp.1027-1037.
- Ryan, J.E., Dhiman, N., Ovsyannikova, I.G., Vierkant, R.A., Pankratz, V.S. and Poland, G.A., 2009. Response surface methodology to determine optimal cytokine responses in human peripheral blood mononuclear cells after smallpox vaccination. *Journal of Immunological Methods*, *341*(1), pp.97-105.
- Sabio, G. and Davis, R.J., 2014, June. TNF and MAP kinase signalling pathways. In *Seminars in immunology* (Vol. 26, No. 3, pp. 237-245). Academic Press.

- Sanderson, C.M., Hollinshead, M. and Smith, G.L., 2000. The vaccinia virus A27L protein is needed for the microtubule-dependent transport of intracellular mature virus particles. *Journal of General Virology*, *81*(1), pp.47-58.
- Sandvig, K., Skotland, T., van Deurs, B. and Klokk, T.I., 2013. Retrograde transport of protein toxins through the Golgi apparatus. *Histochemistry and Cell Biology*, *140*(3), pp.317-326.
- Sanz, P. and Moss, B., 1999. Identification of a transcription factor, encoded by two vaccinia virus early genes, that regulates the intermediate stage of viral gene expression. *Proceedings of the National Academy of Sciences*, *96*(6), pp.2692-2697.
- Satheshkumar, P.S., Weisberg, A.S. and Moss, B., 2013. Vaccinia virus A19 protein participates in the transformation of spherical immature particles to barrel-shaped infectious virions. *Journal of Virology*, *87*(19), pp.10700-10709.
- Scaplehorn, N., Holmström, A., Moreau, V., Frischknecht, F., Reckmann, I. and Way, M., 2002. Grb2 and Nck act cooperatively to promote actin-based motility of vaccinia virus. *Current Biology*, *12*(9), pp.740-745.
- Schmelz, M., Sodeik, B., Ericsson, M., Wolffe, E.J., Shida, H., Hiller, G. and Griffiths, G., 1994. Assembly of vaccinia virus: the second wrapping cisterna is derived from the trans Golgi network. *Journal of Virology*, *68*(1), pp.130-147.
- Schmitt-John, T., Drepper, C., Mußmann, A., Hahn, P., Kuhlmann, M., Thiel, C., Hafner, M., Lengeling, A., Heimann, P., Jones, J.M. and Meisler, M.H., 2005. Mutation of Vps54 causes motor neuron disease and defective spermiogenesis in the wobbler mouse. *Nature Genetics*, *37*(11), p.1213.
- Schmutz, C., Payne, L.G., Gubser, J., and Wittek, R., 1991. A mutation in the gene encoding the vaccinia virus 37,000-M (r) protein confers resistance to an inhibitor of virus envelopment and release. *Journal of Virology*, *65*(7), pp.3435-3442.
- Schmutz, C., Rindisbacher, L., Galmiche, M.C. and Wittek, R., 1995. Biochemical analysis of the major vaccinia virus envelope antigen. *Virology*, *213*(1), pp.19-27.
- Seaman, M.N., 2004. Cargo-selective endosomal sorting for retrieval to the Golgi requires retromer. *Journal of Cell Biology*, *165*(1), pp.111-122.

- Seaman, M.N., McCaffery, J.M. and Emr, S.D., 1998. A membrane coat complex essential for endosome-to-Golgi retrograde transport in yeast. *The Journal of Cell Biology*, *142*(3), pp.665-681.
- Secher, T., Shima, A., Hinsinger, K., Cintrat, J.C., Johannes, L., Barbier, J., Gillet, D. and Oswald, E., 2015. Retrograde trafficking inhibitor of Shiga toxins reduces morbidity and mortality of mice infected with enterohemorrhagic Escherichia coli. *Antimicrobial Agents and Chemotherapy*, *59*(8), pp.5010-5013.
- Seger, R., Ahn, N.G., Posada, J., Munar, E.S., Jensen, A.M., Cooper, J.A., Cobb, M.H. and Krebs, E.G., 1992. Purification and characterization of mitogen-activated protein kinase activator (s) from epidermal growth factor-stimulated A431 cells. *Journal of Biological Chemistry*, *267*(20), pp.14373-14381.
- Seger, R. and Krebs, E.G., 1995. The MAPK signaling cascade. *The FASEB journal*, *9*(9), pp.726-735.
- Senkevich, T.G., Ojeda, S., Townsley, A., Nelson, G.E. and Moss, B., 2005. Poxvirus multiprotein entry–fusion complex. *Proceedings of the National Academy of Sciences of the United States of America*, *102*(51), pp.18572-18577.
- Senkevich, T.G., White, C.L., Koonin, E.V. and Moss, B., 2002. Complete pathway for protein disulfide bond formation encoded by poxviruses. *Proceedings of the National Academy of Sciences*, *99*(10), pp.6667-6672.
- Shaul, Y.D. and Seger, R., 2007. The MEK/ERK cascade: from signaling specificity to diverse functions. *Biochimica et Biophysica Acta (BBA)-Molecular Cell Research*, *1773*(8), pp.1213-1226.
- Shin, H.B., Choi, M.S., Yi, C.M., Lee, J., Kim, N.J. and Inn, K.S., 2015. Inhibition of respiratory syncytial virus replication and virus-induced p38 kinase activity by berberine. *International Immunopharmacology*, *27*(1), pp.65-68.
- Siniossoglou, S. and Pelham, H.R., 2002. Vps51p links the VFT complex to the SNARE Tlg1p. *Journal of Biological Chemistry*, *277*(50), pp.48318-48324.

- Siniossoglou, S. and Pelham, H.R., 2001. An effector of Ypt6p binds the SNARE Tlg1p and mediates selective fusion of vesicles with late Golgi membranes. *The EMBO Journal*, *20*(21), pp.5991-5998.
- Sivan, G., Martin, S.E., Myers, T.G., Buehler, E., Szymczyk, K.H., Ormanoglu, P. and Moss, B., 2013. Human genome-wide RNAi screen reveals a role for nuclear pore proteins in poxvirus morphogenesis. *Proceedings of the National Academy of Sciences*, *110*(9), pp.3519-3524.
- Sivan, G., Weisberg, A.S., Americo, J.L. and Moss, B., 2016. Retrograde transport from early endosomes to the trans-golgi network enables membrane wrapping and egress of vaccinia virus virions. *Journal of Virology*, *90*(19), pp.8891-8905.
- Smith, G.L., 1999. Vaccinia virus immune evasion. *Immunology Letters*, *65*(1), pp.55-62.
- Smith, G.L., Vanderplasschen, A. and Law, M., 2002. The formation and function of extracellular enveloped vaccinia virus. *Journal of General Virology*, *83*(12), pp.2915-2931.
- Smith, G.L. and Law, M., 2004. The exit of vaccinia virus from infected cells. *Virus Research*, *106*(2), pp.189-197.
- Sodeik, B., Doms, R.W., Ericsson, M., Hiller, G., Machamer, C.E., van't Hof, W., van Meer, G., Moss,B., Griffiths, G., 1993. Assembly of Vaccinia virus: Role of the intermediate compartment between the endoplasmic reticulum and the Golgi stacks. *The Journal of Cell Biology,* 121(3), pp.521-541.
- Spooner, R.A. and Lord, J.M., 2015. Ricin trafficking in cells. *Toxins*, *7*(1), pp.49-65.
- Spooner, R.A., Smith, D.C., Easton, A.J., Roberts, L.M. and Lord, M.J., 2006. Retrograde transport pathways utilised by viruses and protein toxins. *Virology Journal*, *3*(1), p.26.
- Srivastava, A., Shinn, A.S., Lee, P.J. and Mannam, P., 2015. MKK3 mediates inflammatory response through modulation of mitochondrial function. *Free Radical Biology and Medicine*, *83*, pp.139-148.
- Stack, J., Hurst, T.P., Flannery, S.M., Brennan, K., Rupp, S., Oda, S.I., Khan, A.R. and Bowie, A.G., 2013. Poxviral protein A52 stimulates p38 mitogen-activated protein kinase (MAPK) activation by causing tumor necrosis factor receptor-associated factor 6 (TRAF6)

self-association leading to transforming growth factor β-activated kinase 1 (TAK1) recruitment. *Journal of Biological Chemistry*, *288*(47), pp.33642-33653.

- Stechmann, B., Bai, S.K., Gobbo, E., Lopez, R., Merer, G., Pinchard, S., Panigai, L., Tenza, D., Raposo, G., Beaumelle, B. and Sauvaire, D., 2010. Inhibition of retrograde transport protects mice from lethal ricin challenge. *Cell*, *141*(2), pp.231-242.
- Stenmark, H., 2009. Rab GTPases as coordinators of vesicle traffic. *Nature Reviews Molecular Cell Biology*, *10*(8), pp.513-525.
- Südhof, T.C. and Rothman, J.E., 2009. Membrane fusion: grappling with SNARE and SM proteins. *Science*, *323*(5913), pp.474-477.
- Sugimoto, M., Kondo, M., Hirose, M., Suzuki, M., Mekada, K., Abe, T., Kiyonari, H., Ogura, A., Takagi, N., Artzt, K. and Abe, K., 2012. Molecular identification of t w5: Vps52 promotes pluripotential cell differentiation through cell–cell interactions. *Cell Reports*, *2*(5), pp.1363-1374.
- Sung, T.C., Roper, R.L., Zhang, Y., Rudge, S.A., Temel, R., Hammond, S.M., Morris, A.J., Moss, B., Engebrecht, J. and Frohman, M.A., 1997. Mutagenesis of phospholipase D defines a superfamily including a trans-Golgi viral protein required for poxvirus pathogenicity. *The EMBO journal*, *16*(15), pp.4519-4530.
- Sweeney, G., Somwar, R., Ramlal, T., Volchuk, A., Ueyama, A. and Klip, A., 1999. An inhibitor of p38 mitogen-activated protein kinase prevents insulin-stimulated glucose transport but not glucose transporter translocation in 3T3-L1 adipocytes and L6 myotubes. *Journal of Biological Chemistry*, *274*(15), pp.10071-10078.
- Szajner, P., Jaffe, H., Weisberg, A.S. and Moss, B., 2004. A complex of seven vaccinia virus proteins conserved in all chordopoxviruses is required for the association of membranes and viroplasm to form immature virions. *Virology*, *330*(2), pp.447-459.
- Szajner, P., Weisberg, A.S., Lebowitz, J., Heuser, J. and Moss, B., 2005. External scaffold of spherical immature poxvirus particles is made of protein trimers, forming a honeycomb lattice. *The Journal of Cell Biology*, *170*(6), pp.971-981.
- Tai, G., Lu, L., Wang, T.L., Tang, B.L., Goud, B., Johannes, L. and Hong, W., 2004. Participation of the syntaxin 5/Ykt6/GS28/GS15 SNARE complex in transport from the

early/recycling endosome to the trans-Golgi network. *Molecular Biology of the Cell*, *15*(9), pp.4011-4022.

- Tibbles, L.A., Spurrell, J.C., Bowen, G.P., Liu, Q., Lam, M., Zaiss, A.K., Robbins, S.M., Hollenberg, M.D., Wickham, T.J. and Muruve, D.A., 2002. Activation of p38 and ERK signalling during adenovirus vector cell entry lead to expression of the CXC chemokine IP-10. *Journal of Virology*, *76*(4), pp.1559-1568.
- Tong, L., Smyth, D., Kerr, C., Catterall, J. and Richards, C.D., 2004. Mitogen-activated protein kinases Erk1/2 and p38 are required for maximal regulation of TIMP-1 by oncostatin M in murine fibroblasts. *Cellular signalling*, *16*(10), pp.1123-1132.
- Tournier, C., Dong, C., Turner, T.K., Jones, S.N., Flavell, R.A. and Davis, R.J., 2001. MKK7 is an essential component of the JNK signal transduction pathway activated by proinflammatory cytokines. *Genes & Development*, *15*(11), pp.1419-1426.
- Tournier, C., Whitmarsh, A.J., Cavanagh, J., Barrett, T. and Davis, R.J., 1999. The MKK7 gene encodes a group of c-Jun NH2-terminal kinase kinases. *Molecular and Cellular biology*, *19*(2), pp.1569-1581.
- Trousdale, C. and Kim, K., 2015. Retromer: Structure, function, and roles in mammalian disease. *European Journal of Cell Biology*, *94*(11), pp.513-521.
- Tsutsui, K., 1983. Release of vaccinia virus from FL cells infected with the IHD-W strain. *Journal of Electron Microscopy*, *32*(2), pp.125-140.
- Ulaeto, D., Grosenbach, D. and Hruby, D.E., 1996. The vaccinia virus 4c and A-type inclusion proteins are specific markers for the intracellular mature virus particle. *Journal of Virology*, *70*(6), pp.3372-3377.
- van Eijl, H., Hollinshead, M., Rodger, G., Zhang, W.H. and Smith, G.L., 2002. The vaccinia virus F12L protein is associated with intracellular enveloped virus particles and is required for their egress to the cell surface. *Journal of General Virology*, *83*(1), pp.195-207.
- Vanderplasschen, A., Hollinshead, M. and Smith, G.L., 1998. Intracellular and extracellular vaccinia virions enter cells by different mechanisms. *Journal of General Virology*, *79*(4), pp.877-887.

- Vanderplasschen, A. and Smith, G.L., 1997. A novel virus binding assay using confocal microscopy: demonstration that the intracellular and extracellular vaccinia virions bind to different cellular receptors. *Journal of Virology*, *71*(5), pp.4032-4041.
- Vasan, N., Hutagalung, A., Novick, P. and Reinisch, K.M., 2010. Structure of a C-terminal fragment of its Vps53 subunit suggests similarity of Golgi-associated retrograde protein (GARP) complex to a family of tethering complexes. *Proceedings of the National Academy of Sciences*, *107*(32), pp.14176-14181.
- Vasquez-Rifo, A., Bossé, G.D., Rondeau, E.L., Jannot, G., Dallaire, A. and Simard, M.J., 2013. A new role for the GARP complex in microRNA-mediated gene regulation. *PLoS Genetics*, *9*(11), p.e1003961.
- Vlahopoulos, S. and Zoumpourlis, V.C., 2004. JNK: a key modulator of intracellular signaling. *Biochemistry (Moscow)*, *69*(8), pp.844-854.
- Vliegen, I., Yang, G., Hruby, D., Jordan, R. and Neyts, J., 2012. Deletion of the vaccinia virus F13L gene results in a highly attenuated virus that mounts a protective immune response against subsequent vaccinia virus challenge. *Antiviral Research*, *93*(1), pp.160-166.
- Volz, A., Lim, S., Kaserer, M., Lülf, A., Marr, L., Jany, S., Deeg, C.A., Pijlman, G.P., Koraka, P., Osterhaus, A.D. and Martina, B.E., 2016. Immunogenicity and protective efficacy of recombinant Modified Vaccinia virus Ankara candidate vaccines delivering West Nile virus envelope antigens. *Vaccine*, *34*(16), pp.1915-1926.
- Vora, S., Damon, I., Fulginiti, V., Weber, S.G., Kahana, M., Stein, S.L., Gerber, S.I., Garcia-Houchins, S., Lederman, E., Hruby, D. and Collins, L., 2008. Severe eczema vaccinatum in a household contact of a smallpox vaccinee. *Clinical Infectious Diseases*, *46*(10), pp.1555-1561.
- Walsh, D., Arias, C., Perez, C., Halladin, D., Escandon, M., Ueda, T., Watanabe-Fukunaga, R., Fukunaga, R. and Mohr, I., 2008. Eukaryotic translation initiation factor 4F architectural alterations accompany translation initiation factor redistribution in poxvirus-infected cells. *Molecular and Cellular Biology*, *28*(8), pp.2648-2658.

- Wang, L., Ma, R., Flavell, R.A. and Choi, M.E., 2002. Requirement of mitogen-activated protein kinase kinase 3 (MKK3) for activation of p38α and p38δ MAPK isoforms by TGF-β1 in murine mesangial cells. *Journal of Biological Chemistry*, *277*(49), pp.47257-47262.
- Wang, T.S., Wong, S.W. and Korn, D.A.V.I.D., 1989. Human DNA polymerase alpha: predicted functional domains and relationships with viral DNA polymerases. *The FASEB Journal*, *3*(1), pp.14-21.
- Wagenaar, T.R. and Moss, B., 2009. Expression of the A56 and K2 proteins is sufficient to inhibit vaccinia virus entry and cell fusion. *Journal of Virology*, *83*(4), pp.1546-1554.
- Wang, X. and Tournier, C., 2006. Regulation of cellular functions by the ERK5 signalling pathway. *Cellular Signalling*, *18*(6), pp.753-760.
- Wang, S., Yang, J., Qian, J., Wezeman, M., Kwak, L.W. and Yi, Q., 2006. Tumor evasion of the immune system: inhibiting p38 MAPK signaling restores the function of dendritic cells in multiple myeloma. *Blood*, *107*(6), pp.2432-2439.
- Ward, B.M. and Moss, B., 2000. Golgi network targeting and plasma membrane internalization signals in vaccinia virus B5R envelope protein. *Journal of Virology*, *74*(8), pp.3771-3780.
- Ward, B.M., Weisberg, A.S. and Moss, B., 2003. Mapping and functional analysis of interaction sites within the cytoplasmic domains of the vaccinia virus A33R and A36R envelope proteins. *Journal of Virology*, *77*(7), pp.4113-4126.
- Waskiewicz, A.J., Flynn, A., Proud, C.G. and Cooper, J.A., 1997. Mitogen-activated protein kinases activate the serine/threonine kinases Mnk1 and Mnk2. *The EMBO journal*, *16*(8), pp.1909-1920.
- Waters, M.G., Clary, D.O. and Rothman, J.E., 1992. A novel 115-kD peripheral membrane protein is required for intercisternal transport in the Golgi stack. *The Journal of Cell Biology*, *118*(5), pp.1015-1026.
- Wesche, J., 2001. Retrograde transport of ricin. *International Journal of Medical Microbiology*, *291*(6), pp.517-522.
- Weston, C.R., Lambright, D.G. and Davis, R.J., 2002. MAP kinase signalling specificity. *Science*, *296*(5577), pp.2345-2347.

- Wolffe, E.J., Isaacs, S.N. and Moss, B., 1993. Deletion of the vaccinia virus B5R gene encoding a 42-kilodalton membrane glycoprotein inhibits extracellular virus envelope formation and dissemination. *Journal of Virology*, *67*(8), pp.4732-4741.
- Wolffe, E.J., Katz, E., Weisberg, A. and Moss, B., 1997. The A34R glycoprotein gene is required for induction of specialized actin-containing microvilli and efficient cell-to-cell transmission of vaccinia virus. *Journal of Virology*, *71*(5), pp.3904-3915.
- Wright, C.F. and Coroneos, A.M., 1993. Purification of the late transcription system of vaccinia virus: identification of a novel transcription factor. *Journal of Virology*, *67*(12), pp.7264-7270.
- Wright, C.F., Keck, J.G., Tsai, M.M. and Moss, B., 1991. A transcription factor for expression of vaccinia virus late genes is encoded by an intermediate gene. *Journal of Virology*, *65*(7), pp.3715-3720.
- Wright, C.F., Oswald, B.W. and Dellis, S., 2001. Vaccinia virus late transcription is activated in vitro by cellular heterogeneous nuclear ribonucleoproteins. *Journal of Biological Chemistry*, *276*(44), pp.40680-40686.
- Wysk, M., Yang, D.D., Lu, H.T., Flavell, R.A. and Davis, R.J., 1999. Requirement of mitogen-activated protein kinase kinase 3 (MKK3) for tumor necrosis factor-induced cytokine expression. *Proceedings of the National Academy of Sciences*, *96*(7), pp.3763-3768.
- Yang, Z., Bruno, D.P., Martens, C.A., Porcella, S.F. and Moss, B., 2010. Simultaneous high-resolution analysis of vaccinia virus and host cell transcriptomes by deep RNA sequencing. *Proceedings of the National Academy of Sciences*, *107*(25), pp.11513-11518.
- Yang, Z. and Moss, B., 2009. Interaction of the vaccinia virus RNA polymerase-associated 94-kilodalton protein with the early transcription factor. *Journal of Virology*, *83*(23), pp.12018-12026.
- Yang, G., Pevear, D.C., Davies, M.H., Collett, M.S., Bailey, T., Rippen, S., Barone, L., Burns, C., Rhodes, G., Tohan, S. and Huggins, J.W., 2005. An orally bioavailable antipoxvirus compound (ST-246) inhibits extracellular virus formation and protects mice from lethal orthopoxvirus challenge. *Journal of Virology*, *79*(20), pp.13139-13149.

- Yang, D., Tournier, C., Wysk, M., Lu, H.T., Xu, J., Davis, R.J. and Flavell, R.A., 1997. Targeted disruption of the MKK4 gene causes embryonic death, inhibition of c-Jun NH2-terminal kinase activation, and defects in AP-1 transcriptional activity. *Proceedings of the National Academy of Sciences*, *94*(7), pp.3004-3009.
- Yu, I.M. and Hughson, F.M., 2010. Tethering factors as organizers of intracellular vesicular traffic. *Annual Review of Cell and Developmental Biology*, *26*, pp.137-156.
- Zarubin, T. and Han, J., 2005. Activation and signaling of the p38 MAP kinase pathway. *Cell Research*, *15*(1), p.11.
- Zeh, H.J., Downs-Canner, S., McCart, J.A., Guo, Z.S., Rao, U.N., Ramalingam, L., Thorne, S.H., Jones, H.L., Kalinski, P., Wieckowski, E. and O'malley, M.E., 2015. First-in-man study of western reserve strain oncolytic vaccinia virus: safety, systemic spread, and antitumor activity. *Molecular Therapy*, *23*(1), pp.202-214.
- Zhang, P., Langland, J.O., Jacobs, B.L. and Samuel, C.E., 2009. Protein kinase PKR-dependent activation of mitogen-activated protein kinases occurs through mitochondrial adapter IPS-1 and is antagonized by vaccinia virus E3L. *Journal of Virology*, *83*(11), pp.5718-5725.
- Zhang, W.H., Wilcock, D. and Smith, G.L., 2000. Vaccinia virus F12L protein is required for actin tail formation, normal plaque size, and virulence. *Journal of Virology*, *74*(24), pp.11654-11662.
- Zhou, G., Bao, Z.Q. and Dixon, J.E., 1995. Components of a new human protein kinase signal transduction pathway. *Journal of Biological Chemistry*, *270*(21), pp.12665-12669.
- Zhu, X., Venkataprasad, N., Ivanyi, J. and Vordermeier, H.M., 1997. Vaccination with recombinant vaccinia viruses protects mice against Mycobacterium tuberculosis infection. *Immunology*, *92*(1), p.6.